



**Behaviour of Multi-Celled GFRP Beam Assembly with  
Concrete Infill: Experimental and Theoretical Evaluations**

A thesis submitted by

**Majid Dhahir Muttashar, M Eng.**

For the award of

**Doctor of Philosophy**

2017

## Abstract

Glass Fibre Reinforced Polymer composites (GFRP) have become an attractive construction material for civil engineering applications due to their excellent corrosion resistance, design flexibility, and high stiffness and strength-to-weight ratios. However, research related to the flexural behaviour of concrete filled GFRP tubes is very limited, especially with regards to developing high strength and lightweight composite beams. Therefore, this research project has developed and investigated the behaviour of a new composite beam, termed “multi-celled GFRP beam”, which was made by gluing together a number of pultruded GFRP tubes and then filled with low-strength concrete.

Firstly, the effective elastic properties of the pultruded GFRP tubes were evaluated by testing full-scale specimens with different shear span-to-depth ( $a/d$ ) ratios. The flexural ( $E$ ) and shear ( $G$ ) moduli of the GFRP tubes were then calculated using back calculation ( $BCM$ ) and simultaneous ( $SM$ ) methods. The results showed that the  $BCM$  method gives a more reliable elastic properties of pultruded hollow GFRP sections compared with  $SM$  and coupon tests. In addition, the full-scale test can accurately capture the local buckling failure of the compression flange of the GFRP section and the contribution of shear deformation, which is impossible to capture using a coupon specimen due to the discontinuity of the fibres. The compression buckling failure can significantly affect the ultimate failure load of GFRP sections and result in the section utilising only half of its design capacity.

Secondly, the effect of filling the pultruded GFRP single sections with concrete of different compressive strengths on the flexural behaviour was investigated. Three different compressive strengths of concrete, i.e. 10 MPa, 37 MPa, and 43.5 MPa, were used to fill the hollow pultruded tubes. These beams were then tested under 4-point static bending. The results indicated that the concrete filling improved the flexural behaviour of GFRP tubes. The beams filled with concrete of 10 MPa compressive strength showed a 100% increase in strength, while the beams filled with concrete of 43.5 MPa compressive strength exhibited a 141% increase in strength, compared to the hollow sections. However, both concrete filled beams showed an approximately similar stiffness

suggesting that low-strength concrete is a practical solution to filling the GFRP tubes.

Thirdly, multi-celled GFRP beams were developed, and the flexural behaviour of this new beam concept was investigated. Beams with 1, 2, 3, and 4 cells were tested in hollow and concrete-filled configurations. From the experimental outcomes, it was found that gluing the pultruded GFRP profiles together can help stabilise the section and effectively utilise the high strength of the fibre composite materials. Moreover, the provision of a concrete core in the top cells significantly enhanced the bending strength and stiffness of the GFRP sections, due to the concrete supporting the tube walls and delaying the local buckling. Similarly, the increased number of cells in the cross-section changed the failure mode from compression buckling to bearing.

Finally, a simplified prediction equation, based on the maximum stresses of the GFRP materials and incorporating the shear span-to-depth ratio and local buckling, was developed. This model was used in a parametric study to evaluate the effect of the number of cells, shear span-to-depth ratio, and filling percentage on the flexural behaviour of the multi-celled GFRP beams. The results indicated that the increased number of cells enhanced the capacity of the hollow and concrete-filled beams. Similarly, the failure of the hollow beams will be governed by either the buckling failure of the compression flange of the top cell or the bearing failure, while the concrete filled beams will be affected by either bearing failure of the hollow cell under the filled cells or web buckling of the top-filled cell. It was also established that the multi-celled beams with a concrete infill at the top cell only would have a higher strength-to-weight ratio compared to their hollow beam counterparts. Furthermore, a failure mechanism map was developed to help identifying the possible failure mode for any combinations of GFRP tubes and concrete.

An in-depth understanding of the behaviour of multi-celled GFRP beams, with and without concrete infill, was the significant outcome of this study. Moreover, the newly developed multi-celled GFRP section, filled with a low compressive strength concrete at the top cell only, showed high potential for structural applications that need high strength, high stiffness, and lightweight characteristics.

## Certification of thesis

This thesis is entirely the work of *Majid Muttashar* except where otherwise acknowledges. The work is original and has not previously been submitted for any other award, except where acknowledged.

Student and supervisors signatures of endorsement are held at USQ

*Majid Muttashar*

---

Signature of Candidate

*16 May 2017*

---

Date

### Endorsement

*Professor Karu Karunasena*

---

Signature of Principal Supervisor

*16 May 2017*

---

Date

*Dr Allan Manalo*

---

Signature of Associate Supervisor

*16 May 2017*

---

Date

*Dr Weena Lokuge*

---

Signature of Associate Supervisor

*16 May 2017*

---

Date

## Acknowledgements

Thanks to *Almighty ALLAH* for the gracious kindness in all the endeavours, I have taken up in my life.

I would like to express my sincere greatest appreciation and thanks to my principal supervisor, Professor *Warna (Karu) Karunasena* for the guidance, insight, helpful advice, and constant encouragement provided throughout the course of the dissertation. I am so proud to work with him. I wish to express my sincere gratitude to my associate supervisor *Dr Allan Manalo* for guiding this project and making me realize the importance of perfection and quality. I owe him an unbelievable amount of gratitude for his prominent role in helping me to achieve one of the greatest accomplishments in my life. In addition, my thanks for my associate supervisor *Dr Weena Lokuge* for her advice and valuable comments and suggestions those were essential in improving of my research.

Sincere words of thanks must also go to *Mr Mohammed Alsafi, Mr Wayne Crowell, Mr Martin Geach* and all the staff and postgraduate student at CFM, for their assistance during the fabrication, construction and testing of the specimens and for their support and friendship. I especially thank *Michael Kemp* and all the staff of Wagner's Composite Fibre Technology for providing the GFRP tubes.

My admiration and respect go to my father, my mother, my brothers and sisters for their support, endless love, encouragement and prayers.

I owe my deepest love and appreciation to my dear wife for her steadfast support and continuous encouragement. She was always there to give me the push for this challenge and to face all life obstacles. I cannot present this work without expressing my love to my sons *Ahmed and Mohammed Ridha* and my daughters *Ruqayah and Mariam* who enlightened my life with their smile.

My sincere gratitude and appreciation go to the *Australian Government* for the financial support through Research Training Program (RTP).

My thanks go to *Henk Huijser*, who helped me in editing the thesis.

Finally, to those whom I failed to mention but have been a great part of this endeavour, thank you very much.

## Statements of contributions

The share of the co-authors in the presented publications in this thesis is detail in following:

- **Muttashar M**, Karunasena W, Manalo A, Lokuge W. (2016). "Behaviour of hollow pultruded GFRP square beams with different shear span-to-depth ratios". Journal of Composite Materials. Vol.50, Issue 21, pp. 2925-2940. (IF:1.24, SNIP:1.17)

The overall contribution of **Majid Muttashar** was 70% to the concept development, design of experiments, experiment works, analysis and interpretation of data, drafting and revising the final submission; **Warna Karunasena**, **Allan Manalo**, **Weena Lokuge** were contributed to the concept development, design of experiments, experiment works, analysis and interpretation of data, drafting and providing important technical inputs by 10%, 15% and 5%, respectively.

- **Muttashar M**, Manalo A, Karunasena W, Lokuge W. (2016). "Influence of infill concrete strength on the flexural behaviour of pultruded GFRP square beams". Composite Structures. Vol.145, pp. 58-67. (IF:3.385, SNIP:2.12)

The overall contribution of **Majid Muttashar** was 70% to the concept development, design of experiments, experiment works, analysis and interpretation of data, drafting and revising the final submission; **Allan Manalo**, **Warna Karunasena**, **Weena Lokuge** were contributed to the concept development, design of experiments, experiment works, analysis and interpretation of data, drafting and providing important technical inputs by 15%, 10% and 5%, respectively.

- **Muttashar M**, Manalo A, Karunasena W, Lokuge W. (2017). "Flexural behaviour of multi-celled GFRP composite beams with concrete infill: Experiment and theoretical analysis". Composite Structures. Vol. 159, pp. 21-33. (IF:3.385, SNIP:2.12)

The overall contribution of **Majid Muttashar** was 70% to the concept development, design of experiments, experiment works, analysis and interpretation of data, drafting and revising the final submission; **Allan Manalo**, **Warna Karunasena**, **Weena Lokuge** were contributed to the concept development, design of experiments, experiment works, analysis and interpretation of data, drafting and providing important technical inputs by 15%, 10% and 5%, respectively.

- **Muttashar M**, Manalo A, Karunasena W, Lokuge W. "Prediction model for flexural behavior of pultruded composite beam assembly with concrete infill". Journal of Composites for Construction, (Under review, Submitted on 10 May 2017: IF: 2.5 and SNIP: 1.702).

*Ref. No.: CCENG-2202*

The overall contribution of **Majid Muttashar** was 75% to the concept development, design of experiments, experiment works, analysis and interpretation of data, drafting and revising the final submission; **Allan Manalo**, **Warna Karunasena**, **Weena Lokuge** were contributed to the concept development, design of experiments, experiment works, analysis and interpretation of data, drafting and providing important technical inputs by 15%, 5% and 5%, respectively.

# Table of Contents

Abstract .....	i
Certification of thesis .....	iii
Acknowledgements .....	iv
Statements of contributions .....	v
Table of Contents .....	vii
List of Figures .....	x
List of Tables .....	xi
Chapter 1:        INTRODUCTION .....	1
1.1    Research background and motivation .....	1
1.2    Research objectives.....	5
1.3    Scope and limitations .....	5
1.4    Outline of the thesis .....	6
Chapter 2:        LITERATURE REVIEW .....	10
2.1    Introduction.....	10
2.2    Applications of pultruded GFRP sections in civil engineering .....	11
2.4    Characterization of FRP composites.....	16
2.4.1    Theoretical method .....	16
2.4.2    Experimental methods .....	18
2.5    Instability and failure modes of GFRP beams .....	21
2.5.1    Lateral buckling.....	21
2.5.2    Local Buckling .....	22
2.5.3    Delamination and shear .....	24
2.6    Flexibility in design from assembled pultruded tubes.....	26

2.6.1	Hybrid profiles.....	26
2.6.2	Built up sections .....	27
2.7	Enhancement of strength, serviceability and ductility by filling GFRP tubes with concrete .....	28
2.8	Maintaining the lightweight characteristics of FRP materials .....	32
2.9	Theoretical modelling and capacity prediction .....	34
2.10	Summary.....	36
	<b>Chapter 3: Mechanical Properties of Full-Scale GFRP Tubes.....</b>	<b>38</b>
	Paper I: Behaviour of hollow pultruded GFRP square beams with different shear span-to-depth ratio.....	38
	<b>Chapter 4: Flexural Behaviour of Single Cell GFRP Beams .....</b>	<b>55</b>
	Paper II: Influence of infill concrete strength on the flexural behaviour of pultruded GFRP square beams .....	55
	<b>Chapter 5: Flexural Behaviour of Multi-Celled GFRP Beams .....</b>	<b>66</b>
	Paper III: Flexural behaviour of multi-celled GFRP composite beams with concrete infill; experimental and theoretical analysis.....	66
	<b>Chapter 6: Parametric Investigation on Multi-Celled GFRP Beams.....</b>	<b>80</b>
	Paper IV: Prediction model for flexural behaviour of composite beam assembly partially filled with concrete.....	80
	<b>Chapter 7: CONCLUSIONS and RECOMMENDATIONS .....</b>	<b>110</b>
7.1	Characterization of pultruded GFRP section properties.....	110
7.2	Behaviour of Single cell GFRP beams with concrete infill .....	112
7.3	Behaviour of multi-celled GFRP beams with concrete infill .....	113
7.4	Theoretical study and capacity prediction.....	114
7.5	Contributions of the study.....	116
7.6	Areas of the future research .....	116

List of References.....	118
Appendix A: CONFERENCE PRESENTATIONS .....	130
A.1    Conference Paper I: Flexural and axial behaviour of pultruded GFRP tubes filled with low strength concrete.....	130
A.2    Conference Paper II: Testing and characterization of pultruded glass fibre reinforced polymer (GFRP) beams.....	131
A.3    Conference Paper III: The effect of shear span-to-depth ratio on the failure mode and strength of pultruded GFRP beams.....	132
A.4    Conference Paper IV: Experimental investigation on the flexural behaviour of pultruded GFRP beams filled with different concrete strengths.	133
A.5    Conference Paper V: Behaviour of pultruded multi-celled GFRP hollow beams with low-strength concrete infill.....	134
A.6    Conference Paper VI: Flexural behaviour of glued GFRP tubes filled with concrete .....	135
Appendix B: GLASS FIBRE CONTENT INVESTIGATION.....	136
B.1    Burnout test.....	136
Appendix C: BEARING STRENGTH INVESTIGATION.....	138
C.1    Bearing test .....	138
Appendix D: DUCTILITY OF SINGLE AND MULTI-CELLED BEAMS .....	142
Appendix E: Copyright Information .....	146
E.1    Paper 1 Copyright Information: Behaviour of hollow pultruded GFRP square beams with different shear span-to-depth ratio .....	146
E.2    Paper II Copyright Information: Influence of infill concrete strength on the flexural behaviour of pultruded GFRP square beams .....	149
E.3    Paper III Copyright Information: Flexural behaviour of multi-celled GFRP composite beams with concrete infill; experimental and theoretical analysis.....	155

## List of Figures

Figure 1.1 Common problem of (a) timber (b) steel (c) concrete .....	1
Figure 2.1 Eyecatcher building (Keller 1999) .....	11
Figure 2.2 FRP cooling tower (Bank 2006a) .....	12
Figure 2.3 The all-FRP Lleish Footbridge, city of Lleida, Spain (Gand et al. 2013).....	13
Figure 2.4 Composite decking section footbridge in Aberfeldy, Scotland. (Stratford 2012) .....	13
Figure 2.5 Boardwalk bridge using pultruded FRP tubes by Wagners Composite Technologies Ltd, Australia ( <a href="http://www.compositesworld.com">http://www.compositesworld.com</a> ).....	14
Figure 2.6 Footbridge fabricated from pultruded FRP tubes, Port of Airlie, Australia ( <a href="http://www.wagners.com.au">http://www.wagners.com.au</a> ).....	14
Figure 2.7 FRP DWB girders on Dickey Creek Bridge (Hayes & Lesko 2007) .	15
Figure 2.8 Baoi Bridge in Mossman, Australia. ....	15
Figure 2.9 Levels of consideration and the corresponding types of analysis for composite materials (Kollár & Springer 2003).....	16
Figure 2.10 Principle coordinate axis of unidirectional lamina .....	17
Figure 2.11 Lateral-torsional buckling of an I-shaped pultruded profile (Correia et al. 2011).....	22
Figure 2.12 Local buckling of the compression flange of wide-flange pultruded section transversely loaded (Bank & Yin 1999).....	24
Figure 2.13 Final failure of the wide-flange pultruded section (Bank 2006a).....	24
Figure 2.14 Delamination failure of FRP bridge deck (Keller & Schollmayer 2004).....	26
Figure 2.15 Double web beam (DWB) cross-section: a) 8 inches beam (Hayes & Lesko 2007) b) 36 inches beam (Schniepp 2002).....	27

Figure 2.16 Proposed girder using pultruded section: a) (Keller et al. 2004), b) (Kemp 2008) and c) (Hejll et al. 2005).....	28
Figure 2.17 Existing Concrete filled GFRP tubes .....	31
Figure 2.18 Existing Hybrid FRP-concrete beam designs .....	34
Figure 2.19 Proposed design for a hybrid FRP-concrete beam .....	34
Figure B.1 Coupon samples.....	136
Figure B.2 the orientation of the glass fibre .....	137
Figure C.1 shear test set-up .....	139
Figure C.2 Actual illustration of Bearing test set-up .....	140
Figure C.3 Failure mode of a) hollow beam and b) filled beam.....	140
Figure C.4 Load-displacement curves for hollow beams .....	141
Figure C.5 Load-displacement curves for filled beams .....	141
Figure D.1 Load – displacement behaviour of single cell GFRP hollow and filled beams.....	144
Figure D.2 Load – displacement behaviour of 2 cells GFRP hollow and filled beams.....	144
Figure D.3 Load - displacement behaviour of 3 cells GFRP hollow and filled beams.....	144
Figure D.4 Load - displacement behaviour of 4 cells GFRP hollow and filled beams.....	145

## List of Tables

Table B.1 Details of the sample for burnout test. ....	137
Table B. 2 Summary of the results of burnout test. ....	137
Table B. 3 Summary of the glass fibre content of each ply. ....	137
Table C.1 Summary of the results of coupon shear test .....	140

Table D.1 Summary of the experimental results for single and multi-celled GFRP beams..... 143

# Chapter 1:

## INTRODUCTION

### 1.1 Research background and motivation

Development in all aspects of life encourages engineers and scientists to search for new and better materials for building structures. However, for the construction industry this means faster, better, safer and cheaper structures. Therefore, the new materials have to provide longer life, less maintenance, and they have to withstand aggressive corrosive environments, which is due to the fact that deterioration of timber, corrosion of steel, degradation and marine borer (animals like shipworms) attack of concrete, as shown in Figure 1.1 are considered to be the greatest factors limiting the service life of the conventional materials. One of the best innovative materials considered as an attractive option to solve the abovementioned problems is fibre reinforced polymers (FRP) composites.



Figure 1.1 Common problem of (a) timber (b) steel (c) concrete

In the last decade, FRP profiles have become more accepted in civil construction applications. The innovation of the FRP composites started during the Second World War to cater for the need of the defence sector for Radomes (a dome or other structure protecting radar equipment) (Hollaway 2010). Since then, a significant improvement in their quality, and noticeable cost reductions of using FRPs in different applications, have been achieved. The innovation of pultrusion technology in addition to the advancements in specific resins, catalysts and accelerators represent the potential elements of the fundamental development of glass fibre reinforced polymer composites (GFRP) in the building and

construction industries. This technology, in fact, gives both the manufacturer and the designer opportunities to produce structures with different shapes and forms, and in addition to the tolerability of composite materials, this means they can have higher strength in some parts of the structure (Nordin & Täljsten 2004).

There is a great potential to utilize fibre reinforced composites and, in general, glass fibre reinforced polymer pultruded sections in civil engineering structural applications due to its many unique advantages. However, if these materials are to be used effectively, complete information on their physical and mechanical properties as well as a detailed understanding of their structural performance under loading are critical. While a number of theoretical equations have been developed to estimate the mechanical properties of pultruded composite profiles (Barbero et al. 1991; Nagaraj & GangaRao 1997; Omidvar 1998), these models require accurate information on the processing details, such as the properties of fibre and resin, the volume fraction of the fibre, and the composition of the laminate, which, most of the time, is not available. Moreover, several researchers (Davalos et al. 1996; Manalo et al. 2012; Roberts & Masri 2003) have indicated that the results from a theoretical evaluation may not always agree with experimental values since the fibres themselves exhibit some degree of anisotropy, and fibre properties are very sensitive to fabrication conditions. Therefore, it is generally preferred to determine the material properties of pultruded FRP sections experimentally and not to rely only on theoretical models. These tests should be designed to accurately account for the complex internal structure of the composite and/or the variation of the mechanical properties within the element, to achieve realistic design properties. While several standards suggest determining the mechanical properties from tests using coupons specimens, full-scale testing is recommended to obtain the effective flexural and shear rigidities of an FRP composites section, which in turn are very important in the design and performance evaluation.

In most applications, the design of structures utilising GFRP composite materials is governed by deflection and buckling limitations instead of strength, due to their relatively low elastic modulus and thin-walled section (Ascione et al. 2013a; Neto & Rovere 2007). Thus, several researchers have filled the FRP profile with

concrete to create a stiffer structure. The FRP tubes, in this system, provide a corrosion resistant element, lateral and longitudinal reinforcement, and lightweight permanent formworks, in addition to confining the inner concrete core. On the other hand, the concrete core prevents the local buckling failure of the section. The effectiveness of this system as compressive members has been demonstrated by several researchers (Abouzied & Masmoudi 2013; Idris & Ozbakkaloglu 2013; Mohamed & Masmoudi 2008; Mohamed & Masmoudi 2010c; Teng et al. 2007; Vincent & Ozbakkaloglu 2013; Zhu et al. 2006) with some studies conducted to investigate its application as flexural members (Fam et al. 2003; Fam, Schnerch, et al. 2005; Fam & Skutezky 2006; Mohamed & Masmoudi 2010b, 2010a). In those studies, the concrete was utilised to fill the composite section completely in order to improve stiffness and capacity. In addition, most of the research has focused on using high compressive strength concrete infill. However, the cost of high strength concrete infill does not justify the enhancement in the stiffness and the strength capacities of the GFRP infilled beams. Therefore, there is a need to investigate the performance of GFRP section filling with different concrete types, including low compressive strength concrete, with a view to determine an optimal concrete filling for GFRP tubes.

The light weight of FRP composites is a key advantage in the replacement work of bridge girders that no longer meet today's requirements, without creating additional load on the existing piers. Many researchers have proven that concrete infill stabilizes the thin-walled sections of FRP pultrusions (Fam et al. 2003; Fam & Rizkalla 2002; Mohamed & Masmoudi 2010a). However, filling the composite section completely with concrete is not optimal for applications governed by bending due to formation of tensile cracking of the concrete, which makes a negligible contribution to its bending resistance. Moreover, this method diminishes the lightweight characteristics of FRP sections. As a result, a number of researchers has created a void in filled concrete near the tensile zone to reduce the excess weight (Fam et al. 2003; Fam, Schnerch, et al. 2005). Their results indicated that providing a concentric void using a GFRP hollow tube improved the strength by 7% more than that of a fully-filled beam. Furthermore, the strength increased by 39% compared with a fully-filled beam when the inner

GFRP hollow tube was shifted towards the tension side. This idea was further extended by Idris and Ozbakkaloglu (2014) when they investigated the flexural behaviour of a double skin tubular beam, which consists of an FRP – high strength concrete – steel section. Their results showed that the composite beam exhibited excellent flexural behaviour with a high inelastic deformation. However, due to the high cost of the manufacturing die, pultruded GFRP tubes are produced in specific cross-section dimensions only. As a result, these sections are not applicable for use in high load applications nor do they comply with the serviceability requirements. Thus, a number of pultruded GFRP sections can be assembled by gluing them together appropriately to produce a larger structural section.

Several studies have developed a number of theoretical models to predict the behaviour of FRP composite beams. These studies employed Classical Lamination Theory (CLT) together with Fibre Model Analysis (FMA), which is based on strain compatibility and force equilibrium to predict the moment capacity and load-deflection behaviour of composite beams (Davalos et al. 1996; Davol et al. 2001; Fam, Mandal, et al. 2005; Mohamed & Masmoudi 2010a; Nagaraj & GangaRao 1997). However, these models ignore the effect of the shear deformation and premature local buckling failure, both of which have a significant effect on the actual behaviour of the composite beam. Thus, it is important to develop a general theoretical model capable of predicting the flexural behaviour of single and multi-celled pultruded GFRP hollow and filled sections.

In this study, a proper method of characterizing the mechanical properties of a full-scale pultruded glass fibre reinforced polymer (GFRP) composites section was determined. These pultruded beams were then filled with concrete with different compressive strengths to determine the effect of concrete filling on the structural behaviour, and to identify a practical concrete filling for GFRP tubes. A number of the GFRP tubes were glued together, and termed “multi-celled GFRP beams”, to evaluate the effect of filling the top cell with concrete on the strength, the failure mode and the stiffness of the beams. A simplified model, accounting for the compressive buckling and shear stresses in GFRP beams, was

also proposed. A parametric investigation to evaluate the effect of the number of cells, shear span-to-depth ( $a/d$ ) ratio, and number of cells to be filled in the “multi-celled GFRP beams”, was also conducted. The results of these studies provide a more detailed understanding of the behaviour of pultruded GFRP sections, thereby enabling their effective usage in construction and civil engineering applications.

## 1.2 Research objectives

The main objective of this study is to evaluate the structural behaviour of multi-celled composite beams made by gluing a number of pultruded GFRP sections, and filled with concrete, through experimental and theoretical investigations. The specific objectives are the following:

1. To evaluate a suitable test method for characterisation of the mechanical properties of full-scale GFRP tubes;
2. To study the effect of compressive strength of concrete infill on the flexural behaviour of pultruded GFRP beams;
3. To investigate the flexural behaviour of multi-celled GFRP beams with concrete infill; and
4. To develop a simplified theoretical model for predicting the flexural behaviour of multi-celled GFRP beams with concrete infill.

## 1.3 Scope and limitations

The study focused on understanding the flexural behaviour of multi-celled GFRP composite beams under a four-point bending test. The composite beams were made from pultruded GFRP square sections (125 mm x 125 mm x 6.5 mm thickness) manufactured by using E-glass fibre reinforcement and vinyl ester resin. The study included experimental and theoretical investigations associated with the proposed multi-celled GFRP filled beam. The scope of the study is summarised below:

- a. The elastic properties of GFRP tubes were evaluated, using full scale beam with different shear span to depth ratios ( $a/d$ ), and tested under four-point bending. In addition, understanding the behaviour of hollow pultruded

GFRP beams at different  $a/d$  ratio was necessary to identify possible failure modes that would hinder the full utilisation of these profiles.

- b. The feasibility of using low strength concrete as a practical infill for the pultruded GFRP tubes, in order to produce a durable, strong and stiff structural beam, was assessed. Five single cell beams and six multi-celled beams were tested under four-point static bending. The tests were used to investigate the effect of concrete strength on the flexural behaviour of GFRP beams.
- c. The performance of the multi-celled GFRP beams was evaluated to identify the possible mode of failure of the bonded beams. The experimental program was designed to investigate the effect of the number of cells and concrete filling on the flexural behaviour of multi-celled beams.

A simplified theoretical model was developed to predict the failure load of the single and multi-celled GFRP beams with and without concrete infill. The model used was based on the maximum stress method, accounting for the combined effect of shear and flexural stresses. The model was then used to predict the failure load of beams with different numbers of cells, shear span-to-depth ( $a/d$ ) ratios and number of cells filled.

#### 1.4 Outline of the thesis

This thesis consists of seven main chapters including this introduction, which presents the research significance, scope and the objectives of the research project.

**Chapter 2** presents the background information on FRP composite in general. In addition, it includes a critical review of the literature concerning the previous work done on the pultruded GFRP tubes, which reports on the available characterisation methods, the use of GFRP tubes, the possible failure mode, the flexibility of assembling GFRP tubes, and the available analytical methods.

**Chapters 3 to 6** present four major studies, which address the specific objectives. The results of each study were presented and published in high quality journals. The details of these manuscripts are listed below:

- **Paper I: Muttashar M**, Karunasena W, Manalo A, Lokuge W. (2016). Behaviour of hollow pultruded GFRP square beams with different shear span-to-depth ratios. *Journal of Composite Materials*. Vol.50, Issue 21, pp. 2925-2940. (IF:1.24, SINP:1.17)
- **Paper II: Muttashar M**, Manalo A, Karunasena W, Lokuge W. (2016). Influence of infill concrete strength on the flexural behaviour of pultruded GFRP square beams. *Composite Structures*. Vol.145, pp. 58-67. (IF:3.318, SINP:2.48)
- **Paper III: Muttashar M**, Manalo A, Karunasena W, Lokuge W. (2017). Flexural behaviour of multi-celled GFRP composite beams with concrete infill: Experiment and theoretical analysis. *Composite Structures*. Vol. 159, pp. 21-33. (IF:3.385, SINP:2.12)
- **Paper IV: Muttashar M**, Manalo A, Karunasena W, Lokuge W. Prediction model for flexural behavior of pultruded composite beam assembly with concrete infill. *Journal of Composites for Construction*, (Under review, Submitted on 10 May 2017: IF: 2.5 and SINP: 1.702).

*Ref. No.: CCENG-2202.*

In addition to the listed journals, the major outcomes of this research were presented in related national and international conferences, which are summarised in *Appendix A*. the copyright information of the published articles are given in *Appendix D*.

**The first specific objective** of this study is to evaluate proper experimental methods to characterize the mechanical properties of GFRP tubes, which has successfully been accomplished and the outcomes were presented in *Paper I*. The elastic material properties were determined by conducting a full-scale test of pultruded GFRP sections with different shear span-to-depth ( $a/d$ ) ratios under four-point bending. Two analysis techniques, using the graphical (simultaneous) and back calculation methods, were employed to evaluate the elastic properties and compare them with the results of the coupon test. The beams were tested up to failure to determine their capacity and failure modes. The effect of shear was analysed considering different  $a/d$  ratios. The measured bending and shear

modulus from the full-scale test was found reliable, and in *Papers II to IV* it was found that it can predict accurately the behaviour of GFRP sections. Furthermore, the results suggested that the flexural behaviour of hollow GFRP beams is highly affected by the premature local failure of the compression flange, which can be prevented by concrete infill. Thus, the beams were filled with concrete and their behaviour was evaluated in *Paper II*.

*Paper II* also addressed **the second specific objective** of the study. The paper presents the effect of the infill concrete strength on the flexural behaviour of GFRP beams. Hollow and filled beams were tested under four-point bending until failure. The load-deflection behaviour, strain response, and failure mode of the beams were examined. The behaviour of filled beams was then compared with their hollow counterparts in order to evaluate the effect of concrete filling on their strength and stiffness. The results of this study show that using low strength concrete as infill materials for GFRP tube is an effective and practical solution to improve the strength and stiffness of the filled beams. The results also highlight that due to the tension cracking of the concrete, filling the entire beams section with concrete is not optimal for applications governed by bending. In addition, this concept diminishes the lightweight characteristics of GFRP composites. This then led to a question about the suitable concept of combining GFRP tubes and concrete to produce a beam, developing good flexural properties and maintaining lightweight characteristics of GFRP composites. The available concepts are reviewed in *Paper III* and a combined section is proposed.

**The third specific objective**, the flexural behaviour of multi-celled composite beams filled with concrete, is achieved in *Paper III*. Initially, the effect of gluing the GFRP tubes together was determined. Then, the effect of filling the section with concrete was studied. The flexural behaviour and the failure mode were thoroughly investigated. The effect of the number of cells, partial filling, and concrete compressive strength were discussed. The results of the extensive experimental program have demonstrated that gluing the GFRP tubes improved the flexural performance of the sections. In addition, filling the section with concrete at the top-most tube prevented the local failure of the section and effectively increased its strength and stiffness. The study identified several

factors affecting the overall behaviour of multi-celled beams, which are presented in *Paper IV*.

**The last and fourth specific objective** of this study is to develop a general theoretical model to predict the behaviour of single and multi-celled GFRP beams, which has been successfully addressed in *Paper IV*. The theoretical model to predict the failure behaviour and failure load single and multi-celled beams, which was developed in *Papers I to III*, was generalised to account for the effects of different  $a/d$  ratios, filling percentages, and the number of filled cells. The model was verified using the available experimental results in the literature and showed a very good agreement. It was determined that the failure of single cell beams are governed by combined shear and bending, while the multi-celled beams failed due to bearing. Similarly, the behaviour of multi-celled beams filled with concrete is governed by either the bearing failure of hollow cells under the concrete-filled cells, or web buckling of the top-filled cell. Furthermore, filling the top cell only with concrete is more effective for the structure application, in terms of increase in the strength-to-weight ratio and stiffness-to-weight ratio of the partially filled beams.

**Chapter 7** presents the conclusion that summarizes the main findings of the study and suggests recommendations for future work.

## **Chapter 2:**

### **LITERATURE REVIEW**

#### **2.1 Introduction**

Fibre reinforced polymer (FRP) composite materials are mainly made from a combination of fibres and polymers (matrix). The fibre is the load carrying element, which controls the stiffness and strength characteristics of the composite materials. The matrix on the other hand, protects and supports the fibres as well as transfers the local stresses from one fibre to another. Since 1940, FRP composite materials have been developed for use in the defence and aerospace sectors due to their advanced properties (Alampalli et al. 1999). In the mid-1980s, the desire by engineers to use FRP composites as structural materials started due to a need for durable, high strength, lightweight, and high stiffness materials, which could replace the more conventional materials in different environments (Hollaway 2010). As the need for aggressive infrastructure renewal became increasingly evident in the developed world, the pultrusion method was recognized as an effective production technique to manufacture different types of FRP structural shapes (Hollaway 2010). This manufacturing method produced FRP materials for the construction of new infrastructure, or for rehabilitation and replacement of existing structures, at a more reasonable cost.

This chapter gives an overview of the existing applications of GFRP composite in the construction industry. It also reviews the available characterization methods with the aim of finding a suitable method to determine the mechanical properties of GFRP profiles. This chapter further presents important information about the available concepts to overcome the challenges related to the premature failure of GFRP composite tubes. Moreover, it highlights the need for maintaining the lightweight characteristics of FRP composites. Finally, the research on the available analytical models, used to predict the behaviour of the GFRP composite beams, is reviewed and the necessary background is provided on the need to develop a general analytical model.

## 2.2 Applications of pultruded GFRP sections in civil engineering

FRP composite materials have been used effectively in structural engineering applications (Gand et al. 2013). In the early 1980s, the magnetically neutral properties were the key factor in the use of FRP profiles in the computer and electronics industry for Electromagnetic Interference (EMI) test laboratories. A single-story gable frame building was constructed in Virginia, USA, which is considered as the first large structure constructed from FRP composites (Bank 2006b). In 1999, a Swiss composite company called Fiberline Composite constructed a prototype multi-storey frame building, named the Eyecatcher building, which is shown in Figure 2.1. The construction of this building confirmed the potential use of FRP profile shapes in the construction industry (Keller 1999). Another important development in using FRP profiles in building systems was in the cooling tower industry. In the 1980s, Composite Technology Inc. developed an FRP building system for Ceramic Cooling Tower (CCT) and commercialized it as the unilite system (Bank 2006b). This system consisted of a variety of unique FRP pultruded components such as beams, columns, and panels, as shown in Figure 2.2.



Figure 2.1 Eyecatcher building (Keller 1999)



Figure 2.2 FRP cooling tower (Bank 2006a)

In the field of bridge engineering, the light weight and corrosion resistance of the FRP components make them more attractive as bridge elements. Due to these superior properties, in addition to their ease of fabrication and installation, many pedestrian FRP bridges were constructed in less accessible and environmentally restrictive areas without having to use heavy equipment (Hollaway 2010). The Lleida footbridge, which was constructed near Lleida in Spain, as shown in Figure 2.3, utilized all FRP elements (Gand et al. 2013). This pedestrian bridge was constructed on a 38 metre span and consisted of a double-tied arch made of a rectangular hollow FRP cross-section. In 1992, the first cable-stayed pedestrian bridge was developed in the UK and was constructed in Aberfeldy, Scotland, as shown in Figure 2.4. GFRP decks and a tower, as well as the aramid cables, were the main structural components of the bridge. The durability performance of the bridge over 20 years of service has been very satisfactory (Stratford 2012). In 1997, another cable-stayed pedestrian bridge with a span of 40.3 metres was constructed across a railway line, using all FRP profiles, in Kolding, Denmark (Bank 2006b). The use of FRP shapes in the construction of those bridges has enabled rapid and economical construction. A completed boardwalk project was constructed using pultruded FRP tubes by an Australian manufacturer, Wagners Composite Technologies Ltd, as shown in Figure 2.5. The boardwalk was installed in Brisbane, Australia. Considering their long life span, low maintenance, and quick and easy installation, Wagners have supplied FRP pedestrian bridges all across Australia. Figure 2.6 shows a footbridge fabricated

from pultruded FRP tubes and installed at the Port of Airlie, Queensland, in 2012.



Figure 2.3 The all-FRP Leigh Footbridge, city of Lleida, Spain (Gand et al. 2013)



Figure 2.4 Composite decking section footbridge in Aberfeldy, Scotland. (Stratford 2012)



Figure 2.5 Boardwalk bridge using pultruded FRP tubes by Wagners Composite Technologies Ltd, Australia (<http://www.compositesworld.com>)



Figure 2.6 Footbridge fabricated from pultruded FRP tubes, Port of Airlie, Australia (<http://www.wagners.com.au>)

Since 1990, a number of FRP manufacturers have attempted to develop an FRP bridge deck system (Bank 2006b). A decrease in dead weight is considered to be the main advantage of using an FRP bridge deck system to replace a deteriorated reinforced concrete deck. Thus, the live load capacity for the replaced structure can be increased. In 2001, the Strongwell Corporation, Virginia, developed an FRP pultruded deep double web beam (DWB) to be used in bridge construction, as shown in Figure 2.7 (Hayes & Lesko 2007). The beam was composed of E-glass and carbon fibre in a vinyl ester resin. The FRP beams were also used to replace timber beams in a rehabilitation project on Tom's Creek Bridge in Blacksburg. In 2013, Wagners Composite Technologies Ltd built the Baoi

Bridge in Mossman, Australia, which was considered to be the largest full composite bridge in Australia (Figure 2.8). The span of the bridge is 35 metres with a width of 7 metres; the bridge is a fully supported composite structure, which was designed to carry an axial load of heavily-laden cane trucks and agricultural equipment.

In the design and construction of the abovementioned composite structures, the importance of having a detailed understanding of mechanical properties of FRP materials was highlighted. In the next section, the available methods to determine the mechanical properties of FRP composites are evaluated.



Figure 2.7 FRP DWB girders on Dickey Creek Bridge (Hayes & Lesko 2007)



Figure 2.8 Baii Bridge in Mossman, Australia.

## 2.4 Characterization of FRP composites

Complete information on the mechanical properties of FRP material is important for the safe and reliable design of composite structures. Basically, there are two methods to determine the mechanical properties of an FRP composite. The first is the theoretical method, which depends on the individual properties of the matrix and the fibres. The second is the experimental method that takes into account the overall composite behaviour of the FRP. In both methods, one of four levels can be used to characterize an FRP composite material. These levels are: (1) fibre level, (2) lamina level, (3) laminate level, and (4) structure level, as shown in Figure 2.9. The common methods of characterising the mechanical properties of FRP composites are presented in detail in the sections that follow.

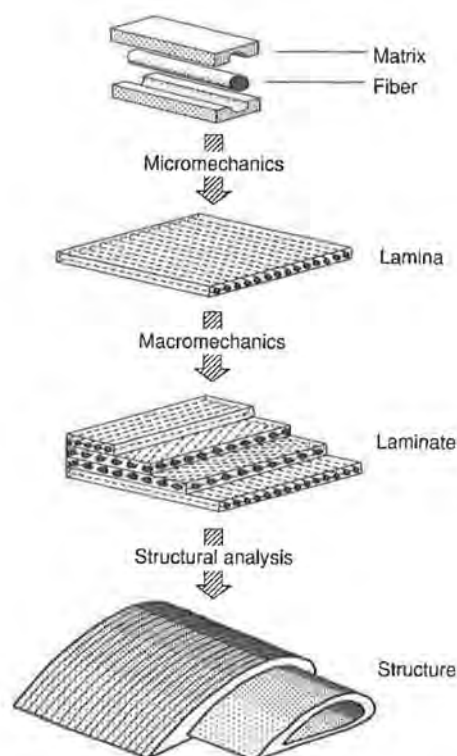


Figure 2.9 Levels of consideration and the corresponding types of analysis for composite materials (Kollár & Springer 2003)

### 2.4.1 Theoretical method

The mechanical properties of FRP composites can be theoretically predicted from the properties of its constituent materials. The physical and mechanical properties

of the composite are strongly influenced by the amount and properties of the fibres and the matrix. The first level of analysis is called the fibre level, also known as Micromechanics. It deals with the state of deformation and stress of the constituents and the interactions between them. In the micromechanics model it is assumed that the fibre and the matrix are made up of homogeneous, isotropic and linear elastic material. The micromechanical level of analysis is important in the study of failure mechanisms, strength and fracture toughness. It is also used to predict the behaviour at the lamina level as a function of constituent properties. The accuracy of using the fibre level to predict the properties of an FRP composite highly depends on the mechanical properties of the fibre and matrix constituents. However, there is no standard format for providing suitable property data of these materials (Bank 2006b)

A lamina is a single ply of a planar FRP composite in which the fibres are aligned in one direction in a matrix. It is also called a unidirectional ply. It is considered to be orthotropic material with its principal material axis defined as 1, 2, and 3, as shown in Figure 2.10. The composite in this level is considered homogenous and anisotropic material where average properties are used in the analysis. This type of analysis is called macro-mechanics level analysis. At this level of analysis, the unidirectional ply is assumed to be a two-dimensional plate with very small thickness compared with its in-plane dimension. In characterizing the behaviour of FRP composites, unidirectional ply plays a key role because it represents the basic building block to calculate the properties of laminate (a stack of lamina).

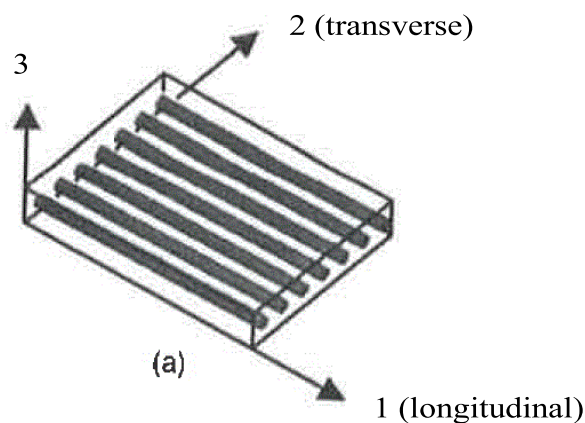


Figure 2.10 Principle coordinate axis of unidirectional lamina

Composite materials are constructed from a stack of arbitrary oriented lamina to form multidirectional laminate. At the laminate level of analysis, the laminate is designated in a manner representing the number, type, orientation, and stacking sequence of the ply. The behaviour of multidirectional laminate totally depends on the properties and the stacking sequence of its individual layers. The so-called classical laminate theory (Bert 1989) is used as a first approximation to predict the behaviour of the laminate.

In analysing a structural level, several studies were conducted to develop micromechanical simulations to predict the flexural and shear modulus properties of full-scale pultruded beams (Barbero et al. 1991; Nagaraj & GangaRao 1997; Omidvar 1998). Similarly, Davalos et al. (1996) conducted a comprehensive analytical program for the analysis of pultruded FRP shapes under bending. They developed a computer program to carry out the analysis of FRP beams from the evaluation of ply stiffness through micromechanics, to the overall member response through the mechanics of laminated beam model. These researchers have highlighted that the accuracy of the theoretical models depends mainly on the individual properties of fibres and resin, the fibre volume fractions, and the composition of laminates (Bank 2006b). However, the distortional effects such as shear-leg, warping, and buckling, which are particularly important for the design of thin-walled FRP sections, most of the time cannot be predicted accurately through theoretical evaluation. Numerous researchers have therefore focused on developing effective experimental methods to accurately determine the mechanical properties of the composite materials and to capture the complex behaviour of composite materials

#### **2.4.2 Experimental methods**

Many experimental methods have been developed to accurately determine the properties of composite materials due to the complexity of the failure mode of FRP profiles. The material characterisation can be conducted using coupon or full-scale specimens, which are discussed in the next sections.

#### *2.4.2.1 Coupon test*

Coupon specimens are normally cut from the fabricated FRP composites part. Both lamina and laminate levels can be evaluated through coupon tests, using small specimens cut from various directions of the FRP profiles. Several researchers have conducted experimental investigations using coupon specimens to determine the mechanical properties of composite materials (Davalos et al. 1996; Roberts & Masri 2003). The results show that the flexural and torsional properties can be determined using coupon test; however, the results were significantly influenced by localised deformation at the supports. Although a number of standard tests were developed based on coupon specimens, several important stiffness and strength properties, such as tensile strength, shear strength, and rotational strength of web-flange junction have to be determined without recourse to standardized test methods (Bai 2013). The implementation of non-standardized methods in characterizing the properties of FRP composites results from the effect of the failure mode of these materials, especially for FRP profiles. The final failure is generally governed by localized cracking and/or separation of one or both flanges from the web. Furthermore, there are limited test methods and equipment to determine the properties of thick composites using coupon tests (Manalo et al. 2012). Due to the limitations in the transverse direction dimension of the common FRP composite profiles, many of the available test standards are not applicable for determining their properties (Cardoso et al. 2014). Due to the fact that the design of pultruded profiles are often controlled by serviceability and buckling limitations, the bending, transverse shear, and torsional rigidity of the full section are required in the design. While these properties can be predicted using theoretical methods, this involves many assumptions relating to the geometry of the profiles, homogeneity and anisotropy. These assumptions generally result in an underestimation of the mechanical properties of the FRP composites. Thus, full-section testing is a preferred method to determine effective properties of FRP profiles.

#### *2.4.2.2 Full scale test*

Small scale coupon tests, using samples fabricated under laboratory conditions, cannot predict the structural behaviour of large scale FRP composite elements

reliably. Furthermore, the strength and stiffness properties of FRP materials are location-dependent within the cross section, due to the heterogeneity and anisotropy characteristics of composite materials. In addition, the complex internal structure and/or the variation of the mechanical properties of FRP composites within the element itself result in a complicated design process of these materials (Muttashar et al. 2015).

One major feature of composite materials, which affects its structural behaviour is its relatively low elastic modulus. Similarly, the low shear modulus of FRP composites results in an increased shear deformation as a percentage of the total deformation, which cannot be captured from coupon tests. Thus, several researchers (Bank 1989; Nagaraj & GangaRao 1997) have used full-scale pultruded FRP beams to account for the shear deformation on the overall bending stiffness. Consequently, they developed standard tests to determine the flexural and shear rigidities. By using full-scale testing, some researchers (Bank 1987; Omidvar 1998) studied the shear coefficient of thin-walled FRP beams, while others (Bank et al. 1995; Barbero & Raftoyiannis 1993; Davalos & Qiao 1997; Mottram 1992; Turvey 1996; Zureick & Scott 1997) have reported that flexural buckling, flexural-torsional buckling, lateral buckling, and local buckling are the main modes of failure of FRP pultruded profiles.

Three or four-point bending tests are the most widely used full-section tests whereby the effective longitudinal modulus is determined from load and mid-span displacement data. Guades et al. (2014) conducted an experimental investigation to determine the mechanical properties of pultruded GFRP sections using coupon and full-section data. They reported that the results from coupon tests are relatively higher than full scale results, regardless of the type of test. They concluded that local buckling of the thin wall and the shear deformation might be the reason for these differences. Bank (1989) and Neto and Rovere (2007) conducted experimental test using different span-to-depth ratios and measured the bending rigidity (EI) and the shear rigidity (GA) of a profile section simultaneously. They concluded that to minimize the effects of the shear deformation, the shear span-to-depth ratio should be at least 20 for the tested beams. The simultaneous method that was developed by those authors has since

been used by a number of researchers and has become an important method to obtain the required properties that can be used in the design. These studies have highlighted that the determination of the accurate mechanical properties of the FRP materials is critical to the effective design and widespread use of these materials in civil engineering and construction.

## **2.5 Instability and failure modes of GFRP beams**

A detailed understanding of the different failure modes of pultruded GFRP profiles is important for their effective usage in civil infrastructure and construction. This section reviews common failure modes of GFRP sections

### **2.5.1 Lateral buckling**

The low in-plane modulus and thin-walled geometry of conventional pultruded GFRP profiles make these composites susceptible to lateral and local buckling. In terms of lateral buckling, the stability becomes a main concern due to its slenderness (Lee 2006). The lateral buckling of composite beams has been demonstrated in numerous studies (Ascione et al. 2011; Kabir & Sherbourne 1998; Lee 2006; Lee et al. 2002; Lin et al. 1996; Lofrano et al. 2013; Sherbourne & Kabir 1995). This type of failure commonly occurs in open-section flexural members, loaded by transverse loads. This failure occurs when the section reaches its critical lateral-torsional buckling load, which results in the flange displacing laterally, relative to the transverse load direction that twists the web, causing the entire beam to move out of its vertical plane, as shown in Figure 2.11. Kabir and Sherbourne (1998) conducted an analytical study on the lateral-torsional buckling of an I section of composite beams, using the Rayleigh-Ritz method. They also studied the effect of shear strain on the lateral stability of thin-walled composite beams (Sherbourne & Kabir 1995). They concluded that for a slender beam section, under transverse loading, the failure modes approach to interactive buckling would result in elastic behaviour with a sudden drop in the section capacity. In addition, they mentioned that the shear strain had a remarkable influence on reducing the lateral stability strength for short spans. Lin et al. (1996) developed a finite element program for the buckling analysis of thin-walled pultruded FRP structural members. They concluded that the buckling load

for members subjected to transverse load and/or bending moment was significantly affected by the shear strain, if the buckling mode was lateral buckling. Lofrano et al. (2013) performed a numerical investigation on the stability of open thin-walled composite beams. They reported that the proposed numerical technique was able to investigate the stability of these sections. Lee et al. (2002) and Lee (2006) developed a one-dimensional finite element model to study the lateral buckling for an I section. They reported that the lateral buckling capacity of the beams is significantly affected by the span-to-height ratio and the location of the applied load, as well as the fibre orientation. The results show that the lateral-torsional effect was increased by 170% with the decrease of span-to-height ratio, which might result in an ineffective utilisation of the design capacity of the composite materials. All reported literature highlighted the effect of lateral buckling on the capacity of thin-walled composites with open cross sections. However, they mentioned that torsional resistance of a closed cross section tube is much higher than that of an opened section, which results in the lateral-torsional buckling not likely being a critical issue for a composite tube.



Figure 2.11 Lateral-torsional buckling of an I-shaped pultruded profile (Correia et al. 2011)

### 2.5.2 Local Buckling

The effect of local buckling plays an important role in the design of thin-walled FRP composite members. Several experimental studies on this topic have demonstrated a reasonable influence of local buckling on the failure load (Barbero & Raftoyiannis 1993; Pecce & Cosenza 2000; Turvey & Zhang 2006). The results of these research studies have shown that the separation of the

compression flange from the web, once the compression flange buckled elastically, is the typical mode of failure in pultruded I beams and box sections. This type of failure is the main reason for bending, and combined shear and bending, failures. Because of the local buckling failure, GFRP beams show limited ductility behaviour which results in brittle failure. Figure 2.12 shows the local buckling of the compression flange of a wide-flange pultruded section under a transverse load (Bank & Yin 1999). This buckling is then followed immediately by in-plane buckling of the thin-unsupported web, which results in the final failure of the section, as shown in Figure 2.13 (Bank 2006b). Mottram (1991) conducted experimental work on 23 pultruded box sections under three point bending with different spans. Two modes of failure were reported in his study. For long-span sections, which a span-to-depth ratio of above 17.7, compression flange buckling (bending failure) was found to be the ultimate mode of failure. Consequently, by assuming this mode as the final mode of failure, the predicted ultimate bending load for the beams was close to the experimental load. On the other hand, for short span beams with a span-to-depth ratio of less than 11.9, the experimental results indicated that the bearing area of the applied load's nose into the fibre reinforced composite had an important effect on the resistance and mode of failure of short-span box beams.

To gain a complete understanding of the structural behaviour of pultruded profiles, and considering the buckling failure as one of the main modes of failure, analytical methods were developed to predict the buckling capacity of FRP composite sections (Ascione et al. 2013a, 2013b; Bank & Yin 1999; Bank et al. 1995; Kollár 2003; Pecce & Cosenza 2000). Bank et al. (1995) reported that the prediction of the local buckling loads in pultruded FRP beams, subjected to flexural loading, was affected by the non-linearity in the experimental data and by the anisotropic and inhomogeneous material properties of the beams. Ascione et al. (2013a), Ascione et al. (2013b) and Pecce and Cosenza (2000) concluded that shear deformability of the composite materials had a significant effect on the prediction of the local buckling load. Among all the analytical methods, Kollár (2003) proposed an approximation method to obtain closed-form equations for buckling of different pultruded profiles, including I, box, channel, and Z-shaped

sections. The results show very good agreement with test results of pultruded profiles and finite element analysis. Furthermore, Kollar's method has the capability to differentiate between flange buckling in beams subjected to flexural loads, and flange buckling in columns subjected to axial loads, due to the assumption of the web restraint, which is given as a function of the end condition of the restraining plate (Bank 2006b). In fact, due to local buckling failure, pultruded FRP profiles failed at 50% of their design capacities (Guades et al. 2014).

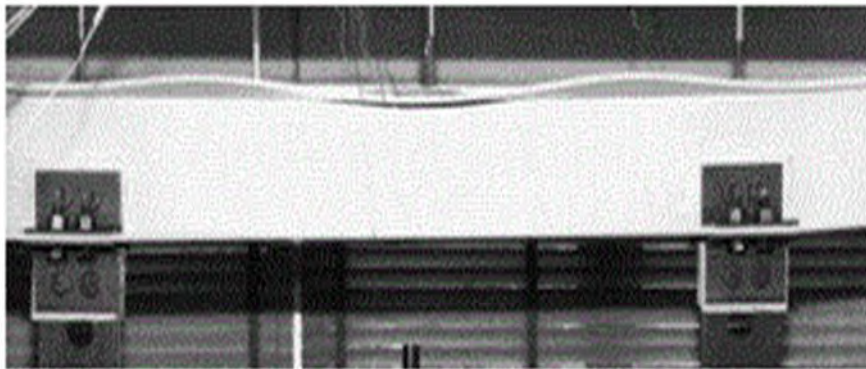


Figure 2.12 Local buckling of the compression flange of wide-flange pultruded section transversely loaded (Bank & Yin 1999)

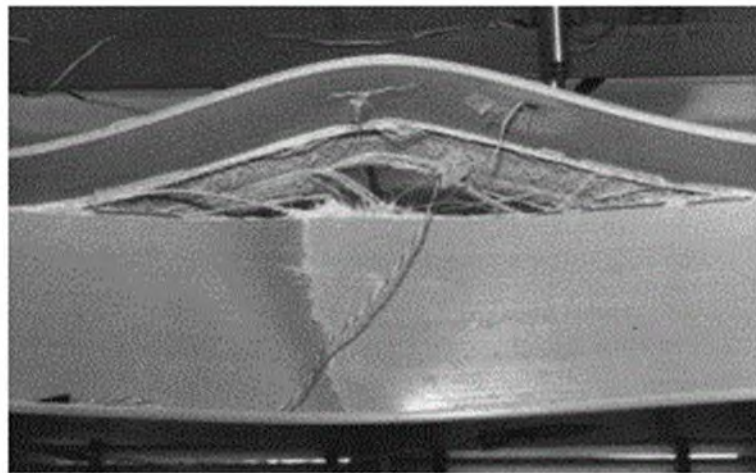


Figure 2.13 Final failure of the wide-flange pultruded section (Bank 2006a)

### 2.5.3 Delamination and shear

Bond, or composite action, between the fibres and the matrix is another factor affecting the mechanical performance of FRP composite materials. The debonding between the two plies of a laminated composite structure is known as delamination. Delamination occurs when the applied stresses exceed the inter-

laminar shear strength of the section, which is normally low for pultruded laminates (Bai et al. 2009). On the other hand, it might occur when the thin resin layer is subjected to extensive in-plane and out-of-plane stresses (Fenske & Vizzini 2001). An example of the delamination failure of an FRP bridge deck is shown in Figure 2.14 (Keller & Schollmayer 2004). Due to large deformation, shear has a significant effect on the delamination failure (Bai et al. 2009). Turvey and Zhang (2006) conducted an experimental investigation on the shear failure strength of glass reinforced polymer wide flange (GRP WF) profiles. They reported that the shear strength at the web-flange junction is only one-seventh of the shear strength of web or flange material. As a result, they concluded that failure often occurs at the web-flange junction due to shear and delamination. Furthermore, shear failure occurred first in the central roving layer along the length of the section prior to the buckling of the profile. Bai and Keller (2009), on the other hand, conducted a theoretical investigation to analyse the geometric and mechanical conditions for pultruded GFRP profiles subjected to axial compression, which could lead to shear failure prior to compression failure. It was found that shear failure can occur prior to compression failure in a pultruded GFRP profile subjected to compression, due to a low shear-to-compression strength ratio. In this regard, different failure criteria were developed to predict the failure strength of FRP composites, such as Maximum Strain or Stress, the Tsai-Wu interaction, or Hashin Criteria (Fenske & Vizzini 2001). The maximum stress criterion suggests that delamination occurs when the maximum shear stress reaches the shear strength of the section (Bai et al. 2009). Fracture mechanics approaches were also used to describe the initiation of the delamination and its propagation (Marannano & Pasta 2007; Wang 1983; Wang & Zhang 2009; Zhang & Wang 2009). Hayes and Lesko (2007) conducted an experimental investigation to identify the failure mode of a full scale composite structural beam. They reported that even though the failure of the beam had the appearance of a delamination failure, the detailed analyses of their study did not confirm their hypothesized mode of failure. The results strongly suggested that compression failure in the top flange near a load patch was the main mode of failure. However, shear and delamination can reduce the flexural buckling load

by up to 10% (Roberts & Masri 2003). The critical analysis of the failure mode of FRP composites helps researchers and designers to propose new techniques to overcome these issues. Therefore, it is important to evaluate these techniques in order to validate their applicability as structural elements.

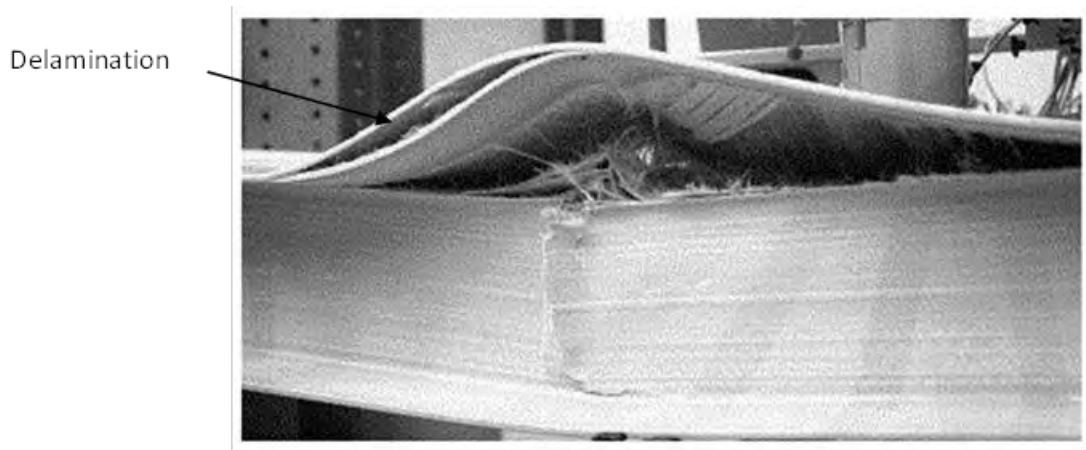


Figure 2.14 Delamination failure of FRP bridge deck (Keller & Schollmayer 2004)

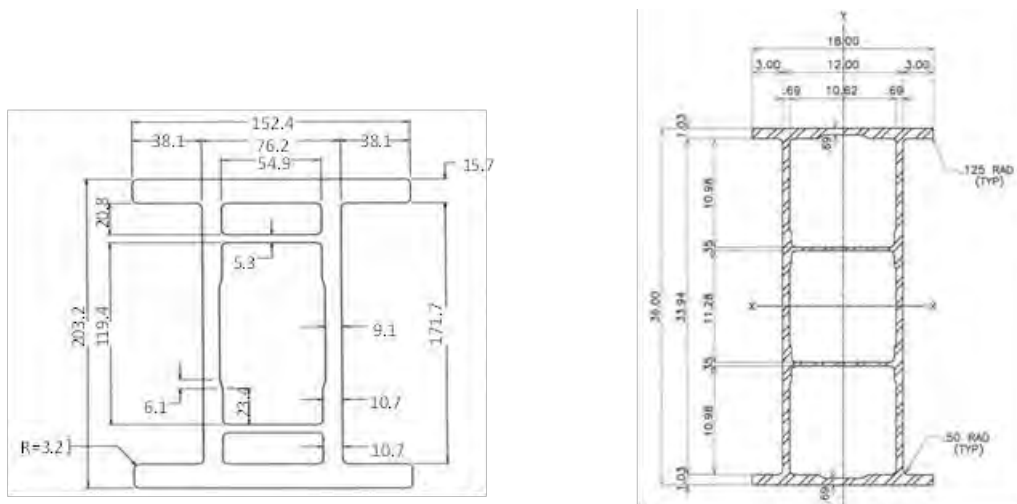
## 2.6 Flexibility in design from assembled pultruded tubes

Two different configurations were proposed, either in the form of one pultruded section (hybrid profile) or a combination of different pultruded sections, to improve the stiffness of the section but still keeping its light weight characteristics.

### 2.6.1 Hybrid profiles

A 200 mm double-web subscale prototype composite beam was manufactured by Strongwell and implemented in the rehabilitation of Tom's Creek Bridge, Virginia, as shown in Figure 2.15a (Hayes & Lesko 2007). Laboratory and field tests were conducted to examine the service load deflection, girder strain, load distribution, degree of composite action, and impact factor. The results indicated a service load deflection of  $L/400$  under moving loads, and a high factor of safety in the composite members against material failure. The results served as a baseline to develop a large double-web beam by the same company in 2002, as shown in Figure 2.15b (Schniepp 2002). Extensive testing and analysis were conducted at Virginia Tech. on the developed double-web beam (DWB) in order to use it in bridge construction. The main goal of this testing was to develop a structural design guide for the DWB. Bending modulus, shear stiffness, failure

mode, and ultimate capacity were the main outputs of the conducted tests. However, while the developed DWB showed good strength and stiffness, the compression failure mode of the carbon fibre plies in the top flange near the point of the applied load affected the design capacity of the beam.



a) All dimensions in mm

b) All dimensions in inches

Figure 2.15 Double web beam (DWB) cross-section: a) 8 inches beam (Hayes & Lesko 2007) b) 36 inches beam (Schniepp 2002)

## 2.6.2 Built up sections

Most of the composite manufacturers use industrialized processes to produce single units rather than continuous production processes. Several research studies have been conducted to bond the FRP composite parts, using epoxy resin adhesives to build up structural elements to be used in construction applications. Keller et al. (2004) conducted an investigation on beam girder, made of adhesively bonded pultruded fibre glass profiles and sandwich panels, as shown in Figure 2.16a. The experimental results showed that it was possible to produce a beam of 20 m length by using this design. The Wagners CFT company of Toowoomba/Australia developed an I-beam girder, using glass fibre composite (GFRP), in their effort to replace wooden bridge girders. Square pultruded profiles, plates, and pultruded angles were the main components of the beam's cross-section, as shown in Figure 2.16b (Kemp 2008). The girder was tested under a four-point flexural test. The test results showed that the failure moment was 20% higher than the required moment, but the stiffness was 7% less than

required. Again however, the local buckling failure of the compression top flange of the section prevented the section from reaching its full capacity. Hejll et al. (2005) presented the manufacturing process and testing of a large scale hybrid composite girder as a part of the European-funded ASSET project, as shown in Figure 2.16c. The main outcome of the project was the ability to develop a complete bridge system using composite profiles. However, due to the cost and time limitations, the girder had not been tested up to failure. As a result, a complete understanding of the structural performance of the girder was not achieved. The combination of FRP tubes together helps to increase the stiffness and the strength capacity of the beam. However, local buckling still remains the main affecting factor in reaching the full capacity of the combined beams. Thus, an evaluation of the use of FRP composite with conventional materials like concrete is one of the solutions to reduce certain deficiencies and disadvantages in construction elements fully made of FRP (Aydin & Saribiyik 2013).

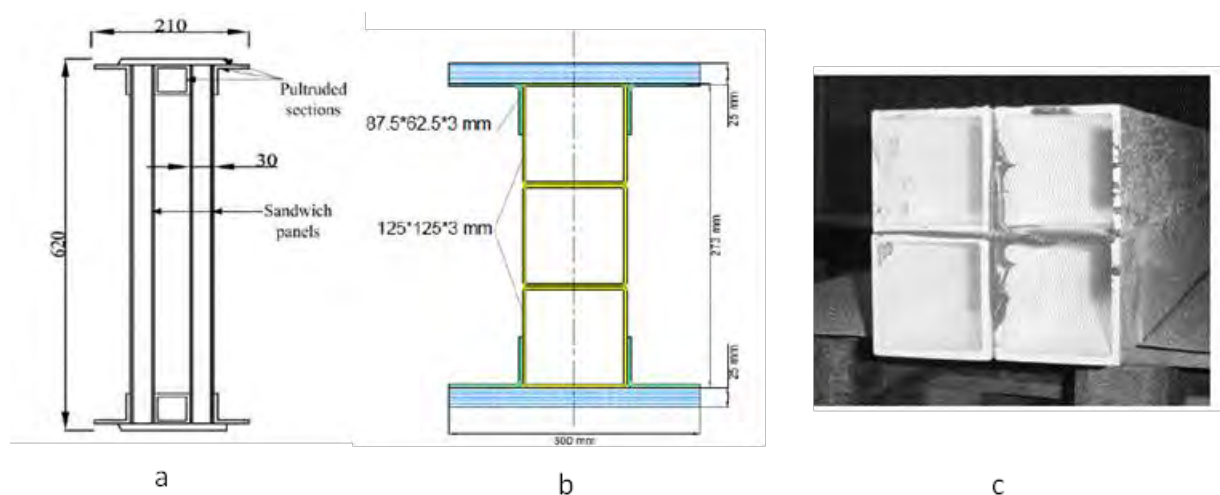


Figure 2.16 Proposed girder using pultruded section: a) (Keller et al. 2004), b) (Kemp 2008) and c) (Hejll et al. 2005)

## 2.7 Enhancement of strength, serviceability and ductility by filling GFRP tubes with concrete

Section 4 highlighted that the local buckling and delamination of the compression flange was the main mode of failure for FRP composite profiles, which prevented the full utilization of the superior properties of these advanced materials. Therefore, it is important to combine FRP tubes with other materials to

improve their behaviour. In fact, it is well known by engineers that combining materials into a composite structural system increases the advantages of the properties inherent in each of its components. One of the classical examples of this is reinforced concrete, which combines a superior load carrying capacity of steel with the compression capability and low cost of concrete (Khalifa & Nanni 2000). Similarly, innovative hybrid construction systems, which combine the FRP profile with conventional concrete, can produce light-weight, non-corrosive and inexpensive sections, which presents another example, shown in Figure 2.17 (Ahmad et al. 2005; Khalifa & Nanni 2000). Similarly, the combination of FRP and concrete as a composite material enables them to take advantage of their superior properties. For instance, it improves their structural performance, not only by decreasing the dead load in terms of replacing the steel reinforcement by FRP, but also the FRP tube also provides a lightweight formwork for concrete, which acts as a non-corrosive reinforcement, reinforcement in the tension side, confinement of concrete in the compression side, shear reinforcement, and protection of the concrete core from aggressive environments, whereas concrete provides the compressive strength for the member and stability for the tube against lateral buckling (Hwang et al. 2000; Mohamed & Masmoudi 2010a). All these features make the composite system a possible alternative to reinforced or pre-stressed concrete to be used as column, piles and beams.

Concrete-filled FRP tubular sections have emerged in beam applications due to their superior performance to carry axial loads, although the benefits of concrete confinement are less in the case of bending as compared to axially loaded members. The major advantages of concrete infill to FRP are the prevention of local buckling failure and the elimination of de-bonding failure and improving the ductility of the beams, which makes this system attractive (Fam & Rizkalla 2002). Fam and Rizkalla (2002) experimentally investigated the effect of concrete filling, cross section configuration, and a different laminate structure on the performance of composite beams by using circular FRP tubes with diameters ranging from 89 to 942 mm and spans ranging from 1.07 to 10.4 metres. The results showed that the flexural behaviour is dependent on the stiffness and diameter to thickness ratio of the tube, while the contribution of concrete

confinement to the flexural strength is insignificant. The strength gain was 250% for the FRP tubes in comparison to a gain of 50% for the steel tubes. The results also indicated that the ductility is greatly improved by filling the tubes with concrete.

Another application of the composite tubes is using them as an alternative to steel spirals for concrete members. Fam et al. (2007) conducted an investigation to check the feasibility of using composite GFRP tubes as an alternative to steel spiral reinforcement in circular concrete members with longitudinal reinforcement. They used six beams with diameters ranging from 219 mm to 324 mm and 2.43 m to 4.2 m long respectively. They reported that, unlike spiral reinforced beams in which the failure was governed by crushing and spalling of concrete cover, GFRP tubes confined a larger area of concrete and contributed as longitudinal reinforcement as well. As a result, members' flexural capacity was increased by up to 113%. Mohamed and Masmoudi (2010b) and Mohamed and Masmoudi (2010a) observed the same behaviour when they performed an experimental 4-point bending test on 6 circular reinforced concrete filled FRP tubes and 4 reinforced concrete beams with a total length of 2000 mm. Their test results indicated that the beam confined by a FRP tube experienced lower deflection, higher stiffness and 55% higher strength than the beam reinforced with steel spirals. Furthermore, the results clearly show that the GFRP tubes increased the ultimate strength and improved the energy absorption of the filled beams. In the process of testing the feasibility of using concrete filled FRP tubes, Fam et al. (2007) investigated the behaviour of concrete filled rectangular filament-wound glass fibre reinforced polymer tubes (CFRFT) for structural members. Three beams (two totally filled and one partially filled with concrete) and five columns were tested. They reported that the CFRFT provided reliable and feasible structural members, that flexural strength is comparable to that of concrete filled steel tubes, and that the strength to self-weight ratio is enhanced by providing a void with a lower strength ratio of about 22 %, which is attributed to the different failure modes of the two beams. While the fibre type and section geometry are important factors affecting the flexural strength of the section, the

adherence between concrete and the FRP section is another factor influencing the final strength of the section.

Aydin and Saribiyik (2013) discussed the flexural behaviour of GFRP produced with different configurations. Providing sand particles in the interior surface of GFRP using epoxy, and wrapping it with extra felt (FRP mat), were the main objectives of their study. They showed that the flexural capacity of these samples was increased approximately three times compared with hollow sections, and two times when compared with hybrid samples. Due to the fact that local failure is the main mode of failure of FRP sections, El-Hacha and Chen (2012) introduced a new type of hybrid beam which was made up of pultruded GRFP hollow section beams, strengthened with a layer of ultra- high performance concrete (UHPC) on the top, and a sheet of carbon FRP or steel FRP on the bottom of the section. They concluded that the flexural strength and flexural stiffness were increased by adding UHPC and CFRP/SFRP to the hollow section. However, the performance of the hybrid beam was limited by the characteristic material properties of the individual material components. Regardless of the advantages associated with filling FRP tubes with concrete, one major drawback of this design is losing the light weight feature, which represents the key reason for using FRP materials. In addition, for structural applications where the behaviour is controlled by pure bending, filling the tubes with concrete does not represent the optimal solution (Abouzied & Masmoudi 2015). Therefore, it is important to utilize the FRP composite in such a way within the structure that the benefit, in terms of mechanical and in-service properties and economics of the complete system, are clearly recognized.

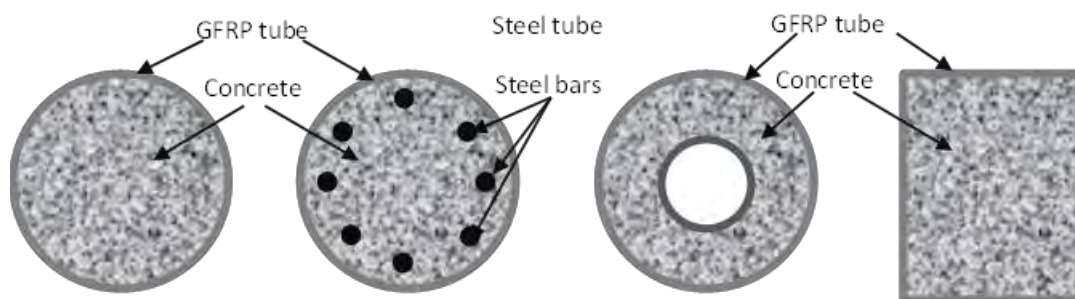


Figure 2.17 Existing Concrete filled GFRP tubes

## 2.8 Maintaining the lightweight characteristics of FRP materials

Combining an FRP section with conventional material is considered to be the best solution to make the best use of the materials, although a filled FRP section completely with concrete is not the optimal solution for applications that are governed by pure bending (Abouzied & Masmoudi 2015). This is due to the fact that in such applications the concrete section is cracked below the neutral axis. As a result, the concrete core slightly contributes to bending resistance and mainly prevents the local buckling of the tube. Therefore, the effective use of concrete to maintain the lightweight properties of the composite system is a crucial issue. Deskovic et al. (1995) proposed a novel hybrid beam design of a composite box section with a layer of concrete on top and a CFRP layer at the bottom of the section. The main concept of their design is to effectively and efficiently use material with high compressive strength and stiffness to cost ratio in the compression side, and use composite material with a failure strain less than that of GFRP in the tension side. The low strain materials will be the first element to fail, giving warning of an imminent collapse. Therefore, they used carbon fibre reinforced plastic (CFRP) for this purpose. In addition, due to the use of concrete in the compression zone, part of the cross section was designed to be a form work for the wet concrete. Figure 2.18a shows the proposed cross section for hybrid FRP concrete beam. The study also includes theoretical analysis, which considers the number of potential failure modes. Web buckling, flexural failure of beam's elements, bond failure between the GFRP section and the concrete slab, and diagonal shear failure of the concrete slab were the observed modes of failure. The experimental results showed that de-bonding failure between the GFRP section and the concrete slab was the common mode of failure. It is the first study that highlighted the potential use of a hybrid composite section consisting of hollow GFRP sections and concrete slabs. However, it reports that the overall behaviour of the hybrid system depends mainly on the quality of the shear bond between the concrete and the GFRP profile. Canning et al. (1999) (Figure 2.18b), Van Erp et al. (2002) (Figure 18c) and Hulatt et al. (2003) (Figure 21d) all conducted experimental investigations on hollow GFRP sections with a thin concrete top layer, using similar concepts to

the one originally proposed by (Deskovic et al. 1995). In their design, they proposed to apply fresh concrete onto a water-based adhesive as the proper method to ensure full composite action taking place between GFRP and the concrete. The results highlighted that failure of the shear bond between the GFRP section and the concrete, and buckling of the composite web of the beam, were the significant modes of failure of these sections. In addition, in such a design the concrete is not fully confined, which decreases the possibility of taking advantage of its increased ductility and strength under confining stresses. Furthermore, they realized that the bond technique was impractical in the site. To address the debonding failure issues associated with the proposed concept, Khennane (2010) and Chakraborty et al. (2011) have taken the idea and developed a novel configuration of a hybrid FRP-concrete beam. They developed a rectangular section using a pultruded GFRP composite profile, a CFRP laminate in the tension zone, and a concrete layer in the compression zone. The whole system was confined with an external filament winding wrapping with fibre orientated at  $\pm 45^\circ$ , as shown in Figure 2.19. The experimental results showed that the proposed approach was successful. However, the beam did not achieve its ultimate capacity due to the premature shear punching failure of the concrete block. This failure subsequently resulted in tearing failure of the pultruded profile, followed by buckling of the unsupported walls. Idris and Ozbakkaloglu (2014) investigated the flexural behaviour of a new composite design known as double-skin tubular beams (DSTBs). This design consisted of an outer FRP tube and a central inner hollow steel section. The gap between the two sections was filled with high strength concrete. Experimental results showed that the proposed section exhibited good load-deflection behaviour with high inelastic deformation. However, the section showed large slippage between the concrete-steel interface. Furthermore, the weight and the bond failure represented the critical drawback of this design. Recently Abouzied and Masmoudi (2015) introduced a rectangular partial concrete-filled fibre-reinforced polymer tube (CFFT) beam with inner voids and steel rebar. The beam was wrapped with filament-wound FRP and it had an inner hollow circular or square FRP tube that was shifted toward the tension zone. The results indicate that a good performance

was achieved in terms of strength and ductility, compared to the conventional reinforced concrete beam. However, the authors suggested that more research is required to optimize the inner GFRP tube contribution to the flexural behaviour. Moreover, they suggested that a simplified analysis method that can accurately describe the overall behaviour of these hybrid construction systems should be developed.

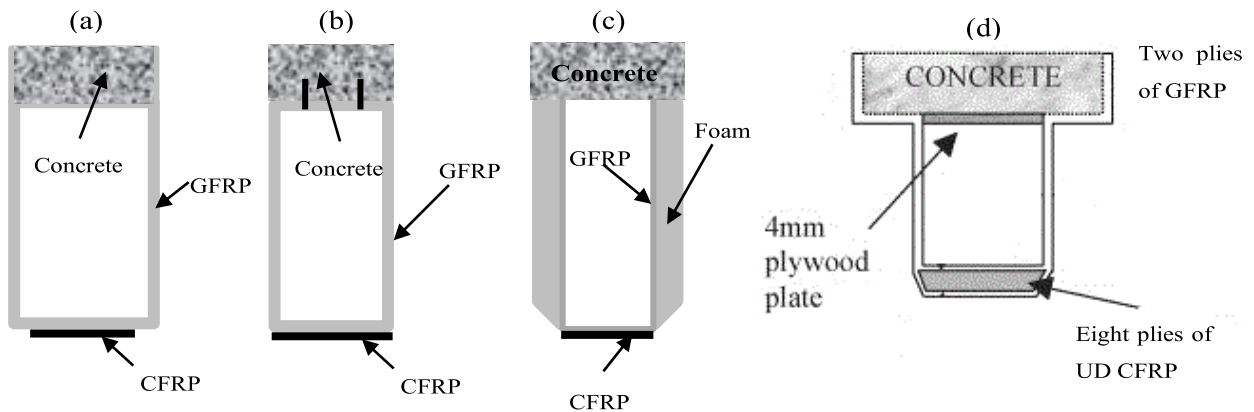


Figure 2.18 Existing Hybrid FRP-concrete beam designs

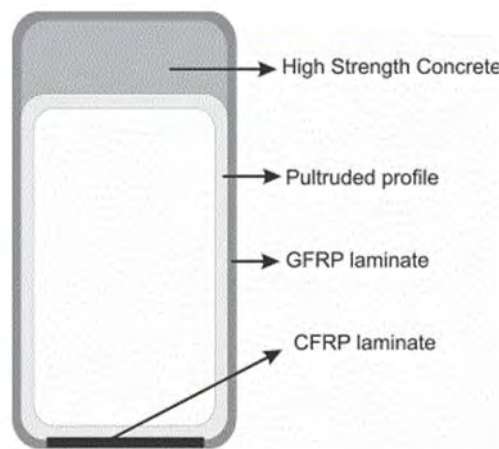


Figure 2.19 Proposed design for a hybrid FRP-concrete beam

## 2.9 Theoretical modelling and capacity prediction

Theoretical and numerical analysis represent an important tool to understand the behaviour of any material, which can reduce the cost and time of testing. In addition, if the mechanical properties of the constitutive materials are provided, a theoretical method of analysis might be considered as an effective solution to predict the behaviour of the section. The accuracy of such methods highly

depends on the initial assumptions. Several studies have been conducted to develop mathematical and constitutive models to understand the behaviour of hollow and concrete filled FRP tubes.

Barbero and Raftoyiannis (1993) undertook an analytical study to investigate the local buckling load as well as the buckling mode of thin walled hollow beams and columns. They pointed out that the prediction of local buckling is important for the prediction of ultimate axial and bending strength of pultruded beams and columns. Kollár (2003), on the other hand, carried out an analytical study to examine local buckling of FRP members with open and closed cross-sections. His study resulted in developing analytical expressions for axially loaded and bent box, C, L and I sections. The main assumption of his research was that he modelled the webs and flanges as separate orthotropic plate objects, rotationally restrained at their edges.

Wu and Bai (2014) and Bai et al. (2013) investigated the possible modes of failure of pultruded glass FRP sections under concentrated loading. They showed that the separation at the web-flange junction is one of the common failure modes of pultruded GFRP beams subjected to bending. In their studies, they proposed a theoretical model to predict the failure load, which considered the combined effect of stresses (modified von Mises criterion) and the bearing resistance of the composite section. These studies take into account the behaviour of the whole section in the calculation of the ultimate failure, instead of the webs and flanges individually. Additionally, they used beam theory to plot how the flexural behaviour depends on the failure load values. Hejll et al. (2005) on the other hand, developed a theoretical derivation that depends on compatibility and equilibrium assumption to predict the flexural behaviour of hybrid FRP composite girder. While the analytical theory provides a good prediction compared with the experimental test, it highly depends on the experimental failure load to calculate the failure deflection. A so-called fibre model analysis (FMA) has been used in several studies to predict the flexural behaviour of hollow and filled composite beams (Abouziied & Masmoudi 2015; Davol et al. 2001; Fam et al. 2003; Fam, Schnerch, et al. 2005; Mohamed & Masmoudi 2010a). A strain compatibility/equilibrium model, using a layer-by-layer method,

is assumed to integrate the forces over the cross-sectional area of the beam. In this model, the FMA methodology is based on first ply failure criteria, which in fact ignore the local buckling effect on the final failure of the section. In addition, it does not account for the shear deformation effect on the flexural behaviour. Therefore, it is important to address the effect of the local buckling and shear in the analysis of the behaviour of GFRP composites in order to predict the behaviour accurately.

## 2.10 Summary

FRP composites have shown significant potential for the development of new structures that have more resistance to the effect of weathering and degradation in severe environments. The critical review of the literature has provided significant details on the feasibility of using GFRP profiles to construct reliable structures for buildings and bridge applications. It has also given an indication on the future application of these materials. To effectively apply FRP composites in the construction industry, designers and structural engineers must have a thorough knowledge of the properties of these materials. This information is important in order to design long lasting strong structures using FRP members. Pertinent characterization methods have been reviewed in this chapter, including theoretical and experimental methods. It was found that the results of theoretical predictions are highly influenced by the properties of fibre and matrix. However, the property data was not reported in standard format. On the other hand, the global deformation represents the main factor affecting the accuracy of the results from a coupon test. Therefore, it was identified that characterisation of the material properties of FRP composites can be effectively determined using testing of full-scale specimens.

As local buckling and delamination mode were the most common failure modes of FRP tubes, several innovation techniques were proposed to overcome these premature failures and effectively utilise the composite materials. One of the most effective ways is to combine or fill the section with concrete to stabilise the thin-walled sections of the composite materials. Previous studies have focussed on using concrete of compressive strength, in a range between 30 to 138 MPa, to

fill the FRP tubes to improve the overall behaviour of the hybrid beams. To the authors' knowledge, there have been no studies conducted investigating the potential use of low strength concrete as an infill to GFRP tubular beams. Although increasing the compressive strength of infill concrete enhanced the FRP tube behaviour, the cost of high strength concrete infill did not justify the enhancement in the stiffness and strength capacities of the hybrid beams. On the other hand, while the concept of filling FRP tubes with concrete represents an effective method to prevent the local buckling of an FRP section, which results in improving its failure capacity, it does also diminish the light weight characteristics of FRP profiles. Therefore, it was identified that a new combination between GFRP tubes and concrete is required to further optimise their usage in a cost-effective alternative for traditional concrete beams. Moreover, the available theoretical methods to predict the flexural behaviour of GFRP composite beams ignored the effect of local buckling shear deformation. Therefore, a good understanding of the effect of these factors on the behaviour of FRP beams is necessary. The above mentioned issues have been the main motivation of this study to conduct an extensive investigation into the behaviour of GFRP sections.

## Chapter 3: Mechanical Properties of Full-Scale GFRP Tubes

### Paper I: Behaviour of hollow pultruded GFRP square beams with different shear span-to-depth ratio

This paper presents an experimental investigation on the behaviour of hollow glass fibre reinforced polymer (GFRP) tubes. The burnout (fibre fraction) test conducted to determine the glass fibre content by weight and the stacking sequence of the plies is reported in **Appendix B**. Full-scale GFRP tubes were used with different shear span to depth ratio ( $a/d$ ) to characterize the effective mechanical properties by measuring the deflection, compression strain and tension strain for up to 20% of the applied load based on ASTM D7250 recommendations. The schematic diagram of the test set-up is shown in **Figure 1** of **Paper I**. Back calculation (*BCM*) and simultaneous (*SM*) methods were then used to analyse the results and to calculate the flexural modulus ( $E$ ) and shear modulus ( $KGA$ ) of the tubes. These full-scale beams were then tested up to failure to evaluate the flexural behaviour of the hollow GFRP tubes under the loading configuration shown in **Figure 2** of **Paper I**. Test of coupons were also conducted and the results were compared to those of the full-scale tests.

From the experimental results, it was found that *BCM* gives more reliable values of  $E$  and  $KGA$  compared with *SM* and coupon tests. The results also showed that the shear deformation has a significant effect on the flexural behaviour of the hollow GFRP beams with lower  $a/d$  ratio. This behaviour was considered in the theoretical evaluation of the flexural behaviour beams investigated in **Papers II to IV**. The results in **Paper I** further showed that the hollow GFRP beams fail prematurely due to local buckling and utilised only 45% of the maximum compressive stress determined from the coupon test. Therefore, filling these sections with concrete is expected to improve their structural performance. Hence, the influence of the low compressive strength concrete infill on the behaviour of GFRP beams was investigated and the results were presented, analysed and discussed in **Paper II**.

# Behaviour of hollow pultruded GFRP square beams with different shear span-to-depth ratios

Majid Muttashar<sup>1,2</sup>, Warna Karunasena<sup>1</sup>, Allan Manalo<sup>1</sup> and Weena Lokuge<sup>1</sup>

## Abstract

It is important to determine accurately the elastic properties of fibre-reinforced polymer composites material, considering that their member design is often governed by deflection rather than strength. In this study, the elastic properties of the pultruded glass fibre-reinforced polymer square sections were evaluated firstly using full-scale with different shear span to depth ( $a/d$ ) ratios and tested under static four-point bending. Back calculation and simultaneous methods were then employed to evaluate the flexural modulus and shear stiffness and were compared with the results of the coupon tests. Secondly, the full-scale beams were tested up to failure to determine their capacity and failure mechanisms. Finally, prediction equations describing the behaviour of the pultruded glass fibre-reinforced polymer square beams were proposed and compared with the experimental results. The results indicate that the back calculation method gives more reliable values of elastic properties of glass fibre-reinforced polymer profiles. In addition, the behaviour of the beams is strongly affected by the  $a/d$  ratios. The shear was found to have a significant contribution on the behaviour of beams with lower  $a/d$  ratios while the flexural stress played a major part for higher  $a/d$  ratios. The proposed equation, which accounts for the combined effect of the shear and flexural stresses, reasonably predicted the failure load of pultruded glass fibre-reinforced polymer square beams.

## Keywords

Elastic properties, characterization, shear, flexural, failure load, GFRP beams

## Introduction

Fibre-reinforced polymer (FRP) composites emerged as a promising material to satisfy the increasing demand for better performing and more durable civil infrastructures.<sup>1</sup> Recently, FRP composites have been used in bridges, because of their high stiffness, strength-to-weight ratios, corrosion resistance and durability.<sup>2</sup> In addition to these superior properties, the process of producing FRP sections allows the designer to specify different material properties for different parts of the cross section.<sup>3</sup> Nevertheless, the use of these advanced materials in structural applications is constrained due to limited knowledge on their material properties and structural behaviour. Therefore, it is of paramount importance to investigate the properties of pultruded FRP sections so that they can be broadly utilised in structural applications.

A number of micromechanical simulations have already been developed to predict the properties of pultruded beams such as flexural and shear modulus.<sup>4–6</sup> The mechanical properties estimated using these models showed a good correlation with the experimental results. However, the models require accurate information on the processing details of the FRP profiles such as individual properties of fibres and resin, the

<sup>1</sup>Centre of Excellence in Engineered Fibre Composites (CEEFC), School of Civil Engineering and Surveying, University of Southern Queensland, Toowoomba, Australia

<sup>2</sup>Department of Civil Engineering, College of Engineering, University of Thi Qar, Iraq

### Corresponding author:

Allan Manalo, Centre of Excellence in Engineered Fibre Composites (CEEFC), School of Civil Engineering and Surveying, University of Southern Queensland, Toowoomba 4350, Australia.  
Email: allan.manalo@usq.edu.au

fibre volume fraction and the composition of the laminates.<sup>7</sup> Therefore, the use of these models as a design tool for structural purposes is likely to complicate the process. Thus, several researchers investigated coupon specimens to determine the effective mechanical properties of the composites and used these properties to predict the behaviour of full scale pultruded FRP profiles.<sup>8,9</sup> Manalo et al.<sup>10</sup> mentioned that there are limited test methods and equipment to characterise the properties of thick FRP composites by using the results of coupon tests. Moreover, the limited dimensions in the transverse direction of the majority of the pultruded GFRP sections added a new obstacle to the applicability of available test standards.<sup>11</sup> The complex internal structure of composites and/or the variation of its mechanical properties within the element itself warrant testing of full scale sections to obtain realistic design properties.

Guades et al.<sup>12</sup> conducted an experimental investigation to characterise the mechanical properties of square pultruded sections (100 mm × 100 mm) using both coupon and full-scale specimens. Although, there was a good agreement between the coupon and full-scale results for single span beams, the effect of shear deformation on the behaviour of the pultruded profiles was neglected as the beam considered in sufficiently long. Bank<sup>13</sup> indicated that the effect of shear on thin walled FRP sections is very significant especially for shorter beams and should be considered in determining the elastic properties of composite material. In support of this, Bank<sup>13</sup> and Neto and Rovere<sup>14</sup> conducted experiments using full-scale sections to determine the flexural ( $E$ ) and shear ( $G$ ) modulus of FRP composite beams. In both situations, three-point bending tests were used to characterise the behaviour of beams with different spans. Even though same test procedure and almost similar section properties were used in both research, there was a huge difference between the calculated  $E/G$  ratios as Bank<sup>13</sup> determined the elastic modulus based on Timoshenko Beam Theory while Neto and Rovere<sup>14</sup> used the graphical (simultaneous) test method. Mottram<sup>15</sup> stated that the sensitivity of the graphical method in determining the slope (of the regression line through the data points) can lead to a significant change in the  $E$  and  $G$  calculations. As a result, there is a need to revisit the graphical method used to find the flexural and shear modulus.

To the authors' knowledge, there are very limited experimental studies conducted to determine the structural properties of full-scale FRP composite beams made of vinyl ester resin with E-glass fibre reinforcement oriented in different directions. In this study, hollow pultruded GFRP square beams with different shear span-to-depth ( $a/d$ ) ratios were tested

using static four-point bending configuration. Graphical (simultaneous) and back calculation methods were used to calculate the  $E$  and  $G$  and compared with the results of the coupon test. In addition, the effect of  $a/d$  ratio on the strength and failure behaviour of the GFRP beams was analysed. Based on the experimental results of this research, a simplified prediction equation to obtain the failure load of the GFRP beams was proposed with due consideration given to the effect of  $a/d$  ratio. These predicted failure loads are then compared with the experimental results.

### Determination of flexural and shear modulus (Beam Theory)

The relatively low elastic modulus of GFRP leads to designs being governed by deflection and buckling limitations, instead of strength.<sup>16,17</sup> In addition, the anisotropic nature of the FRP composites results in low shear modulus to longitudinal elastic modulus ratio. Accordingly, the contribution of shear deformation in the total deformation becomes significant and should be considered in designing composite structures.<sup>3,5,14</sup> This shear contribution can be theorised by using Timoshenko beam theory. This theory incorporates shear deformation of thin walled composite sections in deflection and investigates its effect in a quantitative manner in order to reliably determine the  $E$  and  $G$  for the pultruded FRP section. In this method the controlling equations are:

$$EI \frac{\partial \phi}{\partial x} = M \quad (1)$$

$$\frac{\partial \delta}{\partial x} + \phi = \frac{V}{KGA} \quad (2)$$

where  $I$  is the second moment of area,  $\phi$  is the bending slope,  $M$  is the bending moment,  $\delta$  is the total deflection,  $V$  is the shear force and  $A$  is the cross-sectional area. The shear coefficient  $K$  is a constant which accounts for the shear distribution over the beam cross section. For homogenous box profile,  $K$  can be calculated using the equation recommended by Bank<sup>7</sup>:

$$K = \frac{80}{192 + (v \times G/E)(-12)} \quad (3)$$

where  $v$ ,  $G$  and  $E$  refer to the longitudinal Poisson's ratio, shear modulus and elastic modulus, respectively, of the section. By solving equations (1) and (2) for the case of four-point load bending with the load applied at a distance ( $a$ ) from the support point ( $a = L/3$  in this

case, where  $L$  is the beam span), the total deflection can be obtained as follows:

$$\delta = \frac{23PL^3}{1296EI} + \frac{PL}{6KGA} \quad (4)$$

where  $P$  is the total applied load,  $EI$  is the flexural stiffness and  $KGA$  is the shear stiffness.

Two techniques are commonly used to calculate  $EI$  and  $KGA$  by using the above equation. The first technique is called “back calculation method (BCM)” which was based on the Bernoulli equation to determine the  $EI$  from the strain readings on the outer flange surfaces at mid-span (in the constant moment region):

$$EI = \frac{Mc}{\varepsilon} \quad (5)$$

where  $c$  is the distance from the neutral axis to the outermost fibre, and  $\varepsilon$  is the measured strain. After  $EI$  is calculated, equation (4) can be used to back calculate  $KGA$ .

The second technique is referred to as “simultaneous method (SM)” where at least two different spans should be investigated experimentally. Each test produces a data set for load, deflection and span. These three terms are known in equation (4) with  $EI$  and  $KGA$  as two unknowns. For better interpretation of the method, equation (4) is divided throughout by  $PL/6A$  as follows:

$$\frac{6A\delta}{PL} = \frac{23}{216E} \left(\frac{L}{r}\right)^2 + \frac{1}{KG} \quad (6)$$

This represents a straight line, with  $(L/r)^{-2}$  being the independent variable on the horizontal axis and  $6A\delta/PL$  being the dependent variable on the vertical axis. Herein,  $r$  is the radius of gyration of the section defined by  $r = \sqrt{I/A}$ . By plotting the variable  $6A\delta/PL$  against  $(L/r)^2$ , the elastic modulus can be found from the slope of the straight line and the shear modulus from the intercept on the vertical axis:

$$E = \frac{23}{216 \times \text{slope}} \quad (7)$$

$$KG = \frac{1}{\text{intercept}} \quad (8)$$

## Experiment program

### Material properties

Pultruded GFRP square sections (125 mm × 125 mm × 6.5 mm thickness) produced by Wagner’s

Composite Fibre Technologies (WCFT), Australia were used in this study. These sections are made from vinyl ester resin with E-glass fibre reinforcement. The density of these pultruded profiles is 2050 kg/m<sup>3</sup>. As per standard ISO 1172,<sup>18</sup> the burnout test revealed an overall glass content of 78% by weight in these profiles. The stacking sequence of the plies is [0°/+45°/0°/−45°/0°/−45°/0°/+45°/0°], where the 0° direction aligns with the longitudinal axis of the tube. Table 1 shows the mechanical properties of the pultruded sections determined from coupon tests.

### Characterization of elastic properties for pultruded sections

Following the methodology proposed by Bank,<sup>13</sup> GFRP pultruded profiles with three different  $a/d$  ratios were tested under static four-point bending. The details of the tested specimens are listed in Table 2. The load was applied at the third points of the span and shear span to total length ( $a/L$ ) was maintained at 1/3 for all tests. Figure 1 shows the schematic illustration of the test set-up and the tests were conducted according to ASTM D7250.<sup>19</sup> A 2000 kN capacity servo hydraulic testing machine was used with a loading rate of 2 mm/min. All specimens were tested only up to approximately 20% of the failure load to ensure that the beams are still in the elastic range. The level of the applied load (20% of the failure load) was based on ASTM D7250 recommendation. To validate

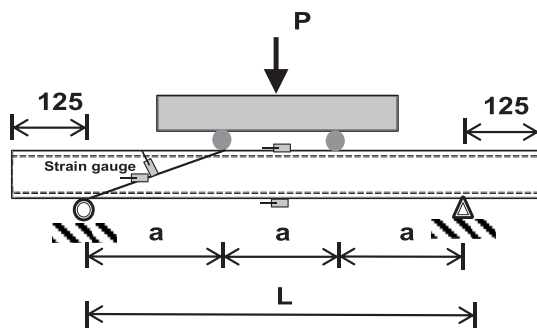
**Table 1.** Mechanical properties from coupon test.

Properties	Average value	SD
Compressive modulus (longitudinal, GPa)	38	1.4
Compressive strength (MPa)	640	37
Tensile modulus (longitudinal, GPa)	42	2
Tensile strength (MPa)	741	39
Flexural modulus (longitudinal) (GPa)	39.3	2.3
Shear modulus (longitudinal) (GPa)	5.7	0.4
Shear strength (MPa)	120	14
Interlaminar shear strength (MPa)	51	2

**Table 2.** Details of the specimens tested for the elastic properties.

Span length (mm)	Shear span, $a$ (mm)	$a/d$
600	200	1.6
900	300	2.4
1200	400	3.2

## All Figures



\*All dimensions are in mm as per Table 2



Figure 1. Experimental set-up for characterisation of elastic properties.

Table 3. Details of the specimens tested for the behaviour of GFRP beams.

Span length (mm)	Shear span, $a$ (mm)	$a/d$
600	150	1.2
900	300	2.4
1200	450	3.6
1800	750	6

the test method, the values of stiffness properties should not be calculated at any applied load level above a point where the specimen exhibits obvious non-linear deflection response due to excessive local deflection. Thus, there were different strain levels depending on  $a/d$ . The strain levels were 410, 620 and 780 micro-strains for  $a/d$  ratios 1.6, 2.4 and 3.2, respectively. Strain gauges (PFL-20-11-1L-120) of 20 mm length were attached to the bottom face at the mid-span of the specimens. Laser displacement transducer was used to measure the mid-span deflection. The applied load and the deflection of the loading ram were recorded using the Systems 5000 data acquisition system.

### Behaviour of hollow pultruded GFRP composite beams

Hollow GFRP pultruded sections with four different  $a/d$  ratios were tested up to failure under static four point bending test. In contrast to Characterization of elastic properties for pultruded sections, the load was applied at the two points with a load span equal to 300 mm. The constant load span was used to keep the upper face of the section under same condition for all specimens and to take account of the limitation on the length of the test frame. Vertical supports were provided to prevent lateral buckling. The details of the tested specimens are listed in Table 3. Figure 2 shows

the experimental set up. A 2000 kN capacity universal machine was used for applying the load. Steel plates were provided at the support and loading points to minimise indentation failure.

### Experimental results and observations

The experimental results for the elastic properties and the behaviour of full scale beams are discussed in this section.

#### Elastic properties of GFRP sections

*E and G using back calculation method.* The load versus deflection curves for all specimens are shown in Figure 3. Linear elastic behaviour up to 20 kN can be observed from these. The variations of  $E$  and  $KGA$  with load for all specimens are shown in Figures 4–6. From these curves, it can be seen that these parameters start at a high value but reduce with increasing load. In order to minimise the errors that might have occurred due to deflection measurements in this study,  $EI$  and  $KGA$  were computed from the average of several points spaced within a range of  $L/800$  to  $L/600$  deflection as suggested by Hayes and Lesko.<sup>20</sup> The average calculated values of  $E$  and  $KGA$  from the BCM are summarized in Table 4. In this table, a calculated value based on 6.35 mm thickness section was used for the moment of inertia. The shear modulus  $G$  is separated from  $KGA$  using the  $k$  determined from equation (3) and the nominal cross section area of the beam. The average value of  $E$  was 47.2 GPa which is 20% higher than the coupon test results. The higher flexural modulus obtained from the full section compared with the coupon specimens can be related to the continuity of  $\pm 45^\circ$  fibres along the length of the pultruded beams. In addition, the shear modulus value of 4 GPa is comparable with the value suggested by Mottram<sup>15</sup> for a standard GFRP pultruded profile.

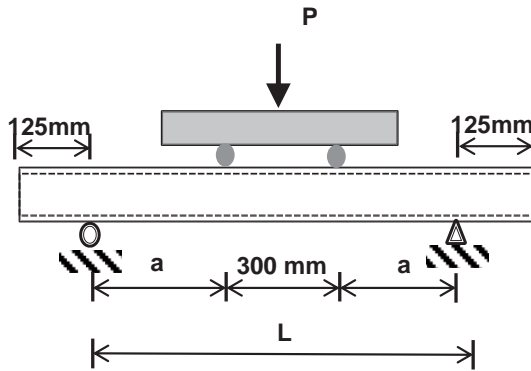


Figure 2. Experimental setup for the behaviour of GFRP beams.

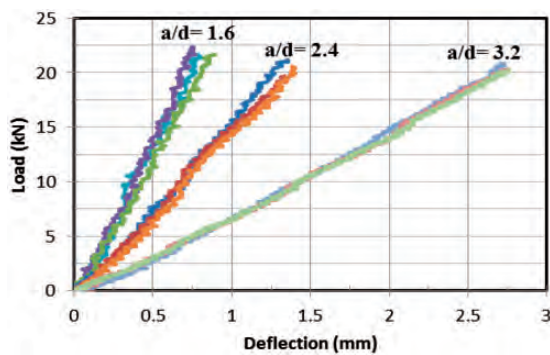


Figure 3. Load–deflection relationship for GFRP beams.

*E and G using simultaneous method.* In order to determine the elastic properties  $E$  and  $G$ , a graph for  $6A\delta/PL$  versus  $(L/r)^2$  was plotted as shown in Figure 7. Each value of  $\delta/P$  was calculated using a selected load,  $P$ , in the range between 0 and 19 kN, and the corresponding measured displacement at mid-span for  $\delta$ . The two points are shown in Figure 7. A linear regression was used to obtain the slope, intercept and the coefficient of correlation, which are also shown in the figure. The  $E$  and  $G$  values were then calculated using equations (7) and (8), respectively. The calculated  $E$  in this method is 56.1 GPa which is higher than the coupon test results by about 43%. In contrast,  $G$  is 3.3 GPa which is less than the average value for standard pultruded profiles by about 17%.

### Behaviour of hollow pultruded GFRP composite beams

*Load–deflection behaviour.* Figure 8 shows the load–deflection curves for the GFRP pultruded beams, which shows a linear behaviour until failure. There is a non-linear response before the final failure for the beams with  $a/d$  ratios of 1.2 and 2.4. This behaviour is possibly due to the crushing of the corners of the specimen at the

support and at the loading points which leads to separation of the web–flange junction. This progressive failure results in the web to continue carrying the applied load. The load carrying capacity of the beam is affected by the variation of the  $a/d$  ratio whereas a decreasing trend was observed with increasing  $a/d$  ratio. All the beams show a brittle failure in both flexural and transverse shear failure modes. For all long span specimens, the ultimate failure was found to occur in the compression flanges beneath the load point starting with compression flange buckling and followed by delamination and shear failure of the flange as shown in Figure 9(a) and (b). On the other hand, for short span specimens, the high applied load result in high buckling in the compression flange and crushing of the web as shown in Figure 9(c). Figure 10 shows a schematic diagram of the observed deformation beneath the load plate and above the support. Table 5 presents a summary of the test results with respect to failure load, corresponding deflection and failure mode.

*Stress–strain behaviour.* The strain measurements for the beams at the top and bottom faces in addition to the strain at the shear path are shown in Figures 11–13. It can be seen that the tension strain at the bottom face is higher than the top face compression strain (i.e. for  $a/d$  ratio of 6 and stress 250 MPa the tension strain reaches 4700 micro strain compared with 4000 micro-strain in the compression side). There was a different trend in the strain on the top and bottom sides. The tension strains increased linearly up to failure, whereas the compression strains began to decrease nonlinearly as the load exceeded approximately 75% of the ultimate failure load. At the top side, the strain was negative demonstrating that the profile is compressed, as expected. With increasing load, however, the values tend to become positive indicating that the top surface is moving from being compressed to tensioned as shown in Figure 11. This behaviour reflects the onset of

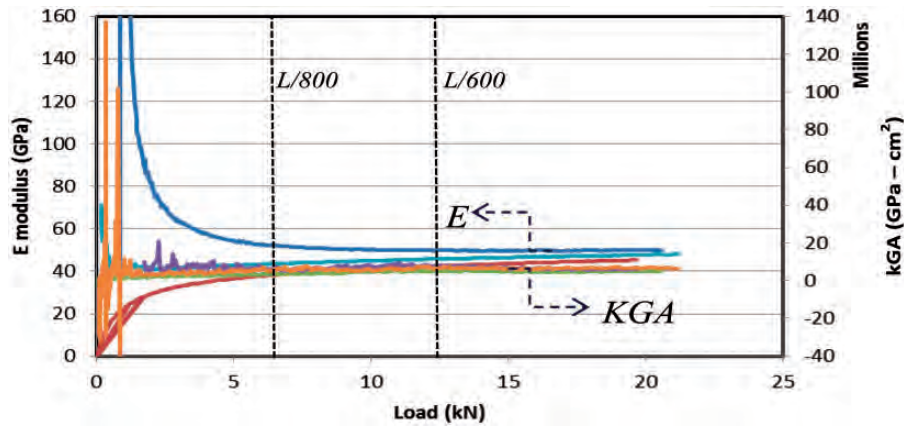


Figure 4. Elastic modulus ( $E$ ) and shear stiffness ( $KGA$ ) versus load for  $a/d = 1.6$ .

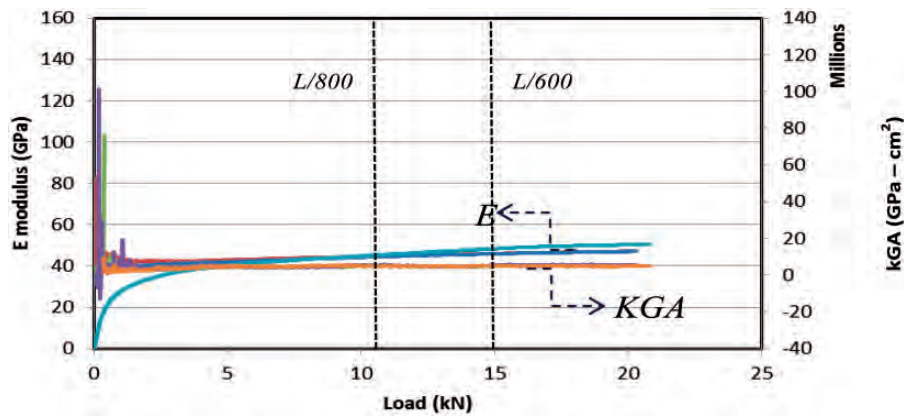


Figure 5. Flexural modulus ( $E$ ) and shear stiffness ( $KGA$ ) versus load for  $a/d = 2.4$ .

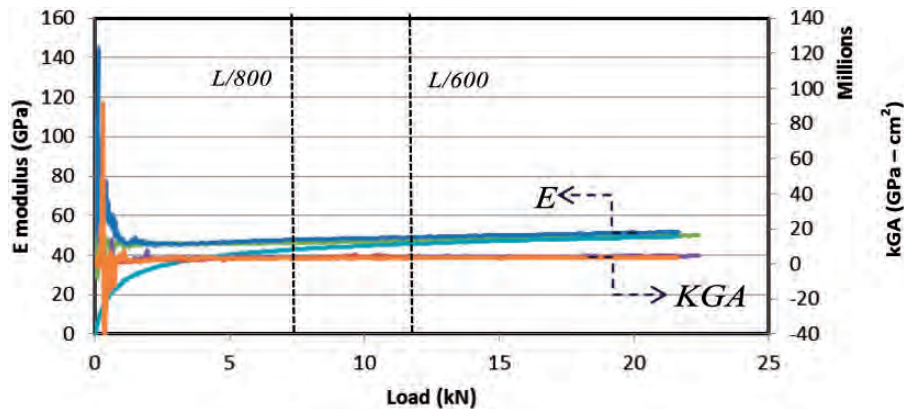


Figure 6. Flexural modulus ( $E$ ) and shear stiffness ( $KGA$ ) versus load for  $a/d = 3.2$ .

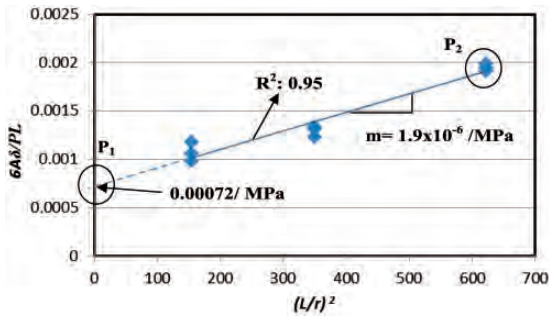
buckling considering that the flange can be assumed to be simply supported at the loading points. Consequently, the increase in the applied load increased the compression component of the moment which results in a local buckling of the flange. Figure 12

shows that the tensile strain decreases with decreasing shear span. The bottom side of the tested specimens were subjected to extensive tensile straining although failure cannot be observed there even after the compression region at the loading zone has failed entirely.

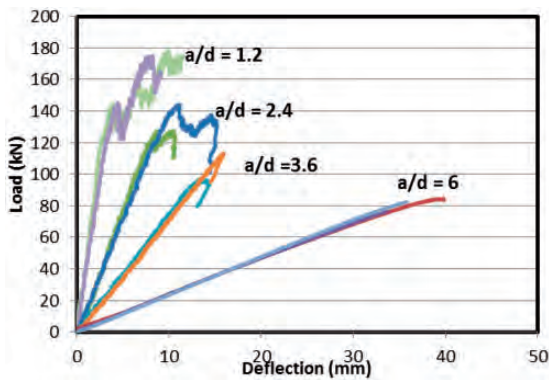
**Table 4.** Summary of average  $E$  and KGA for each span for GFRP beam testing (BCM).

$a/d$	$E$ (GPa)	COV (%)	KGA (GPa cm <sup>2</sup> )	COV (%)	$G$ (GPa)
1.6	47.3	4.4	58.5	10	4.8
2.4	46.2	2.4	49.1	9	4.1
3.2	48.1	2.1	39.3	10	3.3
Ave.	47.2				4

Abbreviation: COV: coefficient of variation.



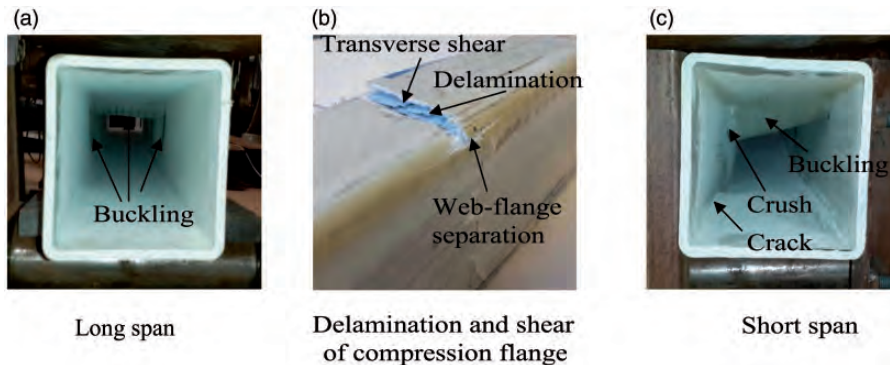
**Figure 7.** Typical graph to determine  $E$  and KG using simultaneous method.



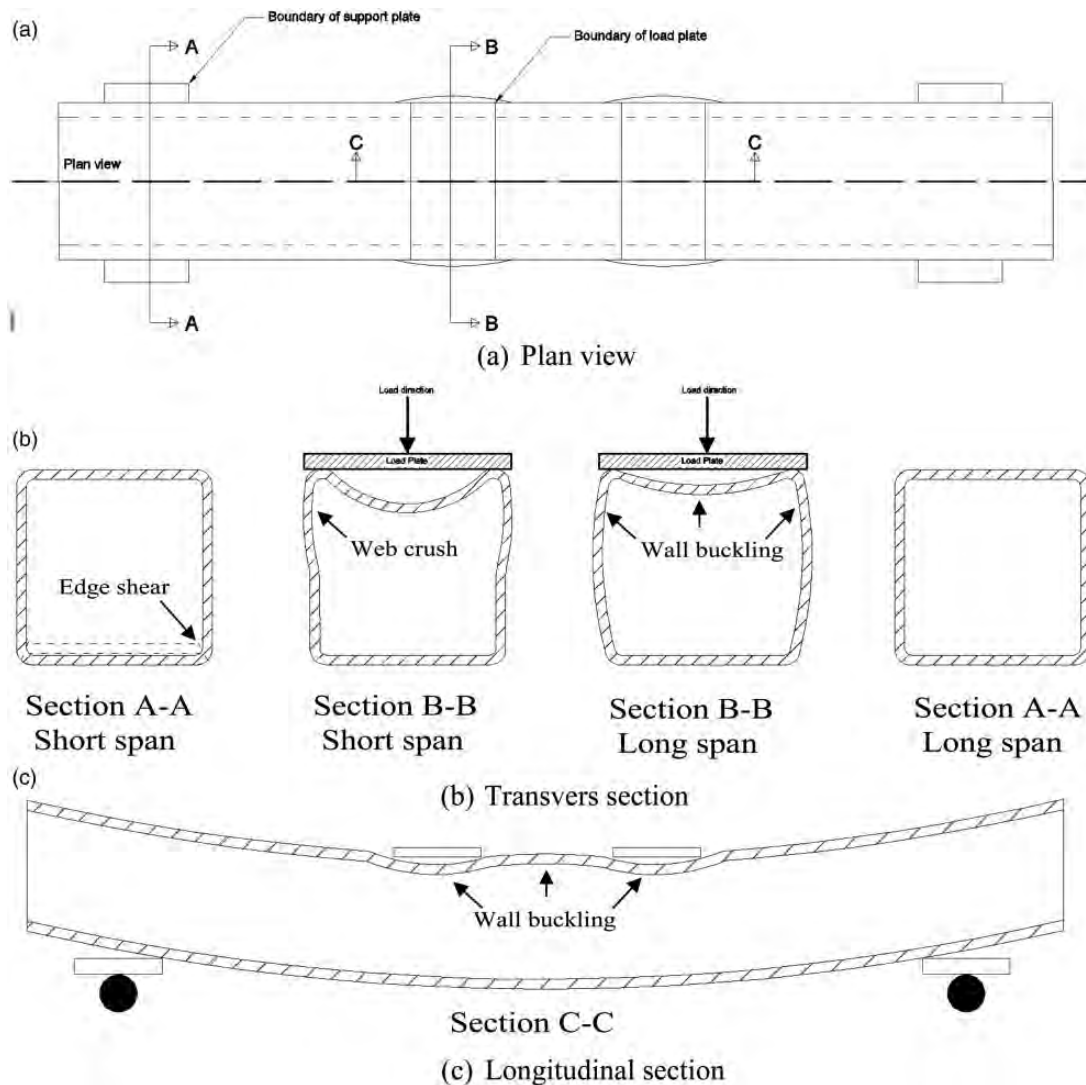
**Figure 8.** Load-deflection curves for GFRP beams.

Figure 13 shows that shear strain increases with decreasing  $a/d$  due to the fact that a significant portion of the shear is transferred directly to the support by an inclined strut. As a result the amount of the direct load transfer increases with decreasing  $a/d$  ratio. In summary, the failure initiated at web-flange junction and followed by buckling and/or crushing in the web depending on the  $a/d$  ratio: beams with higher  $a/d$  ratio experienced buckling failure whereas beams with lower  $a/d$  ratio experienced crushing.

**Failure mode.** The different failure modes of the GFRP beams are shown in Figure 14. The observed failure modes can be classified as flexural failure and transverse shear failure. The shorter beams ( $a/d$  ratios of 1.2 and 2.4) displayed progressive damage accumulation, which is indicated by the drops in the load-deflection curves, with the increasing of the applied load. It was observed that the specimens had cracked and some twisted away from the centre towards one side. The mode of failure observed was transverse shear failure resulting in the delamination and cracking of the fibre along the edges of the pultruded beam in addition to local buckling on the compression flange as shown in Figure 14(a) and (b). Moreover, it was observed that the failure initiated at web-flange junctions and followed by premature buckling and crushing in the webs. This failure behaviour is described as a potential failure for pultruded GFRP sections under concentrated bearing load conditions.<sup>21</sup> For beams with  $a/d$  ratios of 3.6 and 6, the failure occurred at the points of loading and distinct cracks developed on the top surface and side of the tubes. Furthermore, cracks developed at the intersection between the flange and the web due to the buckling, leading to separation between them. It was also observed that delamination crack happened at the compression surface and later progressed into the sides as a result of local buckling initiation as shown in Figure 14(c) and (d). Similar



**Figure 9.** Failure of the long and short span beams.



**Figure 10.** Schematic diagram of the deformation at failure.

**Table 5.** Summary of experimental results for GFRP beams.

Shear span/depth	Average failure load (kN)	Deflection (mm)	Failure mode
1.2	148	8	TS
2.4	132	9	TS
3.6	107.8	14	F
6	80.8	37	F

Abbreviations: TS: transverse shear failure; F: flexural failure.

observation was reported by Guades et al.<sup>12</sup> and Kumar et al.<sup>22</sup> in their investigations on the flexural behaviour of 100 and 76 mm square pultruded FRP tubes. In their studies, however, they reported that the final failure of the specimen occurs mainly due to the effect of the local buckling of the thin wall

(6.35 mm) which results in material delamination and cracking of the fibre along the edges of the beam under the point loads. Shear crack was not observed even for beams with the lowest  $a/d$  ratio. The possible reason for this is the presence of the  $\pm 45^\circ$  plies in addition to the main fibre on the tube which provides a stronger shear resistance along the transverse direction.

### Discussion

**Determination of elastic properties.** Table 6 gives a summary of the properties of the GFRP profiles based on the coupon and full scale tests. It can be seen from this table that there is a significant difference between the results determined from coupon and full scale tests. The main reason between the coupon and full scale results is the effect of discontinuity of the fibres (especially the  $+45^\circ$ ) in the small solid coupon of composite material.

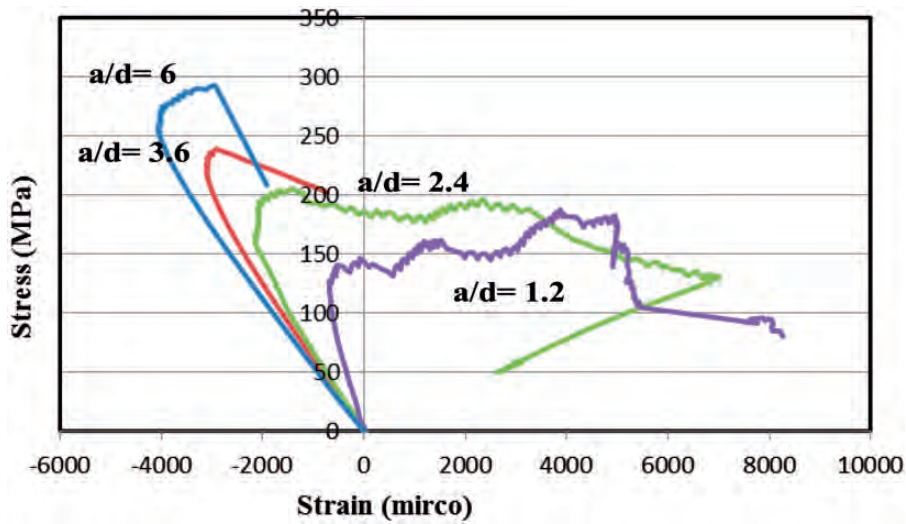


Figure 11. Stress versus compression strain.

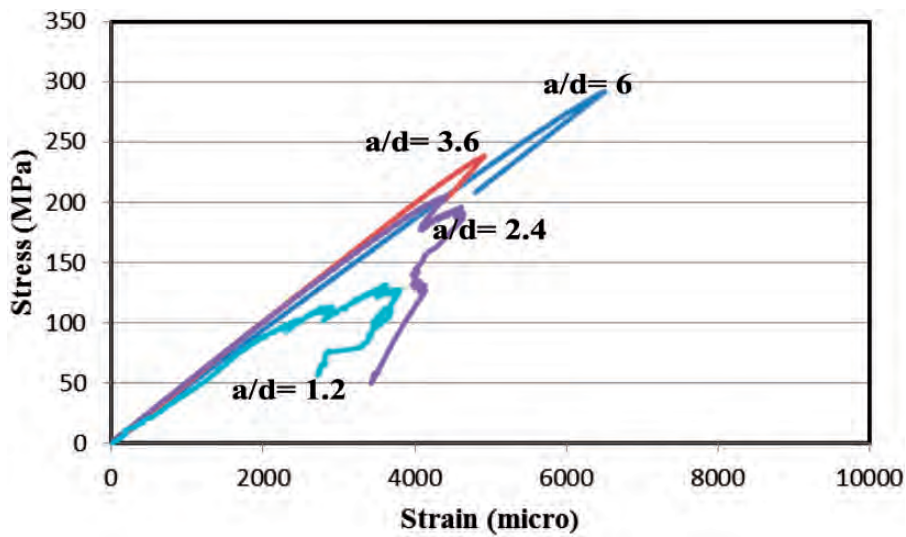


Figure 12. Stress versus tensile strain.

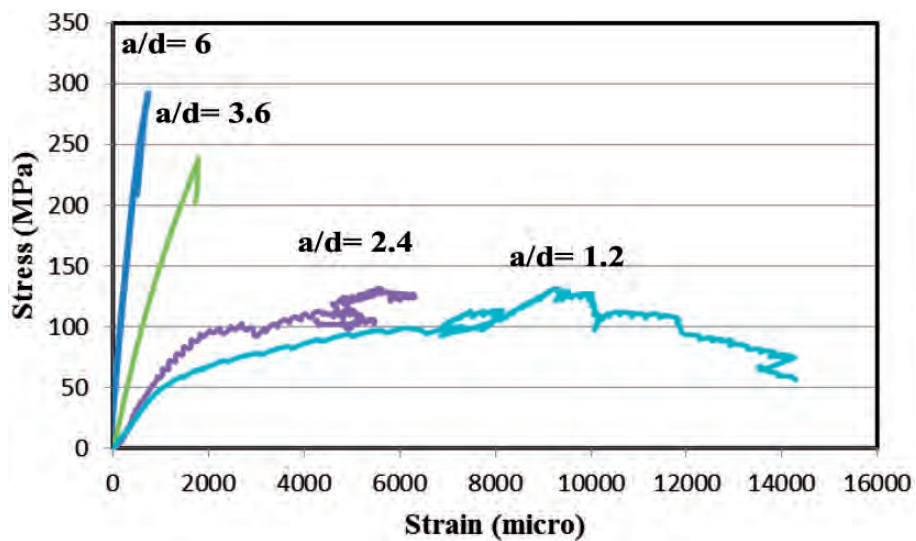
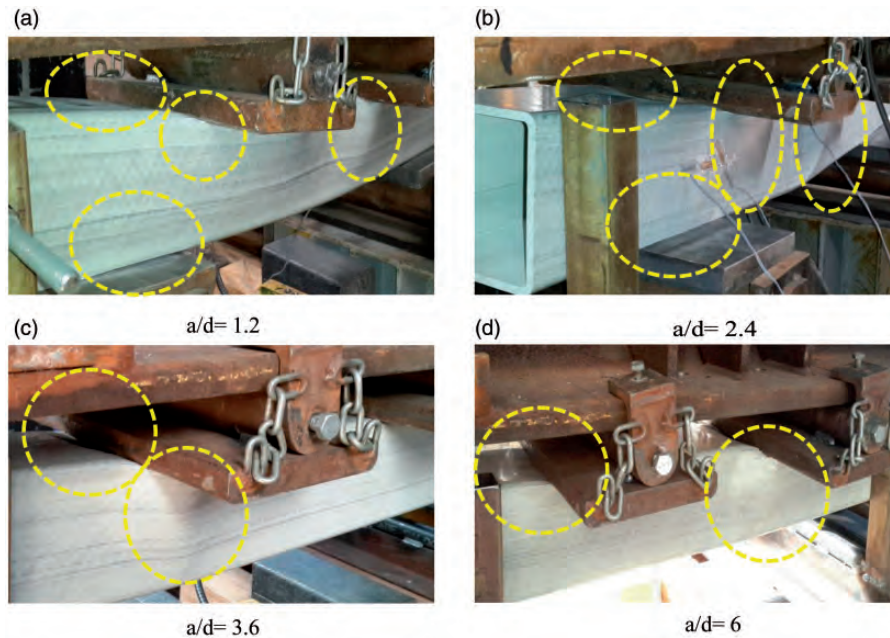


Figure 13. Stress versus shear strain.



**Figure 14.** Failure modes of GFRP beams for different shear span to depth ratios.

**Table 6.** Summary of experimental properties for GFRP beams.

Test type	E modulus (GPa)	G modulus (GPa)
Coupon	39.3	5.7
BCM	47.2	4
SM	56.1	3.3

However, the continuity of the fibres in the full-scale beam results in higher effective elastic properties than the coupon specimens. Using these properties, the load–deflection behaviour of the full-scale pultruded GFRP beams were calculated using equation (4) and compared with the experimental results. Figure 15 displays comparison between the experimental and the predicted deflection calculated by using Timoshenko Beam Theory (equation (4)). The experimental failure load for each beam is used to calculate the corresponding theoretical deflection according to  $a/d$  ratio value. The load values are shown in Figure 15. Elastic properties obtained from full scale test (using BCM and SM) and coupon test have been used to predict the deflection. It can be seen that the Timoshenko Beam Theory provides a good approximation for the curves determined by the experimental tests. It can also be observed from the figure that using the elastic properties from BCM to calculate the beam deflection showed a good correlation with the experimental results for all  $a/d$  ratios. In contrast, analytical results using SM underestimated the experimental results and using coupon test results overestimated the deflection as shown in

Figure 15. SM generally is relatively sensitive to the accuracy of the E measurement. When the span is short and for the same applied load, the deflection is in minimal. This observation is similar with Roberts and Al-Ubaidi<sup>23</sup> wherein they indicated that the measured elastic properties of Pultruded FRP I-profile can change substantially depending on the sensitivity of the graphical method. Therefore, it can be concluded that the elastic properties (E and G) determined using the BCM can reliably predict the behaviour of full scale GFRP beams.

Figure 16 shows the relationship between the flexural and shear deflection percentage of total deflection as a function of  $a/d$  ratio. The flexural and shear deflection was calculated using the average value obtained in this study ( $E/G = 11.6$ ). It can be seen that the flexural deflection constitutes approximately 40% of the total deflection for  $a/d$  of 1.2. In contrast, shear deflection was 60% for the same  $a/d$  ratio. These observations reflect the significant contribution of shear deformation in the total deflection of beams with low shear span to depth ratio. From the figure it can also be observed that the percentage of shear deflection is less than 10% for  $a/d$  of 10 and a ratio of 20 is required to decrease the shear deflection to less than 5%. Therefore, for composite beams with  $a/d \leq 10$  the effect of shear deformation should be accounted in the total deflection calculation.

**Effect of  $a/d$  ratio on shear stress.** The effects of shear span to depth ratio on the shear stress of the GFRP beams

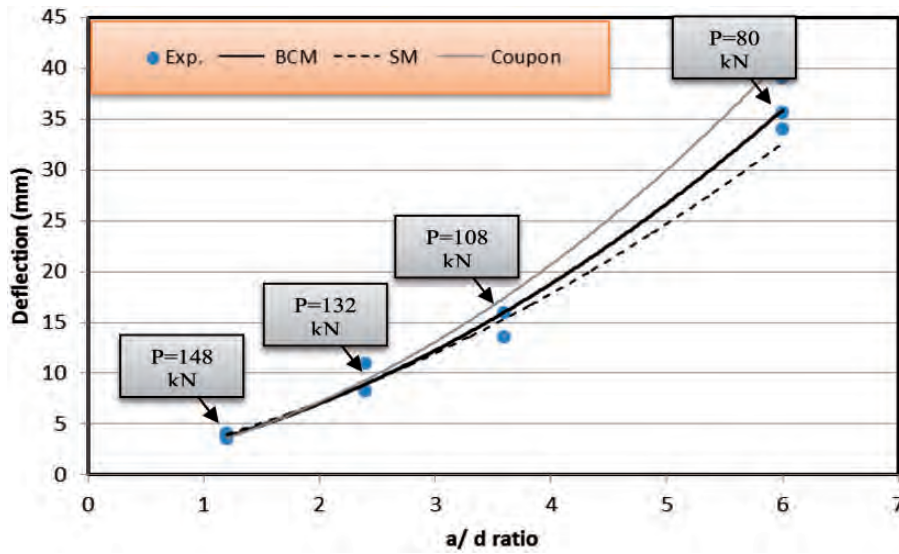


Figure 15. Comparison of theoretical and experimental deflection of beams with different *a/d* ratios.

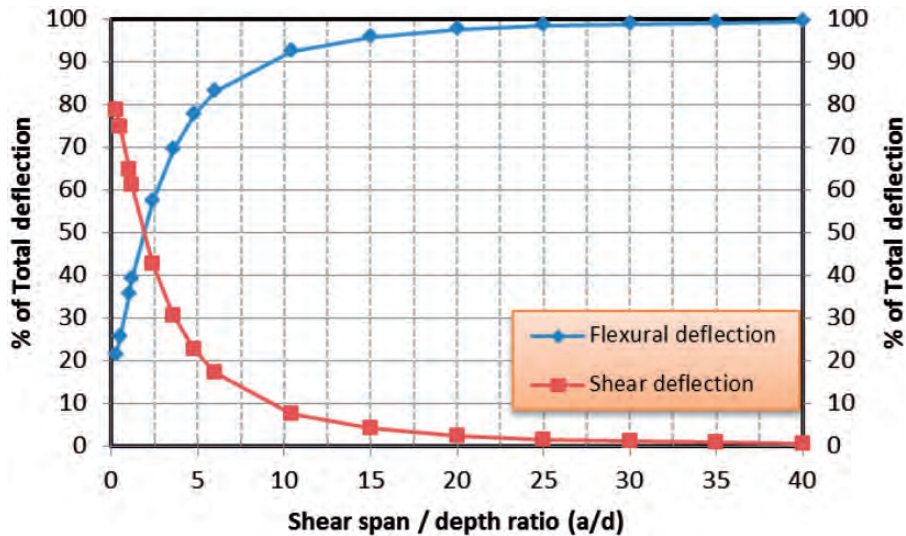


Figure 16. Contribution of flexural and shear deflection for beams with different *a/d* ratios.

were evaluated by calculating the shear stress experienced by the beams using equation 9:

$$\tau = \frac{VQ}{It} = \frac{PQ}{2It} \tag{9}$$

where *V* is the shear force, *Q* is the first moment of area, *I* is the moment of inertia and *t* is the total wall thickness. The calculated values of shear stress at failure for different *a/d* ratios of the GFRP beams are shown in Figure 17. The results showed that the *a/d* ratio has a significant effect on the shear stress experienced by the pultruded GFRP beams. The reason is that the shorter span beams can be subjected to higher failure load which means higher shear force resulting in higher

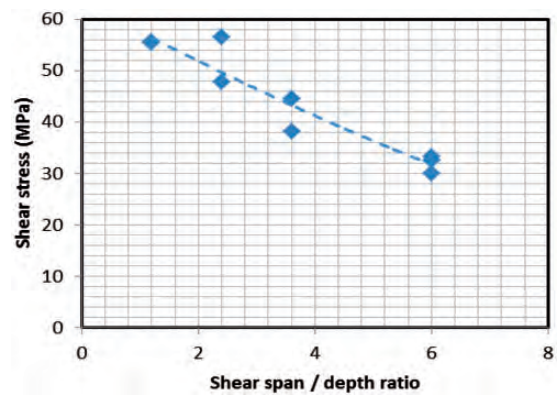


Figure 17. Shear stress versus shear span to depth ratio for GFRP beam.

shear stress according to equation (9). As a result, it can be seen that the shear stress increases with decreasing  $a/d$  ratio. Similar behaviour has been documented for composite sandwich beams and timber beams tested with different  $a/d$  ratios.<sup>24–26</sup> The authors indicated that shorter beam is subjected to a higher shear stress compared with longer span beams. They also mentioned that due to the core weakness, the shorter beams failed due to shear. In this study, no shear cracks were observed on the tested beams at the region of maximum shear even for short span beams.

The relationship between the shear stress and the  $a/d$  ratios seems to be linear. Almost all the tested sections failed in similar mode by local buckling under the applied load followed by cracking at the compression side and the delamination of the plies. Although the tensile strain is low for small  $a/d$  ratios, the bottom face of the beam displays a crushing of fibres at the support without any failure at the mid-span as shown in Figure 14. The reason for this is the higher applied load corresponding to lower  $a/d$  ratio.

The maximum calculated shear stress of the pultruded GFRP beams with shear span to depth ratio of 1.2 and 6 are 55 and 32 MPa, respectively. These shear stresses are 45% and 27%, respectively, of the shear strength of the pultruded profile given in Table 1. These lower percentages indicated that the shear stress is not only the factor which affected the behaviour of the pultruded beams but also the flexural stress. Manalo et al.<sup>10</sup> mentioned that these combined stresses played an important part in understanding the overall behaviour of composites and should be considered in the design and analysis of composite materials.

**Effect of  $a/d$  ratio on flexural stress.** The flexural behaviour of the GFRP hollow sections have been studied by calculating the bending stress using the following equation:

$$\sigma = \frac{Mc}{I} = \frac{Pac}{2I} \quad (10)$$

The calculated bending stresses for GFRP beams with different  $a/d$  ratios are shown in Figure 18. It can be seen that the bending stress increases with increasing  $a/d$  ratio. The maximum bending stress with  $a/d$  ratios of 1.2 and 6 are 98 and 300 MPa, respectively. These bending stress values are 21% and 66% of the compression strength, respectively, and 13% and 41%, respectively, of the tensile strength of the pultruded profile as mentioned in Table 1. This explains the reason why the failure is happening at the compression side. Furthermore, the results indicated that the specimen experiences considerable flexural stresses even at

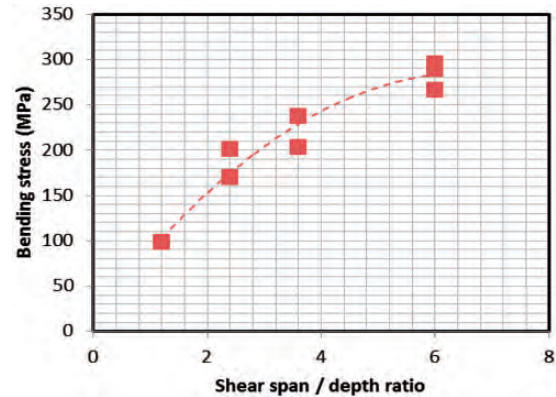


**Figure 18.** Bending stress versus shear span to depth ratio for GFRP beam.

$a/d$  ratio of 1.2 which contributed to the failure mechanisms. Similar result was reported by Turvey and Zhang<sup>27</sup> in their investigation on the shear failure strength of web–flange junctions in pultruded GRP profiles. In their study, however, they reported that failure is a function of combined high shear and bending stresses at the interfaces of different plies.

**Effect of  $a/d$  ratio on failure mode.** The GFRP pultruded beams showed a brittle failure mode. The failure happened without any reduction in the slope of the load–deflection behaviour. The beams with  $a/d$  ratio of more than 3 exhibited a flexural mode of failure. The failure of those beams was controlled by the buckling under the load points followed by cracks and delamination at the compression face in addition to a web–flange junction failure as shown in Figure 14(c) and (d). The beams with  $a/d$  less than 3 showed a transverse shear failure. This type of failure was resulting in the delamination and cracking of the fibre along the edges of the pultruded beam in addition to local buckling on the compression flange as shown in Figure 9. This failure behaviour was reported by Turvey and Zhang<sup>27</sup> and Wu and Bai<sup>21</sup> as a web–flange junction failure which caused mainly by the concentrated bearing load conditions. A change in the slope of the load–deflection behaviour has been noticed. In some cases, it can be seen that there are some drops in the load at the failure progress stage for the beams with spans lower  $a/d$  ratios. This failure response is due to the progressive damage accumulation of the section. No pure shear failure or shear cracks appeared in all of the tested beams. The main reason for that is the stacking sequence of the plies of the GFRP pultruded sections are in the form of  $\pm 45$  degrees. It was clearly noticed that the failure cracks position was closer to the top loading point than to the supports.

## Prediction of failure load for pultruded GFRP beams with different $a/d$ ratio

The contribution of the shear deformation was clearly observed for all  $a/d$  ratios considered in this study. Therefore, in order to estimate the failure load of the pultruded GFRP beams, it is important to account for the shear and the bending stresses in the prediction equation.

### Proposed prediction equation

Based on the experimental results, buckling failure occurred at the concentrated load points and/or near the support locations. The main reason for this behaviour is the high shear forces that typically develop at those locations. Bank<sup>7</sup> stated that, when the beam is subjected to high shear forces and high bending moment, the web is subjected to combined shear stress ( $\tau$ ) and axial compressive or tensile (flexural) stress ( $\sigma$ ). As a result, the combined effect of both stresses is significant and should be accounted for in the prediction of failure load. Structural plastics design manual ASCE<sup>28</sup> recommends using an interaction

equation based on the isotropic plate theory to calculate the critical load which takes into account the combined effect of shear and flexural stresses. This equation expressed in the form:

$$\frac{\sigma_{\text{act}}}{\sigma_{\text{all}}} + \frac{\tau_{\text{act}}}{\tau_{\text{all}}} \leq 1 \quad (11)$$

where  $\sigma_{\text{act}}$  and  $\tau_{\text{act}}$  are the actual flexural and shear stresses, respectively,  $\sigma_{\text{all}}$  and  $\tau_{\text{all}}$  are the corresponding material allowable stresses. In this formula the combined effect of the shear and flexure has been suggested and the failure load can be calculated using the following equation:

$$P = \frac{1}{(ac/2I\sigma_{\text{all}}) + (Q/2It\tau_{\text{all}})} \quad (12)$$

In this study, a linear interaction equation similar to ASCE equation is proposed to predict the failure load of the pultruded GFRP beams which account for the combined effect of shear and flexure. In the proposed equation, buckling stress  $\sigma_{\text{buckling}}$  calculated according to Bank<sup>13</sup> (presented in Appendix 1) has been used instead of the allowable compressive strength due to the fact that almost all the tested hollow pultruded profiles failed with local buckling. Therefore, the predicted failure load of the pultruded GFRP beams can be calculated as:

$$P = \frac{1}{(ac/2I\sigma_{\text{buckling}}) + (Q/2It\tau_{\text{all}})} \quad (13)$$

**Table 7.** Predicted failure load compared with the actual failure load.

$a/d$ ratio	Exp. (kN)	Equation (12) (kN)	Equation (13) (kN)
1.2	148	214	164
2.4	132	170	115
3.6	107.8	142	88
6	80.8	106	60

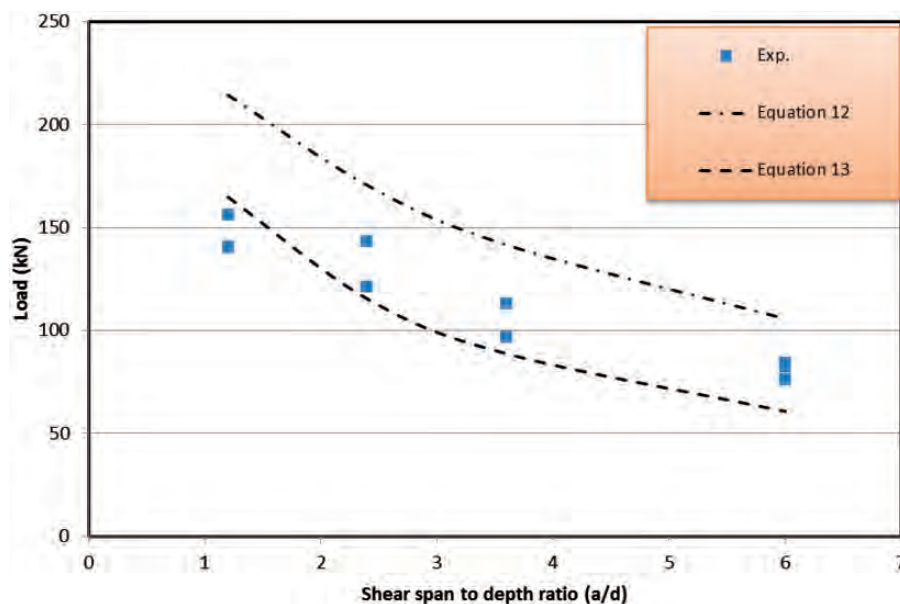


**Figure 19.** Comparison between the predicted and the actual failure loads.

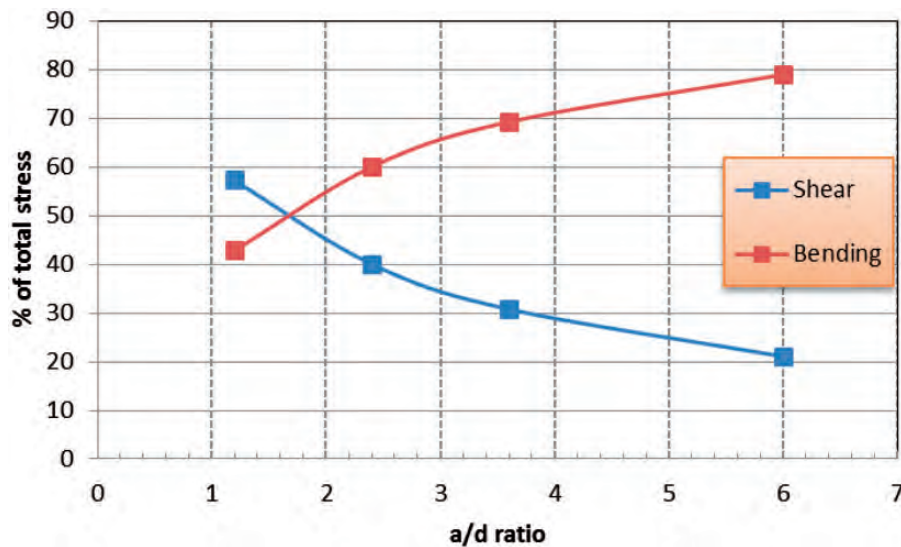


**Figure 20.** Percentages of stress contribution from the total failure stress.

The allowable stresses of the pultruded GFRP material are listed in Table 1.

#### Comparison between predicted and the experimental failure loads

The predicted failure load of the pultruded GFRP beams tested using 4-point load and the percentage difference between the predicted and actual (experimental) average failure loads are summarised in Table 7. For clarity, the comparison is also shown in Figure 19.

It can be seen from Table 7 and Figure 19 that the proposed equation (13) shows a good agreement between the predicted and the actual failure load. For beam with  $a/d$  ratio 1.2, the proposed equation overestimates the failure load by 11%. This indicates that the beams are more likely to fail by transverse shear failure and the shear has the higher effect on the section's failure mode. In contrast, the flexural compression stress is the more dominant stress to cause the failure for pultruded beams with  $a/d$  ratios of 3.6–6. Moreover, it can be clearly noticed that the use of equation (12) to predict the failure load depends on the ultimate flexural stress will overestimate the failure load by as much as 31–44%. Figure 20 shows the percentages of stress contribution from the failure stress of the pultruded beams. As seen from the figure, for beams of  $a/d$  ratio 1.2, shear stress contribution (57%) for the failure load is higher than that for the flexural stress (42%). For beams with higher  $a/d$  ratio, the flexural stress becomes the dominant stress to cause the failure with 79% of the failure load compared with 21% of shear stress, respectively. These percentages showed that the predicted contributions compare well with the experimental contributions for shear and

flexural stresses. In general, the proposed equation 13 provided a conservative but practical estimation of the failure load of the pultruded GFRP beams with different  $a/d$  ratios.

#### Conclusions

The behaviour of GFRP pultruded square beams with different shear span to depth ( $a/d$ ) ratios was investigated using the four-point bending test. Similarly, the elastic properties of the beams were determined by testing full-scale specimens. The following conclusions can be drawn based on the results of the investigation:

1. The back calculation method gives more reliable values of effective flexural and shear moduli of pultruded hollow GFRP square sections compared with simultaneous method and coupon test. This method is based on the Bernoulli equation and uses the strain readings at mid-span of the beam. A good correlation between the predicted and the actual load–deflection behaviour was achieved using the elastic properties determined from this method.
2. The shear deformation contributes by as much as 50% to the total deflection of beams with low  $a/d$  ratio. Thus, it is recommended to account for the shear deflection in the deflection calculation of GFRP beams when ( $a/d$ ) is  $\leq 6$ .
3. The shear stress experienced by the beam decreases with increasing  $a/d$ . In contrast, the flexural stress increases with increasing  $a/d$  ratio.
4. The failure of the beam is governed by the buckling under the loading points followed by cracks and delamination at the web–flange junction at the compression face.

5. The proposed equation accounting for the combined effect of shear and flexural stresses in pultruded GFRP square beams and accounting for the buckling stress of composites reasonably predicted the failure load of full size pultruded GFRP beams.
6. Aside from shear and flexural stresses, it was found that there is a complexity on the overall behaviour of pultruded GFRP square beams with low  $a/d$ , which needs further investigation.

### Acknowledgement

The authors would like to acknowledge the support of Wagner's Composite Fibre Technologies (WCFT) for providing the GFRP pultruded sections. The first author would like to acknowledge the financial support by the Ministry of Higher Education and Scientific Research-Iraq.

### Declaration of Conflicting Interests

The author(s) declared no potential conflicts of interest with respect to the research, authorship, and/or publication of this article.

### Funding

The author(s) received no financial support for the research, authorship, and/or publication of this article.

### References

1. Bakis C, Bank LC, Brown V, et al. Fiber-reinforced polymer composites for construction-state-of-the-art review. *J Compos Constr* 2002; 6: 73–87.
2. Hollaway L. A review of the present and future utilisation of FRP composites in the civil infrastructure with reference to their important in-service properties. *Constr Build Mater* 2010; 24: 2419–2445.
3. Bank LC. Shear coefficients for thin-walled composite beams. *Compos Struct* 1987; 8: 47–61.
4. Barbero EJ, Fu S-H and Raftoyiannis I. Ultimate bending strength of composite beams. *J Mater Civil Eng* 1991; 3: 292–306.
5. Omidvar B. Shear coefficient in orthotropic thin-walled composite beams. *J Compos Constr* 1998; 2: 46–56.
6. Nagaraj V and GangaRao HV. Static behavior of pultruded GFRP beams. *J Compos Constr* 1997; 1: 120–129.
7. Bank LC. *Composite for construction structural design with FRP materials*. NJ: Jone Wiley & Sons, 2006, p.551.
8. Davalos JF, Salim H, Qiao P, Lopez-Anido R and Barbero E. Analysis and design of pultruded FRP shapes under bending. *Compos B: Eng* 1996; 27: 295–305.
9. Roberts T and Masri H. Section properties and buckling behavior of pultruded FRP profiles. *J Reinf Plast Compos* 2003; 22: 1305–1317.
10. Manalo A, Mutsuyoshi H and Matsui T. Testing and characterization of thick hybrid fibre composites laminates. *Int J Mech Sci* 2012; 63: 99–109.
11. Cardoso D, Harries K and Batista E. On the determination of mechanical properties for pultruded GFRP sections. In: *International conference on FRP composites in Civil Engineering*. Vancouver, Canada: International Institute for FRP in Construction, 2014.
12. Guades E, Aravinthan T and Islam MM. Characterisation of the mechanical properties of pultruded fibre-reinforced polymer tube. *Mater Des* 2014; 63: 305–315.
13. Bank LC. Flexural and shear moduli of full-section fiber reinforced plastic(FRP) pultruded beams. *J Test Eval* 1989; 17: 40–45.
14. Neto A and Rovere H. Flexural stiffness characterization of fiber reinforced plastic (FRP) pultruded beams. *Compos Struct* 2007; 81: 274–282.
15. Mottram J. Shear modulus of standard pultruded fiber reinforced plastic material. *J Compos Constr* 2004; 8: 141–147.
16. Chambers RE. ASCE design standard for pultruded fiber-reinforced-plastic (FRP) structures. *J Compos Constr* 1997; 1: 26–38.
17. Parke G and Hewson N. ICE manual of bridge engineering. *History* 2008; 6: 3.
18. ISO 1172. Textile-glass-reinforced plastics, prepregs, moulding compounds and laminates: Determination of the textile-glass and mineral-filler content – calcination methods, 1996.
19. ASTM D7250. *ASTM D7250/D7250M-06 Standard practice for determine sandwich beam flexural and shear stiffness*. West Conshohocken, PA: ASTM International, 2006.
20. Hayes M and Lesko J. The effect of non-classical behaviors on the measurement of the Timoshenko shear stiffness. In: *Proc 2nd inter conf FRP composites in civil engineering – CICE*, 2004, pp. 873–880.
21. Wu C and Bai Y. Web crippling behaviour of pultruded glass fibre reinforced polymer sections. *Compos Struct* 2014; 108: 789–800.
22. Kumar P, Chandrashekhara K and Nanni A. Structural performance of a FRP bridge deck. *Constr Build Mater* 2004; 18: 35–47.
23. Roberts T and Al-Ubaidi H. Flexural and torsional properties of pultruded fiber reinforced plastic I – profiles. *J Compos Constr* 2002; 6: 28–34.
24. Dai J and Hahn HT. Flexural behavior of sandwich beams fabricated by vacuum-assisted resin transfer molding. *Compos Struct* 2003; 61: 247–253.
25. Yoshihara H and Furushima T. Shear strengths of wood measured by various short beam shear test methods. *Wood Sci Technol* 2003; 37: 189–197.
26. Awad ZK, Aravinthan T and Manalo A. Geometry effect on the behaviour of single and glue-laminated glass fibre reinforced polymer composite sandwich beams loaded in four-point bending. *Mater Des* 2012; 39: 93–103.
27. Turvey GJ and Zhang Y. Shear failure strength of web-flange junctions in pultruded GRP WF profiles. *Constr Build Mater* 2006; 20: 81–89.
28. ASCE. *Structural Plastics Design Manual. ASCE manuals and reports on engineering practice 63*. Reston, VA: American Society of Civil Engineering, 1984.

## Appendix I

### Local buckling equation for box profile

According to Bank<sup>7</sup> the compression flange will buckle before one of the webs if  $(\sigma_{ss})_f/(E_L)_f < (\sigma_{ss})_w/(E_L)_w$ . Therefore, the flange will be restrained by both webs. As a result, the spring constant is given as

$$k_{\text{box-flange}} = \frac{4(D_T)_w}{d_w} \left[ 1 - \frac{(\sigma_{ss})_f(E_L)_w}{(\sigma_{ss})_w(E_L)_f} \right]$$

And the local buckling stress for the flange is given as

$$\sigma_{\text{buckling}} = \frac{\pi^2}{b_f^2 t_f} \left[ 2\sqrt{(D_L D_T)(1 + 4.139\xi)} + (D_{LT} + 2D_S)(2 + 0.62\xi^2_{\text{box-flange}}) \right]$$

$$\text{where } (\sigma_{ss})_f = \frac{2\pi^2}{b_f^2 t_f} \left( \sqrt{(D_L D_T)} + D_{LT} + 2D_S \right)$$

$$(\sigma_{ss})_w = \frac{2\pi^2}{d_w^2 t_w} \left( 13.9\sqrt{(D_L D_T)} + 11.1D_{LT} + 22.2D_S \right)$$

$$\xi_{\text{box-flange}} = \frac{1}{1 + 10[(D_T)_f/k_{\text{box-flange}}b_f]}$$

$$D_L = \frac{E_L^c t_f^3}{12(1 - \nu_L \nu_T)}$$

$$D_T = \frac{E_T^c}{E_L^c} D_L$$

$$D_{LT} = \nu_T D_L$$

$$D_S = \frac{G_{LT} t_f^3}{12}$$

$$\nu_T = \frac{E_T^c}{E_L^c} \nu_L$$

where  $b_f$  and  $t_f$  are the width and thickness of the flange, respectively,  $d_w$  and  $t_w$  are the depth and thickness of the web, respectively,  $E_T^c$  is longitudinal compression modulus,  $E_L^c$  is transverse compression modulus,  $G_{LT}$  is the in-plane shear modulus and  $\nu_L$  is the major (longitudinal) Poisson ratio.

## **Chapter 4: Flexural Behaviour of Single Cell GFRP Beams**

### **Paper II: Influence of infill concrete strength on the flexural behaviour of pultruded GFRP square beams**

This paper evaluated the effect of the compressive strength of the infill concrete on the flexural behaviour of pultruded GFRP tubes. Concrete of three different compressive strengths 10 MPa, 37 MPa and 43.5 MPa was used to fill the hollow pultruded tubes. The beams were tested under four point bending with constant shear span to depth ratio of 4.2. The load deflection behaviour, failure strain and mode of failure were reported. Based on the experimental results, the filled beams showed higher failure load compared with hollow beams. The beam filled with concrete of 10 MPa compressive strength showed 100% increase in the failure load while the beam filled with concrete of 43.5 MPa compressive strength showed 141% increase. On the other hand, the filled beams showed approximately similar stiffness. A comparison between the flexural stiffness of the filled beams is shown in *Figure 5* of *Paper II*. Fibre model analysis was implemented to predict the flexural behaviour of hollow and filled beams numerically. The model incorporated the elastic properties of the GFRP tubes determined in *Paper I* and the partial confinement model for the concrete infill.

The presented results in *Paper II* showed that the concrete filling improved the flexural behaviour of GFRP tubes. In addition, the improvement of ductility of the beams is indicated by the increase of the energy absorption, which is determined by comparing the area under the load-deflection curves until ultimate failure. Furthermore, low strength concrete was found as a practical solution to fill the single cell GFRP sections. However, filling the entire hollow section compromised the lightweight characteristics of FRP composites. Hence, a new concept of multi-celled GFRP beams was proposed. An experimental investigation on the flexural behaviour of this new proposed section was conducted and the results are presented, analysed and discussed in *Paper III*.



# Influence of infill concrete strength on the flexural behaviour of pultruded GFRP square beams



Majid Muttashar<sup>a,b</sup>, Allan Manalo<sup>a</sup>, Warna Karunasena<sup>a</sup>, Weena Lokuge<sup>a,\*</sup>

<sup>a</sup> Centre of Excellence in Engineered Fibre Composites (CEEFC), School of Civil Engineering and Surveying, University of Southern Queensland, Toowoomba 4350, Australia

<sup>b</sup> Department of Civil Engineering, College of Engineering, University of Thi Qar, Iraq

## ARTICLE INFO

### Article history:

Available online 2 March 2016

### Keywords:

Composite beam  
Flexural confinement  
Failure load  
GFRP  
Concrete strength  
Flexural behaviour

## ABSTRACT

This paper presents experimental and analytical studies on the effect of the compressive strength of the concrete infill on the flexural behaviour of composite beams. Hollow pultruded Glass Fibre Reinforced Polymer (GFRP) square beams (125 mm × 125 mm × 6.5 mm) filled with concrete having 10, 37 and 43.5 MPa compressive strength were tested under static four-point bending. The results indicate that filled GFRP beams failed at a load 100–141% higher than hollow beams and showed 25% increase in stiffness. However, the increase in concrete compressive strength from 10 to 43.5 MPa increased the ultimate load by only 19% but exhibited almost the same flexural stiffness indicating that a low strength concrete is a practical solution to fill the GFRP profiles to be used as beam applications. Moreover, the concrete infill prevented the premature buckling and web crushing of the GFRP tube. The maximum strain measured at failure is similar to the compressive strain determined from the coupon test indicating the effective utilisation of the GFRP material. Finally, Fibre Model Analysis which considered the partial confined stress–strain curve for the concrete infill gave an accurate prediction of the flexural behaviour of the concrete filled GFRP sections.

© 2016 Elsevier Ltd. All rights reserved.

## 1. Introduction

### 1.1. General

In recent years, fibre reinforced polymers (FRP) have been used in the construction industry due to its advantageous properties such as high stiffness, strength-to-weight ratios, resistance to corrosion and easy installation [1]. However, their relatively low elastic modulus as well as thin-walled sections lead to structural design being governed by deflection and buckling limitations rather than strength [2,3]. These limitations of FRP composite sections can be overcome by infilling with concrete. In such hybrid systems, the deformation capacity is increased by the combined action between the concrete and the thin-walled FRP tube.

Concrete filled FRP tubes (CFFT) became a popular form of hybrid structural elements in rehabilitation or in new construction. In fact, extensive studies have been conducted to investigate the behaviour of CFFTs for bridge columns and piles applications [4–11]. Most of these studies have proven the ability of this system

to take advantage of the confinement provided by the composite shell to the concrete core and the linear elastic nature of the composite section. Similar research has been conducted to investigate the confinement effect of FRP composite on the concrete core [12,13]. These researches showed that FRP confinement has a significant effect on the behaviour of concrete under axial compression. Consequently, various models have been developed [14,15] to predict the stress–strain behaviour of FRP-confined concrete.

The growing popularity of using concrete filled FRP for compression members has motivated researchers to expand the investigation of the system feasibility for bridge beam applications. Under flexural loading, Roeder et al. [16] found that the concrete infill increases local buckling resistance by stiffening the walls of the FRP tube. Davol et al. [17] performed bending tests of large-scale circular FRP shells filled with 45 MPa concrete. They found that increasing the amount of hoop plies around the specimen prevents the occurrence of local buckling on the compression side. Similarly, Fam and Rizkalla [18] carried out large scale flexural tests on hollow and concrete filled GFRP circular tubes wherein the effect of wall thickness ratios with a range of concrete infill strength between 30 and 60 MPa were examined. They reported that the flexural behaviour of concrete filled GFRP circular tubes is affected by the concrete compressive strength and is highly

\* Corresponding author. Tel.: +61 7 3470 4477; fax: +61 7 4631 2526.

E-mail addresses: [majid.alzaidy@gmail.com](mailto:majid.alzaidy@gmail.com) (M. Muttashar), [allan.manalo@usq.edu.au](mailto:allan.manalo@usq.edu.au) (A. Manalo), [karu.karunasena@usq.edu.au](mailto:karu.karunasena@usq.edu.au) (W. Karunasena), [weena.lokuge@usq.edu.au](mailto:weena.lokuge@usq.edu.au) (W. Lokuge).

dependent on the stiffness and diameter-to-thickness ratio of the tube. Prior to this, Mirmiran and Shahawy [6] conducted experiments to investigate the flexural behaviour of concrete-filled FRP tubes as an alternative to the conventional reinforced concrete elements. In addition, Fam et al. [19] studied the behaviour of CFFT box beam to replace the reinforced concrete beam. The results showed that the performance of the concrete filled beams is similar to or better than the conventional reinforced concrete elements. Chen and El-Hacha [20] introduced a new hybrid bridge girder system fabricated from FRP and ultra-high performance concrete (138 MPa). Their results showed that de-bonding at concrete-FRP interface is the main failure mode and it occurs prior to the expected load for flexural failure. Most recently, Aydin and Sari-biyik [21] studied the effect of the adherence between concrete and GFRP profile on the flexural behaviour using sand particles and epoxy which are pasted in the interior surface of the profile. The results indicated that the flexural strength and fracture toughness significantly increased compared to the hollow GFRP section.

Previous studies focussed on using concrete of compressive strength in a range between 30 and 138 MPa to fill the FRP tubes in order to enhance the overall behaviour of the hybrid beams. To the authors' knowledge, there are no studies conducted investigating the potential use of low strength concrete as an infill to the GFRP tube beams. This study investigates the flexural behaviour of hollow and concrete filled square pultruded GFRP tubes. Four-point static bending test was conducted to evaluate the strength, stiffness and failure mechanisms of the concrete filled pultruded GFRP tubes. An analytical model based on force equilibrium, strain compatibility, linear elastic behaviour of FRP and partial stress-strain confinement model for concrete is adopted to predict the behaviour of the tested beams. The results from the theoretical modelling are then compared with the experiment results.

## 1.2. Research motivation

The importance and suitability of concrete filled FRP tubes for compression members has been demonstrated by many researchers. On the other hand, limited studies have been conducted exploring the use of this hybrid system for flexural members [18,19,22,23]. These studies focussed on using concrete of high compressive strength to fill the FRP tubes. However, the cost of high strength concrete infill did not justify the enhancement in the stiffness and strength capacities of the hybrid beams. This study aims at investigating the influence of concrete infill strength on the flexural behaviour of pultruded GFRP square beams including low strength concrete to determine the optimal compressive strength that will result in enhanced strength and stiffness compared to hollow FRP tubes.

## 2. Experimental program

### 2.1. Properties of GFRP tubes and concrete

Square pultruded GFRP sections (125 mm × 125 mm × 6.5 mm thickness) produced by Wagner's Composite Fibre Technologies (WCFT), Australia were used in this study. The tubes were produced using pultrusion process with vinyl ester resin and E-glass fibre reinforcement. Burnout test conducted as per ISO 1172 [24] revealed that the density and the fibre volume fraction are 2050 kg/m<sup>3</sup> and 78% by weight, respectively. Table 1 shows the mechanical properties of the pultruded GFRP profiles. The elastic modulus and shear modulus of the square pultruded GFRP sections were determined previously by Muttashar et al. [25] and are listed in Table 1. On the other hand, coupon tests were conducted to determine the compressive and tensile strength properties for the sections.

**Table 1**  
Properties of the pultruded GFRP profiles.

Material property	Symbol	Property value	Unit
Density	$\rho$	2050	kg/m <sup>3</sup>
Tensile stress	$\sigma_t$	596	MPa
Tensile strain	$\epsilon_t$	16030	Microstrain
Compressive stress	$\sigma_c$	550	MPa
Compressive strain	$\epsilon_c$	11,450	Microstrain
Elastic modulus	$E$	47.2	GPa
Shear modulus	$G$	4	GPa

**Table 2**  
Details of the test specimens.

Specimen ID	Description Concrete strength (MPa)
H-0	–
H-10	10
H-37	37.5
H-43	43.5

Concrete with three different strengths were used as infill in the pultruded sections. Five plain concrete cylinders have been sampled from each batch of three types of concrete and cured under the same conditions as the beam specimens. The 28 day average compressive strengths for the three types of concrete were 10, 37.5 and 43.5 MPa, respectively.

### 2.2. Test specimens

In the experimental works, three hollow GFRP sections and six filled sections were used to investigate the flexural behaviour. The total length of the beams was 2000 mm. Table 2 shows the details of specimens' identification and concrete strength. The specimens were identified using the code listed in the table. The term H-0 indicates the hollow geometry, whereas, H-10, H-37 and H-43 represent GFRP beams filled with concrete having 10, 37 and 43 MPa compressive strength respectively.

### 2.3. Instrumentation and test setup

Four-point bending test was performed over a simply supported clear span of 1800 mm following the ASTM D7250 [26]. The load was applied at two points with a load span of 300 mm. Fig. 1 shows the details of the experimental set up. The load was applied using a 400 kN capacity universal testing machine at a load rate of 3 mm/min. Steel plates were provided at the support and loading points to minimise indentation failure. Four uniaxial strain gauges (types PFL-20-11-1L-120) were used to measure the strain on the top and bottom faces of the beam. The mid-span deflection was measured using a laser displacement transducer. The applied load and the displacement were recorded using "System 5000" data acquisition system. All specimens were tested up to failure to observe the failure mechanisms of the beam.

## 3. Test results and discussion

### 3.1. Load–deflection behaviour

The load–displacement behaviour of the tested beams is presented in Fig. 2. As expected, the hollow beams (H-0) showed a linear elastic behaviour until failure at a load of 80.8 kN and a corresponding mid-span deflection of 39.5 mm. Consequently, the average ultimate flexural stress at the top and bottom of the tested beams was 291 MPa. This value is approximately 45% and

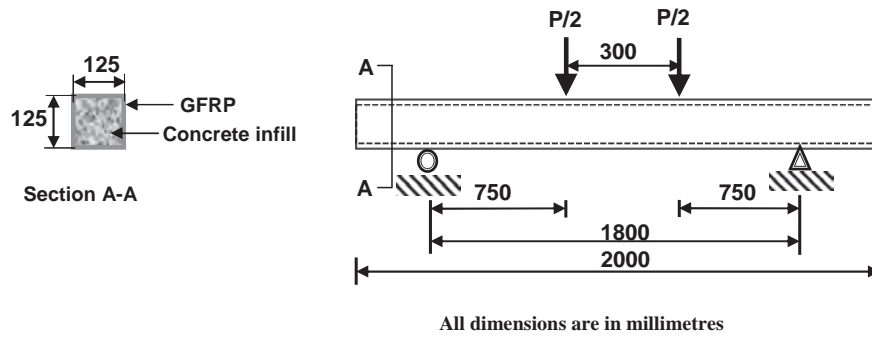


Fig. 1. Details of experimental set up.

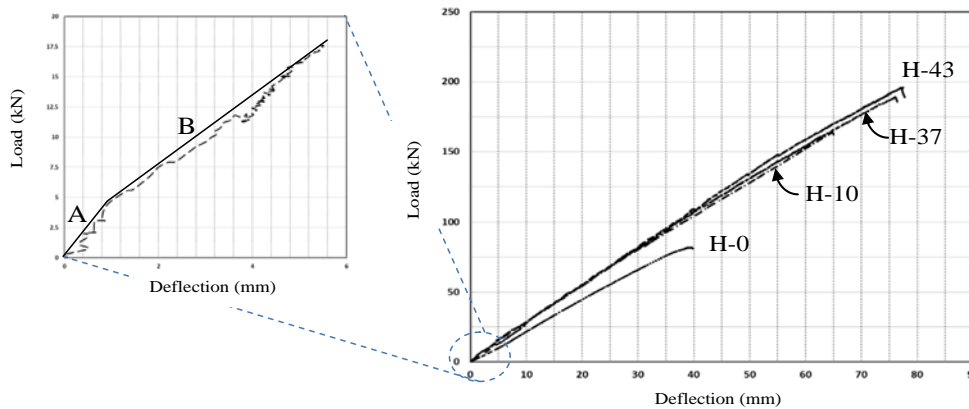


Fig. 2. Load-displacement behaviour of the tested beams.

39% of the compression and tension failure stresses determined from coupon test of the GFRP profile, respectively. The ultimate strength of the GFRP profile was not achieved due to the compressive buckling of the top flange at the constant moment region which led to separation of the web-flange junction, followed by premature buckling, delamination and crushing in the web as shown in Fig. 3. On the other hand, bilinear load–deflection curves were observed for GFRP beams with concrete infill. However, the first part of the curves is insignificant as it forms approximately 3% of the total value (segment A of the curve) as shown in Fig. 2. The curve starts with a high stiffness as the entire concrete cross section is effective. However, once the flexural tensile cracking occurred, the stiffness was reduced but remained almost constant until failure. The H-10, H-37 and H-43 beams failed at an applied load of 163 kN, 189 kN and 195 kN, respectively, as shown in Fig. 2.

There was a significant increase (100–141% higher) in the flexural strength for the filled sections in comparison to those of the hollow sections for all concrete types. This increase reflects the contribution of the concrete core to the section's capacity by

restricting and delaying the local buckling of the GFRP tube, thereby increasing the section ductility and strength. With the increase in concrete strength from 10 to 43.5 MPa (335% increase), however, the improvement in sections' strength is only 19%. This is attributed to two important factors. Firstly, the brittleness of concrete increases with increasing strength, which changes the concrete crack patterns from heterogenic micro-cracks to localised macro-cracks. Secondly, the overall behaviour of the filled beams was controlled by the behaviour of the outside tube. With the internal support provided by concrete core, the pultruded profile is more stable and has smaller tendency to buckle which results in a higher load carrying capacity than hollow tubes. These results are in good agreement with the results reported by Vincent and Ozbakkaloglu [27] when they studied the influence of concrete strength on axial compressive behaviour of FRP tubes filled with normal, high and ultra-high strength concrete. They concluded that the axial performance of FRP-confined concrete reduces as the concrete strength increases. From the current study, this result suggests that the effect of the compressive strength (for 10–43.5 MPa) of infill on the section capacity and stiffness is minimal for the tested beams. This finding is in contrast with the parametric study conducted by Fam and Rizkalla [18]. They reported that increasing the compressive strength of concrete from 20 to 80 MPa resulting in decreasing of the section capacity with noticeable increase in the stiffness. The reported difference in behaviour is more likely to be due to their assumption of using unconfined stress–strain concrete model to predict the behaviour. Fig. 4 shows the strain distribution through the depth of the section at mid-span which clearly shows that the neutral axis depth is higher for lower concrete strength and lower for higher compressive strength. It is obvious that modulus of elasticity becomes higher for high strength concrete however the moment of inertia becomes

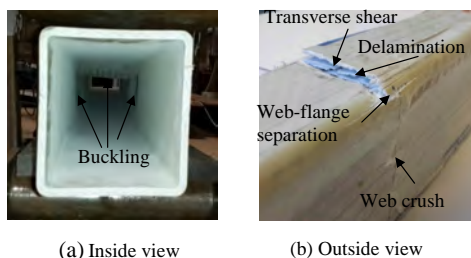


Fig. 3. Failure mode of hollow beams.

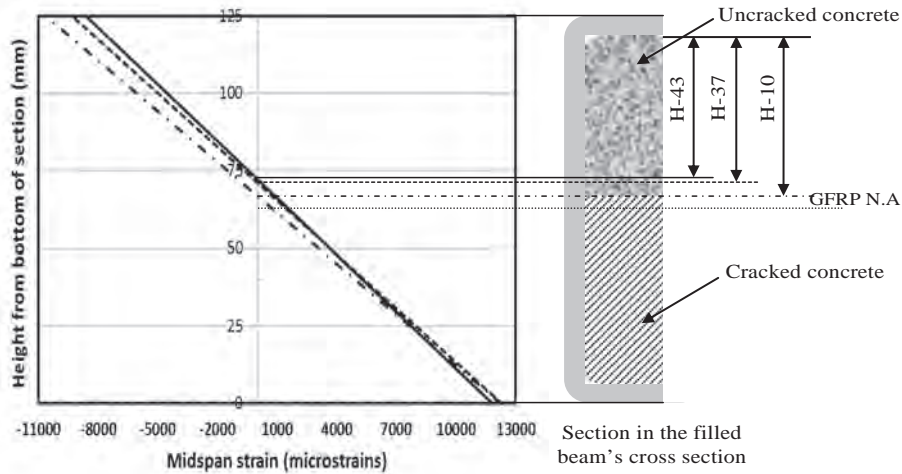


Fig. 4. Mid-span strain distribution at moment capacity of 60 (kN m) for all beams.

lower due to the changes of the neutral axis depth. For example, the neutral axis depth is at a distance of 58 mm from the top of the section for H-10, 53.5 mm for H-37 and 51.5 mm for H-43, at 60 kN m moment capacity. It is noted that 60 kN m moment capacity corresponds to a 160 kN applied load. This result also suggests that the area of concrete contributing to compressive force is lower for a higher strength than a lower strength concrete to achieve internal force equilibrium. Consequently, the ultimate load of the beam is slightly affected by the concrete compressive strength. Even reaching the maximum compressive stress in concrete, the concrete core remains intact and stabilises the hollow GFRP profile until the failure causing some crushing for H-43. This behaviour demonstrates that some level of confinement in concrete is present.

Fig. 5 shows the flexural stiffness of hollow and concrete filled (uncracked and cracked) beams. The average flexural stiffness,  $EI$  of the hollow section is  $2.38 \times 10^{11} \text{ N mm}^2$ . This value was calculated using the equation:

$$EI = \frac{Pa}{48\Delta} (3L^2 - 4a^2) \quad (1)$$

where  $EI$  is the effective flexural stiffness in  $\text{N mm}^2$ ;  $P$  is the applied load in N;  $a$  is the shear span which is the distance between the sup-

port and the nearest point load in mm;  $\Delta$  is the mid-span deflection in mm; and  $L$  is the span in mm. As mentioned earlier in this section, due to the trivial ratio of the first part of the curves in Fig. 3, Eq. (1) can be used to calculate the flexural stiffness of the infilled sections. The uncracked flexural stiffness of the filled beams is  $3.19 \times 10^{11} \text{ N mm}^2$  for 10 MPa concrete and  $4.19 \times 10^{11} \text{ N mm}^2$  for 43 MPa concrete. This result showed that the flexural stiffness of beams with uncracked concrete infill is higher by 34, 55 and 75% for 10, 37 and 43 MPa, respectively, compared to the hollow section. On the other hand, the flexural tensile cracking of the concrete core results in a section with a reduced moment of inertia. In this condition, the flexural stiffness of the beam for all concrete strengths is approximately 26% higher than the hollow section. Interestingly, the flexural stiffness of the beams with concrete infill is almost same. This can be explained by the extent of the depth of the cracked concrete as explained previously. It can also be seen in Fig. 4 that at specific load level, H-10 showed higher compression strain reading compared with H-37 and H-43 while the tension strain seems to be similar for all concrete types. Compared with H-37 and H-43, higher strain reading for H-10 resulting from higher deflection experienced by this beam can be observed. With an increase in the applied load there is an increase in the deflection of the filled beams. The results show that at the specific load level, the mid-span deflection were 60.6, 62.3 and 63.9 mm for H-10, H-37 and H-43, respectively. The main reason for this behaviour is the difference in modulus of elasticity of the concrete core. This is evident from the experimental results that filling the tube with low strength concrete resulted in higher curvature compared with other concrete strengths as shown in Fig. 6. On the other hand, it should be noted that due to the effect of the cracked section, the bottom fibre showed approximately similar tensile strain reading which result in different compression strain values to maintain the balance of the internal forces depending on the strength of the concrete core. This behaviour explains the slightly lower failure load of H-10 compared to H-37 and H-43. Consequently, the beam failed when the top fibre of the GFRP tube reaches a compressive strain near or equal to the maximum compressive strain determined from the coupon test.

### 3.2. Strain response

Fig. 7 shows the load and strain (at mid span at the topmost and bottom most section) relationship of the hollow and concrete filled beams. It can be seen that the hollow section failed at a compress-

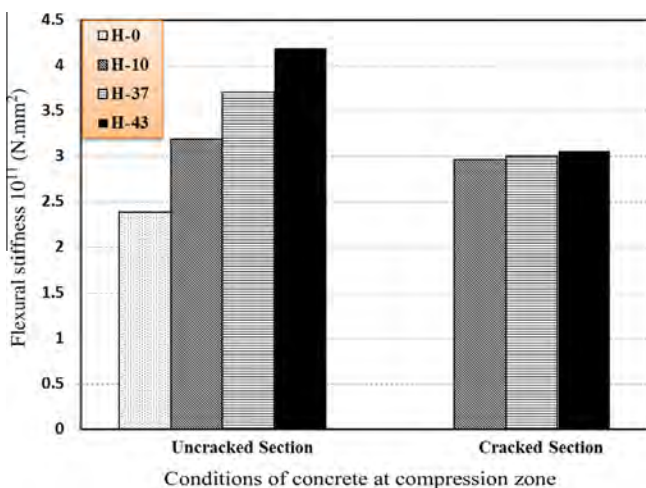


Fig. 5. Comparison of flexural stiffness.

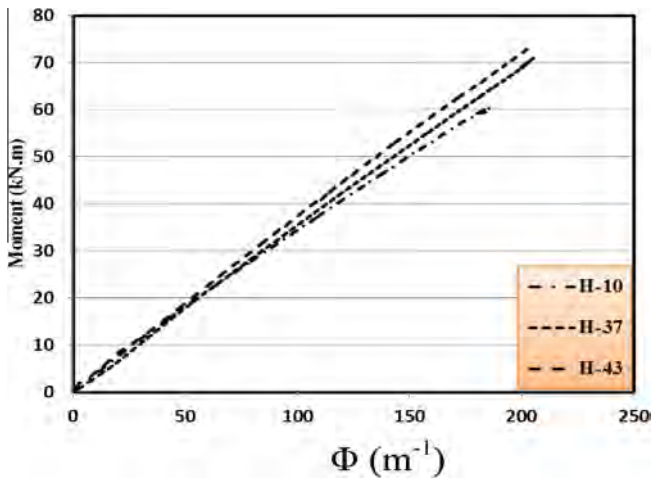


Fig. 6. Moment-curvature behaviour of the tested beams.

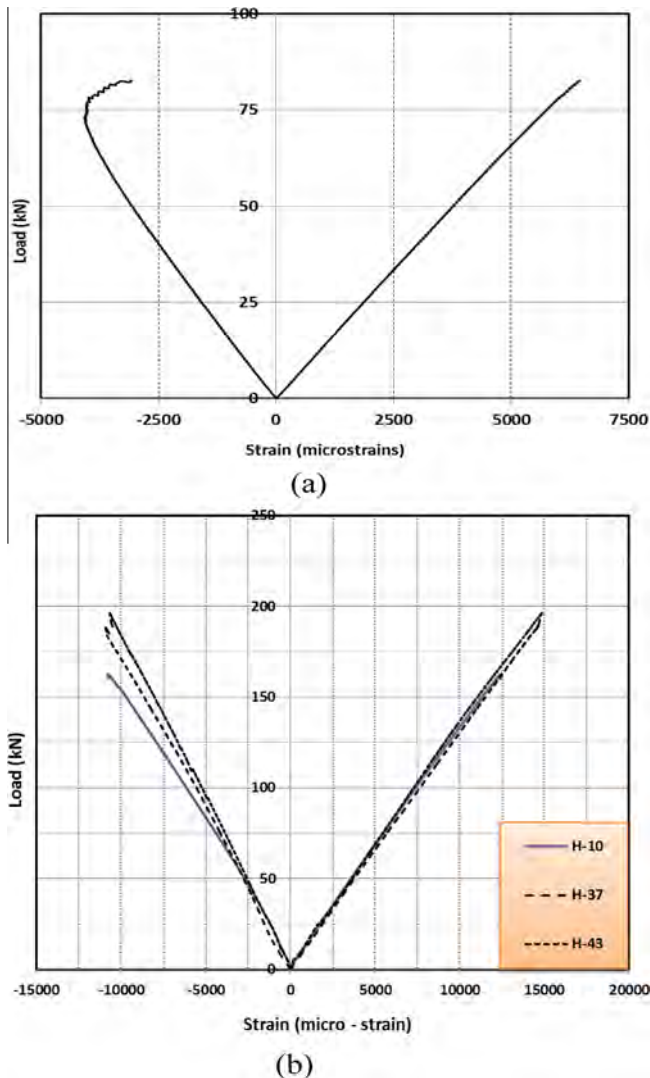


Fig. 7. Load-strain behaviour of the tested beams: (a) hollow, (b) filled.

sive strain of 3140 microstrains and tensile strain of 6100 microstrains. With increasing load, however, the measured strain tend to become positive indicating that the top surface is shifting from compression to tension as shown in Fig. 7a. This behaviour

indicates the initiation of the local buckling of the tube. For beams with concrete infill, a slight decrease in stiffness at a tensile strain of 140 microstrains (load between 3.1 and 4.4 kN) was observed. This decrease in stiffness can be related to the initiation of tensile cracks in the concrete core. The filled sections failed at tensile strains of 12,400, 14,800 and 14,820 microstrains for H-10, H-37 and H-43, respectively as shown in Fig. 7b. These strain levels were approximately 77, 92 and 93% of the maximum strain of pultruded section determined from the test of coupons (Table 1). Thus, it is concluded that no tension failure had occurred at the onset of the final failure. On the other hand, the maximum measured compression strains were 11,100, 11,200 and 11,250 microstrains for H-10, H-37 and H-43, respectively. These values are 97, 98 and 98.5% of the ultimate compressive strains of the pultruded GFRP tubes which indicates that the filled sections failed at onset of the compression failure. Furthermore, the slight differences between the failure compression strains of the filled sections indicate that for all concrete strengths, the concrete core prevents the occurrence of premature local buckling and supported the top wall of the section. As a result, the section failed at strain of 11200 microstrains which represents the highest compression strain achieved in coupon tests. It can also be noticed from Fig. 7 that there was no clear drop in the curve until failure with good strain distribution on both sides indicating that there was no major slip occurred between concrete and the GFRP tube.

### 3.3. Failure mode

Fig. 8(a–d) shows the typical mode of failure of the hollow and filled beams tested under 4-point bending. The experimental results illustrate that the hollow beams failed in a brittle manner. The failure started at the web-flange junctions and followed by premature buckling and crushing in the webs as shown in Fig. 8a. Similar behaviour has been reported in the literature [25,28,29] on flexural behaviour of 125, 100, 76 mm square pultruded GFRP beams. The main reason for this failure is the local buckling in the thin wall which results in material delamination and cracking of the fibres along the edges of the beam under the load application.

Fig. 8(b), (c) and (d) show the failure modes of GFRP beams filled with 10, 37.5 and 43.5 concrete strength, respectively. The failure of all filled beams was due to flexural compression at the constant moment region including cracks in the fibres in the transverse direction. It was observed that delamination crack happened at the compression surface which later progressed into the sides. The complete failure occurred after the fibre cracking in the compression side (at strain level approximately 11,200 microstrains). This strain level is far greater than the failure strain of the hollow section (3140 microstrains) which indicates that the concrete infill prevented the occurrence of local buckling.

The crack pattern in the concrete core was examined by carefully removing the GFRP tube after failure as shown in Fig. 9. The figure clearly shows that flexural cracks were developed at the bottom of the beam between the loading points. Also, the cracks propagated up to the depth of the concrete infill. H-37 and H-43 beams showed distinct flexural cracks as shown in Fig. 9b and c whereas H-10 beam shows fine cracks as can be seen from Fig. 9a. A similar behaviour was reported by Vincent and Ozbakkaloglu [27] and it can be attributed to the brittleness of concrete which increases with increasing concrete compressive strength. As a result, the concrete crack pattern changes from fine microcracks to localised macrocracks. It is also interesting to note that although the complete failure occurred at a strain level of 11,200 microstrains (which is too far away from concrete compression strain of 3000 microstrains), there was no concrete crushing observed at the compression side except the case of section H-43 which might have

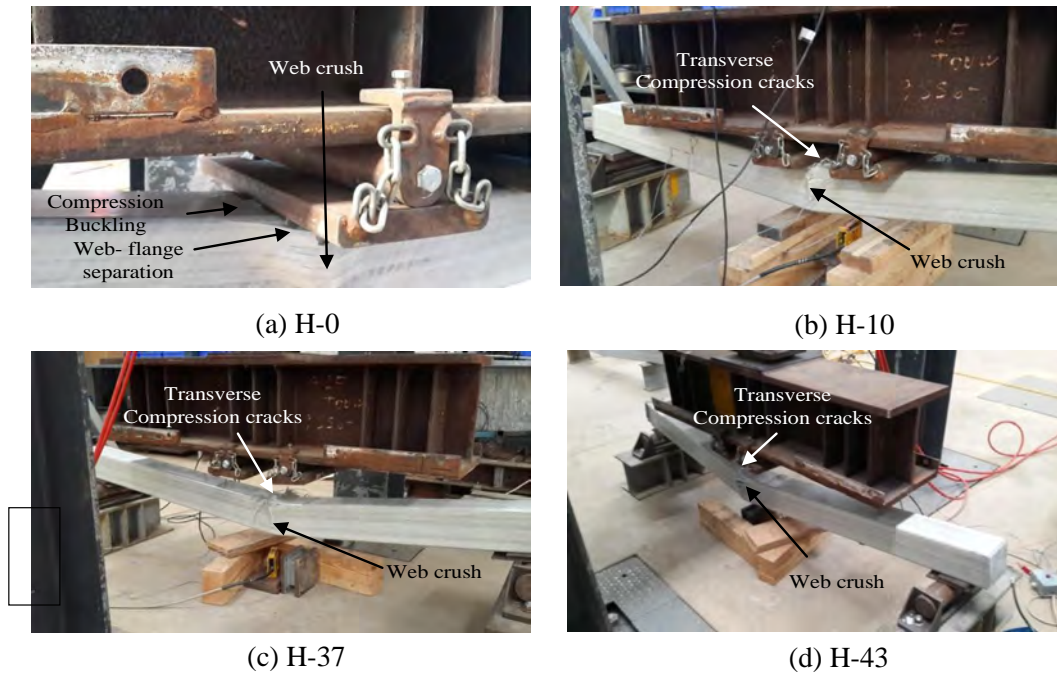


Fig. 8. Failure modes of the tested beams.

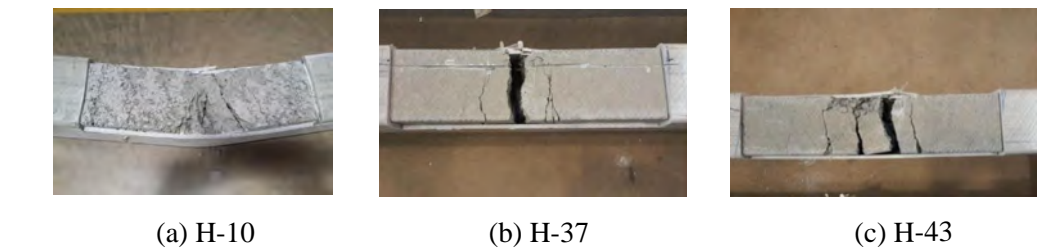


Fig. 9. Crack pattern at failure of the tested beams.

happened after the final failure. This suggests that there is a partial confinement by the GFRP section which in turn kept the concrete under compression intact until failure of the tube.

#### 4. Theoretical analysis

##### 4.1. Analytical model

Fibre Model Analysis (FMA) implemented previously [30] for the analysis of sandwich composite beams is used to predict the flexural behaviour of the concrete filled GFRP beams. The analytical model (as shown in Fig. 10) involves the determination of the position of the neutral axis for a given strain of the extreme compression fibre by using the principles of strain compatibility and cross sectional forces equilibrium. The analytical procedure starts by dividing the cross-section into a number of layers. Based on the appropriate stress-strain model for each material, the stress for each layer is determined depending on the corresponding strain. The internal force at each layer is then calculated by multiplying the stress by the area of layer and the bending moment is obtained by multiplying the force by the distance of the layer from the neutral axis of the section. Using this procedure, the flexural behaviour is determined, and then compared with experimental results.

The assumptions in the analysis include:

- (1) Euler–Bernoulli beam theory.
- (2) Strain distribution throughout the depth of the section is linear.
- (3) Perfect bond between pultruded section and the concrete core.
- (4) Confinement effect is considered.
- (5) Cracked analysis is implemented.
- (6) Pultruded GFRP section behaves linear elastically until failure.
- (7) Stress–strain curve for the GFRP tube was based on full section behaviour (Fig. 11).

The confinement effect plays an important role in choosing the appropriate stress–strain behaviour for concrete. This is considered in the analysis of the flexural behaviour of the concrete filled GFRP tubes. The existing design-oriented stress–strain models for FRP-confined concrete typically followed a bilinear stress–strain curve [31–33]. The bilinear curve consists of a parabolic ascending branch followed by straight line to describe both the ascending and descending branches of the stress–strain curves of confined concrete [34,35]. The parabolic portion is commonly used in several codes of practice such as BS 8110 and Eurocode 2 [35] which was originally proposed by Kent and Park [36]. This curve used to describe the ascending portion of the stress–strain curve of unconfined concrete given by the following equation.

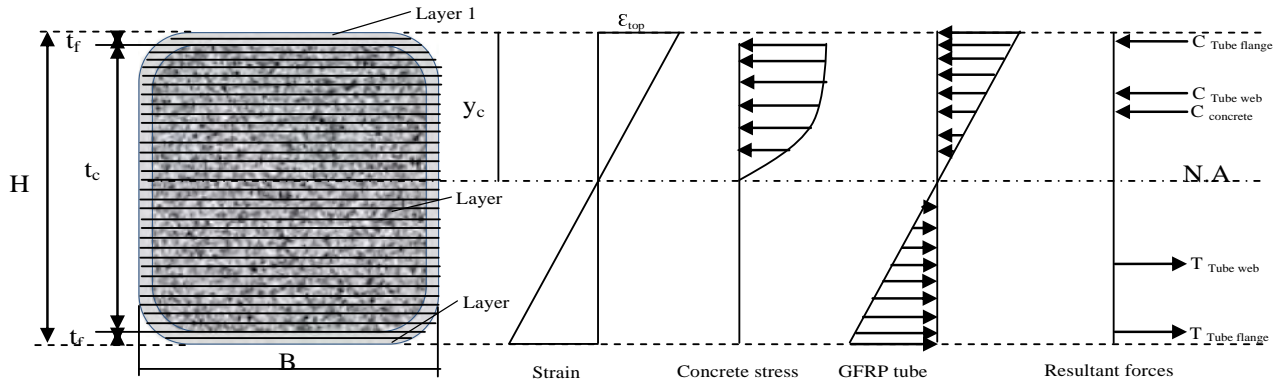


Fig. 10. Assumed strain and stress distribution in the FMA.

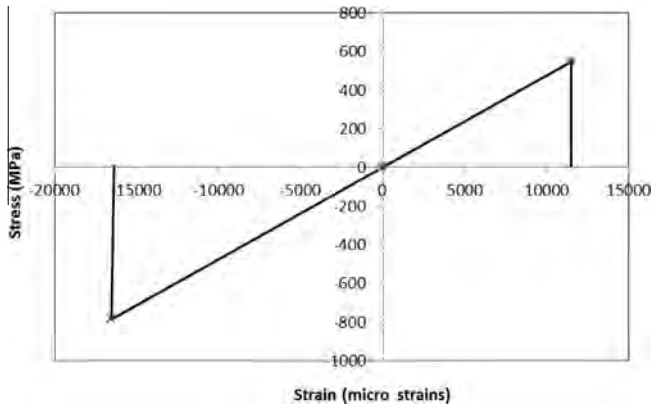


Fig. 11. Stress-strain model for GFRP tube.

branch following [40] which provides the lower bound for the variable confinement model as described in the following equation:

$$\sigma_c = f'_{co} \quad \text{when} \quad \epsilon_c > \epsilon_{co} \quad (3)$$

The partial confinement model is thus described by Eqs. (2) and (3) as shown in Fig. 12. Same model was proposed [38] for hybrid FRP-concrete-steel double skin tubular sections under bending which showed close predictions with the test results. Based on the experimental observations, the ductility and strain of concrete are increased significantly beyond 0.003. It is also well established that failure of concrete filled FRP tubes system is normally governed by local buckling failure of the FRP tube in the compression region before complete failure of the concrete inside. For this failure mode,  $\epsilon_{co}$  can be conservatively assumed to be equal to the design ultimate axial strain obtained from the axial compression tests of hollow FRP tubes due to the fact that the failure strain of the FRP tubes in the filled beams is more than that of hollow tubes.

$$\sigma_c = f'_{co} \left[ \frac{2\epsilon_c}{\epsilon_{co}} - \left( \frac{\epsilon_c}{\epsilon_{co}} \right)^2 \right] \quad \text{when} \quad \epsilon_c \leq \epsilon_{co} \quad (2)$$

where  $\sigma_c$  in MPa and  $\epsilon_c$  represent the stress and strain, respectively, while  $f'_{co}$  in MPa and  $\epsilon_{co}$  are the unconfined concrete cylinder strength and the corresponding strain, respectively. For the definition of the linear second part of the curve, several researches were conducted to determine its slope. In fact, all the conducted research agreed that the FRP confinement is activated once micro-cracks in concrete are initiated under loading which means it is important to determine the correct slope of the second part. Existing studies shows that due to the presence of a strain gradient over the section in flexural, the confinement of FRP to concrete is less effective in sections under bending than in sections under compression [18,37]. However, it is still significant and important to be considered in predicting the load-carrying capacity of the CFFTs [38,39]. Fam et al. [40] suggested that for sections under pure bending unconfined stress-strain curve can be used by considering the effect of strain gradient on the effectiveness of concrete confinement. As a result, they recommended using an ultimate strain higher than that of unconfined concrete, however, their direct use of unconfined stress-strain concrete model result in underestimation of the load-carrying capacity of the filled beams.

In the present study, a similar elastic modulus in both tension and compression has been assumed for the concrete. Tensile cracking was assumed to occur at a tensile strain of 120 microstrains for H-10, H-37 and H-43, respectively. The contribution of the concrete in tension is neglected after tensile cracking. Partial confinement model is used in this study which is composed of a parabolic ascending branch following [34] and a horizontal (zero slope)

#### 4.2. Failure load prediction

The cracking and failure load of the hollow and filled sections were predicted using FMA described in the previous section. In the experimental program, it was observed that the compression failure of the hollow and filled pultruded sections is the dominant mode of failure. For hollow sections, the top fibre compression strain reached 6100 microstrains while the corresponding strain was 11,200 microstrains for the filled sections regardless of the concrete compressive strength. The main reason for the failure of the hollow GFRP profile at lower strain is the local buckling effect. Introducing the concrete infill to the section prevented the local

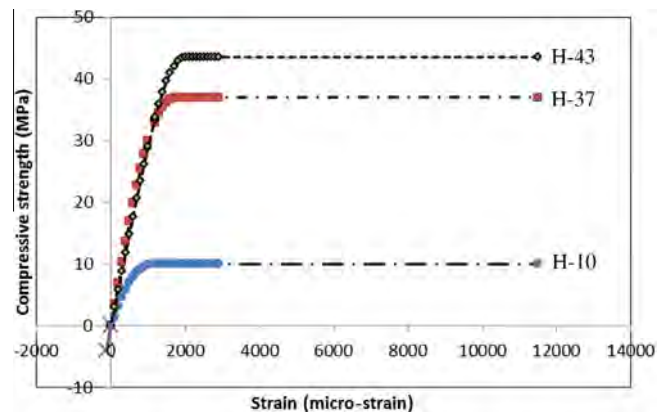


Fig. 12. Stress-strain model for confined concrete.

**Table 3**  
Experimental and predicted failure load of hollow and filled pultruded section.

Sample designation	Experimental load kN		Theoretical prediction kN	
	Cracking	Failure	Cracking	Failure
H-0	–	80.8	–	80.7
H-10	3.1	163	2.98	162.6
H-37	4.25	189	4.2	188.5
H-43	4.38	195	4.28	193.4

buckling of the GFRP tube. As a result, the compression strain reached its highest value. The cracking load was predicted as the load corresponding to a strain of 120 microstrains which was calculated based on the cracking strength of concrete and the modulus of elasticity of the concrete. According to the Australian standard AS 3600 [41], the cracking strength of concrete  $f_{cr}$  in MPa can be calculated as follows:

$$f_{cr} = 0.6\sqrt{f'_c} \tag{4}$$

where  $f'_c$  is the concrete compressive strength at 28 days in MPa. Table 3 shows the predicted cracking and failure loads along with corresponding values. Partial confinement model using Eqs. (2) and (3) has been used to simulate the stress–strain behaviour of the concrete core.

The results indicate that the failure loads of the concrete filled beams can be predicted well using the elastic properties of the full-section GFRP profile and the strength properties determined from coupon tests together with the use of the partial confinement stress–strain model. The predicted cracking and failure loads of all specimens are less than 1% different from the measured values.

4.3. Load–deflection relationship

The FMA was extended to predict the load–deflection behaviour of the hollow and filled pultruded sections using shear deformation theory proposed by Timoshenko in 1921 [42]. In this theory, the contribution of bending and shear deflection has been account for in calculating total deflection. The total deflection at mid span in a simply supported beam under four-point bending can be calculated by:

$$\Delta = M \left[ \frac{a^2}{3EI} + \frac{1}{2EI} \left( \frac{L^2}{4} - a^2 \right) \right] + \frac{Pa}{2KGA} \tag{5}$$

where  $\Delta$  is the deflection at mid span in mm,  $M$  is the applied moment in N mm,  $EI$  is the flexural stiffness in N mm<sup>2</sup>,  $GA$  is the shear stiffness (or transverse shear rigidity) in  $N$  and  $K$  is the shear coefficient. Two configurations of the test specimen-hollow and filled-have been used. As a consequence, two different  $K$  values need to be implemented in the calculations. For homogenous and hollow box profile,  $K$  was calculated using the equation recommended by Bank [43]:

$$K = \frac{80}{192 + (-12 * \nu * G/E)} \tag{6}$$

where  $E$  is the modulus of elasticity in MPa,  $G$  is the shear modulus in MPa and  $\nu$  is the Poisson's ratio. It is well known that the transverse shear rigidity is a function of the shear flow across the section, which depends on the thickness of the cross section. As a result, due to the change of the section configuration from hollow to filled, all cross section is assumed to contribute in the shear deflection calculation. Thus, a value of  $K = 1$  is used for the case of filled section. In Eq. (6),  $\nu$ ,  $G$  and  $E$  refer to the longitudinal Poisson's ratio, shear modulus in MPa and Modulus of Elasticity of the section in MPa, respectively. Fig. 13(a–d) shows comparisons between the

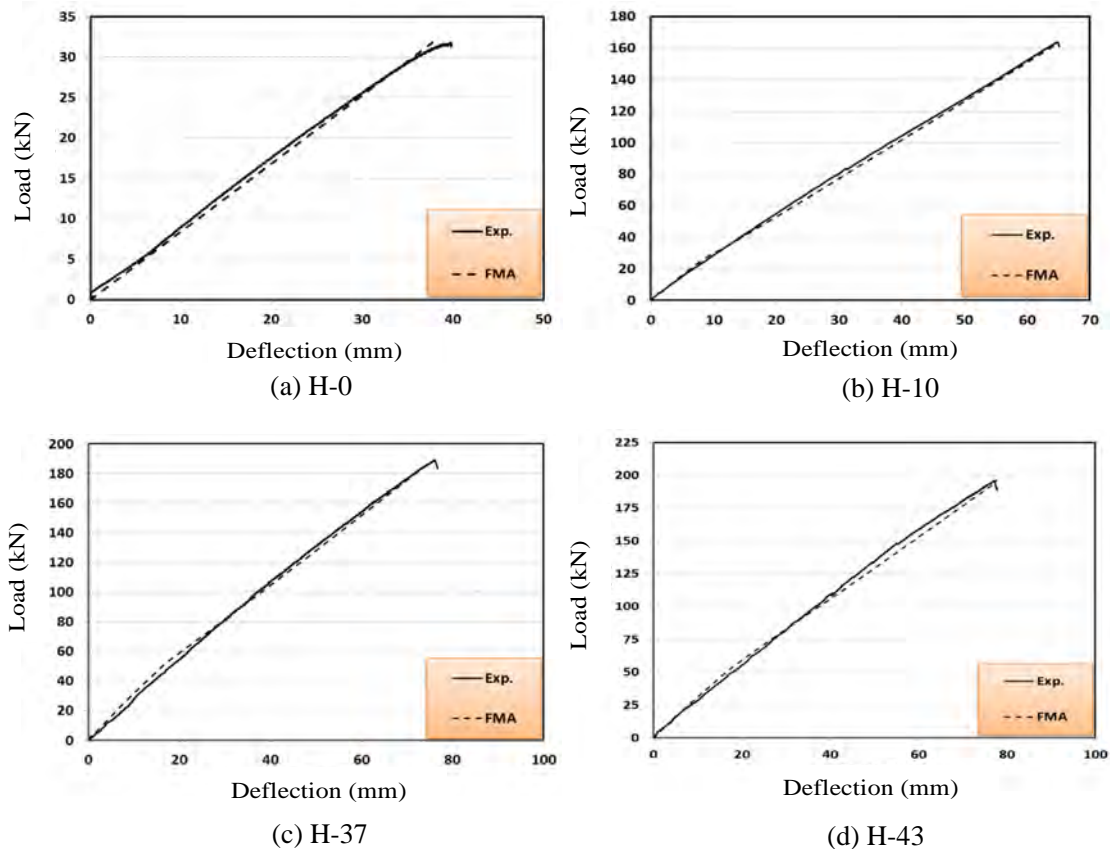


Fig. 13. Comparisons of mid span load–deflection curves.

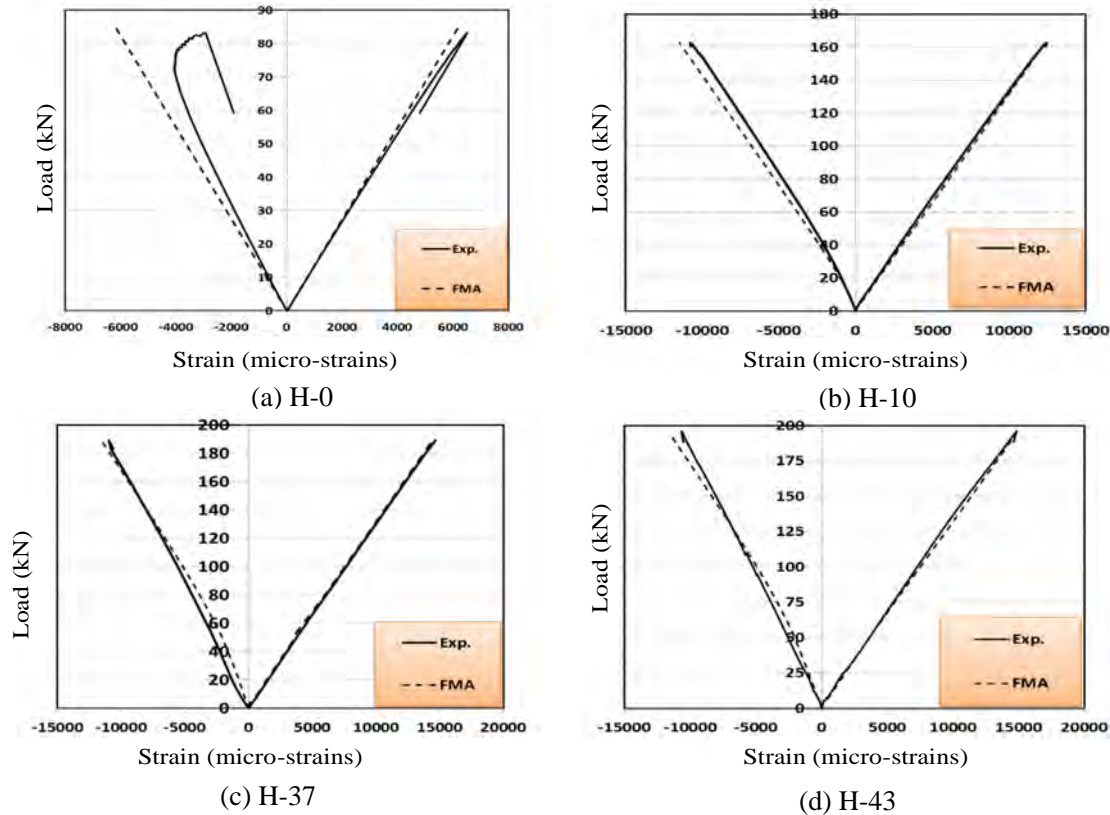


Fig. 14. Comparisons of load–strain curves.

predicted and the experimental mid span load–deflection curves for the hollow and filled beams. Using GFRP properties determined from the full scale test and concrete properties, the theoretical results agree well with the experimental test results up to failure. The figure shows that the difference between the theoretical and the experimental results are less than 1% for all beams. Similarly, it is evident from the curves that the assumed value of  $K = 1$  for beams with concrete infill was valid for all concrete strength.

#### 4.4. Load–strain relationship

Fig. 14(a–d) shows comparisons of predicted and experimental load–strain curves for hollow and filled sections. The strain values presented are those of the extreme fibre at the mid-span. The experimental results shows a linear relationship in tension and bilinear in compression side. For the hollow section, there is a slight difference between the analytical and the experimental results in the compression side. The main reason for this divergence is the effect of local buckling which is not considered in the theoretical model. On the other hand, the analytical results agree well with predicted load–strain relation in tension.

The good agreement between the analytical and experimental results for all concrete types confirms the validity of the partial confined model in predicting the load–strain relation. Similarly, the load–strain relationship shows a higher strain in the tension compared with compression side, which confirms the tensile cracking of the concrete and decreasing its contribution in the flexural stiffness. Finally, the assumption of compatibility of strains through the depth of the section and the equilibrium of the internal force resultants are valid.

## 5. Conclusions

This study has presented the results of four point bending tests on hybrid concrete filled GFRP tubes. The main parameter examined in this study is the compressive strength of concrete core. A simple theoretical model was implemented and used to predict the behaviour of the tested beams. Based on the results, the following conclusions can be drawn:

- Hollow beams failed due to premature buckling and web crushing of the GFRP tube at 291 MPa. This level of stress is only 45% of the compressive strength determined from the coupon tests.
- The concrete filled GFRP sections failed at a load 100–141 % higher than its hollow counterpart and exhibited 25% higher stiffness. The failure of these beams was compressive failure of the GFRP tube at a strain similar to the compressive strain determined from the coupon tests.
- The increase in concrete compressive strength from a low 10 MPa to a high strength 43.5 MPa increased the ultimate load by 19%. Similarly, the flexural stiffness of the beam with concrete infill is almost the same after the initiation of the flexural tension cracks in the concrete core.
- Use of low strength concrete can be considered as a practical solution to fill the GFRP tubes to prevent local buckling and improve the overall flexural behaviour.
- The simplified Fibre Model Analysis can accurately predict the flexural behaviour of the hollow and concrete filled GFRP tubes. For the hybrid beams, partial confinement of the concrete infill should be considered.

- The theoretical prediction of the concrete cracking and the failure loads for the concrete filled GFRP tubes using the elastic properties of the full-section GFRP tubes and the strength properties determined from the coupon test is in close agreement with the experimental results.

## Acknowledgements

The authors are grateful to Wagner's Composite Fibre Technologies (WCFT), Australia for providing all the GFRP tubes in the experimental programme. The first author would like to acknowledge the financial support by the Ministry of Higher Education and Scientific Research-Iraq.

## References

- [1] Hollaway L. A review of the present and future utilisation of FRP composites in the civil infrastructure with reference to their important in-service properties. *Constr Build Mater* 2010;24:2419–45.
- [2] Ascione L, Berardi VP, Giordano A, Spadea S. Buckling failure modes of FRP thin-walled beams. *Compos B Eng* 2013;47:357–64.
- [3] Neto A, Rovere H. Flexural stiffness characterization of fiber reinforced plastic (FRP) pultruded beams. *Compos Struct* 2007;81:274–82.
- [4] Fam AZ, Rizkalla SH. Confinement model for axially loaded concrete confined by circular fiber-reinforced polymer tubes. *ACI Struct J* 2001;98.
- [5] Fam AZ, Rizkalla SH. Behavior of axially loaded concrete-filled circular fiber-reinforced polymer tubes. *ACI Struct J* 2001;98.
- [6] Mirmiran A, Shahawy M. A new concrete-filled hollow FRP composite column. *Compos B Eng* 1996;27:263–8.
- [7] Mohamed HM, Masmoudi R. Axial load capacity of concrete-filled FRP tube columns: experimental versus theoretical predictions. *J Compos Constr* 2010;14:231–43.
- [8] Ozbakkaloglu T. Axial compressive behavior of square and rectangular high-strength concrete-filled FRP tubes. *J Compos Constr* 2012;17:151–61.
- [9] Ozbakkaloglu T, Oehlers DJ. Concrete-filled square and rectangular FRP tubes under axial compression. *J Compos Constr* 2008;12:469–77.
- [10] Ozbakkaloglu T. Concrete-filled FRP tubes: manufacture and testing of new forms designed for improved performance. *J Compos Constr* 2012;17:280–91.
- [11] Ozbakkaloglu T, Akin E. Behavior of FRP-confined normal-and high-strength concrete under cyclic axial compression. *J Compos Constr* 2011;16:451–63.
- [12] Xiao Y, Wu H. Compressive behavior of concrete confined by carbon fiber composite jackets. *J Mater Civ Eng* 2000;12:139–46.
- [13] Teng J, Lam L. Behavior and modeling of fiber reinforced polymer-confined concrete. *J Struct Eng* 2004;130:1713–23.
- [14] Yu T, Teng J. Design of concrete-filled FRP tubular columns: provisions in the Chinese technical code for infrastructure application of FRP composites. *J Compos Constr* 2010.
- [15] Binici B. An analytical model for stress–strain behavior of confined concrete. *Eng Struct* 2005;27:1040–51.
- [16] Roeder CW, Lehman DE, Bishop E. Strength and stiffness of circular concrete-filled tubes. *J Struct Eng* 2010;136:1545–53.
- [17] Davol A, Burgueno R, Seible F. Flexural behavior of circular concrete filled FRP shells. *J Struct Eng* 2001;127:810–7.
- [18] Fam AZ, Rizkalla SH. Flexural behavior of concrete-filled fiber-reinforced polymer circular tubes. *J Compos Constr* 2002;6:123–32.
- [19] Fam A, Cole B, Mandal S. Composite tubes as an alternative to steel spirals for concrete members in bending and shear. *Constr Build Mater* 2007;21:347–55.
- [20] Chen DS, El-Hacha R. Flexural behaviour of hybrid FRP-UHPC girders under static loading. In: Proceedings of 8th International Conference on Short and Medium Span Bridge Niagara Falls, Canada; 2010.
- [21] Aydin F, Saribiyik M. Investigation of flexural behaviors of hybrid beams formed with GFRP box section and concrete. *Constr Build Mater* 2013;41:563–9.
- [22] Fam A, Flisak B, Rizkalla S. Experimental and analytical modeling of concrete-filled fiber-reinforced polymer tubes subjected to combined bending and axial loads. *ACI Struct J* 2003;100.
- [23] Mohamed HM, Masmoudi R. Flexural strength and behavior of steel and FRP-reinforced concrete-filled FRP tube beams. *Eng Struct* 2010;32:3789–800.
- [24] ISO 1172. Textile-glass-reinforced plastics, prepegs, moulding compounds and laminates: Determination of the textile-glass and mineral-filler content-Calcination methods; 1996.
- [25] Muttashar M, Karunasena W, Manalo A, Lokuge W. Behaviour of hollow pultruded GFRP square beams with different shear span-to-depth ratios. *J Compos Mater* 2015. 0021998315614993.
- [26] ASTM D7250. ASTM D7250/D7250M-06 Standard practice for determine sandwich beam flexural and shear stiffness. West Conshohocken, (PA): ASTM International; 2006.
- [27] Vincent T, Ozbakkaloglu T. Influence of concrete strength and confinement method on axial compressive behavior of FRP confined high- and ultra high-strength concrete. *Compos B Eng* 2013;50:413–28.
- [28] Guades E, Aravinthan T, Islam MM. Characterisation of the mechanical properties of pultruded fibre-reinforced polymer tube. *Mater Des* 2014;63:305–15.
- [29] Kumar P, Chandrashekhara K, Nanni A. Structural performance of a FRP bridge deck. *Constr Build Mater* 2004;18:35–47.
- [30] Manalo A, Aravinthan T, Karunasena W, Islam M. Flexural behaviour of structural fibre composite sandwich beams in flatwise and edgewise positions. *Compos Struct* 2010;92:984–95.
- [31] Fardis MN, Khalilii HH. FRP-encased concrete as a structural material. *Mag Concr Res* 1982;34:191–202.
- [32] Samaan M, Mirmiran A, Shahawy M. Model of concrete confined by fiber composites. *J Struct Eng* 1998.
- [33] Saafi M, Toutanji H, Li Z. Behavior of concrete columns confined with fiber reinforced polymer tubes. *ACI Mater J* 1999;96.
- [34] Hognestad E. Study of combined bending and axial load in reinforced concrete members. University of Illinois Engineering Experiment Station Bulletin; no 399; 1951.
- [35] Lam L, Teng J. Design-oriented stress–strain model for FRP-confined concrete. *Constr Build Mater* 2003;17:471–89.
- [36] Kent DC, Park R. Flexural members with confined concrete. *J Struct Div* 1971;97:1969–90.
- [37] Wu Z, Li W, Sakuma N. Innovative externally bonded FRP/concrete hybrid flexural members. *Compos Struct* 2006;72:289–300.
- [38] Yu T, Wong Y, Teng J, Dong S, Lam E. Flexural behavior of hybrid FRP-concrete-steel double-skin tubular members. *J Compos Constr* 2006;10:443–52.
- [39] Mirmiran A, Shahawy M, Samaan M. Strength and ductility of hybrid FRP-concrete beam-columns. *J Struct Eng* 1999;125:1085–93.
- [40] Fam A, Flisak B, Rizkalla S. Experimental and analytical modeling of concrete-filled FRP tubes subjected to combined bending and axial loads. *ACI Struct J* 2003;100:499–509.
- [41] AS3600. Concrete structure. Australian Standards; 2009.
- [42] Timoshenko SP, Young DH, Weaver W. Vibration problems in engineering. In: Vibration problems in engineering. New York: Wiley; 1974.
- [43] Bank LC. Composite for construction structural design with frp materials. New Jersey: Jone Wiley & Sons; 2006.

## Chapter 5: Flexural Behaviour of Multi-Celled GFRP Beams

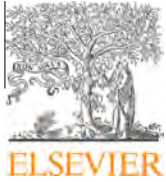
### Paper III: Flexural behaviour of multi-celled GFRP composite beams with concrete infill; experimental and theoretical analysis

This paper presents the flexural behaviour of multi-celled GFRP beams under four-point static bending test. The test parameters were the number of cells in the cross-section, concrete compressive strength and the percentage of concrete filling. Sample preparation and assembly process were described and presented in *Figure 1 of Paper III*. The tubes were glued together vertically to improve the stiffness capacity of the beams. Beams with 1, 2, 3, and 4 cells were tested in hollow and concrete-filled configurations. Based on the experimental results, the filled beams showed good improvement in failure load, stiffness and ductility than their hollow counterparts, which can be observed by comparing the area under the load-deflection curves of hollow and filled beams. Furthermore, the increased number of cells in the cross-section resulted in a change in the failure mode from compression failure of the top most fibre to a bearing failure. Bearing failure test was then conducted for hollow and filled beams to determine their bearing capacity. The test results were presented in *Figure C.1 of Appendix C*. The experimental results of the bearing test support the conclusion made for bearing failure in *Paper III*.

Theoretical model was proposed to predict the failure load of multi-celled hollow and filled beams based on maximum stress theory which assumed that the failure of flexural beam will occur when the sum of the ratios of the actual shear and flexural stresses to that of the allowable stresses approaches unity as given by:

$$\frac{\sigma_{act}}{\sigma_{all}} + \frac{\tau_{act}}{\tau_{all}} \leq 1$$

where  $\sigma_{act}$ ,  $\tau_{act}$ ,  $\sigma_{all}$  and  $\tau_{all}$  are the actual and allowable flexural and shear stresses, respectively. In general, the model gave reliable estimation of the failure load of the multi-celled beams. Moreover, the results of the study enabled the identification of several parameters that affect the behaviour of multi-celled beams such as number of cell, shear span-to-depth ratio and filling percentages. The effect of these parameters were investigated theoretically to come up with a simplified prediction equation and developed a failure mechanisms map for multi-celled GFRP beam sections, which was the focus of *Paper IV*.



# Flexural behaviour of multi-celled GFRP composite beams with concrete infill: Experiment and theoretical analysis



Majid Muttashar<sup>a,b</sup>, Allan Manalo<sup>a,\*</sup>, Warna Karunasena<sup>a</sup>, Weena Lokuge<sup>a</sup>

<sup>a</sup> Centre for Future Materials (CFM), School of Civil Engineering and Surveying, University of Southern Queensland, Toowoomba 4350, Australia

<sup>b</sup> Department of Civil Engineering, College of Engineering, University of Thi Qar, Iraq

## ARTICLE INFO

### Article history:

Received 1 July 2016

Revised 6 September 2016

Accepted 16 September 2016

Available online 20 September 2016

### Keywords:

Composite beam

Multi-cell beams

Flexural confinement

Failure load

GFRP

Concrete in-fill

Concrete strength

Flexural behaviour

## ABSTRACT

This research introduces multi-celled glass fibre reinforced polymer (GFRP) beam sections partially filled with concrete. Hollow pultruded GFRP square tubes (125 mm × 125 mm × 6.5 mm) were bonded together using epoxy adhesives to form the beams using 2–4 cells. Concrete with 15 and 32 MPa compressive strengths was used to fill the top cell of the multi-cell beams. These beams were then tested under static four-point bending and their behaviour was compared with hollow beams. The results showed that up to 27% increase in strength was achieved by using multi-cell beams compared to a single cell beam. Filling in the top cell of the beams with concrete enhanced the capacity as well as the stiffness of the beams. The multi-celled GFRP beams filled with concrete at the top cell failed at 38–80% higher load and exhibited 10–22% higher stiffness than their hollow counterparts. The increase in the compressive strength of the concrete infill from 15 MPa to 32 MPa resulted in up to 14% increase in the failure load but did not enhance the flexural stiffness. Finally, the proposed prediction equation which account for the combined effect of shear and flexural stresses showed a good agreement with the experimental results for hollow cells and up to 3 cells of concrete filled beams. The bearing stress equation gave a better estimation for 4-cell filled section.

© 2016 Elsevier Ltd. All rights reserved.

## 1. Introduction

The corrosion of steel reinforcement is considered the greatest factor limiting the service life of reinforced concrete structures. Thus, innovative and cost-effective materials offering long-term durability and requiring less maintenance, like glass GFRP, are becoming attractive for use in civil engineering applications. Several projects in the construction industry have benefited from the low cost to high-strength of pultruded GFRP thin-walled tubes [1–3]. Despite their many advantageous properties, the relatively low elastic modulus of pultruded GFRP composites resulted in their design governed by serviceability requirements which prevented the full utilisation of their high tensile strength. Similarly, their hollow sections are prone to compression (bending) buckling failure [4,5], web-flange junction failure in the compression zone [6,7] and local buckling of walls due to in-plane compression

[8–10]. These limitations of pultruded GFRP sections should, therefore, be addressed for their wide acceptance and use in civil engineering applications.

Several researches proposed different geometrical configurations and material combinations to improve the structural performance of hollow pultruded FRP profiles. Hejll et al. [11] experimentally investigated the flexural behaviour of composite beams made by gluing together square GFRP profiles with a layer of carbon FRP bonded to the flanges. They concluded that assembling the profiles together provided a system with a higher stiffness than individual GFRP profiles to satisfy the requirement for a composite bridge. However, the composite beams failed at a strain of around 7500 microstrains, which are only 60% of the strain capacity determined from the coupon tests. They documented that this behaviour mainly resulted from the buckling failure of the top flange of the square pultruded profile. Kumar et al. [12] and Kumar et al. [13] conducted experimental investigations on 76 mm square hollow pultruded GFRP tubes to evaluate their flexural performance. Two, four and eight layered tubes were bonded together using epoxy adhesive and tested under four-point bending test. In the four and eight layered assembly, the layers of FRP tubes glued together such that each layer is perpendicular to the ones above

\* Corresponding author at: Centre of Excellence in Engineered Fibre Composites (CEEFC), School of Civil Engineering and Surveying, University of Southern Queensland, Toowoomba, Queensland 4350, Australia.

E-mail addresses: [majid.alzaidy@gmail.com](mailto:majid.alzaidy@gmail.com) (M. Muttashar), [allan.manalo@usq.edu.au](mailto:allan.manalo@usq.edu.au) (A. Manalo), [karu.karunasena@usq.edu.au](mailto:karu.karunasena@usq.edu.au) (W. Karunasena), [weena.lokuge@usq.edu.au](mailto:weena.lokuge@usq.edu.au) (W. Lokuge).

or below it. They mentioned that the proposed combination showed a good flexural performance and met the strength requirement and the other necessary performance criteria of bridge deck applications. However, web-flange junction failure and twisting of the top layer were observed followed by debonding failure between the layers due to the increased number of tubes in the four- and eight-layered beams. In contrast, the two-layered beams exhibited local buckling failure. Satasivam and Bai [14] and Satasivam and Bai [15] conducted experimental investigations on modular web-flange FRP-steel composite systems and GFRP web-flange sandwich systems for beam and slab applications. The modular sandwich systems were prepared via adhesive or novel bolted connections. The results show that the FRP – steel composite systems failed due to premature local crushing of the box profiles situated directly underneath the loading point. On the other hand, the GFRP web-flange sandwich systems showed shear crack originating from the region of maximum shear for specimens with low shear span to depth ratio ( $a/d = 8$ ) while longer specimens ( $a/d = 24$ ) failed by separation of the web-flange junction and buckling of the web. In another study, Hayes et al. [16] and Schniepp [17] conducted experimental work on pultruded double web beams (DWB) under three- and four-point bending. The beam composed of both E-glass and carbon fibres in a vinyl ester resin. The beams consistently failed within compression flange at the interface between carbon and glass fibres. Again, the delamination within the compression flange was the final failure mechanism of the DWB. Hayes and Lesko [18] indicated that the relatively thick flange and the free edge effect for these type of composite beams have played a major role in the initiation of the delamination at the interface between the laminates.

Hybrid structural systems wherein GFRP box beam sections were combined with a concrete layer cast onto the top flange and/or a thin layer of carbon fibre bonded to the tension side were developed to prevent the local buckling in the compression flange and delamination failure of the hollow composites sections [19–21]. Moreover, it can also increase the stiffness and strength of the composite section and reduce the deflection at failure [22]. The addition of stiffer carbon fibres on the bottom flange can further improve the stiffness of the hybrid composite beams. However, most hybrid composite beams failed in a brittle manner due to the failure in the adhesion between the pultruded section and the concrete layer [23]. In order to prevent the adhesion failure, several researchers completely filled the hollow composite sections with concrete instead of just bonding them on top flanges [24–27]. This approach is not optimal for applications governed by pure bending due to tension cracking in the concrete which decreases the concrete core contribution to the bending resistance [28]. Furthermore, this method diminishes the light weight characteristics of FRP profiles. Therefore, several researchers developed hybrid composite beam systems wherein inner GFRP tube is provided to create a void near the tensile zone [25,29,30]. The results indicated that the strength and stiffness of the hybrid beams with inner hole are increased compared with those of a totally filled tube. In a recent study on hybrid composite beam where the concrete was reinforced with steel to minimise tensile cracking and a void was introduced towards the tensile zone [28], the behaviour of the composite beam was compared with a conventional RC beam of the same size. The results showed that the flexural strength of the composite beam is 229% higher than that of a conventional RC beam. However, these researches highlighted that failure due to inward buckling, relatively large slippage between concrete and inner steel or GFRP tube are the main factors that affected the flexural behaviour of the tested beams. Additionally, in the applications which required larger beam sizes, the flexural compression strength failure decreases as the beam size increases [31]. Furthermore, the addition weight of the inner tube and the bond between concrete and GFRP remain critical issues in this combination.

The abovementioned previous studies highlighted the following points: (i) effectiveness of GFRP profiles in the construction industry; (ii) instability and failure of hollow beams due to local buckling and delamination of the compression flange; (iii) flexibility in design from assembled pultruded tubes together; (iv) enhancement of strength and serviceability by filling GFRP tubes with concrete; and (v) maintaining the lightweight characteristics of FRP materials by creating voids in the tension zone of infilled concrete. Based on these important characteristics, the concept of assembling pultruded sections together is explored in this study in order to get benefit of the high sectional moment of inertia of the multi-celled section and flexibility in design. This multi-celled beam concept was achieved by gluing together 2, 3, and 4 GFRP sections with 125 mm × 125 mm cross section. Moreover, partial filling is introduced by filling only the top cell of the multi-celled beams with concrete having two different compressive strengths to prevent local buckling failure but keeping the weight minimum. An experimental investigation was then conducted to evaluate the flexural behaviour of these beams and comparison was made with the behaviour of their hollow counterparts. The comparison includes the moment and deflection behaviour, ultimate capacity, and failure mechanism. Simplified prediction methods were also proposed to determine the failure load of the hollow and filled multi-celled beams accounting for the combined effect of shear and flexural stresses. The predicted failure load was then compared with the experimental results.

## 2. Experimental program

### 2.1. Material properties

The hollow pultruded GFRP square tubes (125 mm × 125 mm × 6.5 mm) used in this study are made up of vinyl ester resin and E-glass fibre reinforcement. The tubes consisted of nine plies of  $[0^\circ/+45^\circ/0^\circ/-45^\circ/0^\circ/-45^\circ/0^\circ/+45^\circ/0^\circ]$  E-glass fibre manufactured using pultrusion process by Wagner's Composite Fibre Technologies (WCFT), Australia. Tensile and compressive strength properties along the longitudinal direction were evaluated by testing coupon specimens following ASTM Standard D 695 [32] and ISO 527-2 [33] standards and are reported in Table 1. On the other hand, the elastic modulus and shear modulus were determined from tests of the whole section in a previous study by the authors [34]. The burnout test conducted as per ISO 1172 standard [35] revealed that the density and the fibre volume fraction are 2050 kg/m<sup>3</sup> and 78% by weight, respectively. Two types of concrete were used to fill the beams, i.e. Bastion premix concrete and cement grout.

### 2.2. Sample preparation

Fig. 1 shows the preparation of specimens wherein the square pultruded section represents the main component of the multi-cell beams. Prior to bonding, the surfaces of the square sections

**Table 1**  
Properties of the pultruded GFRP profiles.

Material property	Symbol	Property value	unit
Density	$\rho$	2050	kg/m <sup>3</sup>
Tensile stress	$\sigma_t$	596	MPa
Tensile strain	$\epsilon_t$	16,030	microstrain
Compressive stress	$\sigma_c$	550	MPa
Compressive strain	$\epsilon_c$	11,450	microstrain
Inter-laminar shear	$\tau$	86	MPa
Elastic modulus	$E$	47.2	GPa
Shear modulus	$G$	4	GPa



Fig. 1. Preparation process of pultruded sections assembly.

to be glued were properly ground and cleaned with acetone (Fig. 1a). GFRP profiles were then assembled and bonded together in 2, 3, 4 cells (Fig. 1b). The adhesives used for bonding the profiles are the Techniglué-HP R26 supplied by ATL composites Pty Ltd. It is a thixotropic, solvent free, toughened epoxy resin which is mixed with H26 hardener and with mechanical properties listed in Table 2. Approximately 1 mm thick bond line was applied (Fig. 1c). The bonded sections were then clamped (hand tight) to provide the necessary bond pressure during adhesive curing (Fig. 1d). The excess adhesives were removed from the sides of the bonded beams. After that, the beams were left to harden for 5 days at ambient temperature.

Fig. 2 shows the filling process of the pultruded beams with concrete. The beams were fixed in a vertical position prior to cast-

ing. The concrete was prepared and mixed for 10 min and then poured into the beams. Five concrete cylinders were sampled from each batch for strength testing and cured under the same conditions as the beam specimens. The 28 day average compressive strength for the Bastion premix concrete and the cement grout were 15 and 32 MPa, respectively. The reason for using two types of concrete infill is to investigate their strength effect on the behaviour of the filled beams. After filling, the specimens were cured for 28 days at ambient temperature before they were tested. Prior to the test, plastic square inserts were used for the hollow and filled beams at the loading and support points to prevent any indentation and/or crushing failure at those points and to allow the beam to fail at the location of the maximum and constant bending moment as shown in Fig. 3a.

Table 2

Mechanical properties of TENCHIGLUE-HP R26 epoxy adhesive.

Property	Symbol	Value	Test method
Tensile strength	$f_t$	34.1 MPa	ISO 527-2
Tensile Modulus	$E_t$	2409 MPa	ISO 527-2
Lap shear strength	$f_v$	11.9 MPa	ASTM D3161
Heat deflection temperature	HDT	85 °C	ISO 75

Notes:

1. The properties in the table are per the ATL Engineering data sheet.
2. The values in the table are based on a cure schedule of 24 h @ ambient + 8 h @ 80 °C.

### 2.3. Specimen details

The details of the tested beams are given in Table 3. In the table, the specimens were identified by codes. The specimen length depends on the total depth of the beam to maintain the shear span to depth ratio ( $a/d$ ) at 4.2. The beams were then divided into three groups according to the section configurations as hollow (H), filled with low strength concrete (H-15) and filled with cement grout (H-32). In the identifications 1C, 2C, 3C and 4C, the first number represents the number of cells and the letter C indicates that they are bonded cells. Two beams were tested for each combination.



**Fig. 2.** Filling process of the pultruded beams with concrete. (a) Plastic inserts, (b) Steel angles and steel chains.

#### 2.4. Test setup and experimental procedure

A static four – point bending test of the pultruded beams (Fig. 4) was performed following the ASTM D7250 [36] standards. The load was applied at two points with a load span of 300 mm. A 2000 kN universal testing machine was used for applying the load at a rate of 3 mm/min. A laser displacement transducer was used to measure the mid span deflection. Additional steel angles and steel chains were used at the supports to avoid any rotation or lateral buckling (Fig. 3b). Uni-axial strain gauges (type PFL-20-11-1L-120) were used to measure the strain at the top and bottom faces of the beams. The applied load and the displacement were measured and recorded using a data logger System 5000. All specimens were tested up to failure to observe the failure mechanisms of the beams.

### 3. Experimental results and observations

#### 3.1. Flexural behaviour

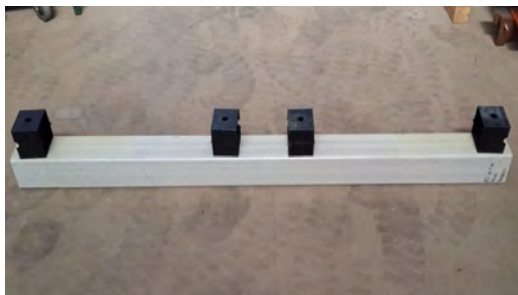
The test results of the flexural behaviour of single and multi-cell GFRP pultruded beams under four-point bending are given in

Table 4 and the moment – displacement behaviour of the tested beams with 1, 2, and 3 cells are presented in Figs. 5–7, respectively. The figures illustrate that the moment increased almost linearly with the deflection up to failure for all the tested beams. Failure of hollow beams was identified as a compressive buckling of the top flange at the constant moment region, while the filled sections failed due to the initiation of compression failure on the top fibres of the section. The failure moment was calculated for each beam based on the failure load and the shear span. Top and bottom failure strains are corresponding to the failure loads. The mode of failure for each specimen is also shown in Table 4.

The table and the figures show that the failure moment increased by 105%, 63%, 58% and 38% for 1, 2, 3 and 4 cells beams filled with 32 MPa infill, respectively, compared with hollow specimen. Single cell specimen filled with 32 MPa compressive strength concrete exhibited approximately 14% higher failure moment than specimen filled with 15 MPa compressive strength concrete. A similar behaviour was observed in specimens with 2 and 3 bonded cells and the top cell filled with concrete. The results also showed that single and multi-celled sections filled with 32 MPa concrete failed at slightly higher compression strains compared to beams filled with 15 MPa concrete. This behaviour reflects the contribution of the concrete core in the strength of the composite beam. However, the failure compression strains values vary depending on the number of bonded specimens. The filled beams failed at approximately 65, 41, 40 and 18% higher strains than the hollow beams for the specimens' 1C-H, 2C-H, 3C-H and 4C-H, respectively. The main reason of this variation is the relationship between the depth of the specimens and the distance between the applied loads. When the number of bonded cells is increased, the stress concentration increased with a constant loading distance. As a result, the section behaves in a same manner like three point bending moment.

#### 3.2. Failure mode

The experimental investigations showed that flexural compression failure was the dominant failure mode of all the tested beams in this study. It is worth noting that there were no lateral instability problems observed by the section during the entire experimental investigation. Fig. 8 shows the failure mode of the beams of 1, 2, 3, and 4 bonded cells with hollow and filled configurations. The failure mode of hollow sections initiates due to the local buckling (LB) of the thin walls which eventually result in material degradation and total failure of the beam. The failure occurred under one of the point load and varied cracks appeared on the top surface of the top cell of the section. The cracks developed perpendicular to the longitudinal axis of the section and then progressed to the web-flange junction due to the effect of buckling and finally these cracks propagated into the web, leading to the final failure of the speci-



(a) Plastic inserts



(b) Steel angles and steel chains

**Fig. 3.** Supporting procedure of the tested beams.

**Table 3**  
Descriptions of the pultruded GFRP tested beams.

Specimen	Illustration	$B$ (mm)	$D$ (mm)	$L_t$ (mm)	$L$ (mm)	$a$ (mm)	$f'_c$ MPa
1C-H-0		125	125	2000	1350	525	–
1C-H-15		125	125	2000	1350	525	15
1C-H-32		125	125	2000	1350	525	32
2C-H-0		125	250	2750	2400	1050	–
2C-H-15		125	250	2750	2400	1050	15
2C-H-32		125	250	2750	2400	1050	32
3C-H-0		125	375	3700	3450	1575	–
3C-H-15		125	375	3700	3450	1575	15
3C-H-32		125	375	3700	3450	1575	32
4C-H-0		125	500	5000	4500	2100	–
4C-H-32		125	500	5000	4500	2100	32

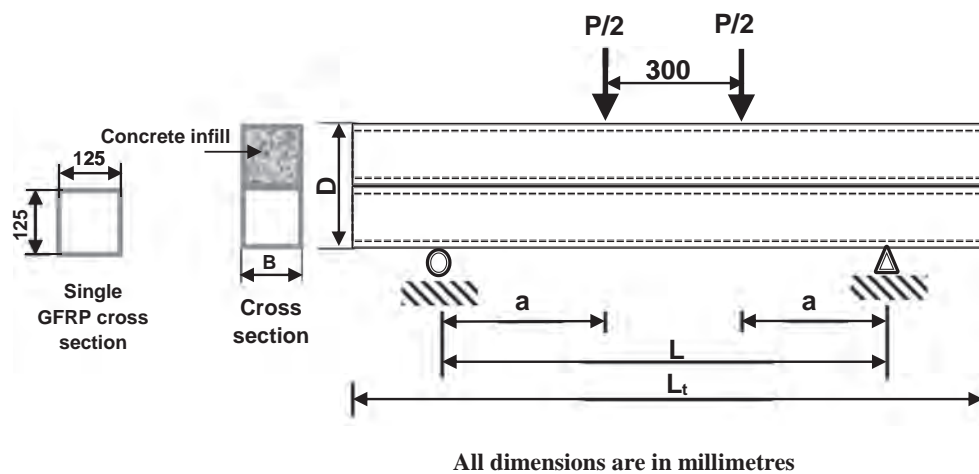


**Fig. 4.** Flexural test set-up for single and multi-cell beams.

mens. Fig. 8a, c and e shows the failure mode of 1C-H-0, 2C-H-0 and 3C-H-0, respectively. It is of interest to mention that no damage was observed in the second and third cells. In addition, there was no delamination or slipping occurred on the glue line. These results suggest that an efficient glue joint was achieved between the pultruded sections, which was provided by the structural epoxy adhesive used.

Fig. 8b, d and f shows the failure mode of the filled specimens 1C-H-32, 2C-H-32 and 3C-H-32, respectively. It can be seen from the figure that the failure of the filled beams was similar to that of hollow beams. However, those beams failed at higher moment due to the contribution of the concrete core. Furthermore, the presence of the concrete core, however, prevented the local buckling of the compression flange which resulted in higher failure strain com-

pared with the hollow beams. Again, the failure started at the compression flange with fibre damage, matrix cracking and delamination. The failure then progressed into the web due to the progress of the flexural cracks with the application of the load and the failure of the concrete core. In contrast, the four bonded cell section showed different mode of failure as shown in Fig. 8g. The specimen 4C-H-32 failed due to flange-web junction failure of the second cell resulting from bearing pressure of the top cell, delamination and fibre cracks at the top flange, web fibre cracks, and de-bonding between the top and second cell. This type of failure might occur due to the high bearing load level applied to the section. Furthermore, the top filled cell played an important role by applying bearing pressure on the second top cell which results in high level of inter-laminar shear at the flange-web junction. It is

**Table 4**  
Summary of the experimental test results for pultruded GFRP beams.

Specimen	<i>D</i> (mm)	<i>L</i> (mm)	<i>a</i> (mm)	Failure load (kN)	Failure moment (kN m)	Deflection (mm)	Bottom strain $\mu\epsilon$	Top strain $\mu\epsilon$	Failure mode
1C-H-0	125	1350	525	90.6	23.8	18.8	5500	4000	<sup>a</sup> LB
1C-H-15				161.5	43	29.8	9104	8113	<sup>b</sup> CF
1C-H-32				186.6	49	34	10,329	8443	CF
2C-H-0	250	2400	1050	151.2	79.4	34.7	6324	4242	LB
2C-H-15				217	114	42.7	7520	6675	CF
2C-H-32				247.6	130	48	8947	7679	CF
3C-H-0	375	3450	1575	187.5	147.6	42.4	5496	3979	LB
3C-H-15				261.6	214	55.8	7331	6928	CF
3C-H-32				294.6	232	60.5	7708	7090	CF
4C-H-0	500	4500	2100	225	236.5	48	5400	4490	LB
4C-H-32				348	365	63.9	6409	5338	<sup>c</sup> B

<sup>a</sup> LB = Local buckling failure.

<sup>b</sup> CF = GFRP material failure at the compression side.

<sup>c</sup> B = Bearing failure.

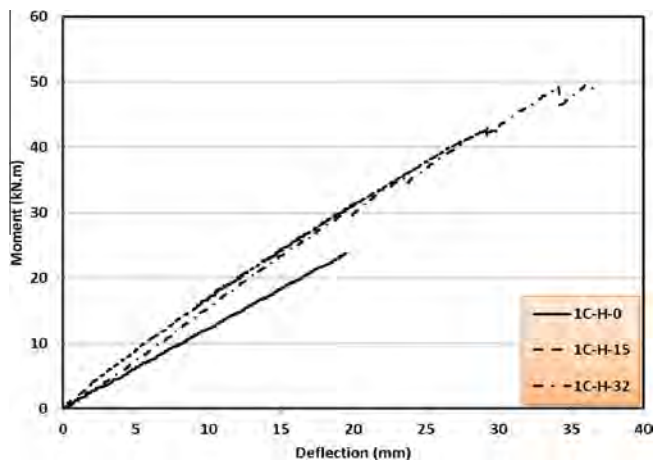


Fig. 5. Moment-displacement behaviour of 1 cell GFRP pultruded beams.

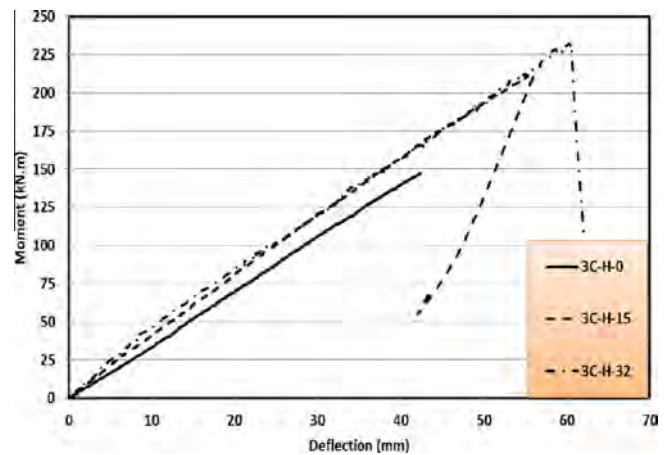


Fig. 7. Moment-displacement behaviour of 3 cells GFRP pultruded beams.

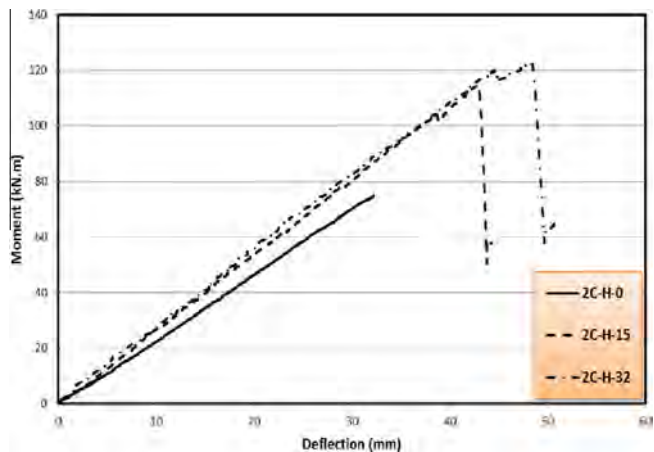


Fig. 6. Moment-displacement behaviour of 2 cells GFRP pultruded beams.

interesting to see that the failure of the multi-cell sections was due to top cell failure which did not result in a total collapse of the beam. This behaviour might be considered to be appropriate for structural engineering designs, as the failure was not really catastrophic.

Crack pattern of the concrete core was examined by removing the pultruded GFRP section after failure. Fig. 9 shows the flexural cracks of the specimens filled with concrete (15 MPa) and cement grout (32 MPa). It can clearly be seen from the figure that flexural

cracks developed at the bottom of the beam between the loading points. Furthermore, the cracks spread up to the depth of the concrete infill for single section and the bonded sections. 1C-H-32, 2C-H-32 and 3C-H-32 beams showed distinct flexural cracks as shown in Fig. 9 b, d, f and g while 1C-H-15, 2C-H-15 and 3C-H-15 beams showed fine cracks (Fig. 9a, c and e). This behaviour might be attributed to the brittleness of cement grout which increases with increasing compressive strength. Therefore, different crack patterns were observed. Fig. 6 also shows a slight difference between the number of cracks and the cracking area of single cell specimens compared with double and triple cell specimens. These differences are related to the core contribution in the compression zone. On the other hand, similar crack patterns were observed for 4C-H-32 specimen compared with 1C-H-32 specimen due to the effect of de-bonding failure between the layers of the 4 cells beam which increased the deflection of the top cell. It is interesting to note that crushing did not occur for the concrete core at the maximum moment zone although the complete failure occurred at a strain much higher than the ultimate concrete compression strain (Fig. 9). These results indicate that there is a partial confinement effect of the GFRP tube to the concrete core which in turn kept the concrete under compression intact until failure of the tube.

#### 4. Analysis and discussion

The effect of different parameters investigated on the flexural behaviour of multi-celled GFRP beams are analysed and discussed in this section.

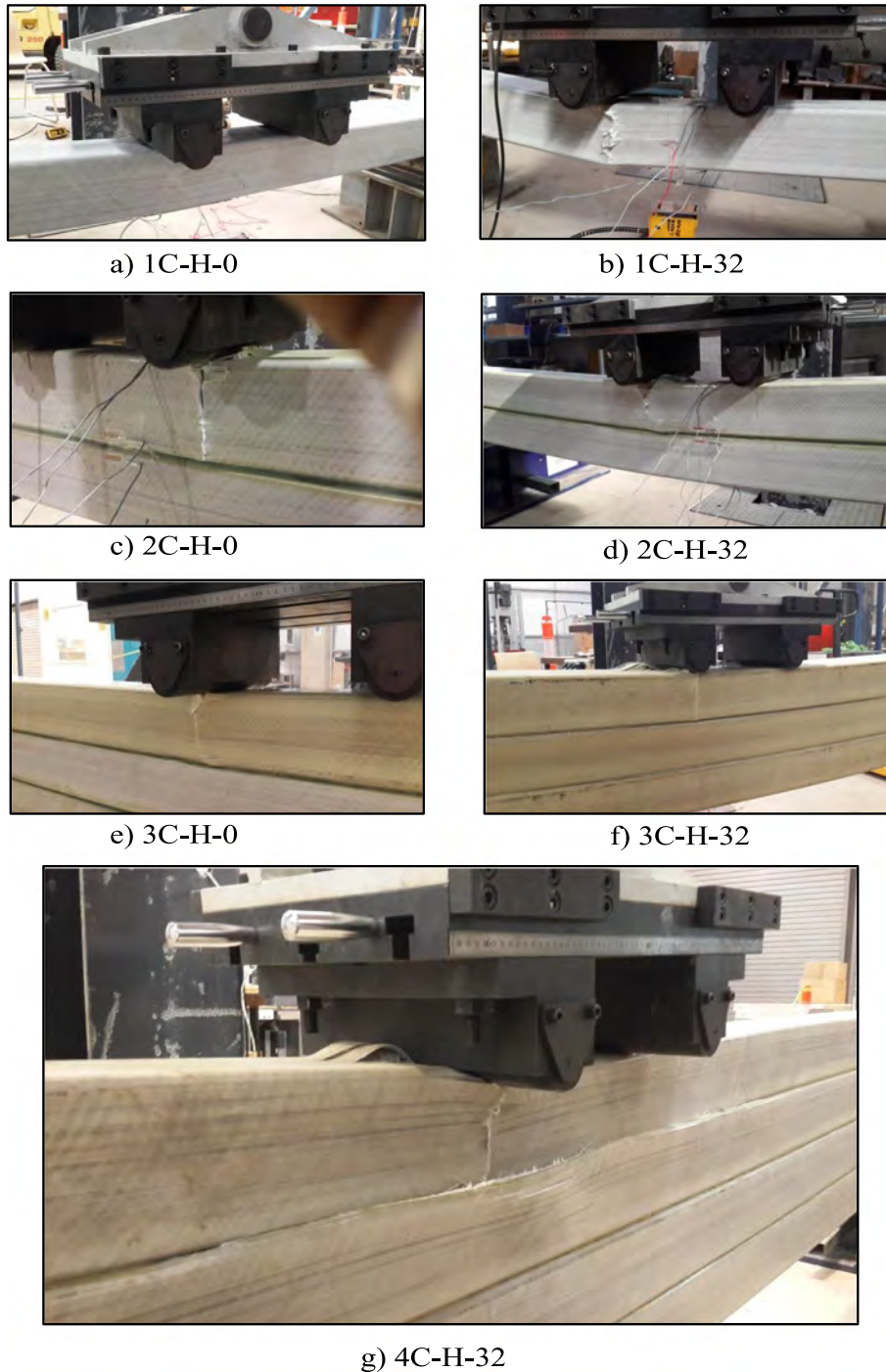


Fig. 8. Failure modes of hollow and filled pultruded GFRP beam.

#### 4.1. Effect of number of cells

##### 4.1.1. Hollow sections

The effect of the number of cells on flexural strength was evaluated by the maximum bending stress experienced by the GFRP beams using the below equation:

$$\text{Bending stress} = \frac{M_b c}{I} \quad (1)$$

where  $M_b$  is the bending moment,  $c$  is the distance from the neutral axis to the outer top fibre and  $I$  is the moment of inertia of hollow section. The relationship of the bending stress and the number of

cells is shown in Fig. 10. It can be seen that the single cell pultruded beam failed at a bending stress of 227 MPa. This result represents approximately 41% of the design capacity of the section based on coupon test results. By gluing the pultruded sections together in 2, 3 and 4 cells resulted in higher level of bending stress at failure compared to single cells. Beams with 2, 3, and 4 bonded cells failed at stresses of 280, 254, and 237 MPa, respectively. These stress values are 43%, 46% and 51% of the design capacities of the section based on coupon test results, respectively. The better performance of multi-cell than single cell can be attributed to the better stability provided by the flanges in the glue lines. However, the beam with 2 cells performed better than 3 and 4 cells. This could be due to the

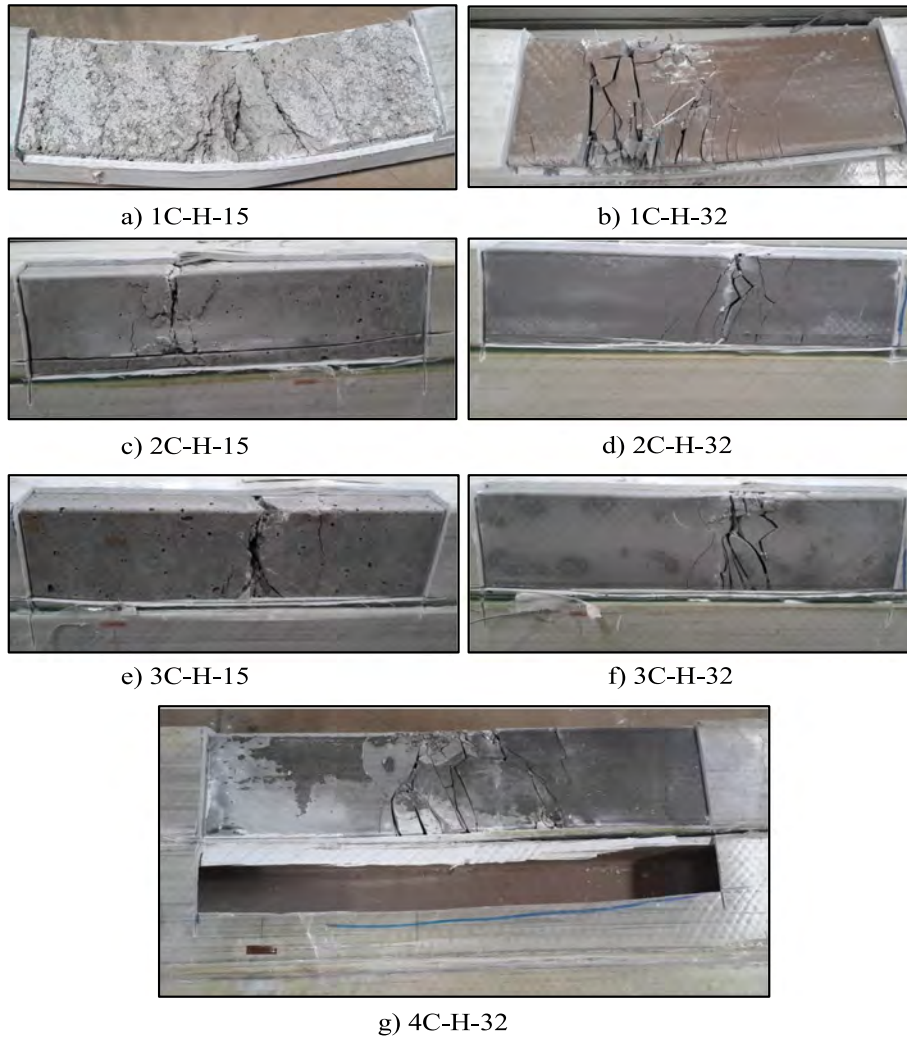


Fig. 9. Crack patterns at failure of the tested beams.

higher level of load needed to fail the 3 and 4 cells than 2 cells as shown in Table 4. As the area under the loading point resisting the applied load is the same for all the beams, the beams with 3 and 4 cells are subjected to a higher level of bearing stress at the loading point which increases the tendency of micro-cracks formation in this zone. The same behaviour was observed by [37,38] wherein they indicated that the failure strain and failure stress decrease as the beam depth increases due to the micro-cracks concentration at the failure zone. Therefore, the failure of the beam is directly related to the compressive strength of the beam under the vertical loads.

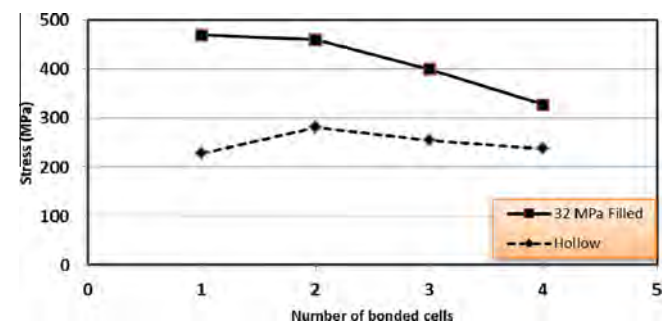


Fig. 10. Bending strength for the bonded pultruded GFRP sections.

The effective flexural stiffness,  $EI$  of the single and multi-cell beams was also evaluated based on the slope of the linear elastic portion of the load and mid-span deflection curve using the relation:

$$EI_{eff} = \frac{L^2 a}{48} \left( 3 - \frac{4a^2}{L^2} \right) \left( \frac{\Delta P}{\Delta v} \right) \quad (2)$$

where  $P$  is the total applied load,  $L$  denotes the span length,  $a$  is the shear span,  $(\Delta P/\Delta v)$  is the slope of the load–deflection curve,  $EI_{eff}$  is the effective flexural stiffness. The apparent stiffness modulus,  $E_{app}$  of the tested beams was then computed by dividing  $EI_{eff}$  by the second moment of inertia  $I$  of the hollow beam sections. Fig. 11 shows the relationship between the apparent modulus and the number of cells. The results show that the  $E_{app}$  of the single cell section is almost equal to that of the bonded cell beams. This behaviour clearly shows that the apparent stiffness is not affected by the number of bonded cells indicating that the contribution of the shear deformation to the total deflection is similar as a result of using same shear span to depth ratio ( $a/d = 4.2$ ) for all the tested beams. In another study, Muttashar et al. [34] found that shear deformation contributes approximately 30% to the total deflection of beams with  $a/d = 4$ . Another possible reason for this behaviour is the failure of single and multi-cell beams is almost similar due to the effect of local buckling. These results suggest that the multi-cell sections will provide stronger beams while maintaining the

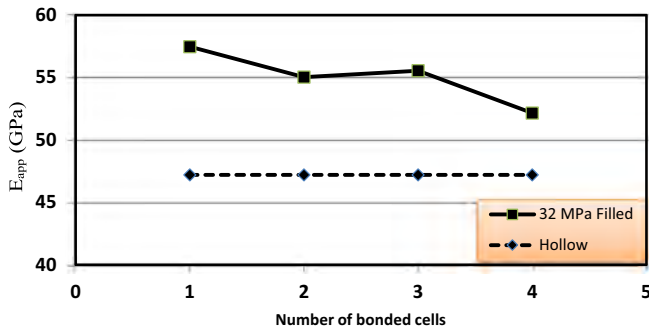


Fig. 11. Apparent stiffness modulus for the bonded pultruded GFRP beams.

same effective modulus compared with single cell. However, it is noteworthy that the failure stress values of the hollow single and multi-cell specimens represent approximately only 50% of the stress level determined from coupon test due to the fact that the failure is controlled by the local buckling failure of the compression.

#### 4.1.2. Partially filled concrete beams

Fig. 10 shows the maximum bending stress of the single and multi-cell GFRP beams with 32 MPa compressive strength concrete infill. The maximum bending stress was calculated using Eq. (1). The figure shows that single cell specimens filled with concrete exhibited 105% higher strength than hollow specimens. This is attributed to the contribution of the concrete core to reduce the local deformation and improve the strength of the section. Similarly filling the top cell of beams with 2, 3, and 4 cells improved the flexural strength by 63, 57, and 38%, respectively, compared to their hollow counterparts which reflects the positive effect of concrete infill in preventing local buckling failure. However, the effectiveness of the concrete infill decreases with increasing cell numbers. These observations can be explained by the following. First, the flexural strength of the beams is governed more by the GFRP sections and less by the concrete infill. For all GFRP beams tested, failure occurred in a brittle manner due to compression failure of the topmost compression fibre near the loading point. With increasing number of cells, the effect of concrete filling on the bending strength becomes lower due to the higher level of load needed to fail beams compared with single cells which results in high stress concentration between the loading points. The authors believe that the percentage of improvement of the flexural strength becomes higher if the stress concentration is minimised.

Fig. 11 also illustrates the effect of concrete infill on the apparent stiffness modulus  $E_{app}$  of single and multi-cell specimens. Firstly, the effective flexural stiffness  $EI_{eff}$  was calculated based on the slope of the linear elastic portion of the load and mid-span deflection after tensile cracking (Fig. 12) using Eq. (2) then the  $I$  of the hollow sections has been used to calculate  $E_{app}$ . It is found that the concrete infill has a noticeable effect on the apparent modulus for single and multi-cell beams. It can be seen from the figure that the  $E_{app}$  of the single cell specimens increased by 22% compare to hollow specimens while the beams with 2, 3 and 4 cells improved by 18, 17 and 10%, respectively over their counterpart hollow specimens.

The failure behaviour also changes by filling the top GFRP section with concrete as shown in Figs. 5–8. It also improved the flexural stiffness of the beams to some extent. The deformation of the infilled beams increases with the increase in the external load. This deformation becomes higher for 2, 3 and 4 cells section due to the increase in the applied load. Furthermore, the infilled beams show high deflection which means high curvature. Due to the effect of

shear span to depth ratio in addition to high deflection, maximum compressive stresses is located at the top section along the longitudinal direction of the beam and compressive stresses was also developed in the shear span along the line connecting load and support. These stresses might result in high compressive stress near the load point due to the effect of local stress concentration. Consequently, the effect of concrete infill tends to be less for beams with higher cell numbers in the cross section. In addition, it is obvious that the total stiffness of the composite sections is a combination of those of their components. However, due to tensile cracking of concrete and the increase of the number of bonded cells, lower contribution of the concrete infill was achieved. On the other hand, even though the improvement in the flexural stiffness decreases with increased number of cells, these percentages represent the improvement in the flexural stiffness from the overall stiffness of each section. That means 10% increase in the overall stiffness of 4 cell beams is more effective than the 22% increase for single cell beams as only 25% of the section is filled while 100% is filled for the single section. The experimental results suggested that, in the construction of multi-cell pultruded beams, filling the top cell with concrete will result in stronger and stiffer beam than the hollow beams.

#### 4.2. Effect of concrete compressive strength

Fig. 13 shows the influence of concrete compressive strength on the flexural strength of beams with 1, 2 and 3 cells. The beams filled with 32 MPa compressive strength exhibited higher flexural strength than beams filled with 15 MPa by 16, 13 and 10% for 1, 2 and 3 cells, respectively. These percentages are minimal compared to the increase in concrete compressive strength from 15 MPa to 32 MPa. The possible reason for the limited increase in the flexural strength is that the failure of those sections is governed by the compression failure of the pultruded profiles. In addition, the difference in the neutral axis location might be another reason for this variation. Concrete of low strength shows higher neutral axis depth which results in higher contribution in the calculation of the flexural strength. However, single specimen shows higher strength gain compared with other specimens due to the difference in the failure mode between single and multi-cells sections.

Fig. 14 shows the influence of concrete compressive strength on the flexural stiffness of the 1, 2 and 3 cell beams. The flexural stiffness,  $EI$  was also evaluated based on the slope of the linear elastic portion of the load and mid-span deflection curve after flexural tensile cracking of the concrete using Eq. (2). The main reason for considering the  $EI$  at the cracked concrete section is that most concrete structures are already cracked in actual service but up to within allowable width. The figure indicates that the flexural stiffness of the beams filled with 15 MPa compressive strength concrete is almost similar to those beams filled with 32 MPa concrete. It is seen that 1, 2 and 3 cells specimens filled with 32 MPa concrete are only 2.2, 1.2, and 0.4% stiffer, respectively, than beams filled with 15 MPa concrete. Two possible reasons may explain this behaviour. Firstly, it is clear from the experimental results that the overall behaviour of the tested beams is governed by the GFRP profile's mode of failure due to the fact the failure occurred at a very high strain level compared with strain failure of concrete. Secondly, due to the difference in modulus of elasticity between the two concrete types and after the occurrence of tensile cracks, higher area of low strength concrete infill is required to maintain the equilibrium in the internal forces compared with higher strength concrete. Consequently, the concrete compressive strength shows a limited effect on the flexural capacity. On the other hand, although the concrete core is located in the compression zone for beams of 3 cells or more, the mode of failure is slightly different from that of beams of 1 and 2 cells. Figs. 8 and 9

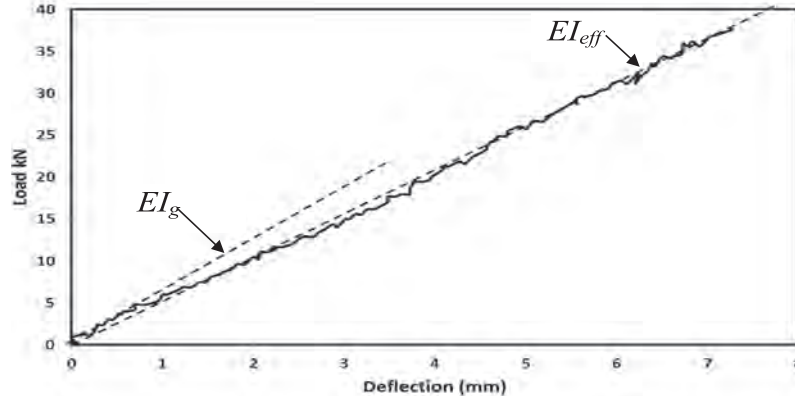


Fig. 12. Section stiffness.

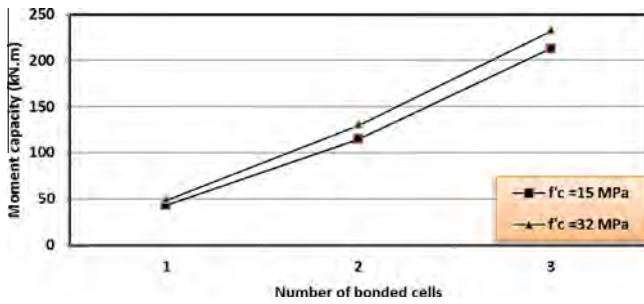


Fig. 13. Effect of concrete compressive strength on the moment capacity of the beams with 1, 2 and 3 cells.

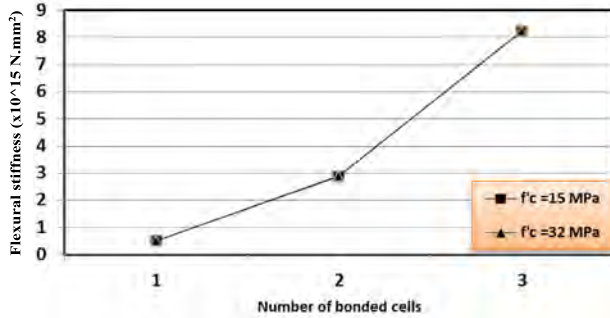


Fig. 14. Effect of concrete compressive strength on the flexural stiffness of the 1, 2 and 3 cells pultruded GFRP sections.

show that the concrete core cracked and local buckling failure happened in the cell located under the filled cell. This behaviour explains the limited contribution of the concrete core on the stiffness. It can be concluded that the flexural behaviour of the tested specimens in this study was not significantly affected by the increase in the compressive strength.

## 5. Theoretical analysis and evaluation

### 5.1. Failure load prediction

The observed failure mode of hollow beams was local buckling of the compression flange under the loading points in addition to a shear crack in the shear span (Fig. 8). At the location of loading, the maximum bending moment and shear forces exist. Manalo [39] and Awad et al. [40] highlighted that for composite beams with a shear span-to-depth ratio ( $a/d$ ) less than 4.5, failure will occur

due to a combined effect of shear and flexural stress. In the current study, the tested beams have an  $a/d = 4.2$ . Similarly, Bank [1] stated that, when the beam is subjected to high shear force and bending moment, the web will experience a combination of shear stress ( $\tau$ ) and flexural (compressive or tensile) stress ( $\sigma$ ). Under this condition, the failure of the multi-celled composite beams is expected to occur when the sum of the ratios of the actual shear and flexural stresses to that of the allowable stresses approaches unity as given by:

$$\frac{\sigma_{act}}{\sigma_{all}} + \frac{\tau_{act}}{\tau_{all}} \leq 1 \quad (3)$$

where  $\sigma_{act}$  is the actual flexural compressive stress carried by the topmost fibre of the GFRP tube calculated as:

$$\sigma_{act} = \frac{Mc}{I} = \frac{Pac}{2I} \quad (4)$$

where  $P$  is the applied load,  $a$  is the shear span,  $c$  is the distance from the neutral axis of the section to the topmost fibre, and  $I$  is the second moment of inertia of the section. On the other hand, the actual shear stress  $\tau_{act}$  can be determined using the below equation:

$$\tau_{act} = \frac{VQ}{It} = \frac{PQ}{2It} \quad (5)$$

where  $V$  represents the shear force ( $P/2$ ),  $Q$  is the first moment of area, and  $t$  is the total thickness of the section. As the elastic instability of the pultruded GFRP sections in compression is governed by the local buckling [41], Muttashar et al. [34] suggested to use buckling stresses,  $\sigma_{cr}^{local}$  instead of the allowable compressive stresses in Eq. (3). An approximate expression to determine the buckling stresses for free and rotationally restrained orthotropic plates has been proposed by Kollár [42]. In this method, the local buckling stress of the section is calculated by considering the web and flange to be separate from each other and assuming them as orthotropic plates subjected to uniaxial compression and elastically restrained along their common edge. This buckling stress equation is given below:

$$\sigma_{cr}^{local} = \min\{\sigma_{loc,f}, \sigma_{loc,w}\} \quad (6)$$

where  $\sigma_{loc,f}$  and  $\sigma_{loc,w}$  are the critical normal stresses of flanges and webs, respectively. The critical normal stresses of the flanges and the webs can then be written as [41].

$$\sigma_{loc,f} = \frac{\pi^2}{b_f^2 t_f} [2\sqrt{(D_L D_T)(1 + 4.139\xi)} + (D_{LT} + 2D_S)(2 + 0.62\xi^2_{box-flange})] \quad (7)$$

$$\sigma_{loc,w} = \frac{\pi^2}{d_w^2 t_w} [13.9\sqrt{(D_L D_T)} + 11.1 D_{LT} + 22.2 D_S] \quad (8)$$

The compression flange will buckle before one of the webs if  $(\sigma_{ss}^{ss})_f / (E_L)_f < (\sigma_{ss}^{ss})_w / (E_L)_w$ . In this case, the web restrains the rotation of the flanges and the spring constant is given as:

$$k_{box-flange} = \frac{4(D_T)_w}{d_w} \left[ 1 - \frac{(\sigma_{ss}^{ss})_f (E_L)_w}{(\sigma_{ss}^{ss})_w (E_L)_f} \right] \quad (9)$$

where

$$(\sigma_{ss}^{ss})_f = \frac{2\pi^2}{b_f^2 t_f} (\sqrt{(D_L D_T)} + D_{LT} + 2D_S) \quad (10)$$

$$(\sigma_{ss}^{ss})_w = \frac{2\pi^2}{d_w^2 t_w} (13.9\sqrt{(D_L D_T)} + 11.1 D_{LT} + 22.2 D_S) \quad (11)$$

$$\xi_{box-flange} = \frac{1}{1 + 10[(D_T)_f / k_{box-flange} b_f]} \quad (12)$$

$$D_L = \frac{E_L t_f^3}{12(1 - \nu_L \nu_T)} \quad (13)$$

$$D_T = \frac{E_T^c}{E_L^c} D_L \quad (14)$$

$$D_{LT} = \nu_T D_L \quad (15)$$

$$D_S = \frac{G_{LT} t_f^3}{12} \quad (16)$$

$$\nu_T = \frac{E_T^c}{E_L^c} \nu_L \quad (17)$$

where  $b_f$  and  $t_f$  are the width and thickness of the flange, respectively,  $d_w$  and  $t_w$  are the depth and thickness of the web, respectively,  $E_T^c$  is longitudinal compression modulus,  $E_L^c$  is transverse compression modulus,  $G_{LT}$  is the in-plane shear modulus, and  $\nu_L$ ,  $\nu_T$  are the major (longitudinal) and minor (transverse) Poisson ratios, respectively. On the other hand, the web buckles first when  $(\sigma_{ss}^{ss})_f / (E_L)_f > (\sigma_{ss}^{ss})_w / (E_L)_w$ . In this case, Kollár [42] suggested to take  $K = 0$  as a conservative estimate.

In terms of the shear stress, the web of the GFRP tube is highly susceptible to buckle in location of high shear forces while flange buckling which typically occurs under the loading point or near the supports. The critical shear buckling stress of an orthotropic web can be determined using the relation (18) proposed by [43]:

$$\tau_{cr}^{local} = \frac{4k_{LT} \sqrt{D_L D_T^3}}{d_w^2 t_w} \quad (18)$$

where

$$k_{LT} = 8.125 + 5.045K \quad \text{for } K \leq 1 \quad (19)$$

and

$$K = \frac{2D_S + D_{LT}}{\sqrt{D_L D_T}} \quad (20)$$

For the infilled section, the flexural buckling stress ( $\sigma_{cr}^{local}$ ) is different. Wright [44] highlighted that the infill concrete will contribute in delaying or eliminating the local buckling in the compression flange. However, it has a minimum effect on the buckling of the webs due to the insufficient connection between the tube and the concrete. As a result, the section will develop more resistance to the applied load and will reach its maximum allowable compressive stress (Table 1). Under such condition, Eq. (3) can be used to predict the failure of 1, 2 and 3 cells sections but with considering  $\tau_{cr}^{local}$  as the effective shear stress instead of  $\tau_{all}$ . With these assumptions, the predicted failure load,  $P_H$  of single and multi-celled hollow beams is given by Eq. (21) while the predicted failure load,  $P_F$  of their counterpart filled beams is given by Eq. (22).

$$P_H = \frac{1}{\frac{ac}{2I\sigma_{cr}^{local}} + \frac{Q}{2It\tau_{cr}^{local}}} \quad (21)$$

$$P_F = \frac{1}{\frac{ac}{2I\sigma_{all}} + \frac{Q}{2It\tau_{cr}^{local}}} \quad (22)$$

### 5.2. Predicted results and comparison with the experiments

Table 5 summarises the predicted failure load for single and multi-cell beams with and without concrete infill. The percentage difference between the experimental and predicted failure loads is also given in Table 5. It is clear that the predicted failure load using combined effect of shear and flexural stresses given in Eq. (21) showed a very good agreement with the experimental results for single and multi-celled hollow beams. The equation over predicts the failure load by only 4.5% for single cell section. In addition, the equation overestimate the failure load for 2,3 and 4 cells section by only 3.3%, 0.5% and 1.1%, respectively. On the other hand, the predicted failure load in Eq. (22) is only 2.7% higher compared to the experimental failure load for 1, 2 and 3 cells filled beams, respectively. However, for the filled beam with 4 cells, Eq. (22) overestimated the predicted failure load by 8%. This relatively high difference between the predicted and the actual failure load can be due to the complex state of stress under the loading point for the infilled beams with 4 cells. It is noted from Fig. 8g that the beam with 4 cells exhibited a bearing failure by flange-web junction separation of the second top cell. This failure is due to the high inter-laminar stress at the flange-web junction which has exceeded the shear capacity limit of the pultruded section. Wu and Bai [45] indicated that pultruded FRP beams subject to concentrated loads in the plane of the web are more likely to show inter-laminar shear failure due to bearing stresses at the web-flange junction. They then proposed an equation to estimate the nominal web crippling capacity of the pultruded GFRP beams:

$$R_N = f_s \times A_{shear} \quad (23)$$

where

**Table 5**  
Predicted failure load and difference with the experimental failure load.

Number of cells	Hollow section			Filled section				
	Exp.	Eq. (21)	% Diff.	Exp.	Eq. (22)	% Diff.	Eq. (23)	% Diff.
1	90.6	95	4.5	186.6	192	2.7	326.5	42.8
2	151	156	3.3	247.6	250	1.3	326.5	24.1
3	187.5	188	0.5	294.6	299	1.7	326.5	9.7
4	243	245	1.1	348	378	8.1	326.5	-6.1

$$A_{shear} = 2 \times t_w \times b_{plate} \quad (24)$$

and  $b_{plate}$  represents the width of the bearing plate and  $f_s$  is the inter-laminar shear strength of the section. Using this equation, the failure load of the filled beam sections was calculated and presented in Table 5. Comparison between the predicted and actual failure load showed only a 6.1% difference. The difference between the predicted and the measured failure load is probably due to the slightly higher actual sheared area. Thus, it can be concluded that the failure load of 1, 2 and 3 cells filled beams can be accurately predicted using linear combination of shear and flexural stresses while the bearing stress formula gives a better prediction of the failure load for the filled beam with 4 cells.

## 6. Conclusions

This study presented the results of four point bending tests on hybrid multi-cell hollow and concrete filled GFRP tubes. The main parameters examined in this study are number of cells, cell configuration and compressive strength of concrete core. A simple theoretical model was implemented and used to predict the flexural behaviour of multi-celled GFRP beams. Based on the results, the following conclusions can be drawn:

- Multi-cell hollow beams show better flexural performance than single cell. The single cell beams failed with 40% of its design capacity based on coupon tests while the failure of the multi-cell beams reached 51%. Although, there is an improvement in the failure stress levels for multi-cell beams, these levels are still lower than the stress level determined from coupon test due to the fact that the failure is controlled by the local buckling of the compression.
- The failure of the multi-cell sections was due to the compression failure in the top cell which did not result in a total collapse of the beam. This behaviour might be considered to be appropriate for structural engineering designs, as the failure was not really catastrophic.
- The flexural strength of beams filled with concrete at the top-most section is 105%, 63%, 57% and 38% for 1, 2, 3 and 4 cell sections, respectively, higher than that of hollow section. This reflects the positive effect of concrete infill in preventing local buckling failure.
- Compression flange failure associated with fibre breakage, matrix cracking and delamination was the main mode of failure of the filled beams. The failure then progressed into the webs with increasing applied load due to the effect of flexural cracks in the concrete core.
- Concrete infill has a noticeable effect on the apparent modulus for single and multi-cell beams. The  $E_{app}$  increased by as much as 22% compared to the hollow beam section.
- Beams filled with 32 MPa compressive strength exhibited 14% higher flexural strength than beams filled with 15 MPa. However, increasing the compressive strength from 15 to 32 MPa has a minimal effect on the flexural stiffness of the filled beams due to the fact that the behaviour of the tested beams controlled by the behaviour of GFRP tubes.
- The combined effect of shear and flexural stresses should be considered to reliably predict the failure load of hollow and filled multi-celled beams but with some modifications. Using the buckling stresses in bending and shear instead of the allowable stresses gives a reliable estimation of the failure load for hollow sections while using the allowable compressive stress and critical shear stress is accurate for the filled section.
- The failure of filled beams with 4 cells is governed by inter-laminar shear failure at the web-flange junction and the failure

load can be estimated reasonably well by calculating the nominal web crippling capacity of the pultruded GFRP beam.

## Acknowledgement

The authors are grateful to Wagner's Composite Fibre Technologies (WCFT), Australia for providing all the GFRP tubes in the experimental programme. The first author would like to acknowledge the financial support by the Ministry of Higher Education and Scientific Research-Iraq.

## References

- [1] Bank LC. Application of FRP composites to bridges in the USA. Japan Society of Civil Engineers (JSCE), Proceedings of the international colloquium on application of FRP to bridges, January 20, 2006. p. 9–16.
- [2] Ryall M, Stephenson R. Britannia bridge: from concept to construction. Proceedings of the ICE-Civil Engineering; Thomas Telford; 1999. p. 132–43.
- [3] Gand AK, Chan T-M, Mottram JT. Civil and structural engineering applications, recent trends, research and developments on pultruded fiber reinforced polymer closed sections: a review. *Front Struct Civ Eng* 2013;7:227–44.
- [4] Mottram J. Lateral-torsional buckling of a pultruded I-beam. *Composites* 1992;23:81–92.
- [5] Davalos JF, Qiao P. Analytical and experimental study of lateral and distortional buckling of FRP wide-flange beams. *J Compos Constr* 1997;1:150–9.
- [6] Bai Y, Keller T, Wu C. Pre-buckling and post-buckling failure at web-flange junction of pultruded GFRP beams. *Mater Struct* 2013;46:1143–54.
- [7] Turvey GJ, Zhang Y. Shear failure strength of web-flange junctions in pultruded GRP WF profiles. *Constr Build Mater* 2006;20:81–9.
- [8] Bank LC, Nadipelli M, Gentry TR. Local buckling and failure of pultruded fiber-reinforced plastic beams. *J Eng Mater Technol* 1994;116:233–7.
- [9] Barbero EJ, Fu S-H, Raftoyiannis I. Ultimate bending strength of composite beams. *J Mater Civ Eng* 1991;3:292–306.
- [10] Hai ND, Mutsuyoshi H, Asamoto S, Matsui T. Structural behavior of hybrid FRP composite I-beam. *Constr Build Mater* 2010;24:956–69.
- [11] Hejll A, Täljsten B, Motavalli M. Large scale hybrid FRP composite girders for use in bridge structures—theory, test and field application. *Compos B Eng* 2005;36:573–85.
- [12] Kumar P, Chandrashekhar K, Nanni A. Testing and evaluation of components for a composite bridge deck. *J Reinf Plast Compos* 2003;22:441–61.
- [13] Kumar P, Chandrashekhar K, Nanni A. Structural performance of a FRP bridge deck. *Constr Build Mater* 2004;18:35–47.
- [14] Satasivam S, Bai Y. Mechanical performance of bolted modular GFRP composite sandwich structures using standard and blind bolts. *Compos Struct* 2014;117:59–70.
- [15] Satasivam S, Bai Y. Mechanical performance of modular FRP-steel composite beams for building construction. *Mater Struct* 2016;49:4113–29.
- [16] Hayes M, Lesko J, Haramis J, Cousins T, Gomez J, Masarelli P. Laboratory and field testing of composite bridge superstructure. *J Compos Constr* 2000.
- [17] Schniepp TJ. Design manual development for a hybrid, FRP double-web beam and characterization of shear stiffness in FRP composite beams; 2002.
- [18] Hayes MD, Lesko JJ. Failure analysis of a hybrid composite structural beam. *Compos A Appl Sci Manuf* 2007;38:691–8.
- [19] Triantafillou T, Meier U. Innovative design of FRP combined with concrete. *Adv Compos Mater Bridge Struct* 1992:491–9.
- [20] Canning L, Holloway L, Thorne A. Manufacture, testing and numerical analysis of an innovative polymer composite/concrete structural unit. *Proc ICE-Struct Build* 1999;134:231–41.
- [21] Van Erp G, Heldt T, Cattell C, Marsh R. A new approach to fibre composite bridge structures. Proceedings of the 17th Australasian conference on the mechanics of structures and materials, ACMSSM17, Australia; 2002. p. 37–45.
- [22] Manalo AC, Aravinthan T, Mutsuyoshi H, Matsui T. Composite behaviour of a hybrid FRP bridge girder and concrete deck. *Adv Struct Eng* 2012;15 (4):589–600.
- [23] Chakraborty A, Khennane A, Kayali O, Morozov E. Performance of outside filament-wound hybrid FRP-concrete beams. *Compos B Eng* 2011;42:907–15.
- [24] Aydin F, Saribiyik M. Investigation of flexural behaviors of hybrid beams formed with GFRP box section and concrete. *Constr Build Mater* 2013;41:563–9.
- [25] Fam AZ, Rizkalla SH. Flexural behavior of concrete-filled fiber-reinforced polymer circular tubes. *J Compos Constr* 2002;6:123–32.
- [26] Gautam BP, Matsumoto T. Shear deformation and interface behaviour of concrete-filled CFRP box beams. *Compos Struct* 2009;89:20–7.
- [27] Muttashar M, Manalo A, Karunasena W, Lokuge W. Influence of infill concrete strength on the flexural behaviour of pultruded GFRP square beams. *Compos Struct* 2016;145:58–67.
- [28] Abouzied A, Masmoudi R. Structural performance of new fully and partially concrete-filled rectangular FRP-tube beams. *Constr Build Mater* 2015;101:652–60.

- [29] Khennane A. Manufacture and testing of a hybrid beam using a pultruded profile and high strength concrete. *Aust J Struct Eng* 2010;10:145–56.
- [30] Idris Y, Ozbakkaloglu T. Flexural behavior of FRP-HSC-steel composite beams. *Thin-Walled Struct* 2014;80:207–16.
- [31] Kim J-K. Size effect on flexural compressive strength of concrete specimens; 2000.
- [32] ASTM Standard D 695. Standard test method for compressive properties of rigid plastics. Philadelphia, USA: ASTM International; 2010.
- [33] ISO 527-2. Plastics: Determination of tensile properties; 1996.
- [34] Muttashar M, Karunasena W, Manalo A, Lokuge W. Behaviour of hollow pultruded GFRP square beams with different shear span-to-depth ratios. *J Compos Mater* 2015;0021998315614993.
- [35] ISO 1172. Textile-glass-reinforced plastics, prepegs, moulding compounds and laminates: Determination of the textile-glass and mineral-filler content- Calcination methods; 1996.
- [36] ASTM Standard D7250. Standard practice for determine sandwich beam flexural and shear stiffness. ASTM Standard D7250/D7250M-06. Philadelphia: ASTM International; 2006.
- [37] Kim J-K, Yi S-T, Kim J-Hj. Effect of specimen sizes on flexural compressive strength of concrete. *ACI Struct J* 2001:98.
- [38] Kim J-K, Yi S-T. Application of size effect to compressive strength of concrete members. *Sadhana* 2002;27:467–84.
- [39] Manalo A. Behaviour of fibre composite sandwich structures under short and asymmetrical beam shear tests. *Compos Struct* 2013;99:339–49.
- [40] Awad ZK, Aravinthan T, Manalo A. Geometry effect on the behaviour of single and glue-laminated glass fibre reinforced polymer composite sandwich beams loaded in four-point bending. *Mater Des* 2012;39:93–103.
- [41] Tomblin J, Barbero E. Local buckling experiments on FRP columns. *Thin-Walled Struct* 1994;18:97–116.
- [42] Kollár LP. Local buckling of fiber reinforced plastic composite structural members with open and closed cross sections. *J Struct Eng* 2003;129:1503–13.
- [43] Bank LC. Composite for construction structural design with FRP materials. New Jersey: John Wiley & Sons; 2006.
- [44] Wright H. Local stability of filled and encased steel sections. *J Struct Eng* 1995;121:1382–8.
- [45] Wu C, Bai Y. Web crippling behaviour of pultruded glass fibre reinforced polymer sections. *Compos Struct* 2014;108:789–800.

## Chapter 6: Parametric Investigation on Multi-Celled GFRP Beams

### **Paper IV: Prediction model for flexural behaviour of composite beam assembly partially filled with concrete**

This paper proposed a general theoretical model based on the maximum stresses of the GFRP materials and incorporating the effect of shear span-to-depth ratio and local buckling. The analytical model formulated in *Paper III* was used as a benchmark of the proposed model. The model integrates the material constitutive relationships from *Paper I* and *Paper II*. The accuracy of the model was verified by the experimental results reported in the literature and those presented in *Papers I to III*. A parametric study was then performed using the theoretical model to study further the effect of several parameters such as number of cell in the cross-section, shear span-to-depth ( $a/d$ ) ratio and the concrete filling percentage on the flexural behaviour of the multi-celled GFRP beams. The results showed that the increased number of cell enhanced the capacity of the hollow beams however their strength capacity is governed by either the failure of the top cells by compressive buckling of the top flange or bearing failure. On the other hand, either the bearing failure of the hollow cells under the concrete filled cells or web buckling of the top filled cell governs the behaviour of multi-celled beams with concrete infill. The increase of  $a/d$  ratio of hollow multi-celled resulted in a higher strength-to-weight ratio than beams with lower  $a/d$  ratio. Furthermore, multi-celled beams with concrete infill at the top cell only shows high strength-to-weight ratio than its hollow beams counterpart for all  $a/d$  ratios. Finally, a failure mechanism map was developed to help identify the possible failure mode of any combination of GFRP tubes with concrete. This failure map is also a useful tool for designers to identify the appropriate equation to calculate the failure load of multi-celled GFRP beams. Finally, the results obtained from this paper suggested that the proposed multi-celled GFRP system filled with concrete in the top cells can provide a higher strength and stiffer beams compared to hollow sections but maintain the lightweight characteristics of composite materials. In order to effectively use this system in applications such as bridges, it is important to investigate the dynamic behaviour and fatigue on its flexural behaviour which result from the effect of moving loads.

# Prediction Model for Flexural Behavior of Pultruded Composite Beam Assembly with Concrete Infill

Majid Muttashar<sup>1,2</sup>, Allan Manalo<sup>3</sup>, Warna Karunasena<sup>4</sup> and Weena Lokuge<sup>5</sup>

## ABSTRACT

This paper presents a theoretical model based on maximum stress theory to predict the behaviour of multi-celled hollow and concrete filled glass fibre reinforced polymer (GFRP) beams subjected to bending. The model accounts for the effect of local buckling of the flange and the web of the tube in addition to the effect of shear span-to-depth ratio ( $a/d$ ). The reliability of the model is verified using experimental results reported in the literature wherein a good agreement was obtained. A parametric study was then conducted to investigate the effect of number of cells in the cross-section,  $a/d$  ratio, and the percentage of concrete filling on the failure mode and failure load of the multi-celled composite beams. The results showed that either the bearing failure or compressive buckling of the hollow cells governs the behaviour of the multi-celled beams. A failure map plot to help ascertain the possible failure for multi-celled GFRP beams with and without concrete infill was also developed.

**Keywords:** Theoretical prediction, multi-cell GFRP beams, flexural behaviour, failure load, concrete infill, shear span-to-depth ratio, Failure mode map

<sup>1</sup>PhD candidate, Centre of Future Materials, Faculty of Health, Engineering and Sciences, University of Southern Queensland, Toowoomba, Queensland, 4350, E-mail: [majid.alzaidy@gmail.com](mailto:majid.alzaidy@gmail.com)

<sup>2</sup>Lecturer, Civil Engineering Department, Thi-Qar University, Thi-Qar, Iraq.

<sup>3</sup>Senior Lecturer, Centre of Future Materials, Faculty of Health, Engineering and Sciences, University of Southern Queensland, Toowoomba, Queensland, 4350, E-mail: [allan.manalo@usq.edu.au](mailto:allan.manalo@usq.edu.au)

<sup>4</sup>Professor, Centre of Future Materials, Faculty of Health, Engineering and Sciences, University of Southern Queensland, Toowoomba, Queensland, 4350, E-mail: [Karu.karunasena@usq.edu.au](mailto:Karu.karunasena@usq.edu.au)

<sup>5</sup>Senior Lecturer, Centre of Future Materials, Faculty of Health, Engineering and Sciences, University of Southern Queensland, Toowoomba, Queensland, 4350, E-mail: [Weena.lokuge@usq.edu.au](mailto:Weena.lokuge@usq.edu.au)

## INTRODUCTION

Glass fibre reinforced plastic (GFRP) composites are becoming an attractive materials for civil engineering and construction due to their high strength-to-weight ratio and durability (Fam et al. 2002). FRP composites are generally used as walkways and bridges in corrosive environment, water treatment plants, cooling towers and non-electromagnetic interference building (Bakis et al. 2002). Moreover, pultruded GFRP sections provide some distinct advantages in terms of lightness and simplicity in the design and construction of new-build structures. However, the thin walled of these composite sections prevent the full utilisation of their superior strength properties. These sections are susceptible to premature failures including compression buckling, web buckling and web-flange junction failures (Bank 2006, Muttashar et al. 2016). Research by Bai et al. (2013) and Muttashar et al. (2016) has shown that these type of failures result in the pultruded composite sections utilising only around 45% of the maximum compressive strength determined from the coupon tests .

Several concepts were developed and implemented to use the GFRP profiles effectively in the construction industry. The first concept was dealing with assembling small pultruded sections using glue or bolts to produce a large structural member to carry high loads and provide high stiffness (Hejll et al. 2005, Kumar et al. 2004, Satasivam et al. 2014). Despite of the lightweight characteristics and good flexural performance of the assembled composite sections, these sections were susceptible to failure by twisting of the top layer, web-flange junction failure and premature local buckling of the flange underneath the loading point. Accordingly, the use of GFRP composites in combination with concrete as filling material for pile and bridge girder applications was investigated as another concept (Muttashar et al. 2016, Fam et al. 2001, Mirmiran et al. 1996, Davol et al. 2001). The concrete infill eliminated the local buckling of the thin walled GFRP section, which significantly improved the load-carrying capacity and stiffness of the structural system. At the same time, the composite tube provided a non-corrosive protection to the concrete thereby increasing its durability. Nonetheless, the lightweight characteristic of the FRP composites was compromised in this hybrid structural form. As a result, this concept was modified by providing a hole in the filled concrete to improve the strength and the stiffness of the section and at the same time to reduce the total weight of the section. Several researchers developed hybrid structural systems in which an inner hole in the filled concrete was provided near the tensile zone (Fam et al. 2002, Khennane 2010, Idris et al. 2014). These studies pointed out that the inner hole in the concrete infill maintained the lightweight of the composite section and it had positive

effect on its strength and stiffness. However, a premature local buckling of the top layer of glued section, the flexural compression failure of the filled beams and the bond failure between the concrete and GFRP tube represented the main disadvantages of this system. In order to overcome the disadvantages of each concept and get benefit of their advantages, Muttashar et al. (2017) proposed a multi-celled beam partially filled with concrete which represents a combination of concepts 1 and 2. The partial filling of this system depends on the total filling of the individual cell in the multi-celled beam section. This design provided more flexibility in the filling procedure of the section, significantly reduced the effect of bond failure between the concrete and the GFRP tube by reducing the contact surface due to the use of small tubes. In addition, bonding small cells together allowed the effective usage of the composites and concrete. The results showed a good flexural performance of the tested beam where the failure mode changed from local buckling to failure of the GFRP profile. The results also highlighted that the increase of number of cells in the cross-section improves the load carrying capacity of the beam. In addition, the concrete filling enhanced the failure stress and the flexural stiffness of the beams. However, the work was limited to one shear span to depth ratio, only up to four celled beams and concrete filled in the top cells only. While the effects of these various parameters can be investigated experimentally, this is a very expensive and time-consuming exercise. Therefore, the development of theoretical model and verification with available experimental results is critical and important for the better understanding, analysing and designing the multi-celled beams with different dimensions and configurations.

Several analytical models were developed to predict the flexural behaviour of single cell hollow beams and concrete filled FRP beams. These models employed the Classical Lamination Theory (CLT) together with traditional section analysis or the so-called Fibre Model Analysis (FMA) which was developed based on strain compatibility and force equilibrium to predict the moment capacity and load-deflection behaviour of the composite beams (Davalos et al. 2001, Fam et al. 2005, Davalos et al. 1996, Nagaraj et al. 1997, Mohamed et al. 2010). These models have been verified for composite beams with only limited test results. Similarly, the CLT requires accurate information on the processing details of the FRP profile to predict its mechanical properties, which is not always available. In addition, the proposed models ignore the effect of the shear deformation and premature local buckling failure, which have a significant effect on the actual behaviour of the composite material.

Since the existing mathematical models have several limitations in terms of incorporating shear and local buckling effect, it is important that this paper presents a general theoretical model capable in predicting the flexural behaviour of single and multi-celled pultruded GFRP hollow and filled sections. The accuracy of the developed model was verified by experimental results from previous works by the authors and other studies reported in the literature. The model was also used to study the effect of a range of key parameters on the behaviour and failure mode of both hollow and filled GFRP tubes.

### **BEHAVIOUR OF ASSEMBLED COMPOSITES BEAM**

Extensive experimental works were conducted to investigate the behaviour of assembled GFRP beams under four-point bending. In the first stage, hollow pultruded GFRP beams were tested with different shear span-to-depth ( $a/d$ ) ratios (Muttashar et al. 2016). The results showed that the beams with  $a/d$  ratio of more than 4 exhibited a flexural mode of failure. The failure was controlled by the buckling under the load points followed by cracks and delamination at the compression face in addition to a web-flange junction failure as shown in Fig.1a. The beams with  $a/d$  less than 2 showed a transverse shear failure. the failure started with delamination and cracking of the fibre along the edges of the pultruded beam in addition to local buckling on the compression flange as shown in Fig.1b. The results of this stage suggested that shear deformation has a significant effect on the failure mode of the GFRP hollow beams. In the second stage, concrete of different compressive strengths were used to fill the GFRP tubes (Muttashar et al. 2016). The concrete infill enhanced the flexural performance of the beams by restricting and delaying the local buckling of the thin walls, thereby increasing the ductility and the strength of the section. The failure of the filled beams was due to flexural compression at the constant moment region including cracks in the fibres in the transverse direction as shown in Fig.2. It was observed that the delamination cracks occurred at the compression face, which later progressed into the sides. The results suggested that concrete filling has an important role in preventing the local buckling failure, which resulted in higher failure strength of the filled beams. The behaviour of multi-celled GFRP beams of 2, 3 and 4 cells were was investigated under four-bending configurations at the last stage (Muttashar et al. 2017). The failure of hollow sections initiates due to the local buckling of the thin walls of the top cell, which eventually resulted in material degradation and total failure as shown in Fig.3. The failure of filled beams was similar to that of hollow beams. However, those beams failed at higher moment due to the contribution of the concrete core. On the other hand, the four bonded cell section showed different mode of failure as shown in

Fig.4. the beam failed due to flange-web junction failure of the hollow cell under the filled cell which results from bearing pressure of the top cell. The results suggested that number of cell has important effect on the failure mode of multi-celled beams. More importantly, the results of these experimental investigations enabled the identification of several parameters that affect the behaviour of multi-celled beams such as number of cells, shear span-to-depth ratio and filling percentages.

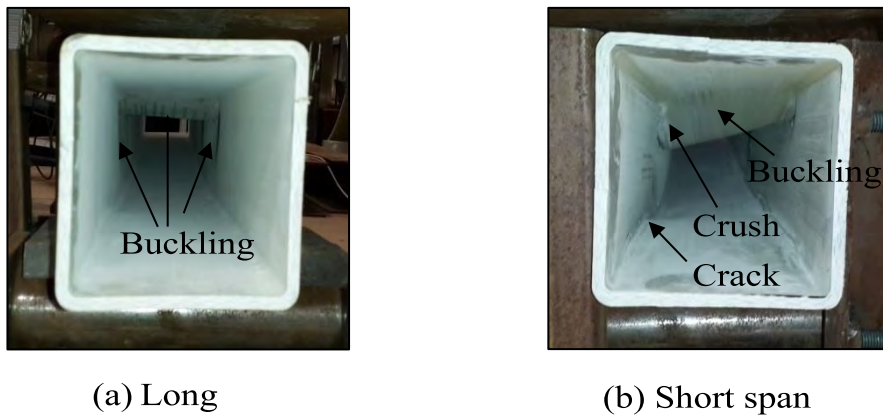


**Fig. 1.** Failure mode of long and short GFRP hollow beams

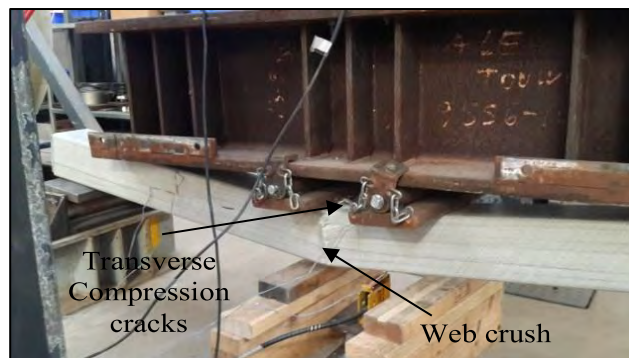


**Fig. 2.** Failure mode of GFRP filled beam

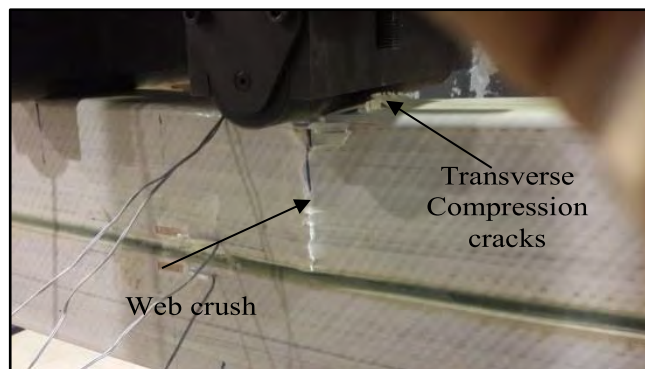


**Fig. 3.** Failure mode of multi-celled hollow beam

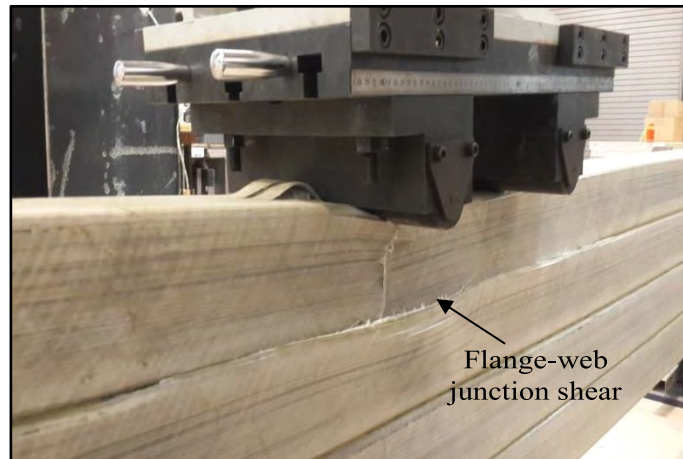


**Fig. 4.** Failure mode of 4 cell filled beams

## **PARAMETERS AFFECTING ASSEMBLED BEAM BEHAVIOUR**

### **Number of cells**

The concept of assembling a number of panels or sheets together to produce large structural beam section is not new. Timber engineers used this technique in glue-laminated (glulam) lumber where several smaller pieces of wood horizontally or vertically laminated to produce large section in order to carry higher loads (Manalo et al. 2010). Although the composite materials demonstrate high strength and high stiffness, the limitation on their shape size confines their wide use for civil engineering applications. Manalo et al. (2010) conducted experimental investigations onto the behaviour of glue-laminated fibre composite sandwich beams. The beams consisted of 1, 2, 3, and 4 innovative composite sandwich panels glued together in the flatwise and edgewise positions to produce a structural beam section. The authors specified that gluing the composite sandwich beams together in edgewise position resulted in a stronger and more stable section than the individual sandwich beams alone. They found that the increase of the bending strength was due to the contribution of the vertical skins in preventing the widening of the core flexural tensile cracks, which prevented the premature failure of the beam. Due to the high cost of the manufacturing die, the pultruded GFRP tubes are produced in specific cross-section dimensions only. For high load applications and to comply with the serviceability requirements, a number of these pultruded sections can be assembled together by gluing them appropriately. Kumar et al. (2004), (Kumar et al. 2003) investigated the flexural behaviour of two, four and eight layered tubes bonded together by epoxy adhesive and tested under four-point bending test. The results showed that the failure load significantly increase with the increase of the layers' number.

They also indicated that joining technique provides flexibility in the design to have adequate stiffness to limit deflections or any deformations that may adversely affect the strength or serviceability of the structure. These studies have shown that the concept of gluing GFRP sections together provides additional flexural strength and stiffness, facilitate fast installation and provides flexibility in the design. However, local buckling of the thin walls of the top layer contributed to most of the failure mode. Therefore, an investigation on the effect of number of cells in both hollow and with concrete infill multi-celled sections is important to determine the optimum number of layers that will effectively utilise the high strength properties of the composite section while enhancing its stiffness properties.

### **Shear span to depth ratio**

The shear span-to-depth ( $a/d$ ) ratio has a noticeable effect on the failure mode of the composite beams but the research determining its effect on concrete filled FRP tubes is limited. In such system, shear failure which is governed by the  $a/d$  ratio took the form of FRP web buckling instead of diagonal cracking or concrete web crushing (Fam et al. 2006). Shawkat et al. (2008) investigated the effect of  $a/d$  ratio on the structural behaviour of GFRP tubes totally filled with concrete. The results showed that the moment capacity of concrete filled pultruded GFRP beams increase with the increase of  $a/d$  ratio from 1 to 3. Furthermore, the authors present a second order polynomial equation for the relationship between the variation of the mid tensile strain and  $a/d$  ratio depends on the experimental results. According to the trend of the proposed equation, they suggested that the full flexural strength of the section could be achieved when  $a/d$  ratio exceeded 5. In addition, the results indicated that the longitudinal tensile strains in the flange at which failure occurred was dependent on  $a/d$  ratio. Ahmad et al. (2005) conducted experimental and theoretical investigations on the shear strength of deep concrete-filled FRP tube (CFFT) beams with different  $a/d$  ratios (0.5, 0.75 and 0.9). The results showed that shear may not be a critical issue for CFFT beams compared with their reinforced concrete counterpart for  $a/d$  ratios as low as 1. On the other hand, they mentioned that the contribution of flexural stress increased beyond  $a/d$  ratio of 0.9. Furthermore, for CFFT beams with  $a/d=0.5$ , the shear contribution of GFRP tubes became negligible and the concrete resisted most of the shear. This behaviour is due to the increase in major compression strut angle and the decrease in the effective length of the tube. A composite system consisting of rectangular GFRP tubes connected to concrete slab was tested by Fam et al. (2006). The beam – slab system had  $a/d$  ratios of 2.85 and 6.45. The results showed that the beam with  $a/d$  ratio of 6.45 failed in flexural by reaching its full tensile strain

of the flange in flexure. On the other hand, the results showed that the  $a/d$  of 4 is a critical ratio at which flexural tension failure of the GFRP bottom flange and GFRP web buckling may occur which considered as a combined failure. Due to the low shear modulus of GFRP tubes and the high possibility of local buckling failure, the  $a/d$  is an important parameter that needs proper consideration in the theoretical evaluation of the flexural behaviour of composite beams with partial concrete infills.

### **Filling percentage**

Concrete – filled tubes (CFFTs) is an innovative structural system due to their high performance and durability (Son et al. 2008). However, filling the FRP tube completely with concrete was not optimal due to the flexural tensile cracking of the concrete core which do not provide bending resistance but just add weight to the beam (Abouzied et al. 2015). Therefore, partial filling of the FRP tubes was proposed by several researchers to reduce the excess weight of the cracked concrete below the neutral axis. Fam et al. (2002) conducted experimental investigation on the effect of an inner hole on the flexural behaviour of circular CFFT beams with an outer identical GFRP tube of 168 mm diameter. Two different beam configurations were tested in order to compare the flexural behaviour. The first beam was fully filled with concrete while the second beam had an inner central hole with an area equal to 50% of the cross section. The results showed that providing a central hole is effective as the strength of partially filled beams is only 9% less than that of completely filled beam while its strength to weight ratio is 35% higher. Accordingly, Fam et al. (2005) investigated the effect of an inner hole on the flexural behaviour of rectangular section 266 x 375 mm of filament wound FRP tube. The inner hole size was 60% of the cross section area of the beam (i.e. 40% concrete filling) that offset towards the tension side. The results indicated that the strength of the partially filled section is about 22% lower than that of completely filled beam; however, the overall strength to weight ratio of the partially filled tube was 77% higher. In this system, the buckling of the GFRP flange, which results in debonding from concrete, controlled the overall behaviour. This type of failure did not only reduce the effectiveness of the GFRP flange but also eliminated any partial confinement effect on concrete. Their study also highlighted the need to further optimize the size and the shape of the concrete flange in order to avoid premature compression failure. In another study, Abouzied et al. (2015) investigated the flexural behaviour of full scale rectangular CFFT beams partially filled with concrete. The beam contained rectangular GFRP tubes with inner void of hollow square or circular GFRP tubes (approximately similar cross-section area) shifted toward the tension

zone so that 66% of the cross section was filled with concrete. The results showed that the strength to weight ratio of the partially filled beams is higher than that of fully filled beam by 6%. The beam with circular void showed 7% higher moment capacity compared with a square void. It is clear from the results of the previous research that partial filling has a significant effect on the flexural behaviour of CFFT beams. In addition, the location of the inner hole and the percentage of filling play an important role in the overall behaviour of the composite beams. Therefore, further investigation is required to optimize the concrete filling percentage in order to achieve better performance and to keep the lightweight properties of the composite materials. This study focused on evaluating the strength and stiffness of assembled GFRP tubes by filling the cells with concrete.

### **ANALYTICAL MODEL DEVELOPMENT**

Extensive experimental based research has been conducted to investigate the flexural behaviour of hybrid beams (Fam et al. 2002, Muttashar et al. 2016, Mohamed et al. 2010, Abouzied et al. 2015, Fam et al. 2005). Each study focused on limited parameters such as laminate structure, concrete filling, cross-section, concrete compressive strength, reinforcement type, and partial filling, which affected differently the overall behaviour of the tested beams. Therefore, simplified theoretical studies are important to predict the effect of some of these key parameters. Various studies used the traditional section analysis or the so-called fibre model analysis (FMA) to predict the behaviour of FRP hybrid beams (Fam et al. 2002, Davol et al. 2001, Mohamed et al. 2010, Abouzied et al. 2015, Fam et al. 2005). This fundamental design methodology is often used in analysing steel reinforced concrete and fibre reinforced concrete beams (Manalo et al. 2012). In this analysis method, a layer-by-layer approach based on strain compatibility and force equilibrium is adopted to integrate the stresses over the cross-sectional area of the composite beam. One of the important advantages of this approach is that it can account for the different behaviour of constituent materials. In general, FMA is based on a first ply failure criteria, thus the existing model ignores the effect of local buckling of the section in compression in the analysis which significantly effects on the accuracy of the failure load prediction (Davol et al. 2001). Moreover, its application is limited to structures subjected to pure bending only. Due to the low shear modulus of composite materials, FRP web buckling was considered the main reason of failure especially for low shear span to depth ratio. Therefore, Shawkat et al. (2008) and Fam et al. (2006) developed a simplified strut-and-tie model for a single cell filled beam sections. In the model, a relationship between  $a/d$  and mid span tensile strain was plotted according to the

experimental results. Although, the proposed model showed reasonable predictions of the ultimate loads, which are generally on the conservative side, it neglected the effect of local buckling. As a result, the authors highlighted that the model may only be applicable to their experimental results and may need further verification to generally predict the behaviour of the composite beams.

This study proposed a general theoretical model to predict the failure load of multi-celled composite beams that can account for shear deformation effect and local buckling effect. The model adopted the maximum stress method recommended by the structural plastics design manual ASCE (ASCE 1984) and modified by Muttashar et al. (2015). In the prediction of the failure load, the hollow beams are expected to fail due to local buckling of the flange and the web while the filled beams are assumed to fail by web shear buckling and material failure in the compression side. The contribution of shear deformation was accounted and a perfect bond was assumed between the concrete infill and the GFRP tube as well as between the glue lines of the GFRP tubes. The Microsoft (MS) Excel spreadsheet was used to implement the theoretical analysis of the flexural behaviour of the hybrid composite beams.

### **Prediction of Failure Load**

The failure load was predicted using the maximum stress method which account for the effect of  $a/d$  ratio and local buckling. For a composite beam tested under static bending loads, the modes of failure can be generally classified as: web buckling due to shear stresses causing shear failure; local buckling of compression flange due to normal stresses resulting in flexural failure; lateral buckling failure of the beam; debonding failure at the GFRP-concrete or GFRP- GFRP interface (Deskovic et al. 1995); and web-flange junction failure (bearing failure) (Wu et al. 2014). Muttashar et al. (2015), Muttashar et al. (2016) and Muttashar et al. (2017) however, found that lateral buckling and debonding failure can be eliminated by filling the top cell of the composite beam made from assembly of pultruded GFRP sections. Similarly, debonding failure was unlikely to occur due to the very low magnitude of the inter-laminar shear stresses (relative to shear strength of high quality epoxy adhesive). As a result, shear failure, combined shear and flexural failure, flexural failure, and bearing failure are the main failure modes that are expected for hollow and partially filled composite beams.

The combined effect of the flexural and shear stresses was accounted due to the change in  $a/d$  ratios. Manalo (2013) and Awad et al. (2012) showed that analytical prediction for shear is acceptable for specimens with  $a/d$  less than 2 while the prediction using bending equation is better for  $a/d$  greater than 4.5. In between these  $a/d$  ratios, they suggested to consider the

combined effect of shear and bending. Bank (2006) has the same suggestion in the evaluating of the structural behavior of GFRP composites. Following this, it is expected that the failure of pultruded GFRP beams will occur when the sum of the ratios of the actual shear and flexural stresses to that of their respective allowable stresses approaches unity as given by:

$$\frac{\sigma_{act}}{\sigma_{all}} + \frac{\tau_{act}}{\tau_{all}} \leq 1 \quad (1)$$

The actual flexural compressive stress  $\sigma_{act}$  of GFRP beams is the stress from the overall bending moment  $M$  which can be calculated as:

$$\sigma_{act} = \frac{Mc}{I} \quad (2)$$

where  $c$  is the distance from neutral axis to the section topmost fiber and  $I$  is the moment of inertia of the section transformed into GFRP. Similarly, the GFRP beams will fail in shear, where the actual shear stress  $\tau_{act}$  using Eq. (3) exceeds the allowable shear strength,  $\tau_{all}$ :

$$\tau_{act} = \frac{VQ}{It_w} \quad (3)$$

where  $V$  is the applied shear force,  $Q$  is the first moment of area of the transformed GFRP section, and  $t_w$  is the thickness of the section.

As the elastic instability of the pultruded GFRP sections in compression is governed by the local buckling (Correia et al. 2011), Muttashar et al. (2015) suggested the use of buckling stress,  $\sigma_{cr}^{local}$  instead of the allowable compressive stress in Eq. (1). This  $\sigma_{cr}^{local}$  for free and rotationally restrained orthotropic plates is based on the proposed Eq. (4) by Kollár (2003).

$$\sigma_{cr}^{local} = \min\{\sigma_{loc,f}, \sigma_{loc,w}\} \quad (4)$$

where  $\sigma_{loc,f}$  and  $\sigma_{loc,w}$  are the critical normal stresses of flanges and webs, respectively. In this method,  $\sigma_{cr}^{local}$  of the section is calculated considering the web and flange to be separate from each other and assuming them as orthotropic plates subjected to uniaxial compression and elastically restrained along their common edge. The critical normal stresses of the flanges and the webs can then be written as (Kollár 2003).

$$\sigma_{loc,f} = \frac{\pi^2}{b_f^2 t_f} \left[ 2\sqrt{(D_L D_T)(1 + 4.139\xi)} + (D_{LT} + 2D_S)(2 + 0.62\xi_{box-flange}^2) \right] \quad (5)$$

$$\sigma_{loc,w} = \frac{\pi^2}{d_w^2 t_w} \left[ 13.9\sqrt{(D_L D_T)} + 11.1D_{LT} + 22.2D_S \right] \quad (6)$$

The compression flange will buckle before one of the webs if  $(\sigma_{SS})_f/(E_L)_f < (\sigma_{SS})_w/(E_L)_w$ . In this case, the web restrains the rotation of the flanges and the spring constant is given as:

$$k_{box-flange} = \frac{4(D_T)_w}{d_w} \left[ 1 - \frac{(\sigma_{SS})_f(E_L)_w}{(\sigma_{SS})_w(E_L)_f} \right] \quad (7)$$

where

$$(\sigma_{SS})_f = \frac{2\pi^2}{b_f^2 t_f} \left( \sqrt{(D_L D_T)} + D_{LT} + 2D_S \right) \quad (8)$$

$$(\sigma_{SS})_w = \frac{2\pi^2}{d_w^2 t_w} \left( 13.9\sqrt{(D_L D_T)} + 11.1D_{LT} + 22.2D_S \right) \quad (9)$$

$$\xi_{box-flange} = \frac{1}{1+10[(D_T)_f/k_{box-flange}b_f]} \quad (10)$$

$$D_L = \frac{E_L^c t_f^3}{12(1-\nu_L \nu_T)} \quad (11)$$

$$D_T = \frac{E_T^c}{E_L^c} D_L \quad (12)$$

$$D_{LT} = \nu_T D_L \quad (13)$$

$$D_S = \frac{G_{LT} t_f^3}{12} \quad (14)$$

$$\nu_T = \frac{E_T^c}{E_L^c} \nu_L \quad (15)$$

where  $b_f$  and  $t_f$  are the width and thickness of the flange, respectively,  $d_w$  and  $t_w$  are the depth and thickness of the web, respectively,  $E_T^c$  is longitudinal compression modulus,  $E_L^c$  is transverse compression modulus,  $G_{LT}$  is the in-plane shear modulus, and  $\nu_L$ ,  $\nu_T$  are the major (longitudinal) and minor (transverse) Poisson ratios, respectively. On the other hand, the web buckles first when  $(\sigma_{SS})_f/(E_L)_f > (\sigma_{SS})_w/(E_L)_w$ . In this case, Kollár (2003) suggested to take  $k_{box-flange} = 0$  as a conservative estimate. The buckling stress is then calculated by using Eq. (6).

In terms of the shear stress, the web of the GFRP tube is highly susceptible to buckle in the location of high shear force while flange buckling will typically occur under the loading point or near the supports. The critical shear buckling stress of an orthotropic web can be determined using the relation (18) proposed in (Bank 2006):

$$\tau_{cr}^{local} = \frac{4k_{LT} \sqrt{D_L D_T^3}}{d_w^2 t_w} \quad (16)$$

where

$$k_{LT} = 8.125 + 5.045K \quad \text{for } K \leq 1 \quad (17)$$

and

$$K = \frac{2D_s + D_{LT}}{\sqrt{D_L D_T}} \quad (18)$$

Kollár (2003) highlighted that for the orthotropic materials in conventional GFRP pultruded profiles,  $K < 1$ .

For the filled section, the flexural stress is changed from buckling stress ( $\sigma_{cr}^{local}$ ) to the maximum stress ( $\sigma_{all}$ ) due to the concrete core preventing local buckling in the GFRP section. Wright (1995) highlighted that the infill concrete will contribute in delaying or eliminating the local buckling in the compression flange. However, it has a minimum effect on the buckling of the webs due to the insufficient connection between the tube and the concrete. As a result, the section will develop more resistance to the applied load and will reach its maximum allowable compressive stress. Under such condition, Eq. (1) can be used to predict the failure of multi-celled sections but considering  $\tau_{cr}^{local}$  as the effective shear stress instead of  $\tau_{all}$ . With these assumptions, the predicted failure load,  $P_H$  of single and multi-celled hollow beams is given by Eq. (19) while the predicted failure load,  $P_F$  of their counterpart filled beams is given by Eq. (20).

$$P_H = \frac{1}{\frac{ac}{2I\sigma_{cr}^{local}} + \frac{Q}{2It\tau_{cr}^{local}}} \quad (19)$$

$$P_F = \frac{1}{\frac{ac}{2I\sigma_{all}} + \frac{Q}{2It\tau_{cr}^{local}}} \quad (20)$$

For some cases, the experimental observations by Muttashar et al. (2017) indicated that there is a high possibility for the occurrence of the bearing failure when the number of cells and percentage of filling increases in the section. This failure occurred due to the high inter-laminar stress at the flange-web junction, which has exceeded the shear capacity limit of the pultruded section. Wu et al. (2014) indicated that pultruded FRP beams subject to concentrated loads in the plane of the web are more likely to show inter-laminar shear failure due to bearing stresses at the web-flange junction. They then proposed following Equation to estimate the nominal web crippling capacity of the pultruded GFRP beams:

$$R_N = f_s A_{shear} \quad (21)$$

where

$$A_{shear} = 2 t_w b_{plate} \quad (22)$$

and  $b_{plate}$  represents the width of the bearing plate and  $f_s$  is the inter-laminar shear strength of the section. In this study, Eq.s (19, 20 and 21) combined with Eq.s (1 and 2) are used to predict the failure load of the multi-celled pultruded GFRP beams. The failure load of the section was taken as the minimum value among the calculated failure loads from these proposed equations.

The typical cross section of the hollow and concrete filled beams consists of single and multi-celled square FRP tubes with a web depth  $d$ , flange width  $b$  and thickness of web and flange ( $t_w$  and  $t_f$ , respectively) of 6.5 mm. The concrete infill has a thickness  $c_l$  and width  $b_l$  as shown in Fig. 5. The model takes into the account the round corners of the section. The properties of the materials constituting the cross section are as follows:  $E_F$  is the longitudinal Young's modulus of the GFRP section,  $E_c$  is the Young's modulus of concrete,  $f'_c$  is the compressive strength of concrete, and  $G_f$  is the shear modulus of GFRP section.

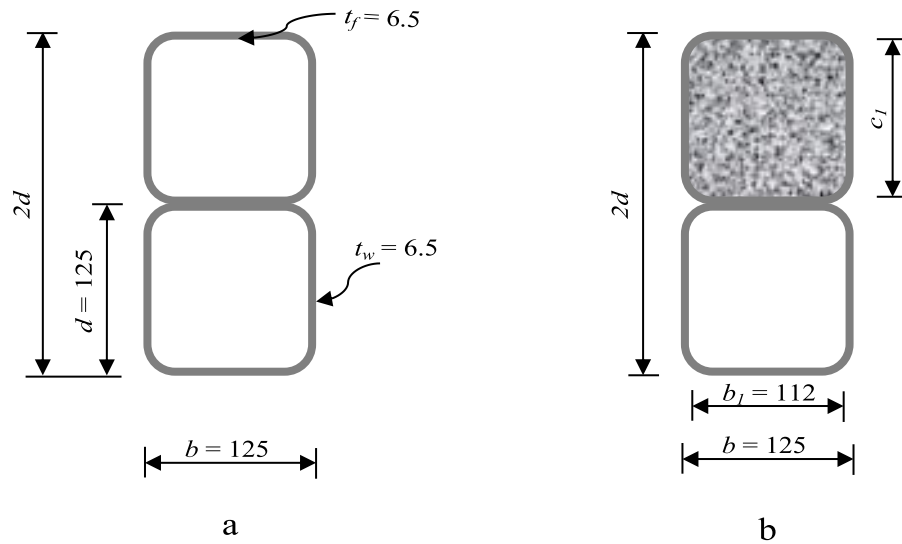


**Fig. 5.** Typical cross-section of GFRP composite beam: a) hollow b) filled.

### Calculation of Flexural Stiffness

The flexural rigidity of the hollow and infilled sections is given by the following:

$$EI = \sum_i^n E_i I_i + E_i A_i (N.A - y_{gi})^2 \quad (23)$$

and

$$N.A = \frac{\sum E_i A_i y_i}{\sum E_i A_i} \quad (24)$$

where  $E_i$  is the modulus of elasticity of element  $i$ ,  $A_i$  is the area of element  $i$ ,  $y_i$  is the distance from the stiffness centroid of the element  $i$  to a chosen fixed point (in present study, the bottom of the cross section) and  $I_i$  is the second moment of area of each element  $i$  around

its own stiffness centroid  $y_{gi}$  as shown in Fig. 6. An equivalent section was used for concrete infill using the modular ratio  $n = E_c/E_f$  where  $E_c$  and  $E_f$  are the concrete and GFRP elasticity modulus, respectively.

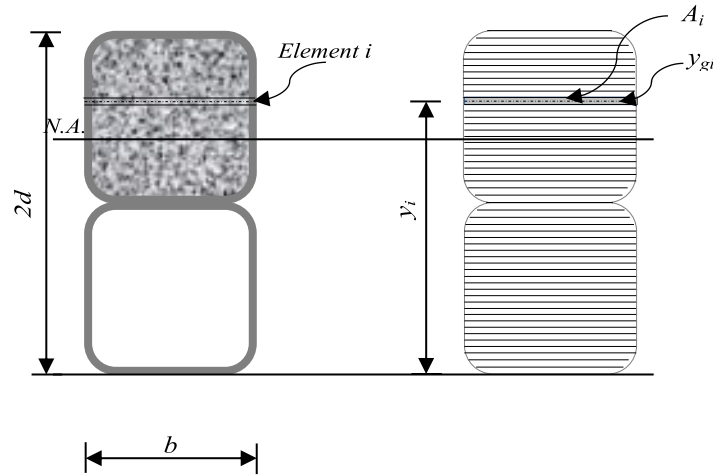


**Fig. 6.** Element geometry.

### Model verification

Eq.s (19, 20 and 21) were used to calculate the failure loads of two (Kumar et al. 2003), four (Muttashar et al. 2015) single cells and three multi-celled hollow GFRP beams in addition to four filled beams (Muttashar et al. 2016, Muttashar et al. 2017). The comparison between the values calculated from the proposed model and those measured from the experiment is presented in the succeeding sections.

### Hollow beams

Eq. (19) was used to predict the failure load of a single cell hollow beam specimens tested by Kumar et al. (2003), Muttashar et al. (2015) and Muttashar et al. (2016). Fig. 7 shows the comparison of the experimental and theoretical prediction failure load of the tested beams. A very good estimation for the failure load was achieved with the discrepancy between the experimental results and theoretical prediction varying between 3% and 10%. The lower predicted value for beams with an  $a/d$  ratio of 1.2 is due to the variation of the cross-section dimension as well as the more complex behaviour in shear of composites as highlighted by Manalo [34]. Fig. 7 also shows that the failure load decreases with the increase of  $a/d$  ratio. The main reason for this behavior is the change of the failure mode from the web-flange junction failure to the local buckling of the thin walls of the compression flange that ultimately results in materials degradation and total failure. Eq.s (19 and 21) were

used to predict the failure load of the multi-celled beams with a/d ratio of 4.2 by Muttashar et al. (2017). Fig. 8 shows the relationship between the number of cells and the predicted failure load. A very good agreement between the predicted and the experimental failure load was observed. A combine shear and flexural mode of failure controlled the behavior of the tested beams. However, the failure mode for 5-celled beams changed to bearing due to the increased rigidity of the beam. The comparison of the failure load between the proposed model and the experimental investigation for single and multi-celled hollow beams showed that the model can reliably predict the failure load of composite beams with different configurations.

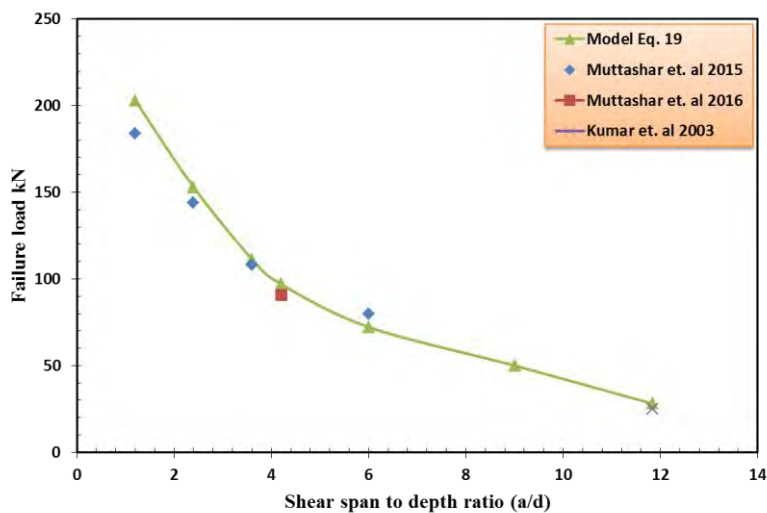


**Fig. 7.** Relationship between failure load and shear span to depth ratio for single cell hollow section.

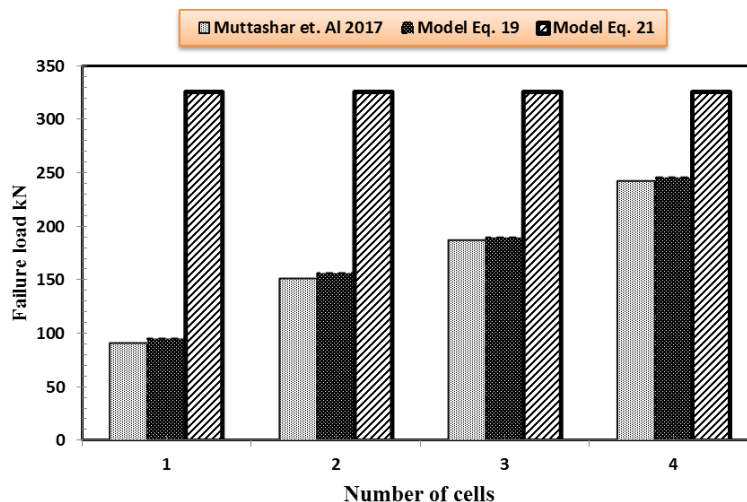


**Fig. 8.** Relationship between failure load and number of cells of multi-celled hollow section.

## Concrete filled beams

Eq.s (20 and 21) were used to predict the failure load of single and multi-celled sections filled with concrete and compared to the experimentally measured failure load by Muttashar et al. (2017). The observed failure mode was either combined shear and flexure (transfer cracks at the topmost fibre in the compression side in addition to outward buckling of the web) or bearing (longitudinal shear cracks at the web-flange junction). Fig. 9 shows the experimental and predicted failure load which shows that the model predicted quite well the failure load due to combined effect of shear and flexure up to 3 cells while the bearing Eq. (21) predicted the failure of 4 celled-beams. The bearing failure of 4 celled beams was due to the increase of the concentrated stresses between the two point's loads caused by the increase of the beams' depth. The failure occurred at the web-flange junction of the hollow cell of the beam while the top filled cell was not affected by the concentrated stresses due to the concrete infill which increased the bearing capacity of the cell. This behavior was valid for hollow and filled multi-celled beams. The increase of number of cells and the decrease of the  $a/d$  ratio resulted in an increase of the section capacity however the failure of the section was controlled by either its stress limit in compression or shear (Table 1).

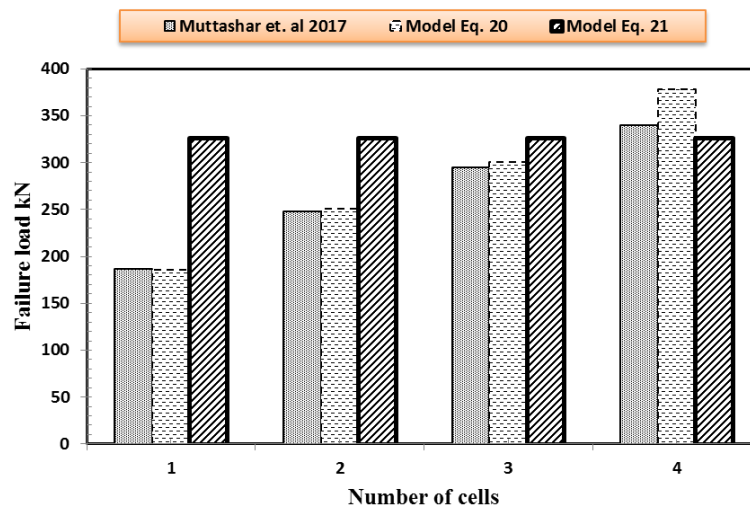


**Fig. 9.** Relationship between failure load and number of cells of multi-celled filled section

## PARAMETRIC STUDY

A parametric investigation of the effect of number of cells, shear span-to-depth ratio and number concrete filled cells on the flexural stiffness and failure load of multi-celled beams was conducted through theoretical evaluation. Muttashar et al. (2016) found that the concrete compressive strength has very minimal effect on the flexural behavior of the multi-celled

beams due to the brittleness of concrete and the small area of concrete contributing to the compressive force. Thus, only the effect of low strength concrete infill was analysed. Four-point bending test configuration with 300 mm distance between the applied loads was used as a case study in order to make comparison and validation of results with the available experimental works. Beams with up to 7 layers of pultruded GFRP tube, a/d ratios of 1.2, 2.4, 3.6, 4.2 and 6, and up to 100% concrete filled cells were also considered. The material properties of GFRP composite and low strength concrete were considered the same of those of (Muttashar et al. 2016) and are given in Table 1.

**Table 1.** Properties of the pultruded GFRP profiles and concrete.

Material property	Symbol	Property value	unit
<b>GFRP tubes</b>			
Density	$\rho$	2050	kg/m <sup>3</sup>
Tensile stress	$\sigma_t$	596	MPa
Tensile strain	$\epsilon_t$	16030	microstrain
Compressive stress	$\sigma_c$	550	MPa
Compressive strain	$\epsilon_c$	11450	microstrain
Inter-laminar shear	$\tau$	85.7	MPa
Elastic modulus	$E$	47.2	GPa
Shear modulus	$G$	4	GPa
<b>Concrete</b>			
Compressive strength	$f'_c$	15	MPa
Modulus of elasticity	$E_c$	20	GPa

### Effect of the number of cells

#### Hollow beam

Table 2 shows the predicted failure loads of the hollow beams with different a/d ratios and number of cells. The loads in the table represent the critical loads (the lowest load) among the predicted loads using Eq.s (1, 2, 19, 20, and 21). For example, the predicted failure load of beam 1C with a/d ratio 3.6 is 111.4 kN which is the minimum load among 136.7 kN, 602 kN, 111.4 kN and 326 kN which represent the failure load calculated according to bending stress, shear stress, combined shear and flexural stresses, and bearing stress, respectively. From the results, it is clear that the failure load increases as the number

of cells increases. It is also noted that expected failure mode changes according to the section capacity. On the other hand, the increase of  $a/d$  ratio results in decreasing load capacity. Similarly, the failure of multi-celled beams is expected to occur either combined effect of shear and flexural stresses or bearing failure. It is clear from the table that no pure shear failure is experienced by the section due to the nature of stacking sequence of the plies of the GFRP section which are arranged in the form of  $\pm 45$  degrees. This result is in good agreement with the experimental investigation by Ahmad et al. (2005) which enlightened that shear is not critical for CFFT beams. Furthermore, this behaviour agreed well with the experimental results of pultruded GFRP beams documented by Muttashar et al. (2016) and Wu et al. (2014). In addition, no pure bending failure is dominant for the beams due to the lower contribution of the shear even for the beams with  $a/d$  ratios of 6 and higher where the bending and shear contribution are 93% and 7%, respectively. Similar behaviour was documented in the literature by Fam et al. (2006) documented a similar behaviour for a composite T-beams that failed in flexural with  $a/d$  ratio of 6.45 however there is no mentioned that the failure was due to pure bending. These stress percentages are supported the assumption of the combined shear and bending failure of the beams. However, once the shear stresses under the point load exceeded the shear strength of the section at the web-flange junction, the beam will fail due to bearing. In Table 2, however, two types of failure were presented as the possible mode of failure for the pultruded GFRP hollow beams. The result suggested that the bending failure is not dominant even for beams with  $a/d$  ratios of 6. The behaviour is in contrary with the experimental results conducted by Awad et al. (2012) which highlighted that sandwich beams tested with  $a/d$  ratio of 4.5 will experienced bending failure. The main reason for this behaviour is the differences between the materials property and composition.

#### Filled beam

Table 2 also lists the predicted failure loads for multi-celled filled beams. Again, these loads are the critical loads calculated from Eq.s (1, 2, 20 and 21). It is clear that the failure load increased with increasing number of cells due to the contribution of the added tubes. However, it decreased with increasing  $a/d$ . The effect of concrete filling is more pronounced for higher  $a/d$  ratio compared with low ratios. The failure load of the filled beams shows an increase of 101%, 81%, 53%, 50% and 48% for the beams of 1C, 2C, 3C, 4C and 5C, respectively, compared with its hollow beam counterpart for  $a/d$  ratio of 6. However, the filled beams show less increase of the failure load with 71% and 28% for the beams of 1C

and 5C, respectively, for  $a/d$  ratio of 1.2. The percentage of increase of the failure load decreases at lower  $a/d$  ratio due to the change of the failure mode from combined bending and shear to bearing failure (shear at the web-flange junction). On the other hand, the increase of the failure loads percentages increases at higher  $a/d$  ratio was due to the decrease of the shear effect on the beam.

Table 2 also shows the failure load of multi- celled beams with 2, 3, 4 and 5 cells with the increase the number of filled cells. The general behaviour is similar to that of hollow sections such that the failure load increases as the cell's numbers in the cross-section increases while it decreased with the increase of  $a/d$  ratio. For  $a/d$  ratio of 1.2, the increase of the number of cells in the section showed insignificant effect on the failure load of the beam because the failure mode was governed by the bearing failure regardless of the number of cells. Although, the effect of bearing deceases with the increase of  $a/d$  ratio, the percentage of increase of the failure load shows less increase with the increase number of filled cells in the section due to the fact that the concrete core below the neutral axis is cracked and does not contribute much to the strength. The partially filled beams demonstrate about 20 – 25 % lower failure strength compared with the totally filled beams however their strength to weight ratio was higher. This behaviour is well agreed with the experimental results conducted by Fam et al. (2005). Similar to hollow beams, the results suggested that only two types of failure (combined bending and shear and bearing failure) are expected to occur for the filled beams.

**Table 2.** Predicted failure load of the multi-celled filled beams.

No. of cells	Filled	a/d				
		1.2	2.4	3.6	4.2	6
1	0C	244 <sup>a</sup>	153 <sup>a</sup>	111.4 <sup>a</sup>	98 <sup>a</sup>	72.2 <sup>a</sup>
	1C	417 <sup>d</sup>	290 <sup>b</sup>	210.7 <sup>b</sup>	185.4 <sup>b</sup>	145 <sup>b</sup>
2	0C	326 <sup>c</sup>	271 <sup>a</sup>	182 <sup>a</sup>	156.5 <sup>a</sup>	110 <sup>a</sup>
	1C	326 <sup>c</sup>	326 <sup>c</sup>	274.6 <sup>b</sup>	251 <sup>b</sup>	199.3 <sup>b</sup>
	2C	417 <sup>d</sup>	417 <sup>d</sup>	340.4 <sup>b</sup>	295.6 <sup>b</sup>	211.8 <sup>b</sup>
3	0C	326 <sup>c</sup>	303.6 <sup>b</sup>	216.8 <sup>b</sup>	189.7 <sup>b</sup>	138 <sup>b</sup>
	1C	326 <sup>c</sup>	326 <sup>c</sup>	326 <sup>c</sup>	299.9 <sup>b</sup>	212 <sup>b</sup>
	2C	326 <sup>c</sup>	326 <sup>c</sup>	326 <sup>c</sup>	326 <sup>c</sup>	282.9 <sup>b</sup>
	3C	417 <sup>d</sup>	417 <sup>d</sup>	417 <sup>d</sup>	394 <sup>b</sup>	283 <sup>b</sup>
4	0C	326 <sup>c</sup>	326 <sup>c</sup>	281 <sup>b</sup>	245.8 <sup>b</sup>	178.5 <sup>b</sup>
	1C	326 <sup>c</sup>	326 <sup>c</sup>	326 <sup>c</sup>	326 <sup>c</sup>	267.6 <sup>b</sup>
	2C	326 <sup>c</sup>	326 <sup>c</sup>	326 <sup>c</sup>	326 <sup>c</sup>	326 <sup>c</sup>
	3C	326 <sup>c</sup>	326 <sup>c</sup>	326 <sup>c</sup>	326 <sup>c</sup>	326 <sup>c</sup>
	4C	417 <sup>d</sup>	417	417 <sup>d</sup>	417 <sup>d</sup>	366.7 <sup>b</sup>
5	0C	326 <sup>c</sup>	326 <sup>c</sup>	326 <sup>c</sup>	301.6 <sup>b</sup>	219 <sup>b</sup>
	1C	326 <sup>c</sup>	326 <sup>c</sup>	326 <sup>c</sup>	326 <sup>c</sup>	326 <sup>c</sup>
	2C	326 <sup>c</sup>	326 <sup>c</sup>	326 <sup>c</sup>	326 <sup>c</sup>	326 <sup>c</sup>
	3C	326 <sup>c</sup>	326 <sup>c</sup>	326 <sup>c</sup>	326 <sup>c</sup>	326 <sup>c</sup>
	4C	326 <sup>c</sup>	326 <sup>c</sup>	326 <sup>c</sup>	326 <sup>c</sup>	326 <sup>c</sup>
	5C	417 <sup>d</sup>	417 <sup>d</sup>	417 <sup>d</sup>	417 <sup>d</sup>	417 <sup>d</sup>
6	0C	326 <sup>c</sup>	326 <sup>c</sup>	326 <sup>c</sup>	326 <sup>c</sup>	283 <sup>b</sup>
7	0C	326 <sup>c</sup>	326 <sup>c</sup>	326 <sup>c</sup>	326 <sup>c</sup>	326 <sup>c</sup>

<sup>a</sup> combined shear and bending (Eq. 19); <sup>b</sup> combined shear and bending (Eq. 20); <sup>c</sup> bearing failure hollow (Eq.21); <sup>d</sup> bearing failure filled (Eq.21)

### Effect of shear span to depth ratio ( $a/d$ )

Strength to weight ratio

Fig.10 shows the effect of  $a/d$  ratio on the strength to weight ratio of single and multi-celled hollow beams. The bending strength ( $M$ ) of each beam was determined by ( $M = Pa/2$ ) where ( $P$ ) represents the failure load as shown in Table 2 and ( $a$ ) is the shear span. The

strength then divided by the weight of the section per meter length to calculate the strength to weight ratio. The weight of the beam was determined by considering the GFRP section density (Table 1) and a concrete density of  $2400 \text{ kg/m}^3$ . The results show that strength to weight ratio of the beams with  $a/d$  ratio of 1.2 was the lowest compared with other  $a/d$  ratios for single and multi-celled beams. This behaviour clearly demonstrates the negative effect of bearing failure on the strength capacity of the beams. With the increase in  $a/d$ , the strength-to-weight ratio increases. This effectiveness increases with the increase in the number of cells. For example, the strength-to-weight ratio of beams with single cells is at 0.01 at an  $a/d=1.2$  and increases to 0.15 at  $a/d$  of 6. On the other hand, the strength-to-weight ratio of 5 celled beams is at 0.06 at  $a/d=1.2$  and 0.22 at  $a/d$  of 6 or almost 4 times increase. These results suggest that GFRP beams at higher  $a/d$  is more effective than at lower  $a/d$  as it utilises better the high flexural strength of fibre composites but still maintaining its lightweight.

Fig. 11 displays the effect of  $a/d$  ratio on the strength to weight ratio of single and multi-celled beams with only top cell filled. The figure shows that the strength to weight ratio increases with the increase of  $a/d$  for both single and multi-celled beams. However,  $a/d$  ratio beyond 3.6 has a minimal effect on the strength to weight ratio for the beams of 1C, 2C and 3C, respectively. This is because of the similarity of the failure mode where the beams failed due to combined effect of shear and bending. On the other hand, the increase of  $a/d$  ratio shows a significant effect on the strength to weight ratio for the beams consist of 4 cells and higher. This behaviour reflects the decrease of the shear deformation effect with the increase of  $a/d$  ratio. Again, the results show that filled the top cell with concrete is more effective at higher  $a/d$  ratio compared with lower  $a/d$  ratio. Furthermore, the results indicate that the strength to weight ratio of the filled beams was higher than its counterpart hollow beams for all  $a/d$  ratios which reflects the positive contribution of the concrete infill on the failure behaviour of the beams.

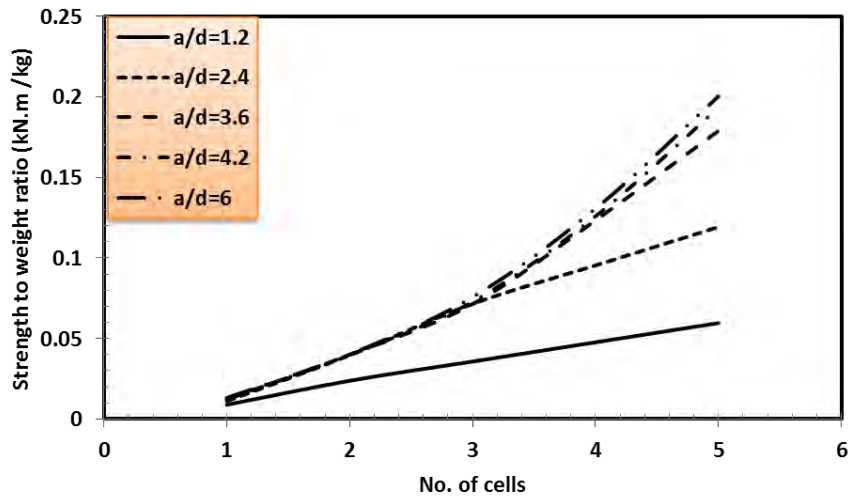


**Fig. 10.** Relationship between strength-to-weight ratio and a/d ratios for hollow section.

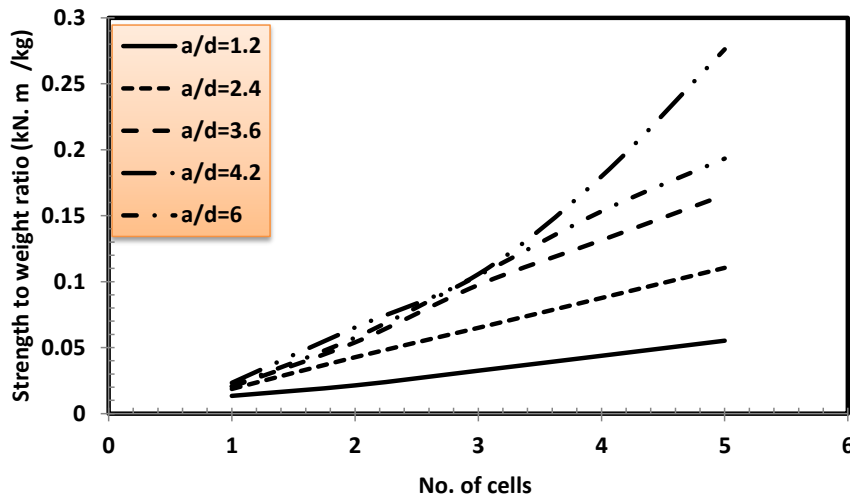


**Fig. 11.** Relationship between strength-to-weight ratio and a/d ratios for filled section.

### Effect of number of filled cells with concrete

#### Strength to weight ratio

The strength-to weight ratio of the composite beam with different number of cells filled with concrete was analysed. Fig. 12 shows the variation of the strength-to weight ratio with the number of filled cells. The results showed that filling the top cell of the section with concrete is an effective method to enhance the strength capacity of the multi-celled composite beams. The top filled section has the highest strength to weight ratio for beams with up to 4 cells. The increase in the strength-to-weight ratio is attributed to the effect of concrete infill in preventing the local buckling failure of the section. It can also be noted from the figure that the strength-to-weight ratio is highest for beams with 5 cells. However, filling the cells of the

beams with 5 cells did not enhance its strength-to-weight ratio. This is because the failure mode is governed by bearing failure for both hollow and filled sections. Instead, the section with higher number of filled cells shows lower strength-to-weight ratio compared with beams that has one cell filled. This behaviour might be resulted from two reasons; firstly, the increase of the number of filled cells in the cross-section changed the mode of failure from combined shear and bending to bearing failure. Secondly, due to the effect of concrete tension cracks, the additional concrete filling will contribute in lower percentage to the strength while it will add more weight to the total weight of beam. Although, increasing the number of filled cells in the section displays decreasing of the strength to weight ratio, it shows noticeable improvement compared with the hollow beams. The results suggested that filling the beam with concrete represents an effective solution in terms of increasing the strength to weight ratio for multi-celled composite beams. Still, strength to weight ratio of the beam with filling the top cell only with concrete is significantly greater than that of hollow and totally filled beams.

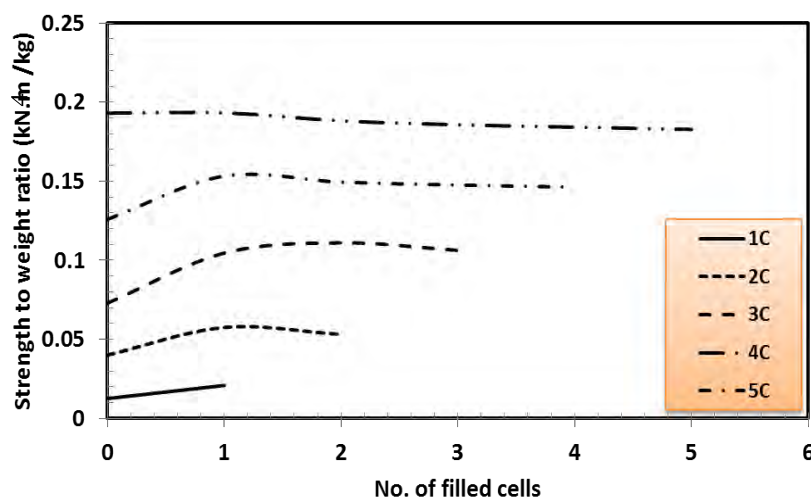


**Fig. 12.** Relationship between strength to weight ratio with number of filled cells of single and multi-celled beams.

#### Stiffness to weight ratio

The effect of concrete filling on the stiffness-to-weight ratio is presented in Fig. 13. The figure indicated that the stiffness-to-weight ratio increased with filling the top cell of the section with concrete compared with hollow beam. The main reason for that is the contribution of the concrete core in increasing the moment of inertia and the apparent modulus of the section. A similar observation was reported in the literature Fam et al. (2006) and Chakraborty et al. (2011). Beyond this, the stiffness-to-weight ratio of filled beams starts

to decrease to the point even lower than the hollow beams. This is because the concrete core infill near the neutral axis of the section did not contribute as much stiffness but significantly adding to the weight. The results show that filling the top cell of the section with concrete is more effective in increasing the stiffness to weight ratio compared with hollow and totally filled beams.

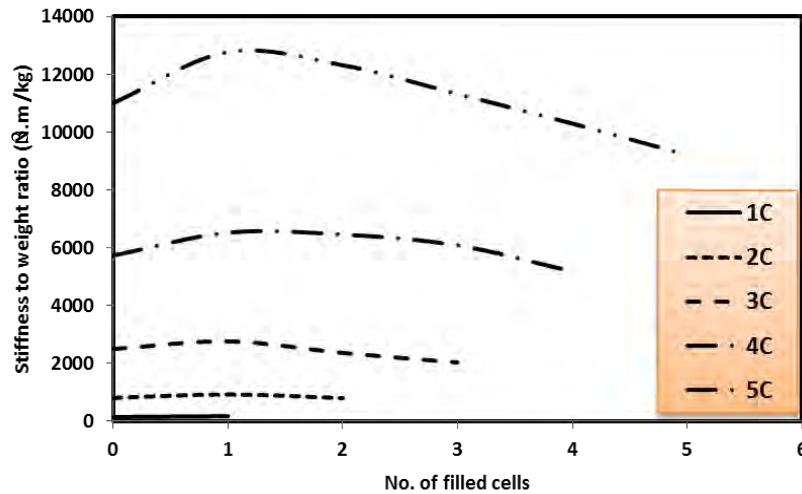


**Fig. 13.** Relationship between stiffness to weight ratio with number of filled cells of single and multi-celled beams.

### FAILURE MODE MAP

A failure mode map representing the different failure modes of composite beams was developed using the failure load Equations. This diagram was established by considering the relationship between the geometric non-dimensional variables or geometric and physical variables (Awad et al. 2012). In this study, the numbers of cells in the GFRP beam section and the  $a/d$  ratios were considered as the non-dimensional geometric properties, and the failure mode represents the physical variable. Of all the failure modes described previously, it is clear that the observed mode will be that which occurs at the lowest load. Considering the experimental results presented in (Muttashar et al. 2015) and (Muttashar et al. 2017), the failure mode of the GFRP beams is affected by the variations of  $a/d$  ratio and the number of cells in the cross-section in addition to the number of filled cells. Therefore, a failure map plot of  $a/d$  ratio in the x-axis and the number of filled cells in the y-axis was prepared to show the possible mechanisms of failure for multi-celled GFRP beams with different geometry. As listed previously, two failure modes (bearing (B) and combined shear and flexural failures (S+F)) have been defined in the failure map of the multi-celled GFRP composite beams using the proposed analytical model. Fig. 14 shows the final failure map of

the multi-celled GFRP hollow and filled beams. This results agreed well with the experimental results presented by (Muttashar et al. 2015). It is clear from the figure that the bearing failure can be avoided even at lower  $a/d$  ratio for single celled beams. On the other hand, to prevent the bearing failure of multi-celled hollow beams, higher  $a/d$  ratio should be used. The results also suggested that hollow beam with more than 6 cells in the cross-section has high tendency to fail in bearing.

Filling the sections with concrete will result in changing of the failure boundaries. While the section with filled concrete at the top showed highest strength-to-weight and stiffness-to-weight ratio, the tendency for bearing failure to occur becomes higher. From an  $a/d$  of 0.65 for hollow beams, single celled beam section with concrete infill needs to have at least an  $a/d$  of 1.5 to prevent the bearing failure. Furthermore, the figure shows that the slope of one cell filled is lower than hollow line, which further demonstrated the higher tendency for bearing failure. In addition, further increase in the possibility of the occurrence of bearing failure is expected when 2 and more cells filled with concrete. This behaviour is clearly shown in the figure as the line of 2 cells filled is lower than the other lines. Moreover, the failure mode map in Fig. 14 represents a useful and simply tool for the designers to calculate the failure load for any combination of GFRP tube and concrete. For example, by referring to the Failure mode map, a designer can identify that a multi-celled beam consisting of 3 cells, filled with concrete at the top, and with an  $a/d$  of 4 will fail by combined shear and bending. Following this, Eq. (20) should be used to calculate the failure load. Moreover, for 3-celled beams with top sections infill, the designer should specify an  $a/d$  of at least 4 to prevent bearing failure of the beam.

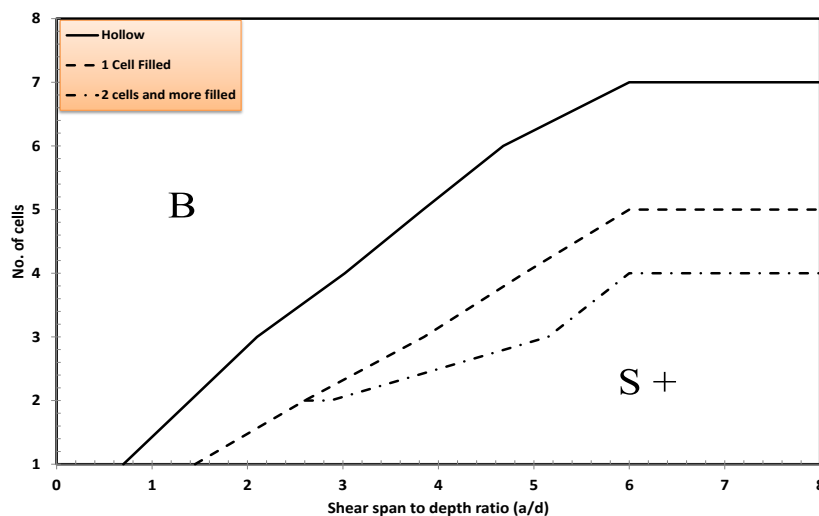


Fig. 14. Failure map of multi-celled GFRP beams.

## CONCLUSIONS

In this study, a general theoretical model to predict the failure load of multi-celled composite beams with concrete infill was established and calibrated with experimental results reported in the literature. The model was based on maximum stress method, which was modified to account for the effect of local buckling of GFRP tubes and the shear span-to-depth ratio. The proposed model agreed very well with the experimental results. The prediction model was then used to evaluate the effect of the number of cell in the cross-section, shear-span to depth ratio and the number of concrete filled cells on the flexural behaviour of GFRP tubes. A general failure map was then developed following the results of the parametric studies. The following conclusions are drawn from the results of the study:

- Increasing the number of cells increase the capacity of the hollow beams. Its strength capacity is, however governed by either failure of the top cells by compressive buckling of the top flange or bearing failure.
- The behaviour of the multi-celled beams with concrete infill is governed either by the bearing failure of the hollow cells under the concrete filled cells or web buckling of the top filled cells.
- Hollow multi-celled beams with a higher  $a/d$  ratio has higher a strength-to-weight ratio than beams with a lower  $a/d$ . Up to 400% increase in the strength-to-weight ratio for 5 celled beams was calculated by changing the  $a/d$  from 1.2 to 6.
- The strength-to-weight ratio of the multi-celled beams with concrete infill at the top cell is higher than its counterpart hollow beams for all  $a/d$  ratios. This reflects the positive contribution of concrete filling in stabilising the top cell and increasing the failure of the beam but adding minimal weight to the section.
- Filling the top cells only with concrete is better than filling all the cells. This is due to the mode of failure changing from combined shear and bending to bearing. Moreover, the stiffness-to-weight ratio of filled beams starts to decrease due to the concrete infill near the neutral axis that significantly add to the weight.
- A failure map plot to help ascertain the possible failure for multi-celled GFRP beams with and without concrete infill was developed. This plot can be also a useful tool for designers to identify the appropriate equation to calculate the failure load of multi-celled GFRP beams. Moreover, this can be an important preliminary tool to identify the design parameters that will prevent bearing failure of the beams and effectively utilise the high flexural strength of fibre composite materials.

## ACKNOWLEDGEMENT

The authors are grateful to Wagner's Composite Fibre Technologies (WCFT), Australia for providing all the GFRP tubes in the experimental programme. The first author would like to acknowledge the financial support by the Ministry of Higher Education and Scientific Research-Iraq.

## REFERENCES

- Fam, A. Z., and Rizkalla, S. H. (2002). "Flexural behavior of concrete-filled fiber-reinforced polymer circular tubes." *Journal of Composites for Construction*, 6(2), 123-132.
- Bakis, C., Bank, L. C., Brown, V., Cosenza, E., Davalos, J., Lesko, J., Machida, A., Rizkalla, S., and Triantafillou, T. (2002). "Fiber-reinforced polymer composites for construction-state-of-the-art review." *Journal of Composites for Construction*, 6(2), 73-87.
- Bank, L. C. (2006). *Composite for Construction Structural Design with FRP Materials*, John Wiley & Sons, New Jersey.
- Muttashar, M., Karunasena, W., Manalo, A., and Lokuge, W. (2016). "Behaviour of hollow pultruded GFRP square beams with different shear span-to-depth ratios." *Journal of Composite Materials*, 50(21), 2925-2940.
- Bai, Y., Keller, T., and Wu, C. (2013). "Pre-buckling and post-buckling failure at web-flange junction of pultruded GFRP beams." *Materials and structures*, 46(7), 1143-1154.
- Muttashar, M., Manalo, A., Karunasena, W., and Lokuge, W. (2016). "Influence of infill concrete strength on the flexural behaviour of pultruded GFRP square beams." *Composite Structures*, 145, 58-67.
- Hejll, A., Täljsten, B., and Motavalli, M. (2005). "Large scale hybrid FRP composite girders for use in bridge structures—theory, test and field application." *Composites Part B: Engineering*, 36(8), 573-585.
- Kumar, P., Chandrashekhara, K., and Nanni, A. (2004). "Structural performance of a FRP bridge deck." *Construction and Building Materials*, 18(1), 35-47.
- Satasivam, S., and Bai, Y. (2014). "Mechanical performance of bolted modular GFRP composite sandwich structures using standard and blind bolts." *Composite Structures*, 117, 59-70.
- Fam, A. Z., and Rizkalla, S. H. (2001). "Behavior of axially loaded concrete-filled circular fiber-reinforced polymer tubes." *ACI Structural Journal*, 98(3).
- Mirmiran, A., and Shahawy, M. (1996). "A new concrete-filled hollow FRP composite column." *Composites Part B: Engineering*, 27(3), 263-268.
- Davol, A., Burgueno, R., and Seible, F. (2001). "Flexural behavior of circular concrete filled FRP shells." *Journal of structural engineering*, 127(7), 810-817.
- Khennane, A. (2010). "Manufacture and testing of a hybrid beam using a pultruded profile and high strength concrete." *Australian Journal of Structural Engineering*, 10(2), 145-156.
- Idris, Y., and Ozbakkaloglu, T. (2014). "Flexural behavior of FRP-HSC-steel composite beams." *Thin-Walled Structures*, 80, 207-216.
- Muttashar, M., Manalo, A., Karunasena, W., and Lokuge, W. (2017). "Flexural behaviour of multi-celled GFRP composite beams with concrete infill: Experiment and theoretical analysis." *Composite Structures*, 159, 21-33.
- Fam, A., Mandal, S., and Rizkalla, S. (2005). "Rectangular filament-wound glass fiber reinforced polymer tubes filled with concrete under flexural and axial loading: Analytical modeling." *Journal of Composites for Construction*, 9(1), 34-43.
- Davalos, J. F., Salim, H., Qiao, P., Lopez-Anido, R., and Barbero, E. (1996). "Analysis and design of pultruded FRP shapes under bending." *Composites Part B: Engineering*, 27(3), 295-305.
- Nagaraj, V., and GangaRao, H. V. (1997). "Static behavior of pultruded GFRP beams." *Journal of Composites for Construction*, 1(3), 120-129.
- Mohamed, H. M., and Masmoudi, R. (2010). "Flexural strength and behavior of steel and FRP-reinforced concrete-filled FRP tube beams." *Engineering Structures*, 32(11), 3789-3800.
- Manalo, A., Aravinthan, T., and Karunasena, W. (2010). "Flexural behaviour of glue-laminated fibre composite sandwich beams." *Composite structures*, 92(11), 2703-2711.

- Manalo, A., Aravinthan, T., Karunasena, W., and Islam, M. (2010). "Flexural behaviour of structural fibre composite sandwich beams in flatwise and edgewise positions." *Composite Structures*, 92(4), 984-995.
- Kumar, P., Chandrashekhara, K., and Nanni, A. (2003). "Testing and evaluation of components for a composite bridge deck." *Journal of reinforced plastics and composites*, 22(5), 441-461.
- Fam, A., and Skutezky, T. (2006). "Composite T-beams using reduced-scale rectangular FRP tubes and concrete slabs." *Journal of Composites for Construction*, 10(2), 172-181.
- Shawkat, W., Fahmy, W., and Fam, A. (2008). "Cracking patterns and strength of CFT beams under different moment gradients." *Composite Structures*, 84(2), 159-166.
- Ahmad, I., Zhu, Z., Mirmiran, A., and Fam, A. (2005). "Shear strength prediction of deep CFFT beams." *Fiber reinforced polymers (FRP) for reinforced concrete structures VII*, 1085-1102.
- Son, J.-K., and Fam, A. (2008). "Finite element modeling of hollow and concrete-filled fiber composite tubes in flexure: Model development, verification and investigation of tube parameters." *Engineering Structures*, 30(10), 2656-2666.
- Abouzied, A., and Masmoudi, R. (2015). "Structural performance of new fully and partially concrete-filled rectangular FRP-tube beams." *Construction and Building Materials*, 101, 652-660.
- Fam, A., Schnerch, D., and Rizkalla, S. (2005). "Rectangular filament-wound glass fiber reinforced polymer tubes filled with concrete under flexural and axial loading: experimental investigation." *Journal of Composites for Construction*, 9(1), 25-33.
- Manalo, A., and Aravinthan, T. (2012). "Behaviour of glued fibre composite sandwich structure in flexure: experiment and fibre model analysis." *Materials & Design*, 39, 458-468.
- ASCE (1984). "Structural Plastics Design Manual." *ASCE Manuals and Reports on Engineering Practice 63*, American Society of Civil Engineering, Reston, VA.
- Muttashar, M., Karunasena, W., Manalo, A., and Lokuge, W. (2015). "Behaviour of hollow pultruded GFRP square beams with different shear span-to-depth ratios." *Journal of Composite Materials*, 0021998315614993.
- Deskovic, N., Triantafillou, T. C., and Meier, U. (1995). "Innovative design of FRP combined with concrete: short-term behavior." *Journal of Structural Engineering*, 121(7), 1069-1078.
- Wu, C., and Bai, Y. (2014). "Web crippling behaviour of pultruded glass fibre reinforced polymer sections." *Composite Structures*, 108, 789-800.
- Manalo, A. (2013). "Behaviour of fibre composite sandwich structures under short and asymmetrical beam shear tests." *Composite Structures*, 99, 339-349.
- Awad, Z. K., Aravinthan, T., and Manalo, A. (2012). "Geometry effect on the behaviour of single and glue-laminated glass fibre reinforced polymer composite sandwich beams loaded in four-point bending." *Materials & Design*, 39, 93-103.
- Correia, J. R., Branco, F., Silva, N., Camotim, D., and Silvestre, N. (2011). "First-order, buckling and post-buckling behaviour of GFRP pultruded beams. Part 1: Experimental study." *Computers & Structures*, 89(21), 2052-2064.
- Kollár, L. P. (2003). "Local buckling of fiber reinforced plastic composite structural members with open and closed cross sections." *Journal of Structural Engineering*, 129(11), 1503-1513.
- Wright, H. (1995). "Local stability of filled and encased steel sections." *Journal of structural engineering*, 121(10), 1382-1388.
- Chakraborty, A., Khennane, A., Kayali, O., and Morozov, E. (2011). "Performance of outside filament-wound hybrid FRP-concrete beams." *Composites Part B: Engineering*, 42(4), 907-915.

## Chapter 7: CONCLUSIONS and RECOMMENDATIONS

Glass fibre reinforced polymers (GFRP) profiles have become an attractive material for use in civil engineering applications due to their high strength, stiffness-to-weight ratio, non-corrosive and lightweight characteristics. To date, numerous research studies have demonstrated the suitability of combining pultruded FRP tubes and concrete for compression members but relatively few studies have been conducted to evaluate their flexural behaviour. Moreover, most of these studies have focused on utilising high compressive strength concrete infill to increase the strength and stiffness of the pultruded FRP tubes. By contrast, this study explored the usage of low compressive strength concrete infill for pultruded GFRP tubes to come up with a strong, stiff, and cost-effective beam section. The concept of multi-celled beams with concrete infill only at the top cells was also introduced to maintain the lightweight characteristics of composite materials. In order to have a complete understanding of the behaviour of these new beams, the study was conducted in the following four phases:

1. Determination of a suitable test method for characterisation of the mechanical properties of full-scale GFRP tubes. In addition, the study examined the effect of shear span-to-depth ratio on the failure capacity and failure mode.
2. Evaluation of the effect of compressive strength of the concrete infill on the flexural behaviour of pultruded GFRP beams using a four-point bending test.
3. Investigation of the behaviour of multi-celled GFRP beams with concrete infill with different numbers of bonded cells and different concrete filling percentages using a four-point bending test.
4. Examination of the influence of numbers of cells on the cross-section, shear span-to-depth ratio, and of the filling percentage on the flexural behaviour and failure mode.

The major findings of this study are summarized in the following sections.

### 7.1 Characterization of pultruded GFRP section properties

This study has experimentally investigated the flexural behaviour of full-scale hollow GFRP beams. Beams with different  $a/d$  ratios were considered in order to evaluate the flexural and shear moduli of the GFRP tubes, using the graphical (simultaneous) and

back calculation methods. These properties were then compared with the results from the coupon tests. A theoretical prediction equation, describing the behaviour of the tested beams, was also proposed. Based on the results of this investigation, the following conclusions are drawn:

- Material characterisation using full-scale specimens was an effective method to determine the elastic properties of the pultruded GFRP section. This test method can accurately capture the global properties of pultruded GFRP sections and the typical failure behaviour of compressive buckling and delamination at the web-flange junction at the compression face, which may not be covered by a test of coupons.
- The discontinuity of the fibres (especially the  $\pm 45^\circ$ ) in the coupon specimens resulted in a lower strength and effective elastic properties of the composite materials, compared to the properties obtained from the full-scale beam tests. Moreover, the small dimension of the section in the transverse direction limited the determination of the material properties using coupon specimens. This resulted in the overestimation of beam deflection by up to 7 %.
- The back calculation method, which was based on the Bernoulli equation and used the strain readings at the mid-span of the beam, gave a more reliable value of effective flexural and shear moduli of pultruded hollow GFRP square sections compared with a simultaneous method and coupon test. A maximum of 1.5% variation between the predicted and the actual load-deflection behaviour was achieved using the elastic properties determined from this method.
- The shear span-to-depth ( $a/d$ ) ratio has a significant effect on the flexural behaviour of the GFRP beams. While shear failure was not observed for beams with low  $a/d$  ratio, the shear deformation contributed by as much as 52% to the total deflection of beams. Thus, it is recommended to account for the shear deflection in the deflection calculation of GFRP beams when the  $a/d$  ratio is less than, or equal to, 6.
- A simplified theoretical model accounting for the combined effect of shear and flexural stresses as well as the compressive buckling stress in pultruded GFRP square beams can reasonably predict the failure load of full size pultruded GFRP beams. Comparison between the predicted and experimental results

showed only a maximum of 11% difference in the failure load for beams with low  $a/d$  ratios.

- The failure of the full-scale pultruded GFRP beam was governed by the compressive buckling under the loading points, followed by cracks and delamination at the web-flange junction at the compression face. The section failed at a stress level of 291 MPa, which denotes only 45% of the compressive strength capacity of the GFRP tube, as determined from the coupon test.

The above demonstrates that conducting a full-scale test is necessary to evaluate the effective mechanical properties of pultruded GFRP sections for its design to be reliable and safe. Furthermore, the results highlighted that local buckling and shear deformations have a significant effect on the flexural behaviour and failure mechanism of GFRP profiles. Filling these sections with concrete is anticipated to improve their structural performance and effectively utilise their high strength characteristics.

## **7.2 Behaviour of Single cell GFRP beams with concrete infill**

The effect of the compressive strength of concrete infill on the flexural behaviour of beams, with a view of determining a lower cost infill for GFRP profiles, was investigated. Experimental and theoretical investigations on hollow GFRP square sections (of 125 mm x 125 mm x 6.5 mm) filled with concrete, with 10 MPa, 37 MPa and 43.5 MPa compressive strength, were tested under 4-point static bending. The conclusions related to this study are summarised as follows:

- The provision of concrete filling prevented the local buckling of the thin walls of the GFRP tube by providing internal support, and it improved the section capacity due to its contribution to the internal compression forces. The concrete filled GFRP sections failed at a 100% to 141 % higher load than its hollow counterpart, and exhibited at least 25% higher stiffness.
- The failure of concrete filled GFRP beams was compressive failure of the GFRP tubes at a strain of 11250 microstrains. This level of strain represents 98% of the ultimate compressive strain of the pultruded GFRP tubes, as determined from the coupon tests, indicating the effective usage of the high-strength properties of the fibre composite materials.

- The use of low compressive strength concrete as infill material was an effective and practical solution to fill the pultruded GFRP tubes. Regardless of the compressive strength of the concrete infill, the flexural stiffness was almost the same after the initiation of the flexural cracks. Similarly, only a 19% higher failure load was observed for beams filled with concrete of 43.5 MPa compared to 10 MPa compressive strength.
- The simplified Fibre Model Analysis (FMA) accurately predicted the flexural behaviour of concrete filled GFRP tubes. The model adopted a partial confinement model for the concrete infill and produced a very good agreement in terms of the load-deflection and load-strain relationships between the theoretical and the experimental results.

From this study, it was further confirmed that the provision of concrete infill, regardless of the compressive strength, can effectively improve the strength and stiffness of pultruded GFRP beam beams. However, filling the entire section diminishes the lightweight properties of GFRP composites. The concept of multi-celled GFRP beams was therefore developed by gluing a number of pultruded sections and filling only the top cell of the beam with concrete. The flexural behaviour and the suitability of this concept for a structural beam were investigated in the next stage

### **7.3 Behaviour of multi-celled GFRP beams with concrete infill**

The flexural behaviour of multi-celled GFRP beams with concrete infill was investigated under four-point loading at an  $a/d$  ratio of 4.2. Beams of 1, 2, 3, and 4 cells with hollow and filled configurations were considered in this study. Concrete with 15 MPa and 32 MPa compressive strengths was used to fill the top cell of the beams. From the experimental and theoretical results, the following conclusions were drawn:

- Multi-celled pultruded GFRP hollow beams behaved linear elastic up to failure. The beams failed at a stress level ranging between 105% and 123% higher than the single-celled beams. This indicated that gluing together the pultruded GFRP profiles can help stabilise the section and effectively utilise the high strength of the fibre composite materials.

- The failure mode of 1, 2 and 3 celled-beams started at the compression flange with fibre breakage, matrix cracking and delamination, which then progressed into the webs because of the concrete core cracking. On the other hand, 4-celled beams show bearing mode failure due to longitudinal shear failure of the fibres at the web-flange junction of the hollow cell.
- Multi-celled beams filled with concrete at the top cell only developed higher strength compared with their hollow beam counterparts before failure as the concrete core delayed the local buckling by supporting the tube walls. This behaviour resulted in 105%, 63%, 57% and 38% higher flexural strength for 1, 2, 3, and 4 cells section, respectively than that of hollow sections. Furthermore, the concrete filling enhanced the flexural stiffness of the beams by as much as 22% compared to the hollow beams.
- Similar to single-celled beams, the compressive strength of the concrete infill has a minor effect on the flexural strength of the multi-celled GFRP beams. Only an increase of 14% in strength was measured for beams with 32 MPa concrete infill compared to 15 MPa. Moreover, the compressive strength of the concrete infill had an insignificant effect on the flexural stiffness, as the overall behaviour of the beam was governed by the GFRP tubes.

Multi-celled GFRP sections filled with concrete at the top cells only, showed high potential for structural beams and maintained the lightweight properties of the composite materials. The study highlighted the effect of several factors on the overall behaviour of multi-celled beams. A theoretical model is therefore needed to assess the effect of those factors on the behaviour of multi-celled beams in order to identify the suitable combination between a GFRP section and concrete infill for effective material usage.

#### **7.4 Theoretical study and capacity prediction**

A simplified theoretical model based on maximum stress theory was developed to predict the failure load and failure mechanisms of multi-celled GFRP beams. The model takes into consideration the local buckling and shear  $a/d$  ratio in its prediction of the flexural behaviour of the beams. The model was then used in a parametric study

to investigate the effects of the number of cells,  $a/d$  ratio, and the number of cells filled with concrete. From the parametric study, the following conclusions were drawn:

- The number of cells in the cross-section has a significant effect on the failure mode of the beam. The failure of single-celled hollow beams was combined shear and bending, while the multi-celled hollow beams failed due to bearing.
- Regardless of the number of cells, the behaviour of the multi-celled beams with concrete infill was governed either by the bearing failure of the hollow cells under the concrete filled cells, when the load exceeded the bearing capacity of the section, or by web buckling of the top filled cell, due to the increase of the compression stresses at the topmost flange-web junction.
- The strength-to-weight and stiffness-to-weight ratio of multi-celled beams filled with concrete at the top cells was significantly higher than that of hollow beams and multi-celled beams fully filled with concrete. Therefore, the multi-celled beams filled with concrete at the top cells could replace the heavy fully filled beam sections to reduce the construction cost and the dead weight of the structure.
- The increase of the  $a/d$  ratio of hollow multi-celled beams resulted in a higher strength-to-weight ratio than beams with a lower  $a/d$  ratio, due to the change of the failure mode from bearing to combined shear and flexural. For example, the strength-to-weight ratio for a 5-celled beam with an  $a/d$  of 6 was four times compared to an  $a/d$  of 1.2. Similarly, the strength-to-weight ratio of multi-celled beams with concrete infill at the top cell was higher than their counterpart hollow beams.

A failure mode map for identifying the possible mechanisms of failure for hollow and concrete filled multi-celled GFRP beams was developed. The failure map considered the numbers of cells in the GFRP beam section and the  $a/d$  ratios as the non-dimensional geometric properties. This map is an important preliminary tool to identify the design parameters that will prevent bearing failure of the beams and effectively utilise the high flexural strength of fibre composite materials.

## **7.5 Contributions of the study**

This study has provided an in-depth understanding of the behaviour of multi-celled GFRP beams with and without concrete infill. Through this study, a suitable test and data analysis method was determined to effectively evaluate the mechanical properties of full-scale pultruded GFRP composite beams. Furthermore, a more detailed understanding of the flexural behaviour of GFRP sections filled with concrete has been gained. This study has allowed the determination of the optimum compressive strength of concrete infill that will result in enhanced strength and stiffness of the hollow GFRP beams. This study has also developed a new type of bonded GFRP tubes (multi-celled beams) for usage in high load and long span applications. The proposed multi-celled beams were filled with concrete in the top cell only, which fully utilises the compressive strength of the composite materials. From the experimental results, simplified design equations were proposed and a failure map was developed to assist designers and engineers to reliably and safely design this type of structure.

## **7.6 Areas of the future research**

The research completed in this study has allowed for a detailed understanding of the effect of a range of parameters on the flexural behaviour of multi-celled GFRP tubes. However, the concept of multi-celled GFRP beams filled with low strength concrete is still in the early stages and requires further experimental and analytical work to increase their acceptance in construction applications. Areas that need further investigation to complete the development of multi-celled GFRP beams are the following:

1. While the low strength concrete infill proved to be a practical solution to fill the GFRP tubes and to enhance the strength and stiffness properties, a study on the effect of lightweight low-strength concrete infill on the flexural behaviour of a single cell GFRP beam is important to maintain the lightweight properties of composite materials.
2. Since the concept of multi-celled GFRP beams with their top cells filled with concrete proved to provide a structural element with high strength, high stiffness and lightweight, it is worth investigating the behaviour of beams with a concrete

filling only along their length, where the bending stresses are at a maximum level.

The multi-celled beams with concrete filling in the top cells only performed satisfactory under a static bending load. However, in real applications such as bridges, a higher cycle loading is expected to occur due to the effect of moving loads. Therefore, it is important to investigate the dynamic behaviour and fatigue on the flexural behaviour of multi-celled GFRP beams.

## List of References

- Abouzieed, A & Masmoudi, R 2013, 'Performance of square concrete-filled FRP tubes versus steel reinforced concrete columns', in Proceedings of 2nd conference on smart monitoring, assessment and rehabilitation of civil structures SMAR2013, Istanbul, Turkey: *proceedings of the Proceedings of 2nd conference on smart monitoring, assessment and rehabilitation of civil structures SMAR2013, Istanbul, Turkey.*
- Abouzieed, A & Masmoudi, R 2015, 'Structural performance of new fully and partially concrete-filled rectangular FRP-tube beams', *Construction and Building Materials*, vol. 101, pp. 652-60.
- Ahmad, I, Zhu, Z, Mirmiran, A, et al. 2005, 'Shear strength prediction of deep CFFT beams', *Fiber reinforced polymers (FRP) for reinforced concrete structures VII*, pp. 1085-102.
- Alampalli, S, O'Connor, J, Yannotti, A, et al. 1999, 'FRPs for bridge construction and rehabilitation in New York', *Materials and construction: Exploring the connection*, ASCE, Reston, VA, pp. 345-50.
- ASCE 1984, *Structural Plastics Design Manual*, ASCE Manuals and Reports on Engineering Practice 63, American Society of Civil Engineering, Reston, VA.
- Ascione, L, Giordano, A & Spadea, S 2011, 'Lateral buckling of pultruded FRP beams', *Composites Part B: Engineering*, vol. 42, no. 4, pp. 819-24.
- Ascione, L, Berardi, VP, Giordano, A, et al. 2013a, 'Local buckling behavior of FRP thin-walled beams: a mechanical model', *Composite Structures*, vol. 98, pp. 111-20.
- Ascione, L, Berardi, VP, Giordano, A, et al. 2013b, 'Buckling failure modes of FRP thin-walled beams', *Composites Part B: Engineering*, vol. 47, pp. 357-64.
- ASTM D7250 2006, *ASTM D7250/D7250M-06 Standard practice for determine sandwich beam flexural and shear stiffness*, ASTM International, West Conshohocken, (PA).
- ASTM D 695 2010, 'Standard test method for compressive properties of rigid plastics', ASTM International, Philadelphia, USA.'.

- Awad, ZK, Aravinthan, T & Manalo, A 2012, 'Geometry effect on the behaviour of single and glue-laminated glass fibre reinforced polymer composite sandwich beams loaded in four-point bending', *Materials & Design*, vol. 39, pp. 93-103.
- Aydin, F & Saribiyik, M 2013, 'Investigation of flexural behaviors of hybrid beams formed with GFRP box section and concrete', *Construction and Building Materials*, vol. 41, pp. 563-9.
- Bai, J 2013, *Advanced fibre-reinforced polymer (FRP) composites for structural applications*, Elsevier.
- Bai, Y & Keller, T 2009, 'Shear failure of pultruded fiber-reinforced polymer composites under axial compression', *Journal of Composites for Construction*, vol. 13, no. 3, pp. 234-42.
- Bai, Y, Vallée, T & Keller, T 2009, 'Delamination of pultruded glass fiber-reinforced polymer composites subjected to axial compression', *Composite Structures*, vol. 91, no. 1, pp. 66-73.
- Bai, Y, Keller, T & Wu, C 2013, 'Pre-buckling and post-buckling failure at web-flange junction of pultruded GFRP beams', *Materials and structures*, vol. 46, no. 7, pp. 1143-54.
- Bakis, C, Bank, LC, Brown, V, et al. 2002, 'Fiber-reinforced polymer composites for construction-state-of-the-art review', *Journal of Composites for Construction*, vol. 6, no. 2, pp. 73-87.
- Bank, L 1987, 'Shear coefficients for thin-walled composite beams', *Composite Structures*, vol. 8, no. 1, pp. 47-61.
- Bank, L 1989, 'Flexural and shear moduli of full-section fiber reinforced plastic(FRP) pultruded beams', *Journal of Testing and Evaluation*, vol. 17, no. 1, pp. 40-5.
- Bank, LC 2006, *Composite for Construction Structural Design with FRP Materials*, Jone Wiley & Sons, New Jersey.
- Bank, LC 2006, 'Application of FRP Composites to Bridges in the USA', in Japan Society of Civil Engineers (JSCE), Proceedings of the International Colloquium on Application of FRP to Bridges, January 20: *proceedings of the Japan Society of Civil Engineers (JSCE), Proceedings of the International Colloquium on Application of FRP to Bridges, January 20* pp. 9-16.
- Bank, LC & Yin, J 1999, 'Failure of web-flange junction in postbuckled pultruded I-beams', *Journal of Composites for Construction*, vol. 3, no. 4, pp. 177-84.

- Bank, LC, Nadipelli, M & Gentry, TR 1994, 'Local buckling and failure of pultruded fiber-reinforced plastic beams', *Journal of engineering materials and technology*, vol. 116, no. 2, pp. 233-7.
- Bank, LC, Yin, J & Nadipelli, M 1995, 'Local buckling of pultruded beams—nonlinearity, anisotropy and inhomogeneity', *Construction and Building Materials*, vol. 9, no. 6, pp. 325-31.
- Barbero, EJ & Raftoyiannis, IG 1993, 'Local buckling of FRP beams and columns', *Journal of Materials in Civil Engineering*, vol. 5, no. 3, pp. 339-55.
- Barbero, EJ, Fu, S-H & Raftoyiannis, I 1991, 'Ultimate bending strength of composite beams', *Journal of Materials in Civil Engineering*, vol. 3, no. 4, pp. 292-306.
- Bert, CW 1989, 'Classical Lamination Theory', in *Manual on Experimental Methods for Mechanical Testing of Composites*, Springer, pp. 11-6.
- Binici, B 2005, 'An analytical model for stress–strain behavior of confined concrete', *Engineering structures*, vol. 27, no. 7, pp. 1040-51.
- Canning, L, Hollaway, L & Thorne, A 1999, 'Manufacture, testing and numerical analysis of an innovative polymer composite/concrete structural unit', *Proceedings of the ICE-Structures and Buildings*, vol. 134, no. 3, pp. 231-41.
- Cardoso, D, Harries, K & Batista, E 2014, 'On the Determination of Mechanical Properties for Pultruded GFRP Sections', in International Conference on FRP composites in Civil Engineering: *proceedings of the International Conference on FRP composites in Civil Engineering* International Institute for FRP in Construction Vancouver, Canada.
- Chakraborty, A, Khennane, A, Kayali, O, et al. 2011, 'Performance of outside filament-wound hybrid FRP-concrete beams', *Composites Part B: Engineering*, vol. 42, no. 4, pp. 907-15.
- Chen, DS & El-Hacha, R 2010, 'Flexural behaviour of hybrid FRP-UHPC girders under static loading', in Proceedings of 8th International Conference on Short and Medium Span Bridge Niagara Falls, Canada: *proceedings of the Proceedings of 8th International Conference on Short and Medium Span Bridge Niagara Falls, Canada*.
- Correia, JR, Branco, F, Silva, N, et al. 2011, 'First-order, buckling and post-buckling behaviour of GFRP pultruded beams. Part 1: Experimental study', *Computers & structures*, vol. 89, no. 21, pp. 2052-64.

- Davalos, JF & Qiao, P 1997, 'Analytical and experimental study of lateral and distortional buckling of FRP wide-flange beams', *Journal of Composites for Construction*, vol. 1, no. 4, pp. 150-9.
- Davalos, JF, Salim, H, Qiao, P, et al. 1996, 'Analysis and design of pultruded FRP shapes under bending', *Composites Part B: Engineering*, vol. 27, no. 3, pp. 295-305.
- Davol, A, Burgueno, R & Seible, F 2001, 'Flexural behavior of circular concrete filled FRP shells', *Journal of structural engineering*, vol. 127, no. 7, pp. 810-7.
- Deskovic, N, Triantafillou, TC & Meier, U 1995, 'Innovative design of FRP combined with concrete: short-term behavior', *Journal of structural engineering*, vol. 121, no. 7, pp. 1069-78.
- El-Hacha, R & Chen, D 2012, 'Behaviour of hybrid FRP-UHPC beams subjected to static flexural loading', *Composites Part B: Engineering*, vol. 43, no. 2, pp. 582-93.
- Fam, A & Skutezky, T 2006, 'Composite T-beams using reduced-scale rectangular FRP tubes and concrete slabs', *Journal of Composites for Construction*, vol. 10, no. 2, pp. 172-81.
- Fam, A, Flisak, B & Rizkalla, S 2003, 'Experimental and analytical modeling of concrete-filled fiber-reinforced polymer tubes subjected to combined bending and axial loads', *ACI Structural Journal*, vol. 100, no. 4.
- Fam, A, Mandal, S & Rizkalla, S 2005, 'Rectangular filament-wound glass fiber reinforced polymer tubes filled with concrete under flexural and axial loading: Analytical modeling', *Journal of Composites for Construction*, vol. 9, no. 1, pp. 34-43.
- Fam, A, Schnerch, D & Rizkalla, S 2005, 'Rectangular filament-wound glass fiber reinforced polymer tubes filled with concrete under flexural and axial loading: experimental investigation', *Journal of Composites for Construction*, vol. 9, no. 1, pp. 25-33.
- Fam, A, Cole, B & Mandal, S 2007, 'Composite tubes as an alternative to steel spirals for concrete members in bending and shear', *Construction and Building Materials*, vol. 21, no. 2, pp. 347-55.

- Fam, AZ & Rizkalla, SH 2001a, 'Confinement model for axially loaded concrete confined by circular fiber-reinforced polymer tubes', *ACI Structural Journal*, vol. 98, no. 4.
- Fam, AZ & Rizkalla, SH 2001b, 'Behavior of axially loaded concrete-filled circular fiber-reinforced polymer tubes', *ACI Structural Journal*, vol. 98, no. 3.
- Fam, AZ & Rizkalla, SH 2002, 'Flexural behavior of concrete-filled fiber-reinforced polymer circular tubes', *Journal of Composites for Construction*, vol. 6, no. 2, pp. 123-32.
- Fenske, MT & Vizzini, AJ 2001, 'The inclusion of in-plane stresses in delamination criteria', *Journal of Composite Materials*, vol. 35, no. 15, pp. 1325-42.
- Gand, AK, Chan, T-M & Mottram, JT 2013, 'Civil and structural engineering applications, recent trends, research and developments on pultruded fiber reinforced polymer closed sections: a review', *Frontiers of Structural and Civil Engineering*, vol. 7, no. 3, pp. 227-44.
- Gautam, BP & Matsumoto, T 2009, 'Shear deformation and interface behaviour of concrete-filled CFRP box beams', *Composite Structures*, vol. 89, no. 1, pp. 20-7.
- Guades, E, Aravinthan, T & Islam, MM 2014, 'Characterisation of the mechanical properties of pultruded fibre-reinforced polymer tube', *Materials & Design*, vol. 63, pp. 305-15.
- Hai, ND, Mutsuyoshi, H, Asamoto, S, et al. 2010, 'Structural behavior of hybrid FRP composite I-beam', *Construction and Building Materials*, vol. 24, no. 6, pp. 956-69.
- Hayes, M, Lesko, J, Haramis, J, et al. 2000, 'Laboratory and field testing of composite bridge superstructure', *Journal of Composites for Construction*.
- Hayes, MD & Lesko, JJ 2007, 'Failure analysis of a hybrid composite structural beam', *Composites Part A: Applied Science and Manufacturing*, vol. 38, no. 3, pp. 691-8.
- Hejll, A, Täljsten, B & Motavalli, M 2005, 'Large scale hybrid FRP composite girders for use in bridge structures—theory, test and field application', *Composites Part B: Engineering*, vol. 36, no. 8, pp. 573-85.
- Hollaway, L 2010, 'A review of the present and future utilisation of FRP composites in the civil infrastructure with reference to their important in-service properties', *Construction and Building Materials*, vol. 24, no. 12, pp. 2419-45.

- Hulatt, J, Hollaway, L & Thorne, A 2003, 'The use of advanced polymer composites to form an economic structural unit', *Construction and Building Materials*, vol. 17, no. 1, pp. 55-68.
- Hwang, S-J, Lu, W-Y & Lee, H-J 2000, 'Shear strength prediction for deep beams', *ACI Structural Journal*, vol. 97, no. 3.
- Idris, Y & Ozbakkaloglu, T 2013, 'Seismic behavior of high-strength concrete-filled FRP tube columns', *Journal of Composites for Construction*, vol. 17, no. 6, p. 04013013.
- Idris, Y & Ozbakkaloglu, T 2014, 'Flexural behavior of FRP-HSC-steel composite beams', *Thin-Walled Structures*, vol. 80, pp. 207-16.
- ISO 527-2 1996, *Plastics: Determination of tensile properties*.
- ISO 1172 1996, *Textile-glass-reinforced plastics, prepegs, moulding compounds and laminates: Determination of the textile-glass and mineral-filler content-Calcination methods*.
- Kabir, MZ & Sherbourne, AN 1998, 'Lateral-torsional buckling of post-local buckled fibrous composite beams', *Journal of engineering mechanics*, vol. 124, no. 7, pp. 754-64.
- Keller, T 1999, 'Towards structural forms for composite fibre materials', *Structural engineering international*, vol. 9, no. 4, pp. 297-300.
- Keller, T & Schollmayer, M 2004, 'Plate bending behavior of a pultruded GFRP bridge deck system', *Composite Structures*, vol. 64, no. 3, pp. 285-95.
- Keller, T, de Castro, J & Schollmayer, M 2004, 'Development of adhesively bonded GFRP sandwich girders', *Journal of Composites for Construction*, vol. 8, no. 5.
- Kemp, M 2008, 'Use of pultruded sections in civil infrastructure', in Proc international workshop on fibre composites in civil infrastructure—Past, present and future, University of Southern Queensland, Toowoomba, Queensland, Australia: *proceedings of the Proc international workshop on fibre composites in civil infrastructure—Past, present and future, University of Southern Queensland, Toowoomba, Queensland, Australia* pp. 29-35.
- Khalifa, A & Nanni, A 2000, 'Improving shear capacity of existing RC T-section beams using CFRP composites', *Cement and Concrete Composites*, vol. 22, no. 3, pp. 165-74.

- Khennane, A 2010, 'Manufacture and testing of a hybrid beam using a pultruded profile and high strength concrete', *Australian Journal of Structural Engineering*, vol. 10, no. 2, pp. 145-56.
- Kim, J-K 2000, 'Size effect on flexural compressive strength of concrete specimens'.
- Kim, J-K & Yi, S-T 2002, 'Application of size effect to compressive strength of concrete members', *Sadhana*, vol. 27, no. 4, pp. 467-84.
- Kim, J-K, Yi, S-T & Kim, J-HJ 2001, 'Effect of specimen sizes on flexural compressive strength of concrete', *ACI Structural Journal*, vol. 98, no. 3.
- Kollár, LP 2003, 'Local buckling of fiber reinforced plastic composite structural members with open and closed cross sections', *Journal of structural engineering*, vol. 129, no. 11, pp. 1503-13.
- Kumar, P, Chandrashekhara, K & Nanni, A 2003, 'Testing and evaluation of components for a composite bridge deck', *Journal of reinforced plastics and composites*, vol. 22, no. 5, pp. 441-61.
- Kumar, P, Chandrashekhara, K & Nanni, A 2004, 'Structural performance of a FRP bridge deck', *Construction and Building Materials*, vol. 18, no. 1, pp. 35-47.
- Lee, J 2006, 'Lateral buckling analysis of thin-walled laminated composite beams with monosymmetric sections', *Engineering structures*, vol. 28, no. 14, pp. 1997-2009.
- Lee, J, Kim, S-E & Hong, K 2002, 'Lateral buckling of I-section composite beams', *Engineering structures*, vol. 24, no. 7, pp. 955-64.
- Lin, Z, Polyzois, D & Shah, A 1996, 'Stability of thin-walled pultruded structural members by the finite element method', *Thin-Walled Structures*, vol. 24, no. 1, pp. 1-18.
- Lofrano, E, Paolone, A & Ruta, G 2013, 'A numerical approach for the stability analysis of open thin-walled beams', *Mechanics Research Communications*, vol. 48, pp. 76-86.
- Manalo, A 2013, 'Behaviour of fibre composite sandwich structures under short and asymmetrical beam shear tests', *Composite Structures*, vol. 99, pp. 339-49.
- Manalo, A & Aravinthan, T 2012, 'Behaviour of glued fibre composite sandwich structure in flexure: experiment and fibre model analysis', *Materials & Design*, vol. 39, pp. 458-68.

- Manalo, A, Aravinthan, T & Karunasena, W 2010, 'Flexural behaviour of glue-laminated fibre composite sandwich beams', *Composite Structures*, vol. 92, no. 11, pp. 2703-11.
- Manalo, A, Mutsuyoshi, H & Matsui, T 2012, 'Testing and characterization of thick hybrid fibre composites laminates', *International Journal of Mechanical Sciences*, vol. 63, no. 1, pp. 99-109.
- Manalo, A, Aravinthan, T, Karunasena, W, et al. 2010, 'Flexural behaviour of structural fibre composite sandwich beams in flatwise and edgewise positions', *Composite Structures*, vol. 92, no. 4, pp. 984-95.
- Marannano, G & Pasta, A 2007, 'An analysis of interface delamination mechanisms in orthotropic and hybrid fiber-metal composite laminates', *Engineering fracture mechanics*, vol. 74, no. 4, pp. 612-26.
- Mirmiran, A & Shahawy, M 1996, 'A new concrete-filled hollow FRP composite column', *Composites Part B: Engineering*, vol. 27, no. 3, pp. 263-8.
- Mirmiran, A, Shahawy, M & Samaan, M 1999, 'Strength and ductility of hybrid FRP-concrete beam-columns', *Journal of structural engineering*, vol. 125, no. 10, pp. 1085-93.
- Mohamed, H & Masmoudi, R 2008, 'Compressive behavior of reinforced concrete-filled FRP tubes', *Special Publication*, vol. 257, pp. 91-108.
- Mohamed, HM & Masmoudi, R 2010a, 'Flexural strength and behavior of steel and FRP-reinforced concrete-filled FRP tube beams', *Engineering structures*, vol. 32, no. 11, pp. 3789-800.
- Mohamed, HM & Masmoudi, R 2010b, 'Deflection Prediction of Steel and FRP-Reinforced Concrete-Filled FRP Tube Beams', *Journal of Composites for Construction*, vol. 15, no. 3, pp. 462-72.
- Mohamed, HM & Masmoudi, R 2010c, 'Axial load capacity of concrete-filled FRP tube columns: Experimental versus theoretical predictions', *Journal of Composites for Construction*, vol. 14, no. 2, pp. 231-43.
- Mottram, J 1991, 'Evaluation of design analysis for pultruded fibre-reinforced polymeric box beams', *Structural Engineer*, vol. 69, pp. 211-20.
- Mottram, J 1992, 'Lateral-torsional buckling of a pultruded I-beam', *Composites*, vol. 23, no. 2, pp. 81-92.

- Mottram, J 2004, 'Shear modulus of standard pultruded fiber reinforced plastic material', *Journal of Composites for Construction*, vol. 8, no. 2, pp. 141-7.
- Nagaraj, V & GangaRao, HV 1997, 'Static behavior of pultruded GFRP beams', *Journal of Composites for Construction*, vol. 1, no. 3, pp. 120-9.
- Neto, A & Rovere, H 2007, 'Flexural stiffness characterization of fiber reinforced plastic (FRP) pultruded beams', *Composite Structures*, vol. 81, no. 2, pp. 274-82.
- Nordin, H & Täljsten, B 2004, 'Testing of hybrid FRP composite beams in bending', *Composites Part B: Engineering*, vol. 35, no. 1, pp. 27-33.
- Omidvar, B 1998, 'Shear coefficient in orthotropic thin-walled composite beams', *Journal of Composites for Construction*, vol. 2, no. 1, pp. 46-56.
- Ozbakkaloglu, T 2012a, 'Axial compressive behavior of square and rectangular high-strength concrete-filled FRP tubes', *Journal of Composites for Construction*, vol. 17, no. 1, pp. 151-61.
- Ozbakkaloglu, T 2012b, 'Concrete-filled FRP tubes: Manufacture and testing of new forms designed for improved performance', *Journal of Composites for Construction*, vol. 17, no. 2, pp. 280-91.
- Ozbakkaloglu, T & Oehlers, DJ 2008, 'Concrete-filled square and rectangular FRP tubes under axial compression', *Journal of Composites for Construction*, vol. 12, no. 4, pp. 469-77.
- Ozbakkaloglu, T & Akin, E 2011, 'Behavior of FRP-confined normal-and high-strength concrete under cyclic axial compression', *Journal of Composites for Construction*, vol. 16, no. 4, pp. 451-63.
- Pecce, M & Cosenza, E 2000, 'Local buckling curves for the design of FRP profiles', *Thin-Walled Structures*, vol. 37, no. 3, pp. 207-22.
- Roberts, T & Masri, H 2003, 'Section properties and buckling behavior of pultruded FRP profiles', *Journal of reinforced plastics and composites*, vol. 22, no. 14, pp. 1305-17.
- Roeder, CW, Lehman, DE & Bishop, E 2010, 'Strength and stiffness of circular concrete-filled tubes', *Journal of structural engineering*, vol. 136, no. 12, pp. 1545-53.
- Ryall, M & Stephenson, R 1999, 'Britannia bridge: from concept to construction', in *Proceedings of the ICE-Civil Engineering: proceedings of the Proceedings of the ICE-Civil Engineering* Thomas Telford, pp. 132-43.

- Satasivam, S & Bai, Y 2014, 'Mechanical performance of bolted modular GFRP composite sandwich structures using standard and blind bolts', *Composite Structures*, vol. 117, pp. 59-70.
- Schniepp, TJ 2002, 'Design manual development for a hybrid, FRP double-web beam and characterization of shear stiffness in FRP composite beams'.
- Shawkat, W, Fahmy, W & Fam, A 2008, 'Cracking patterns and strength of CFT beams under different moment gradients', *Composite Structures*, vol. 84, no. 2, pp. 159-66.
- Sherbourne, AN & Kabir, MZ 1995, 'Shear strain effects in lateral stability of thin-walled fibrous composite beams', *Journal of engineering mechanics*, vol. 121, no. 5, pp. 640-7.
- Son, J-K & Fam, A 2008, 'Finite element modeling of hollow and concrete-filled fiber composite tubes in flexure: Model development, verification and investigation of tube parameters', *Engineering structures*, vol. 30, no. 10, pp. 2656-66.
- Stratford, T 2012, 'The Condition of the Aberfeldy Footbridge after 20 Years in Service'.
- Teng, J & Lam, L 2004, 'Behavior and modeling of fiber reinforced polymer-confined concrete', *Journal of structural engineering*, vol. 130, no. 11, pp. 1713-23.
- Teng, J, Yu, T, Wong, Y, et al. 2007, 'Hybrid FRP–concrete–steel tubular columns: concept and behavior', *Construction and Building Materials*, vol. 21, no. 4, pp. 846-54.
- Triantafillou, T & Meier, U 1992, 'Innovative design of FRP combined with concrete', *Advanced Composite Materials in Bridge and Structures*, pp. 491-9.
- Turvey, G 1996, 'Effects of load position on the lateral buckling response of pultruded GRP cantilevers—comparisons between theory and experiment', *Composite Structures*, vol. 35, no. 1, pp. 33-47.
- Turvey, G & Zhang, Y 2006, 'A computational and experimental analysis of the buckling, postbuckling and initial failure of pultruded GRP columns', *Computers & structures*, vol. 84, no. 22, pp. 1527-37.
- Turvey, GJ & Zhang, Y 2006, 'Shear failure strength of web–flange junctions in pultruded GRP WF profiles', *Construction and Building Materials*, vol. 20, no. 1, pp. 81-9.

- Van Erp, G, Heldt, T, Cattell, C, et al. 2002, 'A new approach to fibre composite bridge structures', in Proceedings of the 17th Australasian conference on the mechanics of structures and materials, ACMSM17, Australia: *proceedings of the Proceedings of the 17th Australasian conference on the mechanics of structures and materials, ACMSM17, Australia* pp. 37-45.
- Vincent, T & Ozbakkaloglu, T 2013a, 'Influence of concrete strength and confinement method on axial compressive behavior of FRP confined high-and ultra high-strength concrete', *Composites Part B: Engineering*, vol. 50, pp. 413-28.
- Vincent, T & Ozbakkaloglu, T 2013b, 'Influence of fiber orientation and specimen end condition on axial compressive behavior of FRP-confined concrete', *Construction and Building Materials*, vol. 47, pp. 814-26.
- Wang, S 1983, 'Fracture mechanics for delamination problems in composite materials', *Journal of Composite Materials*, vol. 17, no. 3, pp. 210-23.
- Wang, S & Zhang, Y 2009, 'Buckling, post-buckling and delamination propagation in debonded composite laminates Part 2: Numerical applications', *Composite Structures*, vol. 88, no. 1, pp. 131-46.
- Wright, H 1995, 'Local stability of filled and encased steel sections', *Journal of structural engineering*, vol. 121, no. 10, pp. 1382-8.
- Wu, C & Bai, Y 2014, 'Web crippling behaviour of pultruded glass fibre reinforced polymer sections', *Composite Structures*, vol. 108, pp. 789-800.
- Wu, Z, Li, W & Sakuma, N 2006, 'Innovative externally bonded FRP/concrete hybrid flexural members', *Composite Structures*, vol. 72, no. 3, pp. 289-300.
- Xiao, Y & Wu, H 2000, 'Compressive behavior of concrete confined by carbon fiber composite jackets', *Journal of Materials in Civil Engineering*, vol. 12, no. 2, pp. 139-46.
- Yu, T & Teng, J 2010, 'Design of concrete-filled FRP tubular columns: provisions in the Chinese technical code for infrastructure application of FRP composites', *Journal of Composites for Construction*.
- Yu, T, Wong, Y, Teng, J, et al. 2006, 'Flexural behavior of hybrid FRP-concrete-steel double-skin tubular members', *Journal of Composites for Construction*, vol. 10, no. 5, pp. 443-52.

- Zhang, Y & Wang, S 2009, 'Buckling, post-buckling and delamination propagation in debonded composite laminates: Part 1: Theoretical development', *Composite Structures*, vol. 88, no. 1, pp. 121-30.
- Zhu, Z, Ahmad, I & Mirmiran, A 2006, 'Seismic performance of concrete-filled FRP tube columns for bridge substructure', *Journal of Bridge Engineering*, vol. 11, no. 3, pp. 359-70.
- Zureick, A & Scott, D 1997, 'Short-term behavior and design of fiber-reinforced polymeric slender members under axial compression', *Journal of Composites for Construction*, vol. 1, no. 4, pp. 140-9.

## **Appendix A: CONFERENCE PRESENTATIONS**

### **A.1 Conference Paper I: Flexural and axial behaviour of pultruded GFRP tubes filled with low strength concrete**

**M Muttashar**, A Manalo, W Karunasena, W Lokuge (2014). Flexural and axial behavior of pultruded GFRP hollow sections filled with low strength concrete. *Australasian Composites Conference (CA 2014)*: Materials for a lighter and smarter world, 7-9 April, Newcastle, Australia.

Abstract: Pultruded hollow composite sections have gained wide acceptance in civil engineering application due to their high strength, lightweight and durability. However, pultruded composite are vulnerable to buckling due to their relatively low modulus of elasticity and thin-walled sections. This paper investigates the benefits of using low strength concrete as an infill to pultruded hollow - glass fibre reinforced polymer (GFRP) section. A total of four composite beams with 125x125 mm section, 6.2 mm wall thickness and 1200 mm span were tested under four point bending. In addition, four specimens with the same cross section and 600 mm height were tested under compressive load. The effect of concrete infill on the strength, stiffness and failure mode was examined. The study showed that using low strength concrete infill is a practical and feasible way to enhance the strength and stiffness as it helps stabilize the pultruded GFRP section. The beam filled with concrete has 145% higher flexural stiffness and failed at 250 % higher load than the hollow section. Similarly, the axial capacity is increased by about 29% compared with the hollow section counterpart.

## **A.2 Conference Paper II: Testing and characterization of pultruded glass fibre reinforced polymer (GFRP) beams.**

**M Muttashar**, W Karunasena, A Manalo, W Lokuge (2015). Testing and characterization of pultruded glass fiber reinforced polymer (GFRP) beams. *Proceeding of the 12th International Symposium on Fiber Reinforced Polymers for Reinforced Concrete Structures (FRPRCS-12) & The 5th Asia-Pacific Conference on Fiber Reinforced Polymers in Structures (APFIS-2015) Joint Conference*, 14-16 December, Nanjing, China.

Abstract: Elastic properties of the fiber reinforced polymer (FRP) composite represent a significant effect on the structural behaviour of this material. Therefore, it is important to use an accurate method to determine these properties as the behaviour is often governed by deflection rather than strength. In this study, full size pultruded glass FRP (GFRP) beams were used to determine the elastic properties using static four-point bending with different shear span to depth ( $a/d$ ) ratios. Two different methods -back calculation and simultaneous - were then employed to evaluate the flexural modulus and shear stiffness and were compared with the results of the test using coupon specimens. The results indicate that the elastic properties determined from full scale test using back calculation method can reliably predict the load - deflection behaviour of the pultruded GFRP beams.

### **A.3 Conference Paper III: The effect of shear span-to-depth ratio on the failure mode and strength of pultruded GFRP beams**

**M Muttashar**, W Karunasena, A Manalo, W Lokuge (2015). The effect of shear span-to-depth ratio on the failure mode and strength of pultruded GFRP beam. *Proceeding of the 12th International Symposium on Fiber Reinforced Polymers for Reinforced Concrete Structures (FRPRCS-12) & The 5th Asia-Pacific Conference on Fiber Reinforced Polymers in Structures (APFIS-2015) Joint Conference*, 14-16 December, Nanjing, China.

Abstract: The use of structural pultruded fibre reinforced polymers (FRP) sections have gained wide acceptance in civil engineering applications due to their favourable structural characteristics like high strength, light weight and durability in severe environmental conditions. However, due to their relatively low modulus of elasticity and thinned walls, these sections are vulnerable to local buckling which can affect their ultimate strength. This paper investigates experimentally the flexural behaviour of pultruded GFRP beams with shear span-to-depth ( $a/d$ ) ratios in the range of 1.2 to 6 using full scale pultruded profiles. Failure modes, strength and crack patterns are the main parameters that were examined in this study. The study shows that shear span has a minor effect on the failure modes of the beams while it has a noticeable effect on the ultimate strength. In addition, fibre model analysis was used to validate the experimental results. Comparison between the experimental and the theoretical analysis results shows a good approximation of the moment - deflection behaviour and failure moment of pultruded GFRP beams.

#### **A.4 Conference Paper IV: Experimental investigation on the flexural behaviour of pultruded GFRP beams filled with different concrete strengths.**

**M Muttashar**, A Manalo, W Karunasena, W Lokuge (2016). Experimental investigation on the flexural behaviour of pultruded GFRP beams filled with different concrete strengths. *Proceeding of the 8th International Conference on Fibre-Reinforced Polymer (FRP) Composites in Civil Engineering (CICE 2016)*, 14-16 December, Hong Kong, China.

Abstract: Glass fibre reinforced polymer (GFRP) pultruded profiles are being increasingly used in the construction industry due to their numerous advantageous over the conventional materials. However, most pultruded GFRP sections fail prematurely without utilising their high tensile strength due to their thin-walled sections. As a result, several hybrid systems made out of GFRP profiles and concrete as a filler material have been proposed in order to enhance their structural performance. Most of these studies utilised high strength concrete wherein the additional cost does not justify the enhancement in the stiffness and strength of the infilled GFRP profiles. This paper presents an experimental investigation on the effect of the compressive strength of concrete infill on the flexural behaviour of beams with a view of determining a lower cost infill for GFRP profiles. Pultruded GFRP square beams (125 mm x 125 mm x 6.5mm) were filled with concrete having 10, 37 and 43.5 MPa compressive strength and tested under static four-point bending. The results showed that the capacity of the filled beam sections increased by 100 to 141% than the hollow sections. However, the compressive strength of the concrete infill has no significant effect on the flexural behaviour of the beams. The increase in concrete compressive strength from 10 to 43.5 MPa increased the ultimate Moment by only 19% but exhibited an almost same flexural stiffness indicating that a low strength concrete is a practical solution to fill the GFRP profiles.

## **A.5 Conference Paper V: Behaviour of pultruded multi-celled GFRP hollow beams with low-strength concrete infill**

**M Muttashar**, W Karunasena, A Manalo, W Lokuge (2016). Experimental investigation on the flexural behaviour of pultruded GFRP beams filled with different concrete strengths. *Proceeding of the 24th Australasian conference on the Mechanics of structures and materials (ACMSM24)*, 6-9 December, Perth, Australia.

Abstract: The structural performance of multi-celled GFRP hollow beams is highly affected by the local buckling failure. Therefore, this study introduces pultruded multi-celled GFRP beams filled with low strength concrete. The flexural behaviour of beams made up of 1, 2 and 3 pultruded GFRP square sections (125 mm x125 mm x 6.5mm) and filled with concrete having low compressive strength was investigated. The composite beams were subjected to four-point static bending test to determine the strength, stiffness and failure mechanisms. The results of the experimental investigations showed that the failure stress of 2 and 3 cells beams is 98% and 85% compared with single cell beam, respectively. However, the filling percentages are 50% and 33%, respectively. All the tested beams were failed due to compression failure of the GFRP profile. Furthermore, the effective stiffness of 2 and 3 cells is 95% and 96%, respectively compared with single cell section.

## **A.6 Conference Paper VI: Flexural behaviour of glued GFRP tubes filled with concrete**

**M Muttashar**, A Manalo, W Karunasena, W Lokuge (2017). Flexural behaviour of glued GFRP tubes filled with concrete. *Proceeding of the 6th Asia-Pacific conference on FRP in structures*, 19-21 July, Singapore. (Accepted)

Abstract: The corrosion of steel reinforcement is considered the greatest factor limiting the service life of reinforced concrete structures. Glass fiber reinforced polymers (GFRPs) are known as cost-effective materials offering long-term durability and less maintenance. As a result, these materials show great potential for use in the civil engineering applications. Due to the high cost of the manufacturing die, pultruded GFRP tubes are produced in specific cross-section dimensions only. For high load applications and to comply with the serviceability requirements, a number of these pultruded sections can be assembled together by gluing them appropriately. This study presents an experimental investigation onto the flexural behavior of glued GFRP tube beams with 1, 2, 3 and 4 - cells filled with concrete under four-point loading. The results show that the strength of the 4 cells glued beams increased by 150 % and 88% for hollow and filled beams, respectively, compared with its counterpart single cell beam. The filled beams failed at 42 – 88 % higher load and showed 10 – 22 % higher stiffness compared with their hollow counterparts. The results also show that gluing small section tubes to produce large section beam is a practical solution to enhance the flexural performance of the composite tubes.

## Appendix B: GLASS FIBRE CONTENT INVESTIGATION

### B.1 Burnout test

Burnout test was conducted to determine the content of glass fibre in the GFRP composite tube. The test was conducted following the standard ISO 1172 (1996). Four coupons of approximately 20 x 30 mm were cut from the four sides of the tube as shown in Figure B.1. The nominal dimension of the sample used in the test is shown in Table B.1. Table B. 2 on the other hand shows a summary of the measured dimensions and results of the test. The specific mass  $\rho$  and glass content  $M_g$  were calculated using Equations B.1 and B.2, respectively.

$$\rho = m_o/v_f \quad (\text{B.1})$$

$$M_g = (m_3 - m_1)/(m_2 - m_1) \times 100 \quad (\text{B.2})$$

where  $m_o$  is the mass of the specimen,  $v_{ff}$  is the volume of the specimen,  $m_1$  is the initial mass of the dry crucible,  $m_2$  is the initial mass of the dry crucible plus dried specimen, and  $m_3$  is the final mass of the crucible plus residue after calcination. The test results displayed that the average specific mass of the tube is 2050 kg/m<sup>3</sup>. On the other hand, the fibre content of the tube is 78%. The results also indicate that the stacking sequence of the plies in the form of  $[0^0/+45^0/0^0/-45^0/0^0/-45^0/0^0/+45^0/0^0]$ , where the 0° direction aligns with the longitudinal axis of the tube as shown in Figure B. 2. In addition, Table B. 3 summarised the content of the glass fibre of each ply.

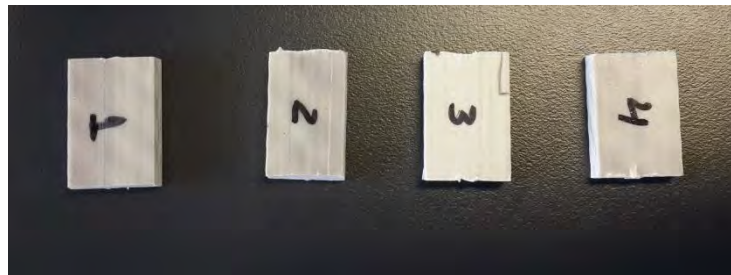


Figure B.1 Coupon samples

Table B.1 Details of the sample for burnout test.

Types	Standard	Width, mm	<i>b</i>	Length, mm	<i>l</i>	Thickness*, mm	<i>t</i>
Burnout	ISO 1172	20		30		6.5	

\* Nominal thickness of the tube

Table B. 2 Summary of the results of burnout test.

Sample No.	Width, b mm	Length, l mm	Thickness, t mm	Specific mass kg/m <sup>3</sup>	Glass content %
1	19.71	29.57	6.51	2043	77.8
2	18.2	29.25	6.13	2027	78.3
3	19.7	29.65	6.57	2035	77.9
4	19.53	29.75	6.15	2091	80.5
Average	19.29	29.31	6.35	2050	78.5
Standard deviation	0.6	0.35	0.2	25	1



Figure B. 2 the orientation of the glass fibre

Table B. 3 Summary of the glass fibre content of each ply.

Ply No.	Ply orientation	Glass content %
1	0°	16
2	+45°	5
3	0°	15
4	-45°	5
5	0°	18
6	-45°	5
7	0°	15
8	+45°	5
9	0°	16

## Appendix C: BEARING STRENGTH INVESTIGATION

### C.1 Bearing test

In this study, in order to evaluate accurately the bearing capacity of the pultruded GFRP section under concentrated loading, coupon shear test was conducted first to determine the shear stress of the GFRP tube. The shear test was conducted according to the ASTM D5379/D5379M (1993) standards. Five coupon samples of a rectangular beam shape with V-notch symmetrically located at the centre were tested as shown in Figure C.1. A universal testing machine with a modified Iosipescu shear test fixture was used to apply the load on the specimens at a constant head speed of 1 mm/min. The applied load was measured with a 22 kN load cell and recorded using a data logger System 5000. The average shear stress is calculated by dividing the applied load by the area of the cross section between the notches using the following relation:

$$\tau_{ave} = \frac{P}{A} \quad (C.1)$$

Table C.1 shows the experimental failure loads and the related shear stresses for the tested coupons. The results demonstrate that the average shear stress of the GFRP sections is 85.7 MPa.

Then a full scale bearing load test was conducted on hollow and filled sections. The sections were placed on a solid base to simulate the worst case of concentrated loading (Wu & Bai 2014). The test was performed on the MTS testing machine. A rigid steel bearing plate with a thickness of 10 mm was used to apply the load on the specimens. The length of the bearing plate was 50 mm for both hollow and filled specimens. The width of the bearing plate was 200 mm, which is sufficient to act cross the full flange width of the GFRP section as shown in Figure C.2. Displacement control mode was used to apply the compressive load at a loading rate of 0.5 mm/min. Figure C.3 shows the failure mode of the tested beams. From the experimental observation, the failure occurred at web-flange junction of the beam with initial cracking of 45°. The cracks then progressed along the edges of the pultruded beam under the bearing plate and then the steel bearing plate broke the longitudinal fibres of the webs. Filled beam showed similar behaviour, however the concrete core enhanced the bearing capacity of the

pultruded beam. The final failure occurred at the web-flange junction under the steel bearing plate as shown in Figure C.3.

The load –displacement relationship of the hollow beam is presented in Figure C.4. The figure shows that the displacement increased linearly with the increase of the load until a certain limit after which the first crack initiated and progressively developed. The section fails at a maximum load of 56 kN. In this study, an equation proposed by Wu and Bai (2014) to estimate the bearing failure load of pultruded section has been adopted. The bearing failure load ( $R_N$ ) was predicted using the proposed equation as follow:

$$R_N = f_s A_{shear} \quad (C.2)$$

where

$$A_{shear} = 2 t_w b_{plate} \quad (C.3)$$

and  $b_{plate}$  represents the width of the bearing plate and  $f_s$  is the inter-laminar shear strength of the section. The predicted load was 54.4 kN which is very well agreed with the experimental results. The proposed equation is adopted to determine the bearing failure load of hollow GFRP beam according to the test configuration. As a result, the predicted bearing failure of hollow GFRP beam is 326 kN. For the filled beam, similar behaviour has been observed as shown in Figure C.5. The displacement increased with the increase of the applied load. The concrete core significantly improved the bearing capacity of the pultruded beam as the final failure occurred at 417 kN.



Figure C.1 shear test set-up

Table C.1 Summary of the results of coupon shear test

Sample No.	Width, $b$ mm	Length, $l$ mm	Thickness, $t$ mm	Failure load kN	Shear stress MPa
S1	18	75	6.51	5986.7	85.7
S2	18	75.3	6.13	5999.4	85.9
S3	18	75	6.47	6016.8	86.1
S4	18	75	6.15	5957.5	85.3
S5	18	75	6.35	5973.2	85.5
Average					85.7

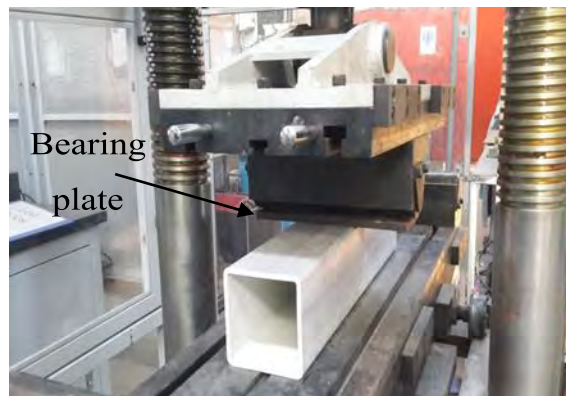


Figure C.2 Actual illustration of Bearing test set-up

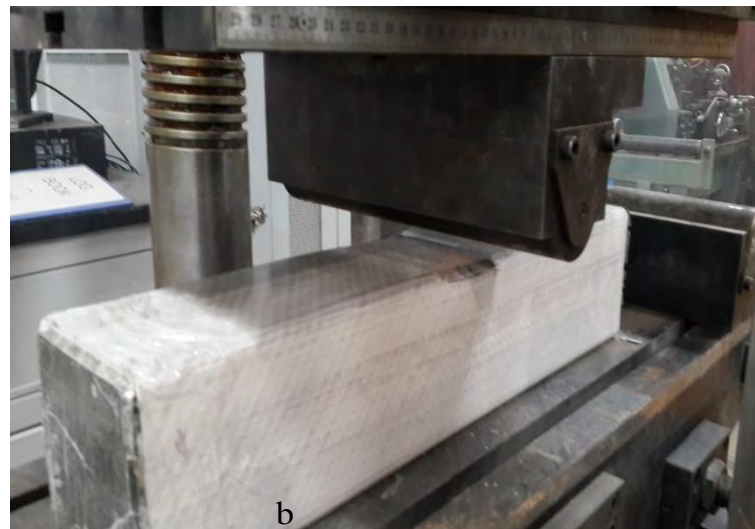


Figure C. 3 Failure mode of a) hollow beam and b) filled beam

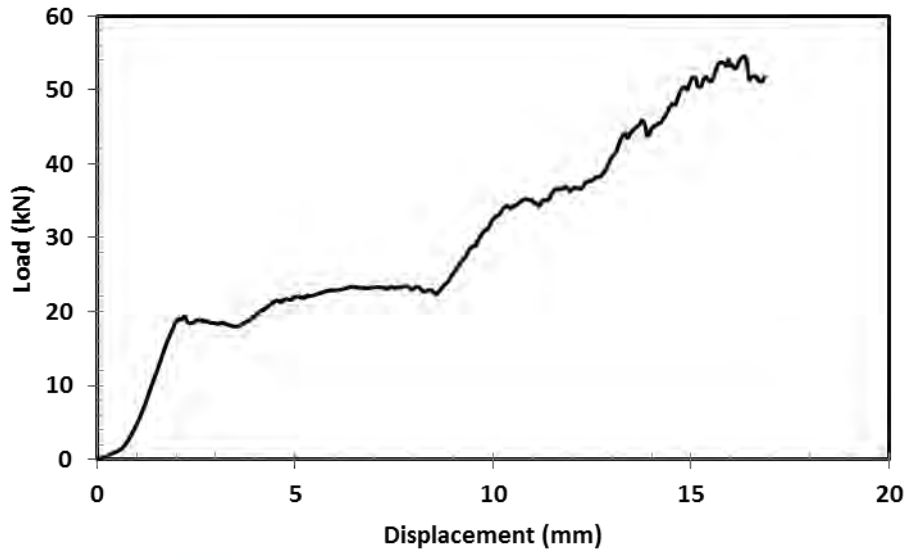


Figure C.4 Load-displacement curves for hollow beams

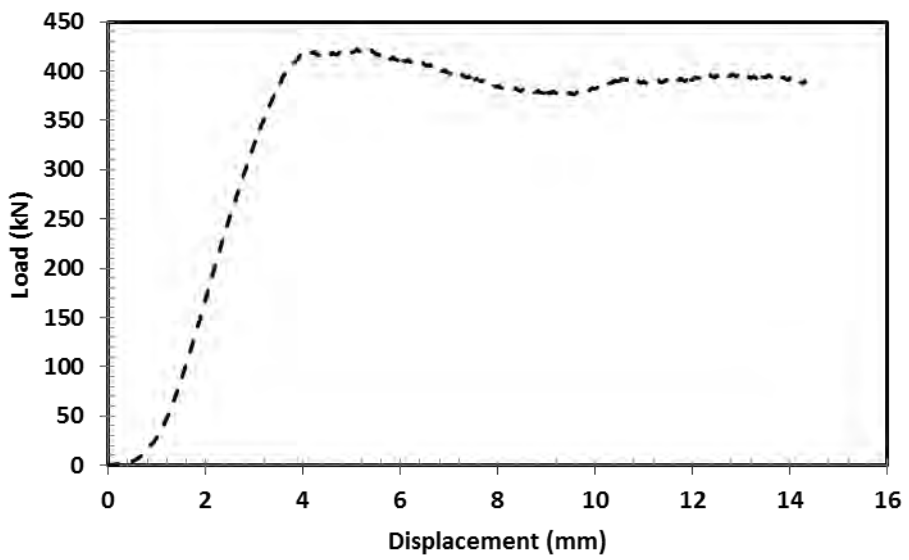


Figure C.5 Load-displacement curves for filled beams

## **Appendix D: DUCTILITY OF SINGLE AND MULTI-CELLED BEAMS**

Ductility of a structural member is defined as the ability to sustain deformations prior to collapse, without loss in strength (Mirmiran et al. 1999). These researchers further suggest that the ductility can be determined by calculating the energy absorption of the beam, which is represented as the area under the load-deflection curve until the ultimate failure. Following this, the ductility of the single and multi-celled hollow and filled beams were determined from their respective load and deformation behaviour presented in Figures D.1 to D.4. The energy absorption of each beam is then listed in Table D.1.

The results show that the ductility of concrete filled beams is significantly greater than that of the hollow beams. For example, the ductility of single cell beam filled with 10 MPa, 37 MPa and 43 MPa concrete is about 230%, 350% and 380%, respectively higher than hollow beams. The increase in strength and energy absorption of the pultruded GFRP beams filled with concrete can be attributed to the concrete filling preventing the local buckling of the tubes. Similarly, the multi-celled beams showed an enhanced ductility after filling with concrete. The ductility of 2-celled beams is increased by up to 127% when filled with concrete at the top section compared to hollow beams. Likewise, 3- and 4-celled beams showed higher ductility than their hollow counterpart beams. The enhancement in the ductility of GFRP sections by filling them with concrete was also reported by Fam and Rizkalla (2002), Mohamed and Masmoudi (2010) and Abouzied and Masmoudi (2015).

The failure behaviour of the GFRP tubes is changed by filling the top layers with concrete. While the failure started at the web-flange junctions and followed by premature buckling and crushing in the webs for hollow beams, the failure of filled beams was due to flexural compression at the constant moment region including cracks in the fibres in the transvers direction. Delamination cracks were observed at the compression surface as well. The complete failure of the filled beams occurred at strain level approximately 11200 microstrains. This strain level is far greater than the failure strain of the hollow section (3140 microstains) which indicated that the concrete infill changed the failure from local failure for hollow beams to flexural

compression failure for filled beams. As a consequence, the deformation of the infilled beams was higher when these beams failed. Moreover, the moment-curvature behaviour of the filled beams increases with the increase of the deflection. The results show that the curvature of concrete filled beams is greater than that of the hollow beams. For example, the curvature of single cell beam filled with 10 MPa, 37 MPa and 43 MPa concrete is about 158%, 173% and 177%, respectively higher than hollow beams. Similarly, the multi-celled beams showed an increase in the curvature after filling with concrete. The curvature of 2-, 3- and 4-celled beams is increased by 53%, 88% and 94%, respectively, when filled with concrete at the top section compared to hollow beams. Although, the concrete filled beams did not present any obvious loss of stiffness prior to failure, the high deformation will give sufficient warning of the impending failure of the structure.

Table D.1 Summary of the experimental results for single and multi-celled GFRP beams

Sample No.	Failure load kN	Deflection MPa	Ductility kN.m	Curvature m <sup>-1</sup>
H-0	80.8	39.5	1.6	72
H-10	163	65	5.3	186
H-37	189	76	7.2	197
H-43	195	78	7.6	200
2C-H-0	151.2	34.7	2.6	42
2C-H-15	217	42.7	4.6	58
2C-H-32	247.6	48	5.9	65
3C-H-0	187.5	42.8	4	25
3C-H-15	261.6	55.8	7.2	36
3C-H-32	294.6	60.5	8.9	47
4C-H-0	225	48	5.4	17
4C-H-32	348	63.9	11.1	33

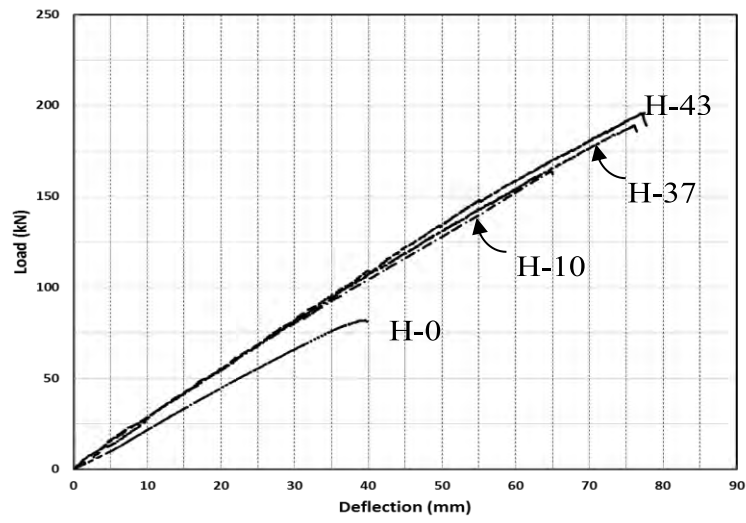


Figure D.1 Load – displacement behaviour of single cell GFRP hollow and filled beams

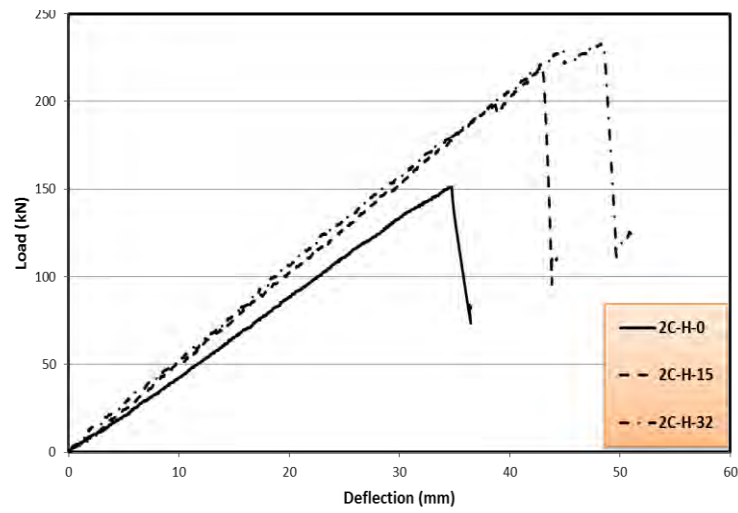


Figure D.2 Load – displacement behaviour of 2 cells GFRP hollow and filled beams

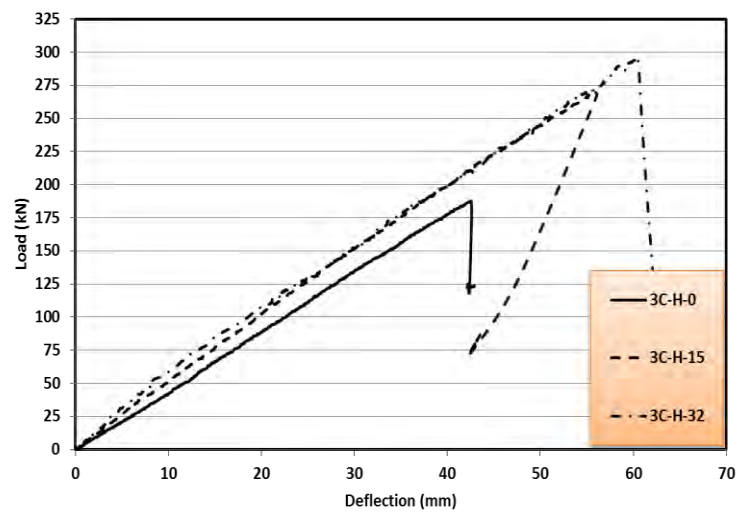


Figure D.3 Load - displacement behaviour of 3 cells GFRP hollow and filled beams

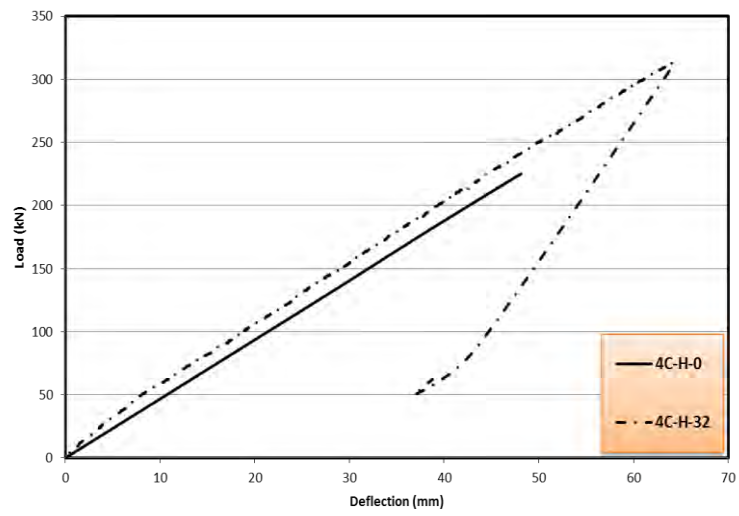


Figure D.4 Load - displacement behaviour of 4 cells GFRP hollow and filled beams

## **Appendix E: Copyright Information**

### **E.1 Paper 1 Copyright Information: Behaviour of hollow pultruded GFRP square beams with different shear span-to-depth ratio**

**Muttashar M**, Karunasena W, Manalo A, Lokuge W. (2016). Behaviour of hollow pultruded GFRP square beams with different shear span-to-depth ratios. *Journal of Composite Materials*. Vol.50, Issue 21, pp. 2925-2940. (IF:1.24, SINP:1.17)



Search: keyword, title  
Search

Cart 0

## Journal Author Archiving Policies and Re-Use

### Authors Re-Using Their Own Work

SAGE Journal authors are able to use their Contribution in certain circumstances without any further permission. It is important to check your signed Contributor Agreement and/or the submission guidelines for the journal to which you have submitted your Contribution to review the journal's policy regarding author re-use.

- [Gold Open Access and SAGE Choice](#)
- [Green Open Access: SAGE's archiving policy](#)

#### Gold Open Access and SAGE Choice

If you wish to re-use an Open Access Contribution published under a Creative Commons License, see [Re-use of Open Access Content](#) for more information.

#### Green Open Access: SAGE's archiving policy

SAGE's Green Open Access policy allows you, as author, to re-use your Contribution as follows:

- You may share the version of the Contribution you submitted to the journal (version 1) anywhere at any time.
- Once the Contribution has been accepted for publication, you may post the accepted version (version 2) of the Contribution on your own personal website, your department's website or the repository of your institution without any restrictions.
- You may not post the accepted version (version 2) of the Contribution in any repository other than those listed above (i.e. you may not deposit in the repository of another institution or a subject repository) until 12 months after first publication of the Contribution in the journal.
- You may use the published Contribution (version 3) for your own teaching needs or to supply on an individual basis to research colleagues, provided that such supply is not for commercial purposes.
- You may use the published Contribution (version 3) in a book authored or edited by you at any time after publication in the journal. This does not apply to books where you are contributing a chapter to a book authored or edited by someone else.
- You may not post the published Contribution (version 3) on a website or in a repository without permission from SAGE.

When posting or re-using the Contribution, please provide a link to the appropriate DOI for the published version of the Contribution on SAGE Journals (<http://online.sagepub.com>) and please make the following acknowledgement: The final, definitive version of this paper has been published in [Journal], Vol/Issue, Month/Year published by SAGE Publishing, All rights reserved.

The chart below includes common requests and an explanation of which 'version' of the article can be used in each circumstance. If the table below indicates that permission is required, please see the instructions for requesting permission at [Journals Permissions](#).

I WANT TO:	CLEARED PERMISSION	REQUIRES PERMISSION
include up to one full article in my unpublished dissertation or thesis	Version 3	
supply my article to my students or use the article for teaching purposes	Version 3	
supply my article to a research colleague at an academic institution	Version 3	
supply my article to a commercial organization for republication, distribution or a web posting	X	
upload my article to my institution repository or department website	Version 2	
upload my article to a repository NOT affiliated with my institution, 12 months after publication	Version 2	
republish my article in a book I am writing or editing	Version 3	
contribute my article to a book edited or written by someone else	X	

VERSION OF CONTRIBUTION	DEFINITION
-------------------------	------------

Version 1 original submission to the journal (before peer review)

---

Version 2 original submission to the journal with your revisions after peer review, often the version accepted by the editor (author accepted manuscript)

---

Version 3 copy-edited and typeset proofs and the final published version

---

If you are the corresponding author of a Contribution, you will receive e-prints which are PDF offprints. See our [Author e-prints policy](#).

It is not SAGE's policy to provide PDFs of the published Contribution (version 3) for posting on servers or depositing in institutional repositories. However, you may update your own version of the article (version 1 or version 2) to reflect changes to the content made during production and convert that article into PDF form.

[back to top](#)

For advice on how to clear permission for a Contribution you intend to submit for publication in a SAGE Journal, please visit our Author Gateway [Copyright and Permissions FAQs](#).

[Rights and Permissions](#)

[Books Permissions](#)

[Journals Permissions](#)

[Journal Author Archiving Policies and Re-Use](#)

[Translations and Subsidiary Rights](#)

---

#### Browse

Books

Journals

Digital Library Products

Digital Solutions for your Course

Catalogs

#### Resources For

Instructors

Societies

Book Authors/Editors

Journal Authors/Editors/Reviewers

Students

Researchers

Librarians

#### About

About SAGE

Contact

News

My Account

Careers

Accessibility

#### Social

[Blog](#)[Facebook](#)[Twitter](#)[LinkedIn](#)[Social Science Space](#)

---

You are in: North America

[Change location](#)

## **E.2 Paper II Copyright Information: Influence of infill concrete strength on the flexural behaviour of pultruded GFRP square beams**

**Muttashar M**, Manalo A, Karunasena W, Lokuge W. (2016). Influence of infill concrete strength on the flexural behaviour of pultruded GFRP square beams. *Composite Structures*. Vol.145, pp. 58-67. (IF:3.318, SINP:2.48)

**ELSEVIER LICENSE  
TERMS AND CONDITIONS**

Feb 24, 2017

This Agreement between Majid Muttashar ("You") and Elsevier ("Elsevier") consists of your license details and the terms and conditions provided by Elsevier and Copyright Clearance Center.

License Number	4055221148074
License date	
Licensed Content Publisher	Elsevier
Licensed Content Publication	Composite Structures
Licensed Content Title	Influence of infill concrete strength on the flexural behaviour of pultruded GFRP square beams
Licensed Content Author	Majid Muttashar,Allan Manalo,Warna Karunasena,Weena Lokuge
Licensed Content Date	10 June 2016
Licensed Content Volume	145
Licensed Content Issue	n/a
Licensed Content Pages	10
Start Page	58
End Page	67
Type of Use	reuse in a thesis/dissertation
Intended publisher of new work	other
Portion	full article
Format	both print and electronic
Are you the author of this Elsevier article?	Yes
Will you be translating?	No
Order reference number	
Title of your thesis/dissertation	FLEXURAL BEHAVIOUR OF HYBRID CONCRETE-GFRP COMPOSITE BEAMS
Expected completion date	Jul 2017
Estimated size (number of pages)	160
Elsevier VAT number	GB 494 6272 12
Requestor Location	Majid Muttashar 4B OXFORD CT  DARLING HEIGHTS, QLD 4350 Australia Attn: Majid Muttashar
Total	0.00 USD
Terms and Conditions	

### INTRODUCTION

1. The publisher for this copyrighted material is Elsevier. By clicking "accept" in connection with completing this licensing transaction, you agree that the following terms and conditions apply to this transaction (along with the Billing and Payment terms and conditions

established by Copyright Clearance Center, Inc. ("CCC"), at the time that you opened your Rightslink account and that are available at any time at <http://myaccount.copyright.com>.

#### GENERAL TERMS

2. Elsevier hereby grants you permission to reproduce the aforementioned material subject to the terms and conditions indicated.

3. Acknowledgement: If any part of the material to be used (for example, figures) has appeared in our publication with credit or acknowledgement to another source, permission must also be sought from that source. If such permission is not obtained then that material may not be included in your publication/copies. Suitable acknowledgement to the source must be made, either as a footnote or in a reference list at the end of your publication, as follows:

"Reprinted from Publication title, Vol /edition number, Author(s), Title of article / title of chapter, Pages No., Copyright (Year), with permission from Elsevier [OR APPLICABLE SOCIETY COPYRIGHT OWNER]." Also Lancet special credit - "Reprinted from The Lancet, Vol. number, Author(s), Title of article, Pages No., Copyright (Year), with permission from Elsevier."

4. Reproduction of this material is confined to the purpose and/or media for which permission is hereby given.

5. Altering/Modifying Material: Not Permitted. However figures and illustrations may be altered/adapted minimally to serve your work. Any other abbreviations, additions, deletions and/or any other alterations shall be made only with prior written authorization of Elsevier Ltd. (Please contact Elsevier at [permissions@elsevier.com](mailto:permissions@elsevier.com)). No modifications can be made to any Lancet figures/tables and they must be reproduced in full.

6. If the permission fee for the requested use of our material is waived in this instance, please be advised that your future requests for Elsevier materials may attract a fee.

7. Reservation of Rights: Publisher reserves all rights not specifically granted in the combination of (i) the license details provided by you and accepted in the course of this licensing transaction, (ii) these terms and conditions and (iii) CCC's Billing and Payment terms and conditions.

8. License Contingent Upon Payment: While you may exercise the rights licensed immediately upon issuance of the license at the end of the licensing process for the transaction, provided that you have disclosed complete and accurate details of your proposed use, no license is finally effective unless and until full payment is received from you (either by publisher or by CCC) as provided in CCC's Billing and Payment terms and conditions. If full payment is not received on a timely basis, then any license preliminarily granted shall be deemed automatically revoked and shall be void as if never granted. Further, in the event that you breach any of these terms and conditions or any of CCC's Billing and Payment terms and conditions, the license is automatically revoked and shall be void as if never granted. Use of materials as described in a revoked license, as well as any use of the materials beyond the scope of an unrevoked license, may constitute copyright infringement and publisher reserves the right to take any and all action to protect its copyright in the materials.

9. Warranties: Publisher makes no representations or warranties with respect to the licensed material.

10. Indemnity: You hereby indemnify and agree to hold harmless publisher and CCC, and their respective officers, directors, employees and agents, from and against any and all claims arising out of your use of the licensed material other than as specifically authorized pursuant to this license.

11. No Transfer of License: This license is personal to you and may not be sublicensed, assigned, or transferred by you to any other person without publisher's written permission.

12. No Amendment Except in Writing: This license may not be amended except in a writing signed by both parties (or, in the case of publisher, by CCC on publisher's behalf).

13. Objection to Contrary Terms: Publisher hereby objects to any terms contained in any purchase order, acknowledgment, check endorsement or other writing prepared by you, which terms are inconsistent with these terms and conditions or CCC's Billing and Payment terms and conditions. These terms and conditions, together with CCC's Billing and Payment terms and conditions (which are incorporated herein), comprise the entire agreement between you and publisher (and CCC) concerning this licensing transaction. In the event of

any conflict between your obligations established by these terms and conditions and those established by CCC's Billing and Payment terms and conditions, these terms and conditions shall control.

14. Revocation: Elsevier or Copyright Clearance Center may deny the permissions described in this License at their sole discretion, for any reason or no reason, with a full refund payable to you. Notice of such denial will be made using the contact information provided by you. Failure to receive such notice will not alter or invalidate the denial. In no event will Elsevier or Copyright Clearance Center be responsible or liable for any costs, expenses or damage incurred by you as a result of a denial of your permission request, other than a refund of the amount(s) paid by you to Elsevier and/or Copyright Clearance Center for denied permissions.

#### LIMITED LICENSE

The following terms and conditions apply only to specific license types:

15. Translation: This permission is granted for non-exclusive world English rights only unless your license was granted for translation rights. If you licensed translation rights you may only translate this content into the languages you requested. A professional translator must perform all translations and reproduce the content word for word preserving the integrity of the article.

16. Posting licensed content on any Website: The following terms and conditions apply as follows: Licensing material from an Elsevier journal: All content posted to the web site must maintain the copyright information line on the bottom of each image; A hyper-text must be included to the Homepage of the journal from which you are licensing at <http://www.sciencedirect.com/science/journal/xxxxx> or the Elsevier homepage for books at <http://www.elsevier.com>; Central Storage: This license does not include permission for a scanned version of the material to be stored in a central repository such as that provided by Heron/XanEdu.

Licensing material from an Elsevier book: A hyper-text link must be included to the Elsevier homepage at <http://www.elsevier.com>. All content posted to the web site must maintain the copyright information line on the bottom of each image.

Posting licensed content on Electronic reserve: In addition to the above the following clauses are applicable: The web site must be password-protected and made available only to bona fide students registered on a relevant course. This permission is granted for 1 year only. You may obtain a new license for future website posting.

17. For journal authors: the following clauses are applicable in addition to the above: Preprints:

A preprint is an author's own write-up of research results and analysis, it has not been peer-reviewed, nor has it had any other value added to it by a publisher (such as formatting, copyright, technical enhancement etc.).

Authors can share their preprints anywhere at any time. Preprints should not be added to or enhanced in any way in order to appear more like, or to substitute for, the final versions of articles however authors can update their preprints on arXiv or RePEc with their Accepted Author Manuscript (see below).

If accepted for publication, we encourage authors to link from the preprint to their formal publication via its DOI. Millions of researchers have access to the formal publications on ScienceDirect, and so links will help users to find, access, cite and use the best available version. Please note that Cell Press, The Lancet and some society-owned have different preprint policies. Information on these policies is available on the journal homepage.

Accepted Author Manuscripts: An accepted author manuscript is the manuscript of an article that has been accepted for publication and which typically includes author-incorporated changes suggested during submission, peer review and editor-author communications.

Authors can share their accepted author manuscript:

- immediately
  - via their non-commercial person homepage or blog
  - by updating a preprint in arXiv or RePEc with the accepted manuscript

- via their research institute or institutional repository for internal institutional uses or as part of an invitation-only research collaboration work-group
- directly by providing copies to their students or to research collaborators for their personal use
- for private scholarly sharing as part of an invitation-only work group on commercial sites with which Elsevier has an agreement
- after the embargo period
  - via non-commercial hosting platforms such as their institutional repository
  - via commercial sites with which Elsevier has an agreement

In all cases accepted manuscripts should:

- link to the formal publication via its DOI
- bear a CC-BY-NC-ND license - this is easy to do
- if aggregated with other manuscripts, for example in a repository or other site, be shared in alignment with our hosting policy not be added to or enhanced in any way to appear more like, or to substitute for, the published journal article.

**Published journal article (JPA):** A published journal article (PJA) is the definitive final record of published research that appears or will appear in the journal and embodies all value-adding publishing activities including peer review co-ordination, copy-editing, formatting, (if relevant) pagination and online enrichment.

Policies for sharing publishing journal articles differ for subscription and gold open access articles:

**Subscription Articles:** If you are an author, please share a link to your article rather than the full-text. Millions of researchers have access to the formal publications on ScienceDirect, and so links will help your users to find, access, cite, and use the best available version. Theses and dissertations which contain embedded PJAs as part of the formal submission can be posted publicly by the awarding institution with DOI links back to the formal publications on ScienceDirect.

If you are affiliated with a library that subscribes to ScienceDirect you have additional private sharing rights for others' research accessed under that agreement. This includes use for classroom teaching and internal training at the institution (including use in course packs and courseware programs), and inclusion of the article for grant funding purposes.

**Gold Open Access Articles:** May be shared according to the author-selected end-user license and should contain a [CrossMark logo](#), the end user license, and a DOI link to the formal publication on ScienceDirect.

Please refer to Elsevier's [posting policy](#) for further information.

18. For book authors the following clauses are applicable in addition to the above: Authors are permitted to place a brief summary of their work online only. You are not allowed to download and post the published electronic version of your chapter, nor may you scan the printed edition to create an electronic version. Posting to a repository: Authors are permitted to post a summary of their chapter only in their institution's repository.

19. Thesis/Dissertation: If your license is for use in a thesis/dissertation your thesis may be submitted to your institution in either print or electronic form. Should your thesis be published commercially, please reapply for permission. These requirements include permission for the Library and Archives of Canada to supply single copies, on demand, of the complete thesis and include permission for Proquest/UMI to supply single copies, on demand, of the complete thesis. Should your thesis be published commercially, please reapply for permission. Theses and dissertations which contain embedded PJAs as part of the formal submission can be posted publicly by the awarding institution with DOI links back to the formal publications on ScienceDirect.

### Elsevier Open Access Terms and Conditions

You can publish open access with Elsevier in hundreds of open access journals or in nearly 2000 established subscription journals that support open access publishing. Permitted third party re-use of these open access articles is defined by the author's choice of Creative Commons user license. See our [open access license policy](#) for more information.

Terms & Conditions applicable to all Open Access articles published with Elsevier :  
Any reuse of the article must not represent the author as endorsing the adaptation of the article nor should the article be modified in such a way as to damage the author's honour or reputation. If any changes have been made, such changes must be clearly indicated.

The author(s) must be appropriately credited and we ask that you include the end user license and a DOI link to the formal publication on ScienceDirect.

If any part of the material to be used (for example, figures) has appeared in our publication with credit or acknowledgement to another source it is the responsibility of the user to ensure their reuse complies with the terms and conditions determined by the rights holder.

Additional Terms & Conditions applicable to each Creative Commons user license:

CC BY: The CC-BY license allows users to copy, to create extracts, abstracts and new works from the Article, to alter and revise the Article and to make commercial use of the Article (including reuse and/or resale of the Article by commercial entities), provided the user gives appropriate credit (with a link to the formal publication through the relevant DOI), provides a link to the license, indicates if changes were made and the licensor is not represented as endorsing the use made of the work. The full details of the license are available at <http://creativecommons.org/licenses/by/4.0>.

CC BY NC SA: The CC BY-NC-SA license allows users to copy, to create extracts, abstracts and new works from the Article, to alter and revise the Article, provided this is not done for commercial purposes, and that the user gives appropriate credit (with a link to the formal publication through the relevant DOI), provides a link to the license, indicates if changes were made and the licensor is not represented as endorsing the use made of the work. Further, any new works must be made available on the same conditions. The full details of the license are available at <http://creativecommons.org/licenses/by-nc-sa/4.0>.

CC BY NC ND: The CC BY-NC-ND license allows users to copy and distribute the Article, provided this is not done for commercial purposes and further does not permit distribution of the Article if it is changed or edited in any way, and provided the user gives appropriate credit (with a link to the formal publication through the relevant DOI), provides a link to the license, and that the licensor is not represented as endorsing the use made of the work. The full details of the license are available at <http://creativecommons.org/licenses/by-nc-nd/4.0>.

Any commercial reuse of Open Access articles published with a CC BY NC SA or CC BY NC ND license requires permission from Elsevier and will be subject to a fee.

Commercial reuse includes:

- Associating advertising with the full text of the Article
- Charging fees for document delivery or access
- Article aggregation
- Systematic distribution via e-mail lists or share buttons

Posting or linking by commercial companies for use by customers of those companies.

20. Other Conditions:

v1.9

Questions? [customer@copyright.com](mailto:customer@copyright.com) or +1-855-239-3415 (toll free in the US) or +1-978-646-2777.

**E.3 Paper III Copyright Information: Flexural behaviour of multi-celled GFRP composite beams with concrete infill; experimental and theoretical analysis**

**Muttashar M**, Manalo A, Karunasena W, Lokuge W. (2017). Flexural behaviour of multi-celled GFRP composite beams with concrete infill: Experiment and theoretical analysis. *Composite Structures*. Vol. 159, pp. 21-33. (IF:3.385, SINP:2.12)

**ELSEVIER LICENSE  
TERMS AND CONDITIONS**

Feb 24, 2017

This Agreement between Majid Muttashar ("You") and Elsevier ("Elsevier") consists of your license details and the terms and conditions provided by Elsevier and Copyright Clearance Center.

License Number	4055211015195
License date	
Licensed Content Publisher	Elsevier
Licensed Content Publication	Composite Structures
Licensed Content Title	Flexural behaviour of multi-celled GFRP composite beams with concrete infill: Experiment and theoretical analysis
Licensed Content Author	Majid Muttashar,Allan Manalo,Warna Karunasena,Weena Lokuge
Licensed Content Date	1 January 2017
Licensed Content Volume	159
Licensed Content Issue	n/a
Licensed Content Pages	13
Start Page	21
End Page	33
Type of Use	reuse in a thesis/dissertation
Intended publisher of new work	other
Portion	full article
Format	both print and electronic
Are you the author of this Elsevier article?	Yes
Will you be translating?	No
Order reference number	
Title of your thesis/dissertation	FLEXURAL BEHAVIOUR OF HYBRID CONCRETE-GFRP COMPOSITE BEAMS
Expected completion date	Jul 2017
Estimated size (number of pages)	160
Elsevier VAT number	GB 494 6272 12
Requestor Location	Majid Muttashar 4B OXFORD CT  DARLING HEIGHTS, QLD 4350 Australia Attn: Majid Muttashar
Total	0.00 USD
Terms and Conditions	

### INTRODUCTION

1. The publisher for this copyrighted material is Elsevier. By clicking "accept" in connection with completing this licensing transaction, you agree that the following terms and conditions apply to this transaction (along with the Billing and Payment terms and conditions

established by Copyright Clearance Center, Inc. ("CCC"), at the time that you opened your Rightslink account and that are available at any time at <http://myaccount.copyright.com>.

#### GENERAL TERMS

2. Elsevier hereby grants you permission to reproduce the aforementioned material subject to the terms and conditions indicated.

3. Acknowledgement: If any part of the material to be used (for example, figures) has appeared in our publication with credit or acknowledgement to another source, permission must also be sought from that source. If such permission is not obtained then that material may not be included in your publication/copies. Suitable acknowledgement to the source must be made, either as a footnote or in a reference list at the end of your publication, as follows:

"Reprinted from Publication title, Vol /edition number, Author(s), Title of article / title of chapter, Pages No., Copyright (Year), with permission from Elsevier [OR APPLICABLE SOCIETY COPYRIGHT OWNER]." Also Lancet special credit - "Reprinted from The Lancet, Vol. number, Author(s), Title of article, Pages No., Copyright (Year), with permission from Elsevier."

4. Reproduction of this material is confined to the purpose and/or media for which permission is hereby given.

5. Altering/Modifying Material: Not Permitted. However figures and illustrations may be altered/adapted minimally to serve your work. Any other abbreviations, additions, deletions and/or any other alterations shall be made only with prior written authorization of Elsevier Ltd. (Please contact Elsevier at [permissions@elsevier.com](mailto:permissions@elsevier.com)). No modifications can be made to any Lancet figures/tables and they must be reproduced in full.

6. If the permission fee for the requested use of our material is waived in this instance, please be advised that your future requests for Elsevier materials may attract a fee.

7. Reservation of Rights: Publisher reserves all rights not specifically granted in the combination of (i) the license details provided by you and accepted in the course of this licensing transaction, (ii) these terms and conditions and (iii) CCC's Billing and Payment terms and conditions.

8. License Contingent Upon Payment: While you may exercise the rights licensed immediately upon issuance of the license at the end of the licensing process for the transaction, provided that you have disclosed complete and accurate details of your proposed use, no license is finally effective unless and until full payment is received from you (either by publisher or by CCC) as provided in CCC's Billing and Payment terms and conditions. If full payment is not received on a timely basis, then any license preliminarily granted shall be deemed automatically revoked and shall be void as if never granted. Further, in the event that you breach any of these terms and conditions or any of CCC's Billing and Payment terms and conditions, the license is automatically revoked and shall be void as if never granted. Use of materials as described in a revoked license, as well as any use of the materials beyond the scope of an unrevoked license, may constitute copyright infringement and publisher reserves the right to take any and all action to protect its copyright in the materials.

9. Warranties: Publisher makes no representations or warranties with respect to the licensed material.

10. Indemnity: You hereby indemnify and agree to hold harmless publisher and CCC, and their respective officers, directors, employees and agents, from and against any and all claims arising out of your use of the licensed material other than as specifically authorized pursuant to this license.

11. No Transfer of License: This license is personal to you and may not be sublicensed, assigned, or transferred by you to any other person without publisher's written permission.

12. No Amendment Except in Writing: This license may not be amended except in a writing signed by both parties (or, in the case of publisher, by CCC on publisher's behalf).

13. Objection to Contrary Terms: Publisher hereby objects to any terms contained in any purchase order, acknowledgment, check endorsement or other writing prepared by you, which terms are inconsistent with these terms and conditions or CCC's Billing and Payment terms and conditions. These terms and conditions, together with CCC's Billing and Payment terms and conditions (which are incorporated herein), comprise the entire agreement between you and publisher (and CCC) concerning this licensing transaction. In the event of

any conflict between your obligations established by these terms and conditions and those established by CCC's Billing and Payment terms and conditions, these terms and conditions shall control.

14. Revocation: Elsevier or Copyright Clearance Center may deny the permissions described in this License at their sole discretion, for any reason or no reason, with a full refund payable to you. Notice of such denial will be made using the contact information provided by you. Failure to receive such notice will not alter or invalidate the denial. In no event will Elsevier or Copyright Clearance Center be responsible or liable for any costs, expenses or damage incurred by you as a result of a denial of your permission request, other than a refund of the amount(s) paid by you to Elsevier and/or Copyright Clearance Center for denied permissions.

#### LIMITED LICENSE

The following terms and conditions apply only to specific license types:

15. Translation: This permission is granted for non-exclusive world English rights only unless your license was granted for translation rights. If you licensed translation rights you may only translate this content into the languages you requested. A professional translator must perform all translations and reproduce the content word for word preserving the integrity of the article.

16. Posting licensed content on any Website: The following terms and conditions apply as follows: Licensing material from an Elsevier journal: All content posted to the web site must maintain the copyright information line on the bottom of each image; A hyper-text must be included to the Homepage of the journal from which you are licensing at <http://www.sciencedirect.com/science/journal/xxxxx> or the Elsevier homepage for books at <http://www.elsevier.com>; Central Storage: This license does not include permission for a scanned version of the material to be stored in a central repository such as that provided by Heron/XanEdu.

Licensing material from an Elsevier book: A hyper-text link must be included to the Elsevier homepage at <http://www.elsevier.com>. All content posted to the web site must maintain the copyright information line on the bottom of each image.

Posting licensed content on Electronic reserve: In addition to the above the following clauses are applicable: The web site must be password-protected and made available only to bona fide students registered on a relevant course. This permission is granted for 1 year only. You may obtain a new license for future website posting.

17. For journal authors: the following clauses are applicable in addition to the above: Preprints:

A preprint is an author's own write-up of research results and analysis, it has not been peer-reviewed, nor has it had any other value added to it by a publisher (such as formatting, copyright, technical enhancement etc.).

Authors can share their preprints anywhere at any time. Preprints should not be added to or enhanced in any way in order to appear more like, or to substitute for, the final versions of articles however authors can update their preprints on arXiv or RePEc with their Accepted Author Manuscript (see below).

If accepted for publication, we encourage authors to link from the preprint to their formal publication via its DOI. Millions of researchers have access to the formal publications on ScienceDirect, and so links will help users to find, access, cite and use the best available version. Please note that Cell Press, The Lancet and some society-owned have different preprint policies. Information on these policies is available on the journal homepage.

Accepted Author Manuscripts: An accepted author manuscript is the manuscript of an article that has been accepted for publication and which typically includes author-incorporated changes suggested during submission, peer review and editor-author communications.

Authors can share their accepted author manuscript:

- immediately
  - via their non-commercial person homepage or blog
  - by updating a preprint in arXiv or RePEc with the accepted manuscript

- via their research institute or institutional repository for internal institutional uses or as part of an invitation-only research collaboration work-group
- directly by providing copies to their students or to research collaborators for their personal use
- for private scholarly sharing as part of an invitation-only work group on commercial sites with which Elsevier has an agreement
- after the embargo period
  - via non-commercial hosting platforms such as their institutional repository
  - via commercial sites with which Elsevier has an agreement

In all cases accepted manuscripts should:

- link to the formal publication via its DOI
- bear a CC-BY-NC-ND license - this is easy to do
- if aggregated with other manuscripts, for example in a repository or other site, be shared in alignment with our hosting policy not be added to or enhanced in any way to appear more like, or to substitute for, the published journal article.

**Published journal article (JPA):** A published journal article (PJA) is the definitive final record of published research that appears or will appear in the journal and embodies all value-adding publishing activities including peer review co-ordination, copy-editing, formatting, (if relevant) pagination and online enrichment.

Policies for sharing publishing journal articles differ for subscription and gold open access articles:

**Subscription Articles:** If you are an author, please share a link to your article rather than the full-text. Millions of researchers have access to the formal publications on ScienceDirect, and so links will help your users to find, access, cite, and use the best available version. Theses and dissertations which contain embedded PJAs as part of the formal submission can be posted publicly by the awarding institution with DOI links back to the formal publications on ScienceDirect.

If you are affiliated with a library that subscribes to ScienceDirect you have additional private sharing rights for others' research accessed under that agreement. This includes use for classroom teaching and internal training at the institution (including use in course packs and courseware programs), and inclusion of the article for grant funding purposes.

**Gold Open Access Articles:** May be shared according to the author-selected end-user license and should contain a [CrossMark logo](#), the end user license, and a DOI link to the formal publication on ScienceDirect.

Please refer to Elsevier's [posting policy](#) for further information.

18. For book authors the following clauses are applicable in addition to the above: Authors are permitted to place a brief summary of their work online only. You are not allowed to download and post the published electronic version of your chapter, nor may you scan the printed edition to create an electronic version. Posting to a repository: Authors are permitted to post a summary of their chapter only in their institution's repository.

19. Thesis/Dissertation: If your license is for use in a thesis/dissertation your thesis may be submitted to your institution in either print or electronic form. Should your thesis be published commercially, please reapply for permission. These requirements include permission for the Library and Archives of Canada to supply single copies, on demand, of the complete thesis and include permission for Proquest/UMI to supply single copies, on demand, of the complete thesis. Should your thesis be published commercially, please reapply for permission. Theses and dissertations which contain embedded PJAs as part of the formal submission can be posted publicly by the awarding institution with DOI links back to the formal publications on ScienceDirect.

### Elsevier Open Access Terms and Conditions

You can publish open access with Elsevier in hundreds of open access journals or in nearly 2000 established subscription journals that support open access publishing. Permitted third party re-use of these open access articles is defined by the author's choice of Creative Commons user license. See our [open access license policy](#) for more information.

Terms & Conditions applicable to all Open Access articles published with Elsevier: Any reuse of the article must not represent the author as endorsing the adaptation of the article nor should the article be modified in such a way as to damage the author's honour or reputation. If any changes have been made, such changes must be clearly indicated.

The author(s) must be appropriately credited and we ask that you include the end user license and a DOI link to the formal publication on ScienceDirect.

If any part of the material to be used (for example, figures) has appeared in our publication with credit or acknowledgement to another source it is the responsibility of the user to ensure their reuse complies with the terms and conditions determined by the rights holder.

Additional Terms & Conditions applicable to each Creative Commons user license:

CC BY: The CC-BY license allows users to copy, to create extracts, abstracts and new works from the Article, to alter and revise the Article and to make commercial use of the Article (including reuse and/or resale of the Article by commercial entities), provided the user gives appropriate credit (with a link to the formal publication through the relevant DOI), provides a link to the license, indicates if changes were made and the licensor is not represented as endorsing the use made of the work. The full details of the license are available at <http://creativecommons.org/licenses/by/4.0>.

CC BY NC SA: The CC BY-NC-SA license allows users to copy, to create extracts, abstracts and new works from the Article, to alter and revise the Article, provided this is not done for commercial purposes, and that the user gives appropriate credit (with a link to the formal publication through the relevant DOI), provides a link to the license, indicates if changes were made and the licensor is not represented as endorsing the use made of the work. Further, any new works must be made available on the same conditions. The full details of the license are available at <http://creativecommons.org/licenses/by-nc-sa/4.0>.

CC BY NC ND: The CC BY-NC-ND license allows users to copy and distribute the Article, provided this is not done for commercial purposes and further does not permit distribution of the Article if it is changed or edited in any way, and provided the user gives appropriate credit (with a link to the formal publication through the relevant DOI), provides a link to the license, and that the licensor is not represented as endorsing the use made of the work. The full details of the license are available at <http://creativecommons.org/licenses/by-nc-nd/4.0>.

Any commercial reuse of Open Access articles published with a CC BY NC SA or CC BY NC ND license requires permission from Elsevier and will be subject to a fee.

Commercial reuse includes:

- Associating advertising with the full text of the Article
- Charging fees for document delivery or access
- Article aggregation
- Systematic distribution via e-mail lists or share buttons

Posting or linking by commercial companies for use by customers of those companies.

20. Other Conditions:

v1.9

Questions? [customer@copyright.com](mailto:customer@copyright.com) or +1-855-239-3415 (toll free in the US) or +1-978-646-2777.